UNIVERSITY OF CALIFORNIA SAN DIEGO

Boundary Feedback Control Design for Classes of Mixed-Type Partial Differential Equations

A dissertation submitted in partial satisfaction of the
requirements for the degree
Doctor of Philosophy

in

Engineering Sciences (Mechanical Engineering)

by

Stephen Chen

Committee in charge:

Professor Miroslav Krstic, Chair
Professor Nikolay Atanasov
Professor Jorge Cortes
Professor Ni Lei
Professor William McEneaney

2019

The dissertation of Stephen Chen is approved, and it is acceptable in quality and form for publication on microfilm and electronically:

_____

_____

_____

_____

_____

Chair

University of California San Diego

2019

DEDICATION

To my parents, Jie Chen and Yan Liu, and my brother, Christopher Chen, for their unconditional support and love.

TABLE OF CONTENTS

LIST OF FIGURES

LIST OF TABLES

ACKNOWLEDGEMENTS

I would like to express the highest gratitude to my advisor, Miroslav Krstic, for his guiding hand in my development as a researcher. His nurturing and guidance has helped shape not only my research skills, but also has imbued me with a strong, deep intuition of control theory, for which I am extremely grateful for.

I would like to thank the members of my Ph.D. committee: Nikolay Atanasov, Jorge Cortes, William McEneaney, Lei Ni for perusing this thesis and for their helpful comments.

I also would like to extend special thanks to Rafael Vazquez for fruitful research discussions and enthusiastic support throughout my tenure as a student. I also would like to thank Scott Moura and Reinhardt Klein for working closely with me on a former ARPA-E project. I would also like to give a special thanks to Andrew Liu for being a mentor during my time at Cymer.

I would also like to give a very special thanks to Claus Danielson for encourging me to continue onto graduate studies in control systems. Without his initial guidance, I would not be in this same position.

I would like to acknowledge former and current graduate students and postdocs of my research group for their enthusiasm, mentoring, and support: Halil Basturk, Shuxia Tang, Greg Mills, Mamadou Diagne, Leobardo Camacho-Solorio, Huan Yu, Shumon Koga, Drew Steeves.

I would like to extend a well-deserved thanks to some of my favorite people for always being supportive and checking up on me regularly: Dennis Wai, Robert Luan, Ben Yee, Jared Porter.

Finally, a special thanks is in order for the crew of Gym Standard and related folks (apologies if I miss some): Daniel, Ryan, Jake, Alena, Carlo, Tony, Jun, Matt, AJ, Carter, Keith, India, Alan, Jakelen, Justin, Edwin, Julian, Jon, Kaidan, Tiffany. I am sure I am missing many of you, but this extends to you all the same. Thanks for keeping me sane and stimulating my creativity, I wouldn't have finished the same way if it weren't for this welcoming and supportive community.

Chapter 2 is a reprint of work published as "Stabilization of an Underactuated Coupled Transport-Wave PDE System" at the American Control Conference (ACC), 2017 co-authored with R. Vazquez and M. Krstic. The dissertation author was the primary investigator and author of this paper.

Chapter 3 is a reprint of work published as "Backstepping Control Design for a Coupled Hyperbolic-Parabolic Mixed Class PDE System" at the Conference on Decision and Control (CDC), 2017 co-authored with R. Vazquez and M. Krstic. The dissertation author was the primary investigator and author of this paper.

Chapter 4 is a reprint of work published as "Backstepping Boundary Control of a 1-D 2X2 Unstable Diffusion-Reaction PDE System with Distinct Input Delays" at the American Control Conference, 2019 co-authored with R. Vazquez and M. Krstic. The dissertation author was the primary investigator and author of this paper.

Chapter 5 is a unpublished work co-authored with R. Vazquez and M. Krstic. The dissertation author was the primary investigator and author of this work.

Chapter 6 is a reprint of work found in "Bilateral Boundary Backstepping Control of a 1-D Unstable Parabolic PDE via a Folding Approach" presented at the 3rd IFAC Joint Workshop on PDE Control and Distributed Parameter Systems (CPDE/CDPS), 2019 co-authored with R. Vazquez and M. Krstic. The dissertation author was the primary investigator and author of this paper. Chapter 6 also contains the extension of this work to state-estimation and output-feedback, which is a reprint of the work "Folding Bilateral Backstepping Output-Feedback Control Design For an Unstable Parabolic PDE," submitted for publication, 2019 co-authored with R. Vazquez and M. Krstic. The dissertation author was also the primary investigator and author of this paper.

Chapter 7 is a reprint of work "A Folding Approach to Bilateral Control of a 1-D Unstable Parabolic PDE with Distinct Input Delays," submitted for publication, 2019 co-authored with R. Vazquez and M. Krstic. The dissertation author was the primary investigator and author of this paper.

Chapter 8 is a reprint of work “Bilateral Boundary Control Design for a Cascaded Diffusion -ODE System Coupled at an Arbitrary Interior Point,” submitted for publication, 2019 co-authored with R. Vazquez and M. Krstic. The dissertation author was the primary investigator and author of this paper.

VITA

2012	Algorithms Intern, Tesla Motors
2013	EECS 192 Teaching Assistant, University of California, Berkeley
2013	B. S. in Electrical Engineering and Computer Sciences with Dean's Honors, University of California, Berkeley
2015	M. S. in Engineering Sciences (Mechanical Engineering), University of California, San Diego
2016	Controls Intern, ASML
2017	MAE 281A Teaching Assistant, University of California, San Diego
2018	MAE 281A Teaching Assistant, University of California, San Diego
2019	Ph. D. in Engineering Sciences (Mechanical Engineering), University of California, San Diego

PUBLICATIONS

S. Chen, R. Vazquez, M. Krstic. "Bilateral Boundary Control Design for a Cascaded Diffusion-ODE System Coupled at an Arbitrary Interior Point". Submitted to Automatica, 2019

S. Chen, R. Vazquez, M. Krstic. "Folding Bilateral Backstepping Output-Feedback Control Design For an Unstable Parabolic PDE". Submitted to IEEE Transactions on Automatic Control, 2019

S. Chen, R. Vazquez, M. Krstic. "Backstepping Boundary Control of a 1-D 2X2 Unstable Diffusion-Reaction PDE System with Distinct Input Delays". American Control Conference, 2019

S. Chen, R. Vazquez, M. Krstic. "Bilateral Boundary Backstepping Control of a 1-D Unstable Parabolic PDE via a Folding Approach". 3rd IFAC Joint Workshop on PDE Control and Distributed Parameter Systems (CPDE/CDPS), 2019

L. Su, S. Chen, J.M. Wang, M. Krstic. "Stabilization of 2X2 Hyperbolic PDEs with Recirculation in the Unactuated Channel". Currently under review in Automatica

S. Chen, R. Vazquez, M. Krstic. "Backstepping Control Design for a Coupled Hyperbolic-Parabolic Mixed Class PDE System". Conference on Decision and Control, 2017

S. Chen, R. Vazquez, M. Krstic. "Stabilization of an Underactuated Coupled Transport-Wave PDE System". American Control Conference, 2017

ABSTRACT OF THE DISSERTATION

Boundary Feedback Control Design for Classes of Mixed-Type Partial Differential Equations

by

Stephen Chen

Doctor of Philosophy in Engineering Sciences (Mechanical Engineering)

University of California San Diego, 2019

Professor Miroslav Krstic, Chair

The work in this dissertation summarizes some advancement in the theory of boundary controller design for coupled partial differential equations (PDEs), including a new interpretation of designing bilateral boundary controllers as equivalent coupled PDEs via a method dubbed "folding." In particular, systems of purely hyperbolic type, purely parabolic type, and mixed (hyperbolic-parabolic) type are all explored in the context of boundary control. The work centers around the method of infinite-dimensional backstepping consisting of an non-trivially invertible spatial transformation mapping to a system with desireable properties, such stability of equilibria and convergence speed. A companion kernel PDE must be solved to properly define the transform.

The transformations across the different classes of PDEs are similiar (and in certain cases, identical); however, curious behavior arises from a heterogeneous mixed type PDE, in which the companion kernel PDE becomes non-standard. The thesis studies some preliminary work into mixed type PDEs in an attempt to recover a more general backstepping design for linear PDE.

In the purely hyperbolic work, a special case of a underactuated hyperbolic system is considered. This is in opposition to pre-existing literature, which assumed a fully actuated system. The classical backstepping boundary controller is modified for the underactuated hyperbolic case, admitting a two-tiered trasnformation approach in which the backstepping controller is augmented by a predictor-based controller to achieve a finite-time stability for the trivial solution of the system. In the purely parabolic work, the notion of the folding approach is introduced as an alternative design method to pre-existing bilateral boundary control design work. The folding approach admits additional design parameters for the control designer, allowing the controls to be biased for differing performance indexes. A complimentary state estimator is designed, which allows for collocated point measurement at any arbitrary point in the domain independent of the control design. The two are combined to achieve an output-feedback control result.

Several results are given for mixed type PDE systems of hyperbolic-parabolic type as well. A first result invovles a scalar system with coupling on the boundary and the interior. The interior coupling necessitates more advanced techniques in the analysis of the companion kernel PDE, particularly in showing well-posedness. These ideas are also applied to other higher-order coupled systems of hyperbolic-parabolic type, including delay compensation for systems of parabolic PDEs, and delay compensation for bilateral controller design of parabolic PDEs.

Both the notion of bilateral boundary control and mixed type PDE systems arise in short-wavelength light generation. In the state-of-the-art light generation at the extreme ultraviolet (EUV) wavelengths, instabilities in the light generation process potentially arise due to coupled plasma interactions with the generating process. Phenomena such as ion-acoustic waves, free-electron plasma diffusion, magnetohydrodynamics, and thermofluidics arise due to the interacting

plasma, introducing potential modes of instability. This instability neceessitates the introduction of feedback control, which can be introduced via two controllers on either boundary of the process domain.

Chapter 1

Introduction

1.1 Motivating example: Extreme ultraviolet light generation in photolithography for semiconductor manufacturing

In the realm of semiconductor manufacturing, the process of photolithography is critical for patterning transistors on silicon. In the photolithography process, as the name may suggest, light is used to expose a layer of photoresist (a light sensitive layer applied on top of the silicon) through a patterned mask. The photoresist interacts with the narrowband light, which is then processed through etching. This process is repeated several times to carve transistors into a silicon wafer.

The size of the transistor is determined by several different factors, but depends linearly on the wavelength of the light. Current state-of-the-art photolithography technology utilizes a spectrum known as deep ultraviolet (DUV), with wavelengths on the order of 280nm. DUV can be generated via a traditionally well understood process – energizing a gas mixture under pressure.

The next stage in light generation focuses on extreme ultraviolet, or EUV, with fundamentally different generation when compared with the aforementioned processes used in DUV. EUV must be generated by ionizing specific metals, that is, energizing droplets of liquid tin until the tin disassociates into tin plasma thereby releasing a photon of the correct wavelength, roughly 13.5nm (this value depends on the intrinsic bandgap of the material being ionized). Repeated ionization events at high frequency lead to sustained light at the correct wavelength.

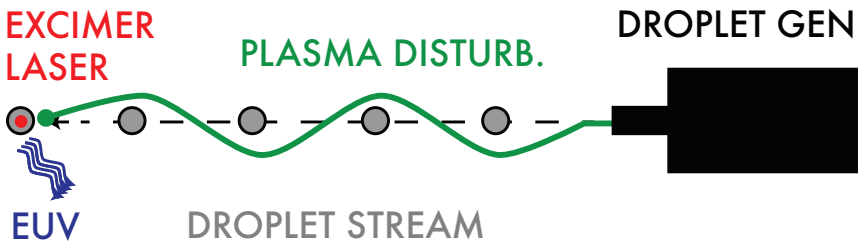

Figure 1.1: A simplified figure of the EUV generation process. Liquid tin is ejected from the generator and ionized by the excimer laser, releasing a photon of EUV light. The resulting tin plasma byproduct (free-electron diffusion, ion-acoustic waves, thermofluidic, and electromagnetic effects) disturbs the transverse displacement of droplets upstream.

The process of generating this sustained light is in fact quite complex. The process is depicted in a very simplifed cartoon (Figure 1.1). A droplet generator squeezes droplets of liquid tin into an evacuated chamber using a piezoelectric sphincter, at high frequencies (75kHz+). The droplets convect in this channel until they reach an excimer laser, which energizes the liquid tin and ideally converts the mass to tin plasma. In reality, because of internal disturbances postulated to be caused by plasma from previous ionization events, the excimer laser does not always have perfect accuracy and the conversion efficiency is not optimal.

The stabilization problem arises in using the excimer laser and droplet generator as control inputs to stabilize the plasma disturbance. It is not difficult to see that the dynamics are inherently infinite-dimensional – the droplet stream convection is modeled by a transport equation (a first-order hyperbolic PDE), while the assorted plasma phenomena can range across many different types of PDE including (but not limited to) wave equations, diffusion equations, and Kortweg-de-Vries equations.

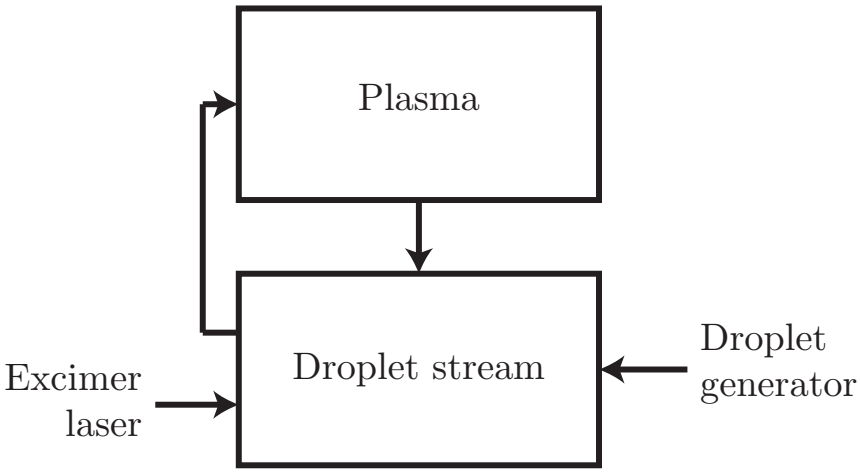

Figure 1.2: A systems perspective of the simple control model. The controls are the excimer laser and the droplet generator, while the coupled plasma and droplet stream dynamics exhibit a feedback loop.

The structure of the proposed control model exhibits feedback between the plasma and droplet stream dynamics, the postulated destabilizing phenomena. The structure of the problem is depicted in Figure 1.3 Thus, the high level control problem can be succinctly stated as: utilizing the droplet generator initial displacement and excimer laser orientation to stabilize the droplet stream and plasma dynamics. The models described in this thesis are motivated by this high level formulation.

1.2 A brief background of the control of backstepping in infinite dimension

Backstepping in infinite dimension has had an explosive growth in researchers working in the field. In the most basic sense, the backstepping approach in infinite dimension utilizes a Volterra integral transformation of the second kind in the spatial variables. It can be thought of as a continuum spatial transformation, which "shifts" certain types of *spatially-causal* interior phenomena into a non-local boundary operator, which can consequently be neutralized via a

control law operating at the boundary. Such is the intuitive idea behind backstepping in infinite-dimension: we apply a spatial transformation which allows us to collect undesirable phenomena into the boundary, where they are compensated by the control law via algebraic cancellation.

There are, of course, several caveats with this design methodology. Most critically, the continuum spatial transformation must be invertible to establish an equivalence relation between the transformed and original systems. The well-posedness of the transform is not immediately obvious in non-classical results, and serves as the main technical challenge in this thesis and much of the ongoing active research. The well-posedness of an invertible Volterra integral transformation of the second kind, however, is well chararcterized by the existence, uniqueness, and regularity of the kernel of the transformation. In the backstepping approach, differential conditions on the kernel are typically imposed – in standard problems, these conditions give rise to a Goursat problem.

The backstepping method has been applied to many classes of linear PDE, and some structured nonlinear PDE problems. For much of the classical infinite-dimensional backstepping work covering standard linear constant coefficient PDEs (heat, wave, transport) as well as some more exotic PDE (Kortweg de Vries, Kuramoto Sivanshinsky, beam models such as shear, Euler-Bernoulli) can be found in [30].

In the realm of more general parabolic PDEs, many results in stabilization and estimation of linear parabolic systems has been investigated. Some initial results on scalar parabolic PDE with spatially-varying diffusion and spatially and temporally varying reaction can be found in [37]. The observer (the dual of the boundary control) was developed initially in [36, 40] for boundary and spatially averaged sensing, respectively. Weakly coupled parabolic PDE has also been investigated rather thoroughly, with [45, 1, 18] having looked at varying state-feedback and output-feedback paradigms, and [10] studying the observer analogue. Some special case of boundary coupling (cascade) has been studied by [41]. More recently, the notion of bilateral (or actuation at both boundaries, in 1-D) has been lightly explored with [43, 8] studying

the stabilization for diffusion reaction and nonlinear viscous Burgers equations. The bilateral methodology for linear parabolic PDE is generalized in [15], which also includes the observer analogue to bilateral control – collocated interior sensing. Finally, some higher dimensional results exist in [44], albeit with a restrictive condition on the shape of the domain.

Hyperbolic PDEs have been just as, if not more, prolific than the parabolic studies. With several key papers [32, 25] studying the state feedback problem of general coupled first-order hyperbolic PDEs. This idea has been expanded to admit additional ideas such as minimum-time control in [3] and bilateral control in [5]. The idea of hyperbolic PDEs as been cast as delays as well, with much literature studying delay problems in the context of hyperbolic PDEs [29].

Typically most coupled PDE system boundary control and observer results are confined to the one type of PDE, or potentially one classification of PDE and ODEs coupled either at the boundary or on the interior. Many results exist in both the former and latter (the former has been discussed prior). The PDE-ODE coupling opens the door for some interesting coupling topologies, which include results of [38, 17, 51, 47, 29, 7].

Interestingly, in the linear case, the backstepping transforms are near identical (for a fixed system-order) across varying classes – a quite unusual property for PDE. In fact, Vazquez in [45] notes the analogy between the kernel PDEs of parabolic and hyperbolic to be similar. These observations, made by the dissertation author as well, prompted the study of mixed-type PDE systems. A mixed-type PDE system can have several differing interpretations depending on the equation structure. One prevalent notion is that in fluid flows, where inviscid free-flow encounters porous media. The free-flow regime is described by a hyperbolic PDE, while the flow through porous media is described by a parabolic PDE, which can be derived from considering both the conservation of mass principle and Darcy's law.

Some work on boundary control for mixed-type systems has been considered, albeit limited. One main result by Krstic [28] considers the scalar first-order hyperbolic PDE boundary cascaded with a scalar parabolic PDE. In this problem, the companion kernel PDE can already be

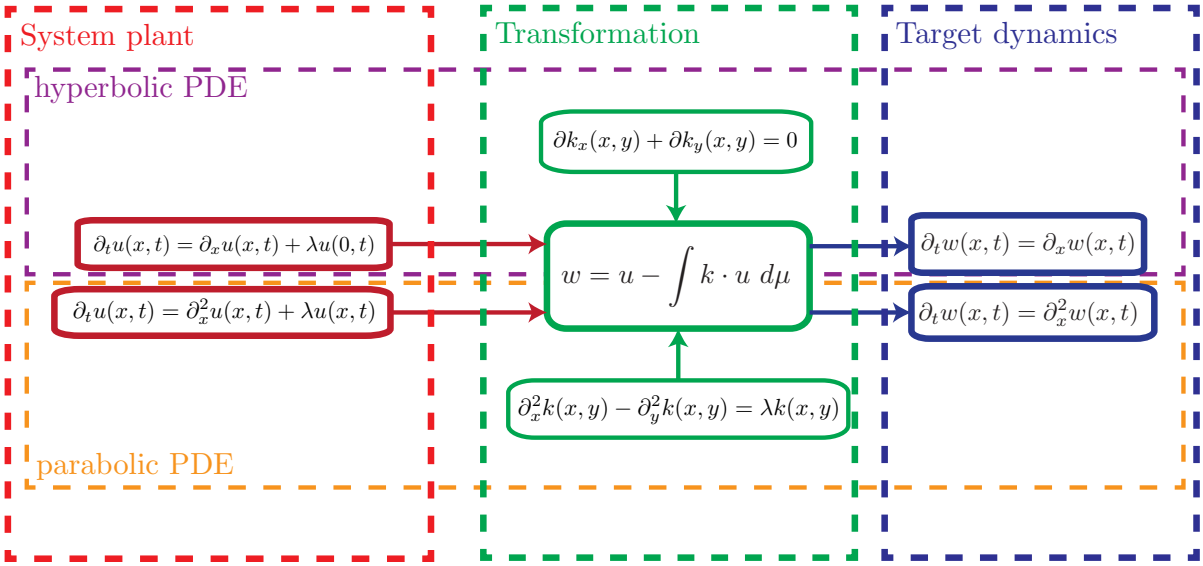

Figure 1.3: Within each (linear) PDE classificiation, associated kernels of transformations are recovered. These kernels are intimately tied to the classification of the PDE.

noted to be different than classical infinite-dimensional backstepping – a PDE of parabolic type. Fortunately, the kernel PDE in [28] exhibits well-studied structure (diffusion-reaction equation with constant coefficients) whose separation property can be exploited for an explicit solution. Other results in mixed-type PDEs include that of Hashimoto [22], which features hyperbolic coupling (delay phenomena) in the interior. The design in [22] depends on *dominance* of the hyperbolic phenomena rather than compensation. A different design method for the same problem considered in [28] is explored by Prieur et al. in [34], which utilizes a property of parabolicity to generate a spectral decomposition of the unstable parabolic PDE into a finite-dimensional unstable system and an infinite-dimensional stable system.

1.3 Organization

The thesis is divided roughly into sections. In Chapter 2, a result in the finite-time stabilization of underactuated hyperbolic systems is presented. A state-feedback methodology, based on a combination of augmented backstepping and predictor control design techniques, is presented. The stabilizing property of this feedback control is shown through two invertible transformations. The well-posedness of the associated kernel PDEs is studied via the method of characteristics, extending the pre-existing methods of solving classical backstepping companion gain kernel PDEs.

In Chapter 3, a first result in the control of a strict feedback mixed-type hyperbolic-parabolic system is given. A novel companion kernel PDE of parabolic type is encountered, motivating the use of Galerkin methods to prove well-posedness, a technique that is typically not used in classical backstepping results. The Galerkin method involves the development of global energy estimates on the kernel domain, which provides the guarantee of well-posedness for the linear kernel PDE. Numerical solutions of the kernel are given, and the closed-loop system simulated to show the effectiveness of the backstepping design.

In Chapter 4, results in delay compensated control of coupled unstable parabolic equations are shown. Surprisingly, although the coupling between the hyperbolic delay and the unstable parabolic equation is "simpler" than that of results in Chapter 3, the higher-order coupled system still mandates more advanced techniques such as the Galerkin method in showing well-posedness of the companion gain kernel PDE. These results extend backstepping designs in coupled, purely parabolic systems to that of a coupled mixed-type coupled hyperbolic-parabolic system.

In Chapter 5, the problem of designing two boundary controllers *bilaterally* (defined on both boundaries of a 1-D PDE) for an unstable parabolic PDE in presence of distinct input delays is investigated. First, a process of designing bilateral control for an unstable parabolic PDE with identical delay is developed, giving rise to an interesting geometric interpretation of

the companion gain kernel PDEs. A method of domain extension, i.e. adding artificial delay, is developed and utilized to establish an equivalence relation between the identical delay and distinct delay cases. However, this artificial delay extension transforms a static state-feedback controller into a dynamic controller. The method of artificial delay extension can be seen to be analogous to dynamic extension in finite-dimensional systems.

In Chapter 6, the problem of bilateral boundary control design for an unstable parabolic PDE is considered with a novel approach termed "folding." This marks an initial step to solving the problem of Chapter 5 without using the dynamic extension technique. The folding technique introduces a design parameter called the *folding point* – mathematically, the single unstable parabolic PDE is folded around this arbitrarily point to generate a coupled parabolic system with exotic boundary conditions. The power of this result is being able to bias the controllers, that is, shift control effort from one controller to another. A complementary state observer is also designed, which analogously uses collocated measurements of the state and flux at any arbitrary point in the interior to generate a converging state estimate. The selection of folding point and sensor locations are *independent* of one another, which is quite powerful. The two designs are combined with an additional proof of the separation principle of design to recover an output feedback result.

In Chapter 7, the result of Chapter 5 is achieved with the folding methodology as opposed to the dynamic extension method. The folding technique is used to design a nominal controller for the parabolic PDE and the results of Chapter 4 are modified to accomodate the folding boundary conditions to recover the delay compensation for bilateral boundary control of unstable parabolic PDEs in presence of distinct input delays.

In Chapter 8, an interesting natural result of the folding approach is investigated, where a finite-dimensional linear ordinary differential equation system is coupled to the parabolic PDE at an arbitrary point on the interior. The folding approach generalizes to this result in a relatively straightforward manner, although care must be taken in the well-posedness proof of the

companion kernel PDE to accommodate the additional coupling.

Chapter 2

Transport-wave

2.1 Introduction

Control of coupled PDE systems has been studied rather extensively, with forays into various coupling structures of varying classes of PDEs. In particular, the study of coupled hyperbolic systems of first order have been explored [25],[32],[31]. Decompositions of wave equations into 2x2 transport systems have also been considered within different contexts [7].

Delay-wave equations have been studied in [48], where it has been shown that for an antistable wave equation with input delay can only be stabilized for delay of even multiples of the wave speed. In fact, any odd multiple delay will result in instability. However in this paper we do not consider an antistable wave equation, rather, one that is marginally stable.

The control of coupled transport systems has been studied in [25], [32], and [31], however, each case has subtle differences from one another. In [32], the case considered is of $n+1$ transport systems, where n transport systems convect in one direction and the controlled system travels in the opposing direction. This was extended to $n+m$ transport systems in [25], however, with the caveat that now the m transport systems each have a controlled boundary (i.e. m control inputs are required). This was further studied in [24].

We study the problem consisting of a coupled wave-transport equation, which consequentially can be decomposed into a system of transport equations. The tools developed in [30] are more readibly applicable to systems of the same class. Such systems are physically motivated by a transport process in which some sort of reaction occurring at the outflow boundary influences the transport dynamics.

A readily available application is in extreme ultraviolet light generation for photolithography. In order to etch transistors into semiconductors, a specific wavelength of light is used. However, to etch smaller and smaller transistors, one must generate light at smaller and smaller wavelengths. Enter extreme ultraviolet: a new, fledging technology which can generate light at sufficiently small wavelengths ($\sim$13nm). However, many issues occur during the generation of this light, which make the application of feedback control attractive. Currently, the extreme ultraviolet generation problem consists of the transport of liquid tin droplets through a stream, which after some travel period are vaporized into plasma by a CO_2 drive laser, thus generating the desired wavelength of light. However, the plasma generated also influences the displacement of droplets further upstream, incurring potentially destabilizing feedback (dependent on the intensity of the drive laser). It is possible to model these plasma mechanisms through wave-like behavior. A more in depth overview of the physics of the system can be found in [46].

In this paper, we consider the case of a coupled transport-wave equation which is decomposed into a $2+1$ first-order hyperbolic system, where the control enters one transport equation with another transport equation traveling in the same direction, and the last traveling in the opposite direction. Hence, this system no longer falls under the $n+1$ class nor the $n+m$ class with m inputs. However, in our case we no longer consider the coupling from the controlled subsystem to the uncontrolled subsystem in the interior, only the boundary. The interior coupling term from the uncontrolled subsystem entering the controlled subsystem is still considered.

The paper is structured as follows: in Section 8.2 we introduce the system model, and transform the system from a transport-wave to a transport-transport type system. In Section 2.3

we introduce the desired target system, study the stability of the target system, and develop a two-part backstepping transformation. The kernel equations of the backstepping transformation are also derived. In Section 2.4 we study the well-posedness of the kernel equations, and derive a solution.

2.2 Problem statement

We consider the model of a coupled transport-wave equation system, where the wave equation state enters the transport equation in an in-domain distributive manner, while the transport equation acts as a boundary source for the wave equation.

$$\partial_t^2 v(x,t) = \mu^2 \partial_x^2 v(x,t) \tag{2.1}$$

$$\partial_t u(x,t) = \partial_x u(x,t) + q(x)v(x,t) \tag{2.2}$$

$$\partial_x v(0,t) = u(0,t) \tag{2.3}$$

$$v(1,t) = 0 \tag{2.4}$$

$$u(1,t) = U(t) \tag{2.5}$$

where $u(x,t)$ is the transport PDE distributed state, $v(x,t)$ the wave PDE distributed state. $q(x)$ is the distributed coefficient coupling the wave PDE to the transport PDE, while $\mu > 0$ is the wave propagation speed. The control input is at the boundary of the transport system u, and is notated $U(t)$. The spatial domain of the system is defined by $x \in [0,1]$.

By defining the following variables $v_0(x,t)$ and $v_1(x,t)$ as

$$v_0(x,t) = \partial_t v(x,t) + \mu \partial_x v(x,t) \tag{2.6}$$

$$v_1(x,t) = \partial_t v(x,t) - \mu \partial_x v(x,t), \tag{2.7}$$

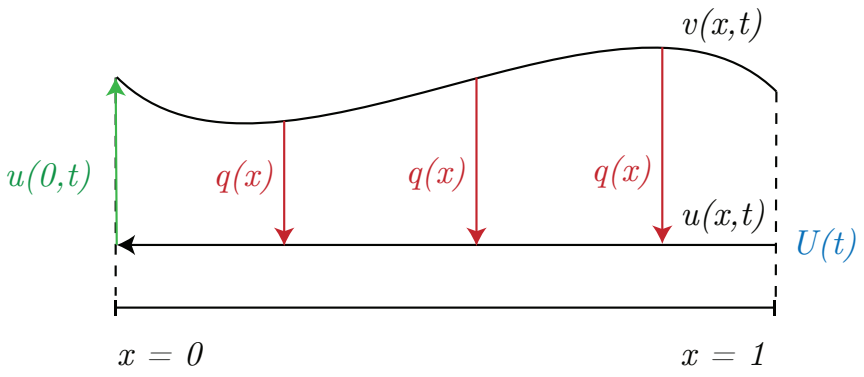

Figure 2.1: Schematic view of coupled transport-wave system.

the wave equation $v(x,t)$ can be decomposed into two transport equations $v_{0,1}(x,t)$ in opposing directions. By utilizing (2.6), (2.7), we can rewrite the system (2.1)-(2.5) as

$$\partial_t v_0(x,t) = \mu \partial_x v_0(x,t) \tag{2.8}$$

$$\partial_t v_1(x,t) = -\mu \partial_x v_1(x,t) \tag{2.9}$$

$$\begin{aligned} \partial_t u(x,t) &= \partial_x u(x,t) \\ &\quad - \frac{q(x)}{2\mu} \int_x^1 [v_0(y,t) - v_1(y,t)] dy \end{aligned} \tag{2.10}$$

$$v_0(1,t) = -v_1(1,t) \tag{2.11}$$

$$v_1(0,t) = v_0(0,t) - 2\mu u(0,t) \tag{2.12}$$

$$u(1,t) = U(t) \tag{2.13}$$

The system now becomes a set of coupled first-order hyperbolic PDEs. One might note that the stability of (v_0, v_1) implies stability in v by imposing the boundary condition (2.4).

The goal is to find a feedback control law $U(t)$ such that the zero equilibrium of the system (2.8)-(2.13) is exponentially stabilized.

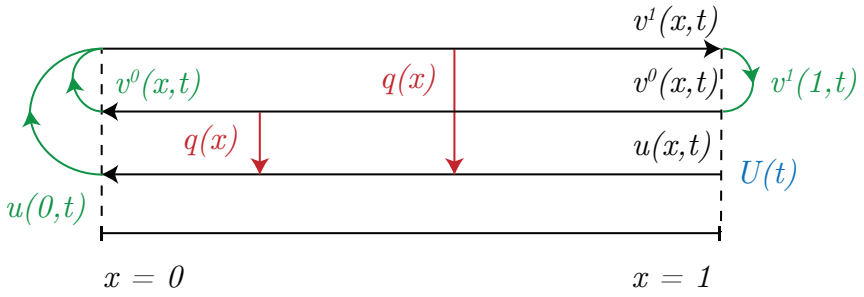

Figure 2.2: Schematic view of coupled transport-transport system.

2.3 Control design

2.3.1 Target system

We utilize backstepping methods to design a control law. We seek to map (2.8)-(2.13) into the following exponentially stable target system:

$$\partial_t v_0(x,t) = \mu \partial_x v_0(x,t) \tag{2.14}$$

$$\partial_t v_1(x,t) = -\mu \partial_x v_1(x,t) \tag{2.15}$$

$$\partial_t w(x,t) = \partial_x w(x,t) \tag{2.16}$$

$$v_0(1,t) = -v_1(1,t) \tag{2.17}$$

$$v_1(0,t) = 0 \tag{2.18}$$

$$w(1,t) = 0 \tag{2.19}$$

Lemma 1. *Consider the system given by* (2.14)-(2.19) *and initial conditions* $v_0(x,0), v_1(x,0)$, $w(x,0) \in \mathcal{H}^1[0,1]$. *The equilibrium* $v_0 = v_1 = w \equiv 0$ *is exponentially stable in the* $\mathcal{L}^2$ *sense.*

Proof. To show that the equilibrium $(v_0(\cdot,t), v_1(\cdot,t), w(\cdot,t)) = 0$ of the target system is exponentially stable, we consider the Lyapunov function inspired by [16]:

$$V(t) = \int_0^1 p_1 e^{\delta x} w(x,t)^2 dx + \int_0^1 \frac{p_2}{\mu} e^{\delta x} v_0(x,t)^2 dx$$

$$+\int_0^1 \frac{p_3}{\mu} e^{-\delta x} v_1(x,t)^2 dx \tag{2.20}$$

where $p_i, \delta > 0, i \in \{1,2,3\}$ are positive coefficients to be chosen. The Lyapunov candidate function V can be bounded by

$$V(t) \geq C_0(||v_0(\cdot,t)||^2 + ||v_1(\cdot,t)||^2 + ||w(\cdot,t)||^2) \tag{2.21}$$

$$V(t) \leq C_1(||v_0(\cdot,t)||^2 + ||v_1(\cdot,t)||^2 + ||w(\cdot,t)||^2) \tag{2.22}$$

where the norm $||\cdot||$ is the $\mathcal{L}^2$ norm, and the constants C_0, C_1 defined by
$C_0 = \max\{p_1, p_2/\mu, p_3 e^{-\delta}/\mu\}$ and $C_1 = \min\{p_1 e^{\delta}, p_2 e^{\delta}/\mu, p_3/\mu\}$. Differentiating $V(t)$ and integrating by parts yields

$$\begin{aligned}
\dot{V}(t) = &-\frac{1}{2} p_1 w(0,t)^2 - \frac{1}{2} p_2 v_0(0,t)^2 \\
&-\frac{1}{2}\left(p_3 e^{-\delta} - p_2 e^{\delta}\right) v_1(1,t)^2 \\
&-\frac{1}{2}\int_0^1 \delta p_1 e^{\delta x} w(x,t)^2 dx \\
&-\frac{1}{2}\int_0^1 \delta p_2 e^{\delta x} v_0(x,t)^2 dx \\
&-\frac{1}{2}\int_0^1 \delta p_3 e^{-\delta x} v_1(x,t)^2 dx
\end{aligned} \tag{2.23}$$

From this, we derive a condition that $p_3 \geq p_2 e^{2\delta}$, which we can enforce by choosing p_2, p_3. Following this, we can bound $\dot{V}(t)$ by

$$\dot{V}(t) \leq -\frac{\delta}{2} V(t) \tag{2.24}$$

From the comparison principle, we can conclude

$$V(t) \leq e^{-\frac{\delta}{2}t} V(0) \tag{2.25}$$

From (2.21) and (2.22),

$$||\gamma(\cdot,t)|| \leq \sqrt{\frac{C_1}{C_0}} e^{-\frac{\delta}{4}t} ||\gamma(\cdot,0)|| \tag{2.26}$$

$$\gamma(x,t) := (v_0(x,t), v_1(x,t), w(x,t)) \tag{2.27}$$

It follows that the equilbirium $(v_0, v_1, w) = 0$ is exponentially stable. □

2.3.2 Backstepping controller

Next, we derive the backstepping feedback control in a two-part process for clarity. The first transformation will be remove the v_0 and v_1 coupling terms in (2.10). The second part involves applying an additive feedfoward to finish stabilizing the system.

Backstepping to remove coupling terms

We seek to use the following transformation to map the original system into an intermediate target system.

$$\begin{aligned}\eta(x,t) = u(x,t) &- \int_0^x k(x,y)u(y,t)dy \\ &- \int_0^1 l(x,y)v_0(y,t)dy - \int_0^1 m(x,y)v_1(y,t)dy\end{aligned} \tag{2.28}$$

Note that for $v_0(x,t), v_1(x,t)$, the backstepping integrals are of the Fredholm-type rather than the typical Volterra-type seen in [30]. This is to account for the nature of the coupling in (2.10). However, as the integral pertaining to the state being transformed ($u(x,t)$) is of the Volterra type, the transformation maintains invertiblility, provided that the kernel functions exist and are bounded (studied in Section 2.4).

The intermediate target system is given as

$$\partial_t v_0(x,t) = \mu \partial_x v_0(x,t) \tag{2.29}$$

$$\partial_t v_1(x,t) = -\mu \partial_x v_1(x,t) \tag{2.30}$$

$$\partial_t \eta(x,t) = \partial_x \eta(x,t) \tag{2.31}$$

$$v_0(1,t) = -v_1(1,t) \tag{2.32}$$

$$v_1(0,t) = v_0(0,t) - 2\mu \eta(0,t) \tag{2.33}$$

$$\eta(1,t) = W(t) \tag{2.34}$$

where $W(t)$ serves as the intermediate control input. Presuming that solutions exist for the control kernel functions, the intermediate control $W(t)$ can be formulated from (8.17) and (2.34) as

$$\begin{aligned} W(t) = U(t) &- \int_0^1 k(1,y)u(y,t)dy \\ &- \int_0^1 l(1,y)v_0(y,t)dy - \int_0^1 m(1,y)v_1(y,t)dy \end{aligned} \tag{2.35}$$

After a executing a tedious derivation of time and space derivatives from (8.17) and imposing (2.16) and related boundary conditions, one can recover a set of coupled kernel PDEs. However, there is a structure in the kernel equations dependent on the domain. We therefore define $l_f(x,y)$ and $l_b(x,y)$ such that

$$l(x,y) := \begin{cases} l_f(x,y) & 0 \le y \le x \le 1 \\ l_b(x,y) & 0 \le x \le y \le 1 \end{cases} \tag{2.36}$$

and similarly, $m_f(x,y)$ and $m_b(x,y)$ such that

$$m(x,y) := \begin{cases} m_f(x,y) & 0 \le y \le x \le 1 \\ m_b(x,y) & 0 \le x \le y \le 1 \end{cases} \tag{2.37}$$

From here, we can find our coupled kernel PDEs as

$$\partial_x k(x,y) + \partial_y k(x,y) = 0 \tag{2.38}$$

$$k(x,0) = -2\mu^2 m_b(x,0) \tag{2.39}$$

$$\partial_x l_b(x,y) + \mu\partial_y l_b(x,y) = -\int_0^y k(x,z)\frac{q(z)}{2\mu}dz \tag{2.40}$$

$$\partial_x l_f(x,y) + \mu\partial_y l_f(x,y) = \frac{q(x)}{2\mu} - \int_0^x k(x,z)\frac{q(z)}{2\mu}dz \tag{2.41}$$

$$\partial_x m_b(x,y) - \mu\partial_y m_b(x,y) = \int_0^y k(x,z)\frac{q(z)}{2\mu}dz \tag{2.42}$$

$$\partial_x m_f(x,y) - \mu\partial_y m_f(x,y) = -\frac{q(x)}{2\mu} + \int_0^x k(x,z)\frac{q(z)}{2\mu}dz \tag{2.43}$$

$$\partial_x l_b(x,0) = m_b(x,0) \tag{2.44}$$

$$(1-\mu)l_f(x,x) = (1-\mu)l_b(x,x) \tag{2.45}$$

$$l_f(0,y) = 0 \tag{2.46}$$

$$(1+\mu)m_b(x,x) = (1+\mu)m_f(x,x) \tag{2.47}$$

$$m_f(x,1) = -l_f(x,1) \tag{2.48}$$

$$m_f(0,y) = 0 \tag{2.49}$$

The boundary conditions (2.46) and (2.49) are found from enforcing the backstepping transformation (8.17), the target system boundary condition (2.33), and the original system boundary condition (2.12). Note that the continuity of $l(x,y)$ and $m(x,y)$ are enforced by the boundary conditions (2.45) and (2.47), despite their piecewise definitions. However, this does not guarantee the differentiability of $l(x,y)$ and $m(x,y)$ on the entire domain. We will study the well-posedness of this system of coupled PDEs in Section 2.4.

Final derivation to target system

Now we must select $W(t)$ such to derive the final target system. This is relatively straightforward, and follows from the direct solutions of (2.29)-(2.34) found using the method of characteristics. The solutions are

$$\eta(x,t) = W(t-(1-x)) \tag{2.50}$$

$$v_0(x,t) = -v_1(1,t-(1-x)/\mu) \tag{2.51}$$

$$v_1(x,t) = v_0(0,t-x/\mu) - 2\mu\eta(0,t-x/\mu) \tag{2.52}$$

By properly combining the solutions (2.50)-(2.52) with appropriate algebraic manipulation, one can derive a causal representation of $W(t)$ as

$$\begin{aligned} W(t) = \frac{(-1)^N}{2\mu} & v_0(0,t+1-2N/\mu) \\ & + \sum_{k=1}^{N} (-1)^{k+1} W(t-2k/\mu) \end{aligned} \tag{2.53}$$

where the value of $N \in \mathbb{Z}_{\geq 0}$ is the smallest possible integer such that $N \geq \mu/2$.

The control $U(t)$ can then be recovered through combining (2.35) and (2.53).

Theorem 2. *Consider the transformed system* (2.8)-(2.13)*, with admissible initial data* $(u(x,0),v_0(x,0),v_1(x,0))$*. Let N be the smallest integer such that* $N \geq \mu/2$*. The control law can be formulated as*

$$\begin{aligned} U(t) = W(t) & + \int_0^1 k(1,y)u(y,t)dy \\ & + \int_0^1 l(1,y)v_0(y,t)dy + \int_0^1 m(1,y)v_1(y,t)dy, \end{aligned} \tag{2.54}$$

where the function $W(t)$ *is an intermediate control defined by* (2.53)*. Then the equilibrium* $(u,v_0,v_1) = 0$ *is exponentially stable in the* $\mathcal{L}^2$ *sense.*

Proof. The proof is straightforward and follows from the invertibility of (8.17) and Lemma 1. □

2.4 Well-posedness of kernel equations

In this section we study the well-posedness of the kernel equations (2.38)-(2.49).

In general, we consider all potential values of μ, but will show this in two cases ($\mu > 1$ and $\mu < 1$) as the structure of the problem changes depending on the value of μ. For the special case of $\mu = 1$, the PDE system degenerates into a simpler problem which can, in fact, be accounted for in both cases.

The k-system is considered first, and an explicit solution can be found using the method of characteristics as

$$k(x,y) = -2\mu^2 m_b(x-y,0) \tag{2.55}$$

Using this, the kernel equations (2.38)-(2.49) can be reduced to a system of four coupled first-order hyperbolic PDEs.

2.4.1 Solving the kernel equations for $\mu < 1$

We first consider the case of solving the kernel equations for $\mu < 1$. Here, the characteristics of the l_f will intercept the boundary $l_f(x,x)$, which are then transferred into $l_b(x,x)$.

From method of characteristics, we can find the solution of $l_f(x,y)$ in terms of $m_b(x,0)$ as

$$\begin{aligned} l_f(x,y) = &\int_0^x \frac{q(s)}{2\mu} ds \\ &+ \int_0^x \int_0^s \mu m_b(s-z,0) q(z) dz ds \end{aligned} \tag{2.56}$$

This solution gives us $l_f(x,1)$ in terms of $m_b(x,0)$, which is needed to solve the $m_f(x,y)$ system. Moreover, it also gives us $l_b(x,x)$, which in conjunction with the boundary condition $l_b(x,0)$ will give us the solution for $l_b(x,y)$.

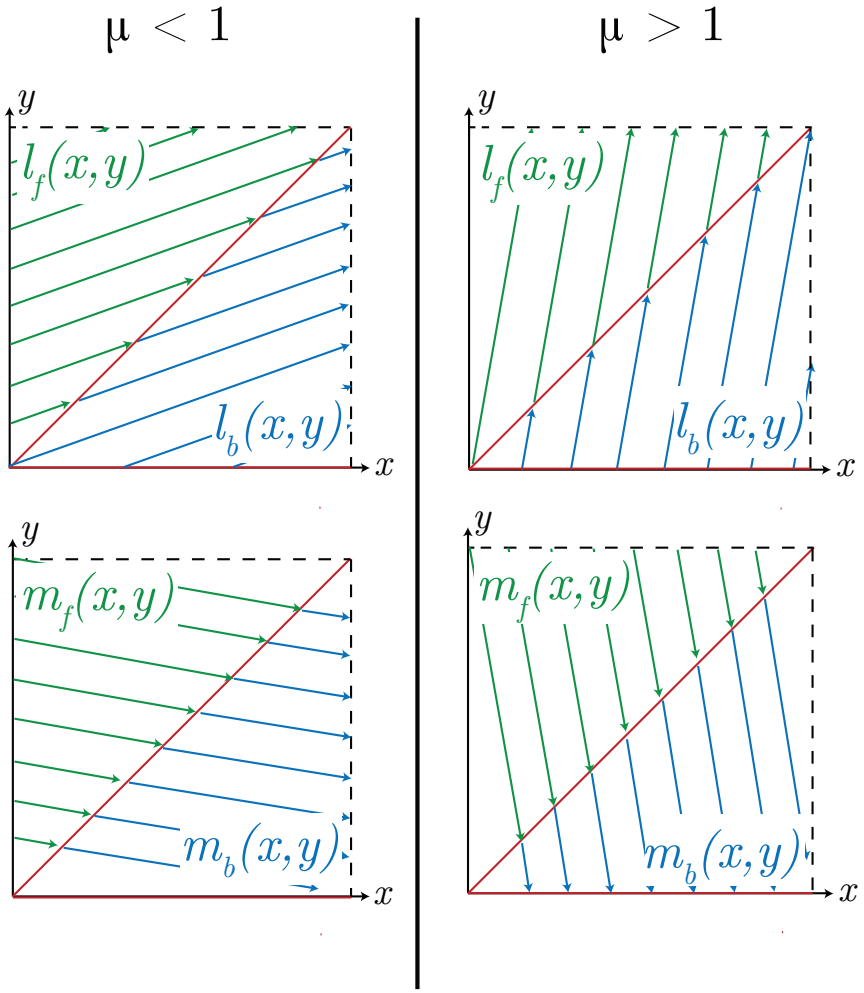

Figure 2.3: Characteristics of **Upper left.** $l(x,y), \mu \leq 1$. **Lower left.** $m(x,y), \mu \leq 1$. **Upper right.** $l(x,y), \mu > 1$. **Lower right.** $m(x,y), \mu > 1$.

Applying method of characteristics to the m_f-system, we find a piecewise solution as

$$m_f(x,y) = \begin{cases} m_{f,1}(x,y) & y > 1-\mu x \\ m_{f,2}(x,y) & y \leq 1-\mu x \end{cases} \tag{2.57}$$

where the functions $m_{f,1}(x,y)$ and $m_{f,2}(x,y)$ are defined by

$$m_{f,1}(x,y) = -l_f\left(\frac{\mu x + y - 1}{\mu}, 1\right) - \int_{\frac{\mu x+y-1}{\mu}}^{x} \frac{q(s)}{2\mu} ds$$

$$- \int_{\frac{\mu x+y-1}{\mu}}^{x} \int_0^s \mu m_b(s-z,0)q(z)dzds \tag{2.58}$$

$$m_{f,2}(x,y) = -\int_0^x \frac{q(s)}{2\mu}ds$$
$$- \int_0^x \int_0^s \mu m_b(s-z,0)q(z)dzds \tag{2.59}$$

From this, one can solve for $m_f(x,x)$ in terms of, which is necessary for solving the m_b-system.

Again, applying the method of characteristics, this time to the m_b-system, the solution $m_b(x,y)$ can be found.

$$m_b(x,y) = m_f\left(\frac{\mu x+y}{\mu+1}, \frac{\mu x+y}{\mu+1}\right)$$
$$- \int_{\frac{\mu x+y}{\mu+1}}^{x} \int_0^{-\mu s+\mu x+y} \mu m_b(s-z,0)q(z)dzds \tag{2.60}$$

By evaluating (2.60) at $y = 0$, we can establish an integral equation in which to solve for $m_b(x,0)$, which is essential for the gain kernels.

$$m_b(x,0) = m_f\left(\frac{\mu x}{\mu+1}, \frac{\mu x}{\mu+1}\right)$$
$$- \int_{\frac{\mu x}{\mu+1}}^{x} \int_0^{\mu(x-s)} \mu m_b(s-z,0)q(z)dzds \tag{2.61}$$

From here, one can note that since $\mu < 1$, the condition $m_f\left(\frac{\mu x}{\mu+1}, \frac{\mu x}{\mu+1}\right) = m_{f,2}\left(\frac{\mu x}{\mu+1}, \frac{\mu x}{\mu+1}\right)$, and therefore the explicit form of the integral equation (2.61) is

$$m_b(x,0) = -\int_0^{\frac{\mu x}{\mu+1}} \frac{q(s)}{2\mu}ds$$
$$- \int_0^{\frac{\mu x}{\mu+1}} \int_0^s \mu m_b(s-z,0)q(z)dzds$$
$$- \int_{\frac{\mu x}{\mu+1}}^{x} \int_0^{\mu(x-s)} \mu m_b(s-z,0)q(z)dzds \tag{2.62}$$

For simplicity, let $\varepsilon = \mu/(1+\mu)$. To solve (2.62), we wil apply the method of successive

approximations. Consider some sequence $\{m_k(x)\}_{k=0}^{k=\infty}$ defined by

$$\begin{aligned} m_k(x) = &-\int_0^{\varepsilon x} \frac{q(x)}{2\mu} ds \\ &-\int_0^{\varepsilon x}\int_0^{s} \mu m_{k-1}(s-z)q(z)dzds \\ &-\int_{\varepsilon x}^{x}\int_0^{\mu(x-s)} \mu m_{k-1}(s-z)q(z)dzds \end{aligned} \tag{2.63}$$

If $m_k(x)$ converges, we can see that $m_k(x) \to m_b(x,0)$. We can define a difference $\Delta m_k(x) := m_{k+1}(x) - m_k(x)$, which admits an update equation

$$\begin{aligned} \Delta m_k(x) = &-\int_0^{\varepsilon x}\int_0^{s} \mu \Delta m_{k-1}(s-z)q(z)dzds \\ &-\int_{\varepsilon x}^{x}\int_0^{\mu(x-s)} \mu \Delta m_{k-1}(s-z)q(z)dzds \end{aligned} \tag{2.64}$$

and also the relation

$$m_b(x,0) = m_0(x) + \sum_{k=0}^{\infty} \Delta m_k(x) \tag{2.65}$$

We now study $|\Delta m_k(x)|$, and its growth with respect to k. Let $m_0(x) = 0$. As one begins computing successive bounds, a general representation can be found as

$$|\Delta m_k(x)| \leq \frac{\varepsilon \mu^k Q^{k+1}}{(2k+1)!} x^{2k+1} \tag{2.66}$$

where $Q = \max |q(x)|$.

We can then conclude uniform convergence of the sum in (2.65) through the Weierstrass M-test, and therefore existence and uniqueness of $m_b(x,0)$ can be concluded. It is straightforward to substitute $m_b(x,0)$ back into derived expressions for $m_b(x,y), m_f(x,y), l_f(x,y)$ to find the respective gain kernels. The derivation of $l_b(x,y)$ is likewise straightforward and is omitted for

space.

2.4.2 Solving the kernel equations for $\mu > 1$

Solving the kernel equations for the $\mu > 1$ case is somewhat similar to that of $\mu < 1$, but with some subtle differences in how the boundary conditions are utilized.

We first solve the l_b-system in terms of $m_b(x,0)$.

$$\begin{aligned} l_b(x,y) &= m_b\left(\frac{\mu x - y}{\mu}, 0\right) \\ &\quad + \int_{\frac{\mu x - y}{\mu - 1}}^{x} \int_0^{\mu s - \mu x + y} \mu m_b(s - z, 0) q(z) dz ds \end{aligned} \tag{2.67}$$

Next we solve the l_f-system with two boundary conditions $l_f(0,y)$ and $l_f(x,x)$.

$$l_f(x,y) = \begin{cases} l_{f,1}(x,y) & y > \mu x \\ l_{f,2}(x,y) & y \leq \mu x \end{cases} \tag{2.68}$$

where $l_{f,1}, l_{f,2}$ are given by

$$\begin{aligned} l_{f,1}(x,y) &= \int_0^x \frac{q(s)}{2\mu} ds \\ &\quad + \int_0^x \int_0^s \mu m_b(s - z, 0) q(z) dz ds \end{aligned} \tag{2.69}$$

$$\begin{aligned} l_{f,2}(x,y) &= l_b\left(\frac{\mu x - y}{\mu - 1}, \frac{\mu x - y}{\mu - 1}\right) + \int_{\frac{\mu x - y}{\mu - 1}}^{x} \frac{q(s)}{2\mu} ds \\ &\quad + \int_{\frac{\mu x - y}{\mu - 1}}^{x} \int_0^s \mu m_b(s - z, 0) q(z) dz ds \end{aligned} \tag{2.70}$$

Following, we solve the m_f-system, which like the l_f-system will be piecewise defined,

considering the boundary conditions $m_f(0,y)$ and $m_f(x,1)$.

$$m_f(x,y) = \begin{cases} m_{f,1}(x,y) & y > 1-\mu x \\ m_{f,2}(x,y) & y \le 1-\mu x \end{cases} \tag{2.71}$$

where $m_{f,1}$ and $m_{f,2}$ are defined as

$$\begin{aligned} m_{f,1}(x,y) &= -l_f\left(\frac{\mu x+y-1}{\mu},1\right) - \int_{\frac{\mu x+y-1}{\mu}}^{x} \frac{q(s)}{2\mu} ds \\ &\quad - \int_{\frac{\mu x+y-1}{\mu}}^{x} \int_0^s \mu m_b(s-z,0) q(z) dz ds \end{aligned} \tag{2.72}$$

$$\begin{aligned} m_{f,2}(x,y) &= -\int_0^x \frac{q(s)}{2\mu} ds \\ &\quad - \int_0^x \int_0^s \mu m_b(s-z,0) q(z) dz ds \end{aligned} \tag{2.73}$$

Finally, we can derive the solution $m_b(x,y)$ in terms of $m_b(x,0)$, which will admit an integral equation.

$$\begin{aligned} m_b(x,y) &= -\int_{\frac{\mu x+y}{\mu+1}}^{x} \int_0^{-\mu s+\mu x+y} \mu m_b(s-z,0) q(z) dz ds \\ &\quad + m_f\left(\frac{\mu x+y}{\mu+1}, \frac{\mu x+y}{\mu+1}\right) \end{aligned} \tag{2.74}$$

By combining all the solutions and evaluating $m_b(x,0)$, the integral equation can be (piecewise) defined as

$$m_b(x,0) = \begin{cases} m_{b,1}(x,0) & x \le \frac{2}{\mu} \\ m_{b,2}(x,0) & x > \frac{2}{\mu} \end{cases} \tag{2.75}$$

where $m_{b,1}$ and $m_{b,2}$ are defined by below. For simplicty of notation, $\varepsilon := \mu/(1+\mu)$.

$$m_{b,1}(x,0) = -\int_0^{\varepsilon x} \frac{q(s)}{2\mu} ds$$

$$
\begin{aligned}
&- \int_0^{\varepsilon x} \int_0^s \mu m_b(s-z,0) q(z) dz ds \\
&- \int_{\varepsilon x}^{x} \int_0^{\mu(x-s)} \mu m_b(s-z,0) q(z) dz ds \qquad (2.76)
\end{aligned}
$$

$$
\begin{aligned}
m_{b,2}(x,0) = &- m_b(x-2/\mu,0) - \int_{\frac{\mu x-2}{\mu-1}}^{\varepsilon x} \frac{q(s)}{2\mu} ds \\
&- \int_{\frac{\mu x-2}{\mu}}^{\frac{\mu x-2}{\mu-1}} \int_0^{\mu s-\mu x+2} \mu m_b(s-z,0) q(z) dz ds \\
&- \int_{\frac{\mu x-2}{\mu-1}}^{\varepsilon x} \int_0^s \mu m_b(s-z,0) q(z) dz ds \\
&- \int_{\varepsilon x}^{x} \int_0^{\mu(x-s)} \mu m_b(s-z,0) q(z) dz ds \qquad (2.77)
\end{aligned}
$$

To prove existence and uniqueness for the system of kernel equations, it is sufficient to show that the the integral equations given by (2.76) and (2.77) have solutions.

The case for $m_{b,1}$ is identical to solving $m_b(x,0)$ in the $\mu < 1$ case, and therefore will be omitted. The case for $m_{b,2}$, however, must be proven through induction.

We will illustrate that $m_{2,b}$ has a solution through the method of successive approximations. To do this, we consider solving iteratively, where domains of length $2/\mu$ are considered in turn.

Let $i \in \{1,...,N\}$, where N is the smallest integer such that $N \geq \mu/2 - 1$. We now consider the domain $I_i = [2i/\mu, \min\{2(i+1)/\mu, 1\}]$, where the minimum is utilized for the corner case $i = N$. First, from (90) we derive an iterating equation

$$
\begin{aligned}
m_{k+1}(x) = &- m_b(x-2/\mu,0) - \int_{\frac{\mu x-2}{\mu-1}}^{\varepsilon x} \frac{q(s)}{2\mu} ds \\
&- \int_{\frac{\mu x-2}{\mu}}^{\frac{\mu x-2}{\mu-1}} \int_0^{\mu s-\mu x+2} \mu m_k(s-z) q(z) dz ds \\
&- \int_{\frac{\mu x-2}{\mu-1}}^{\varepsilon x} \int_0^s \mu m_k(s-z) q(z) dz ds \\
&- \int_{\varepsilon x}^{x} \int_0^{\mu(x-s)} \mu m_k(s-z) q(z) dz ds \qquad (2.78)
\end{aligned}
$$

where if m_k converges in the domain I, it will converge to the true value $m_b(x,0)$ in I. Note

that the term $m_b(x-2/\mu,0)$ already references the well-posedness of m_b, however, containing values on the previous domain I_{i-1}. This is the reason for solving on successive intervals - we are presented with a base case defined by $m_{b,1}$ (already shown to be well-posed), and iterate forward in x.

One can then define a successive difference $\Delta m_k(x) := m_{k+1}(x) - m_k(x)$, which admits an update equation

$$\begin{aligned}\Delta m_k(x) = &-\int_{\frac{\mu x-2}{\mu-1}}^{\frac{\mu x-2}{\mu}} \int_0^{\mu s-\mu x+2} \mu \Delta m_{k-1}(s-z)q(z)dzds \\ &-\int_{\frac{\mu x-2}{\mu-1}}^{\varepsilon x} \int_0^{s} \mu \Delta m_{k-1}(s-z)q(z)dzds \\ &-\int_{\varepsilon x}^{x} \int_0^{\mu(x-s)} \mu \Delta m_{k-1}(s-z)q(z)dzds \end{aligned} \tag{2.79}$$

and assuming that the sequence $m_k(x)$ converges, the function $m_b(x,0)$ on the domain I_i can be written as

$$m_b(x,0) = m_0(x) + \sum_{k=0}^{\infty} \Delta m_k(x), x \in I_i \tag{2.80}$$

Much like the $\mu < 1$ case, instead of studying the convergence of this sequence we will study $|\Delta m_k(x)|$. Then by selecting $m_0(x) = 0$ and computing several successive approximations, we arrive at the bound

$$|\Delta m_k(x)| \leq \frac{(2\mu Q)^k}{(2k)!} M_{i-1} x^{2k} + \frac{\varepsilon (2\mu)^{k-1} Q^{k+1}}{(2k+1)!} x^{2k+1} \tag{2.81}$$

where M_i is defined by $\max |m_b(x,0)| < M_i, x \in I_i$, and $Q = \max |q(x)|$.

Again, by the Weierstrass M-test one can see that for every $i \in \{1,...,N\}$, the summation in (2.80) will converge uniformly, guaranteeing existence and uniqueness of $m_b(x,0)$. Much like the $\mu < 1$ case, it is straightforward to substitute $m_b(x,0)$ and find the solution for all gain kernels.

2.5 Conclusion

A two-part controller is developed for the coupled transport-wave PDE system, in two distinct cases where the transport delay is short when compared to the wave speed ($\mu < 1$), and when the transport delay is long ($\mu > 1$). An extended backstepping transformation is utilized, where Fredholm integrals (as opposed to Volterra) are now required. The gain kernels are solved through exploiting the reflections in the kernel domains to derive an integral equation.

Ongoing work involves developing a state estimation algorithm. In the physical application to extreme ultraviolet light generation, the system is not only underactuated, but also undersensed, leading to additional complexity. Thus, a straightforward backstepping based observer is not feasible, and a novel design must be considered that exploits the system structure.

2.6 Acknowledgements

Chapter 2, in part, is a reprint of the material as it appears in: S.Chen, R. Vazquez, M. Krstic. Stabilization of an Underactuated Coupled Transport-Wave PDE System. American Control Conference, 2017. The dissertation author was the primary investigator and co-author of this paper.

Chapter 3

Heat-transport

3.1 Introduction

The control of coupled partial differential equation systems has developed in great leaps recently, in scenarios involving both boundary and interior coupling structures. This innovation, in part, is due to coupled PDE systems arising naturally in various physical engineering processes such as oil well drilling, biological reactors, extreme ultraviolet lithography (EUV) for semiconductor manufacturing, and more.

Previous work in coupled PDEs has investigated various coupling structures. Almost all of these results involve PDEs of the same class, or of PDE-ODE type (a specific boundary-coupled case). The results for interior-coupled systems explore only the coupling of systems of the same class [25],[32],[45]. For a mixed class system, only a single existing result for a boundary coupled case exists [28]. However, an interior-coupled mixed class had never been explored prior, which this paper will investigate.

The work in this paper was motivated from the authors' previous work in a coupled transport-wave PDE system [13]. It should be noted that the approach applied is very similar, however, the most distinct difference lies in the derivation of the solutions of the gain kernels

involved. Results also exist for the cascade of a hyperbolic-parabolic PDE system in [28], which is very similar but lacks interior coupling. The result in this paper sits naturally between the two aforementioned cases. Both this paper and [45] explore and illustrate the wide applicability of the backstepping control methodology for PDEs across various coupled and mixed class systems.

The notion of a mixed class interior coupled PDE system can be quite difficult to work with theoretically. It is well known that many PDE tools can only be used in the context of a single class, thus making it quite surprising that a tool like backstepping can be applied across different classes. However, depending on the mixed class interior coupled systems in question, certain coupling topologies can be quite difficult to tackle — this paper being a prime example. The coupling in one direction (the one authors have considered) is considerably more tractable than the case where the coupling runs opposite.

The study of a hyperbolic-parabolic mixed class coupled PDE system are naturally motivated by physical problems which include biological chemotaxis (such as tumor and fungal growth), predator-prey population models, and EUV lithography. In particular, a particular part of EUV lithography involves a liquid metal droplet stream convecting through plasma, modeled with a first-order hyperbolic PDE. The plasma, which influences the droplet stream, will diffuse in space, which is modeled using a parabolic PDE, giving arise to the coupled hyperbolic-parabolic mixed-type PDE system [46].

The paper is structured as follows: Section 3.2 establishes the model, Section 3.3 designs the control and proves its exponentially stabilizing property, Section 3.4 explores the existence of a stablizing gain function, and finally Section 3.5 illustrates the effectiveness of the control design through simulation.

3.2 Model

The model under consideration is given below:

$$\partial_t v(x,t) = \varepsilon \partial_x^2 v(x,t) + \lambda v(x,t) \tag{3.1}$$

$$\partial_t u(x,t) = \partial_x u(x,t) + \int_0^x q(x,y) v(y,t) dy \tag{3.2}$$

$$\partial_x v(0,t) = u(0,t) \tag{3.3}$$

$$v(1,t) = 0 \tag{3.4}$$

$$u(1,t) = U(t) \text{ — control} \tag{3.5}$$

The controlled PDE is the transport system u, which convects leftward. The outflow of the transport system drives an unstable (for $\lambda > 0$) reaction-diffusion system as a boundary source. The function $q(x,y)$ represents the coupling kernel, and is assumed to be sufficiently smooth. A schematic representation can be found in Fig. 3.1.

In general, (3.1) can be taken to be any unstable parabolic PDE of the form:

$$\begin{aligned} \partial_t v(x,t) = \varepsilon \partial_x^2 v(x,t) + \sigma(x) \partial_x v(x,t) + \lambda(x) v(x,t) \\ + g(x) v(1,t) + \int_x^1 f(x,y) v(y,t) dy \end{aligned} \tag{3.6}$$

The extension to (3.6) is straightforward, and uses theory developed in [35],[30].

3.3 Control design

A target system is chosen as

$$\partial_t \eta(x,t) = \varepsilon \partial_x^2 \eta(x,t) - c\eta(x,t) \tag{3.7}$$

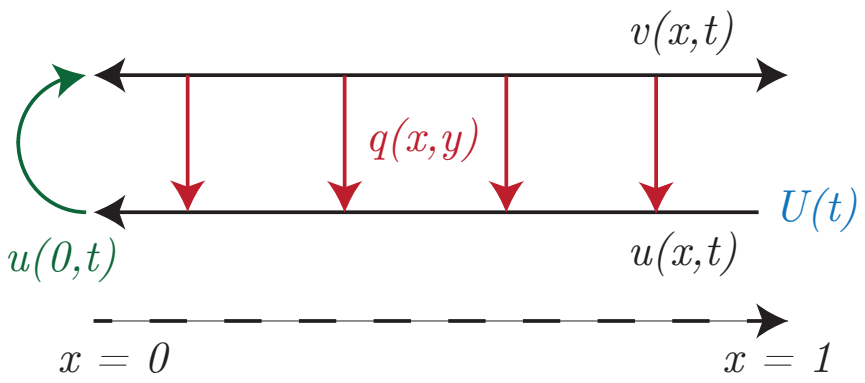

Figure 3.1: A schematic view of the plant.

$$\partial_t \omega(x,t) = \partial_x \omega(x,t) \tag{3.8}$$

$$\partial_x \eta(0,t) = \omega(0,t) \tag{3.9}$$

$$\eta(1,t) = 0 \tag{3.10}$$

$$\omega(1,t) = 0 \tag{3.11}$$

where $c > 0$. Corresponding backstepping transformations for $u \leftrightarrow \omega$ and $v \leftrightarrow \eta$ are formulated as:

$$\eta(x,t) = v(x,t) - \int_x^1 p(x,y)v(y,t)dy \tag{3.12}$$

$$\omega(x,t) = u(x,t) - \int_0^x k(x,y)u(y,t)dy - \int_0^1 l(x,y)v(y,t)dy \tag{3.13}$$

A special note should be made about transformation (8.41). (8.41) is a *Volterra* type transformation. The terms involving $u(x,t)$ and $w(x,t)$ involve only a Volterra integral, while the Fredholm integral in $v(x,t)$ is seen as an "affine" relationship. The only condition we require for invertibility then is the existence of kernels p,k,l of sufficient regularity. This inverse transformation is critical for the proof of stability.

Theorem 3. *Consider the plant model* (3.1)-(3.5) *with the controller*

$$U(t) = \int_0^1 k(1,y)u(y,t)dy + \int_0^1 l(1,y)v(y,t)dy \tag{3.14}$$

$k : [0,1] \times [0,x] \to \mathbb{R}$ *and* $l : [0,1] \times [0,1] \to \mathbb{R}$ *are the solutions of the following coupled hyperbolic-parabolic PDE system:*

$$\partial_x k(x,y) = -\partial_y k(x,y) \tag{3.15}$$

$$k(x,0) = \varepsilon \partial_y l(x,0) \tag{3.16}$$

$$\partial_x l(x,y) = \varepsilon \partial_y^2 l(x,y) + \lambda l(x,y) - F[k](x,y) \tag{3.17}$$

$$\partial_y l(x,0) = 0 \tag{3.18}$$

$$l(x,1) = 0 \tag{3.19}$$

$$l(0,y) = p(0,y) \tag{3.20}$$

where the operator F *is a piecewise defined as*

$$F[k](x,y) = \begin{cases} q(x,y) - \int_y^x k(x,z)q(z,y)dz & y \leq x \\ 0 & \textit{otherwise} \end{cases} \tag{3.21}$$

and $p : [0,1] \times [x,1] \to \mathbb{R}$ *is the solution of the Goursat-type problem*

$$\partial_x^2 p(x,y) - \partial_y^2 p(x,y) = \frac{\lambda + c}{\varepsilon} p(x,y) \tag{3.22}$$

$$p(x,1) = 0 \tag{3.23}$$

$$p(x,x) = \frac{\lambda + c}{2\varepsilon}(x-1) \tag{3.24}$$

Assume arbitrary initial conditions $(u(x,0), v(x,0))$ *compatible with the boundary conditions*

(3.3), (3.4). *Then the closed-loop system is exponentially stable in the* $L^2 \times H^1$ *sense.*

We will prove Theorem 3 in several parts.

3.3.1 Stability analysis for target system

It is relatively easy to see intuitively that the target system (3.7)-(3.11) is exponentially stable — a finite-time stable system ω cascades into the exponentially stable reaction-diffusion equation η (for $c > 0$). The primary difficulty here is in necessitating a higher-order norm in ω—we can only establish stability in the $L^2 \times H^1$ norm.

We first transform the target system into an intermediate form using the following transformation:

$$\zeta(x,t) = \eta(x,t) - (x-1)\omega(0,t) \tag{3.25}$$

By introducing this transformation, we can derive an equivalent target system in (z, ω).

$$\begin{aligned} \partial_t \zeta(x,t) &= \varepsilon \partial_x^2 \zeta(x,t) - c\zeta(x,t) \\ &\quad + (x-1)(c\omega(0,t) - \partial_t \omega(0,t)) \end{aligned} \tag{3.26}$$

$$\partial_t \omega(x,t) = \partial_x \omega(x,t) \tag{3.27}$$

$$\partial_x \zeta(0,t) = 0 \tag{3.28}$$

$$\zeta(1,t) = 0 \tag{3.29}$$

$$\omega(1,t) = 0 \tag{3.30}$$

Lemma 4. *Consider the transformed target system* (3.26)-(3.30) *with arbitrary intial conditions* $(\zeta(x,0), \omega(x,0))$. *Then the equilibrium* $(\zeta, \omega) = 0$ *is exponentially stable in the* $L^2 \times H^1$ *sense.*

Proof. By choosing a Lyapunov function $W(t)$ as

$$W(t) = \frac{1}{2}\int_0^1 \zeta(x,t)^2 dx + \frac{c}{2}\int_0^1 e^{ax}\omega(x,t)^2 dx + \frac{\delta}{2}\int_0^1 e^{bx}\omega_x(x,t)^2 dx \tag{3.31}$$

for $a, b, \delta > 0$ we can prove exponential stability of the transformed target system.

Differentiating (3.31) in time and integrating by parts, we can arrive at

$$\begin{aligned}\dot{W}(t) = &-\varepsilon ||\zeta_x||_{L^2}^2 - c||\zeta||_{L^2}^2 \\ &+ \int_0^1 \zeta(x,t)(x-1)\left(c\omega(0,t) - \partial_x\omega(0,t)\right)dx \\ &- \frac{c}{2}\omega(0,t)^2 - \frac{ac}{2}\int_0^1 e^{ax}\omega(x,t)^2 dx - \frac{\delta}{2}\partial_x\omega(0,t)^2 \\ &- \frac{\delta b}{2}\int_0^1 e^{bx}\partial_x\omega(x,t)^2 dx\end{aligned} \tag{3.32}$$

Applying the Wirtinger inequality [21],

$$\begin{aligned}\dot{W}(t) = &-\left(\varepsilon\frac{\pi^2}{4} - c\right)||\zeta||_{L^2}^2 \\ &+ \int_0^1 \zeta(x,t)(x-1)\left(c\omega(0,t) - \partial_x\omega(0,t)\right)dx \\ &- \frac{c}{2}\omega(0,t)^2 - \frac{ac}{2}\int_0^1 e^{ax}\omega(x,t)^2 dx - \frac{\delta}{2}\partial_x\omega(0,t)^2 \\ &- \frac{\delta b}{2}\int_0^1 e^{bx}\omega_x(x,t)^2 dx\end{aligned} \tag{3.33}$$

Then applying Young's inequality [30] twice, we can arrive at the following expression:

$$\begin{aligned}\dot{W}(t) \leq &-\left(\frac{\varepsilon\pi^2}{4} - \frac{1}{2\gamma}\right)||\zeta||_{L^2}^2 - \frac{5c}{12}\omega(0,t)^2 \\ &- \left(\frac{\delta}{2} - \frac{\gamma}{2}\right)\partial_x\omega(0,t)^2 - \frac{ac}{2}\int_0^1 e^{ax}\omega(x,t)^2 dx\end{aligned}$$

$$-\frac{\delta b}{2}\int_0^1 e^{bx}\partial_x\omega(x,t)^2dx \tag{3.34}$$

where $\gamma > 0$ is a constant to be chosen, arising from one application of Young's inequality. We can note that by selecting $\gamma > 2/(\varepsilon\pi^2)$ and choosing $\delta \geq \gamma$, we can derive a bound that will allow us to prove exponential stability. By doing so, we can further bound $\dot{W}(t)$ by

$$\dot{W}(t) \leq -\min\left\{\frac{\varepsilon\pi^2}{2} - \frac{1}{\gamma}, a, b\right\} W(t) \tag{3.35}$$

From the comparison principle, we can conclude

$$W(t) \leq e^{C(t-t_0)}W(t_0) \tag{3.36}$$

where $C := \left\{\frac{\varepsilon\pi^2}{2} - \frac{1}{\gamma}, a, b\right\}$. Thus, we can conclude exponential stability in the $L^2 \times H^1$ norm. □

Lemma 5. *Consider a Lyapunov function $V(t)$ for the system (η, ω), defined by*

$$V(t) = \frac{1}{2}\int_0^1 \eta(x,t)^2dx + \frac{1}{2}\int_0^1 \partial_x\omega(x,t)^2dx \tag{3.37}$$

Then there exist constants $C_1, C_2 > 0$ such that

$$C_1V(t) \leq W(t) \leq C_2V(t) \tag{3.38}$$

Proof. The lemma follows from expansion and direct application of Cauchy and Agmon inequalities. □

Lemma 6. *Consider the target system* (3.7)-(3.11) *with arbitrary initial conditions $(\eta(x,0), \omega(x,0))$, subject to compatibility conditions. Then the equlibrium (η, ω) is exponentially stable in the $L^2 \times H^1$ sense.*

Proof. From Lemma 4, we have the exponential stability bound

$$W(t) \leq e^{C(t-t_0)} W(t_0) \tag{3.39}$$

By employing Lemma 5 twice, we can transform the bound to be in terms of $V(t)$, and therefore conclude exponential stability in $L^2 \times H^1$.

$$V(t) \leq \frac{C_2}{C_1} e^{C(t-t_0)} V(t_0) \tag{3.40}$$

This concludes the proof. □

3.3.2 Backstepping transformation and gain kernel derivations

Differentiating (3.12) in time once and integrating by parts admits

$$\begin{aligned}
\partial_t \eta(x,t) = {} & \varepsilon \partial_x^2 v(x,t) + \lambda v(x,t) - \varepsilon p(x,1) \partial_x v(1,t) \\
& + \varepsilon p(x,y) \partial_x v(x,t) + \varepsilon \partial_y p(x,1) v(1,t) \\
& - \varepsilon \partial_y p(x,y) v(x,t) - \int_x^1 \varepsilon \partial_y^2 p(x,y) v(y,t) dy \\
& - \int_x^1 \lambda p(x,y) v(y,t) dy
\end{aligned} \tag{3.41}$$

Differentiating (3.12) twice in time gives

$$\begin{aligned}
\partial_x^2 \eta(x,t) = {} & \partial_x^2 v(x,t) + \frac{d}{dx}[p(x,x)] v(x,t) + p(x,x) \partial_x v(x,t) \\
& + \partial_x p(x,x) v(x,t) - \int_x^1 \partial_x^2 p(x,y) v(y,t) dy
\end{aligned} \tag{3.42}$$

From enforcing (3.7) with the relevant boundary conditions, we can derive conditions that comprise the PDE given by (3.22)-(3.24). From [30], we know an explicit form of p can be found

as

$$p(x,y) = -(\lambda + c)(1-y)\frac{I_1(z)}{z} \tag{3.43}$$

$$z = \sqrt{(\lambda + c)((1-x)^2 - (1-y^2))} \tag{3.44}$$

where I_1 denotes a modified Bessel function of the first kind.

Utilizing a similar approach as above, we differentiate (8.41) once in time and integrate by parts to find

$$\begin{aligned}
\partial_t \omega(x,t) = \partial_x u(x,t) &+ \int_0^x q(x,y)v(y,t) - k(x,x)u(x,t) \\
&+ k(x,0)u(0,t) + \int_0^x \partial_y k(x,y)u(y,t)dy \\
&- \int_0^x k(x,y)\int_0^y q(y,z)v(z,t)dzdy \\
&- \varepsilon l(x,1)\partial_x v(1,t) + \varepsilon l(x,0)\partial_x v(0,t) \\
&+ \varepsilon \partial_y l(x,1)v(1,t) - \varepsilon \partial_y l(x,0)v(0,t) \\
&- \int_0^1 \varepsilon \partial_y^2 l(x,y)v(y,t)dy - \int_0^1 \lambda l(x,y)v(y,t)dy
\end{aligned} \tag{3.45}$$

Differentiating (8.41) once in space admits

$$\begin{aligned}
\omega_x(x,t) = u_x(x,t) &+ k(x,x)u(x,t) \\
&- \int_0^x \partial_x k(x,y)u(y,t)dy - \int_0^1 \partial_x l(x,y)v(y,t)dy
\end{aligned} \tag{3.46}$$

Enforcing (3.8) with the relevant boundary conditions will allow us to derive the conditions that comprise the coupled hyperbolic-parabolic PDE system (3.15)-(3.20). This PDE in general will not have an explicit solution, but under the assumption that it is well-posed (to be studied in Section 3.4), numerical methods can yield a sufficiently accurate solution. It is also good to

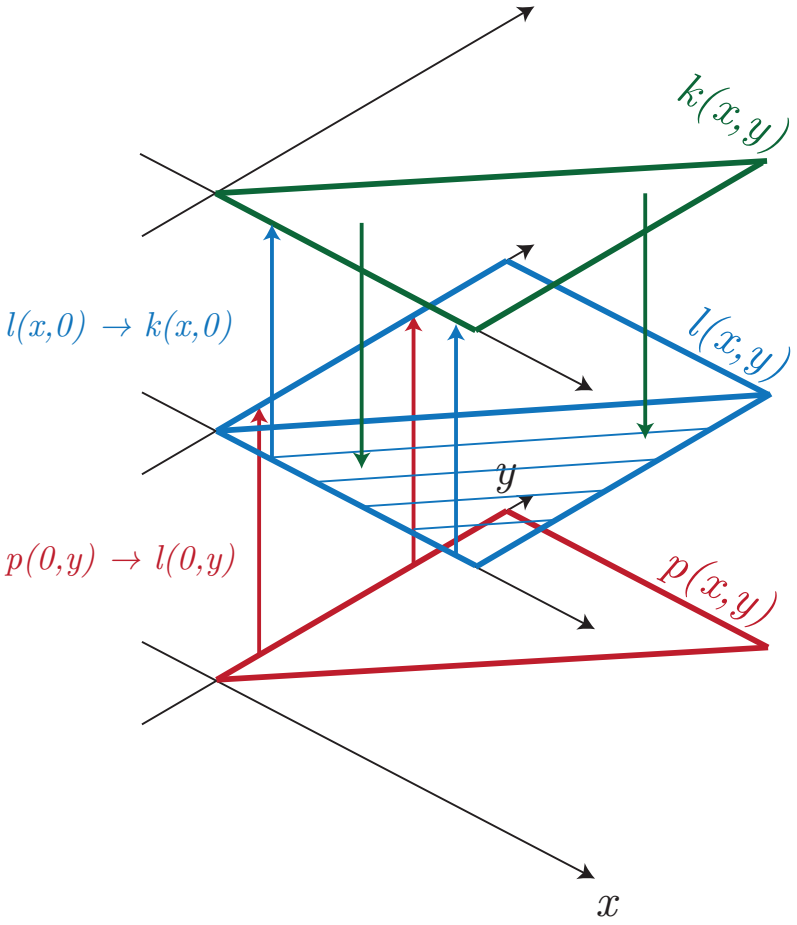

Figure 3.2: Domains and coupling structure of $p(x,y)$ (red), $l(x,y)$ (blue), and $k(x,y)$ (green)

note that we merely require *existence* of a solution and not necessarily uniqueness — as long as the solution fulfills the conditions prescribed, then the target system and original system are equivalent.

With this, we are now equipped to prove Theorem 3.

Proof of Theorem 3. First, we assume that the initial conditions of the target system 3.7-3.11 meet the proper compatibility conditions.

Consider the Lyapunov function

$$\Omega(t) = \frac{1}{2}\int_0^1 [u(x,t)^2 + \partial_x u(x,t)^2 + v(x,t)^2]dx \tag{3.47}$$

Using the inverse transformations (3.12) and (8.41) (which are guaranteed to exist given sufficient regularity of the gain kernels), Young's inequality, and boundedness of the inverse gain kernels we can arrive at the relation

$$||(u,v)||^2 \leq C_3 ||(\eta,\omega)||^2, \quad C_3 > 0 \tag{3.48}$$

Similarly, by considering first the Lyapunov function $V(t)$ defined in (3.37), and using the forward transformations (3.12) and (8.41) with the boundedness of the gain kernels, we can derive

$$||(\eta,\omega)||^2 \leq C_4 ||(u,v)||^2, \quad C_4 > 0 \tag{3.49}$$

Then, from Lemma 6, there exists $a, M_1 > 0$ such that

$$||(\eta,\omega)|| \leq M_1 e^{a(t-t_0)} ||(\eta_0,\omega_0)|| \tag{3.50}$$

By applying (3.48), (3.49), we can finally conclude

$$||(u,v)|| \leq M_2 e^{a(t-t_0)} ||(u_0,v_0)|| \tag{3.51}$$

for some $M_2 > 0$, thus implying exponential stability in the original system. □

3.4 Existence of solutions k, l for the gain kernel PDE system

The first-order hyperbolic PDE for k ((3.15),(3.16)) can be explicitly solved as a function of l as

$$k(x,y) = \varepsilon l(x-y,0) \tag{3.52}$$

Then, showing the existence of gain kernel l is sufficient to show that both k, l exist.

To show the existence of a weak solution, we must first investigate a priori estimates (energy estimates). The interpretation of this a priori estimate is a bound on the solution purely dependent on the nonhomogeneous forcing and initial condition. The result is stated in the following lemma:

Lemma 7 (A priori estimates)**.** *For the system of gain kernel PDEs* (3.15)-(3.21) *and* (3.52)*, one can establish the following $L^2(0,1;H^1)$ a priori estimate on l:*

$$\max_{s\in[0,x]} ||l||_{H^1} + ||l||_{L^2}(0,x;H^1) \leq K(Q, ||p(0,y)||_{H^1}) \tag{3.53}$$

where $Q = ||q||_{L^2(0,1;H^2)}$, and $K : \mathbb{R}_+ \times \mathbb{R}_+ \to \mathbb{R}_+$.

Proof. To begin establishing the energy estimate, we first begin by multiplying (3.17) by $l(x,y)$ and integrating over y. Integrating by parts, and applying Young's inequality several times admits

$$\begin{aligned}\frac{d}{dx}||l||_{L^2}^2 \leq \left(2\lambda + 1 - \frac{\varepsilon}{2}\right)||l||_{L^2}^2 + Q^2 \\ + \varepsilon Q(||l||_{L^2}^2 + \max_{s\in[0,x]} ||l(s)||_{H^1}^2)\end{aligned} \tag{3.54}$$

Next, we differentiate (3.17) once in y, multiply by $l_y(x,y)$, and integrate over y. Following a similar procedure to before, we find

$$\frac{d}{dx}||\partial_y l||_{L^2}^2 \leq \left(2\lambda + 1 - \frac{\varepsilon}{2}\right)||\partial_y l||_{L^2}^2 + Q^2$$

$$+2\varepsilon Q\,||l||_{H^1}^2$$
$$+\varepsilon Q(||l||_{L^2}^2+\max_{s\in[0,x]}||l(s)||_{H^1}^2) \tag{3.55}$$

Combining (3.54),(3.55), and rewriting everything in terms of the highest norms, we arrive at

$$\frac{d}{dx}||l||_{H^1}^2 \leq \left(2\lambda+1-\frac{\varepsilon}{2}+4\varepsilon Q\right)||l||_{H^1}^2$$
$$+2\varepsilon Q\max_{s\in[0,x]}||l(s)||_{H^1}^2+2Q^2 \tag{3.56}$$

To deal with this type of differential inequality, we consider two separate cases – the increasing and decreasing cases (the constant case falls naturally between the two, and is actually trivial). It is important to note that the choice of the case is purely dependent on the parameters $\lambda,\varepsilon,q(x,y)$, which has no effect on the condition of continuous dependence on initial data $l(0,y)$. For the increasing case, we can make note that $\max_{s\in[0,x]}||l(s)||_{H^1}^2=||l(x)||_{H^1}^2$. Thus, (3.56) becomes

$$\frac{d}{dx}||l||_{H^1}^2 \leq \left(2\lambda+1-\frac{\varepsilon}{2}+6\varepsilon Q\right)||l||_{H^1}^2$$
$$+2Q^2 \tag{3.57}$$

which allows us, by the comparison principle, to derive the following H^1 spatial bound on l:

$$||l||_{H^1}^2 \leq \exp\left((2\lambda+1-\frac{\varepsilon}{2}+6\varepsilon Q)x\right)||l(0)||_{H^1}^2$$
$$+\int_0^x \exp\left((2\lambda+1-\frac{\varepsilon}{2}+6\varepsilon Q)(x-z)\right)2Q^2dz \tag{3.58}$$

Noting that $x\in[0,1]$, and $l(0,y)=p(0,y)$ one can certainly find the existence of a function K such that (3.53) is fulfilled for all x. We turn our attention to the opposite case – the decreasing

case. Note that $\max_{s\in[0,x]} ||l(s)||_{H^1}^2 = ||l(0)||_{H^1}^2$. Then (3.56) becomes

$$\frac{d}{dx}||l||_{H^1}^2 \leq \left(2\lambda+1-\frac{\varepsilon}{2}+4\varepsilon Q\right)||l||_{H^1}^2 + 2\varepsilon Q||l(0)||_{H^1}^2 + 2Q^2 \tag{3.59}$$

In a manner similar to the increasing case, we can find the following H^1 spatial bound on l:

$$\begin{aligned}||l||_{H^1}^2 \leq \exp\left((2\lambda+1-\frac{\varepsilon}{2}+4\varepsilon Q)x\right)||l(0)||_{H^1}^2 \\ + \int_0^x \exp\left((2\lambda+1-\frac{\varepsilon}{2}+6\varepsilon Q)(x-z)\right) \\ \times (2Q^2+2\varepsilon Q||l(0)||_{H^1}^2)dz\end{aligned} \tag{3.60}$$

Again, noting that $x\in[0,1]$ and $l(0,y)=p(0,y)$, one can find a different K such that (3.53) is fulfilled for all x. □

Theorem 8. *The kernel PDE defined by* (3.17)-(3.20) *with the operator F defined piecewise as*

$$F[l](x,y) = \begin{cases} q(x,y) - \int_y^x \varepsilon l(x-z,0)q(z,y)dz & y \leq x \\ 0 & \textit{otherwise} \end{cases} \tag{3.61}$$

has a weak solution $l \in L^2[0,1]\times H^1[0,1]$.

Proof. We apply a Galerkin-type argument to prove the existence of weak solutions. Note that most of the proof of well-posedness follows directly from [19], so we merely sketch the proof.

The central idea behind the Galerkin method is to approximate solutions to the PDEs using a truncated sum of weighted orthogonal basis functions. Suppose ϕ_n form an orthogonal basis of n functions for the projected n-th dimensional space. Then, consider the definiton of an "approximate" solution $\hat{l}_m$ as

$$\hat{l}_m(x) := \sum_{k=1}^{m} a_k(x)\phi_k \tag{3.62}$$

Our goal is to choose the coefficients $a_k(x)$ such that $a_k(0) = \langle l(0), \phi_k \rangle$, and such that $\hat{l}_m(x)$ satisfies the projection of (3.17)-(3.19) onto the orthonormal basis ϕ_k.

The PDE "projected" into an m-dimensional subspace give arise to m ordinary differential equations, which by standard differential equation theory, exist and are unique.

We build a sequence $\{\hat{l}_m\}_{m=1}^{\infty}$ (i.e. the sum (3.62) is then taken to infinity). This sequence converges in the weak sense, due to the uniform energy estimates derived in Lemma (7). It is not difficult to see that the uniform bound (7) gives arise to a bound $\left|\left|\hat{l}_m(x)\right|\right|_{L^2} \leq ||l(x)||_{L^2}, \forall m \in \mathbb{N}$, where we have exploited the property of orthonormality. This limit generates a weak solution.

□

3.5 Numerical study

Table 3.1: Simulation parameters

Parameter	Value
ε	0.5
λ	2
c	1
$q(x,y)$	$10(e^y - 1)$

Simulations were executed for a choice of $\varepsilon = 1.5, \lambda = 2, c = 1$ with $q(x,y) = q(y) = 3\exp(1-y)$. The gain kernel $l(x,y)$ was numerically solved using a central finite difference scheme, which leads to the control gains $k(1,y)$ and $l(1,y)$.

It is evident that unstable behavior exists for the choice of parameters in the open-loop simulations shown in Figure 3.6. With the application of feedback control, however, the system exhibits exponentially stable behavior. After some initial transient (due to the initial conditions of the first-order hyperbolic system), the system quickly converges to the zero equililbrium, as seen in Figure 3.7. It should be noted that while purely first-order hyperbolic systems can be stabilized in finite-time, the system of mixed hyperbolic and parabolic equations can only be stabilized

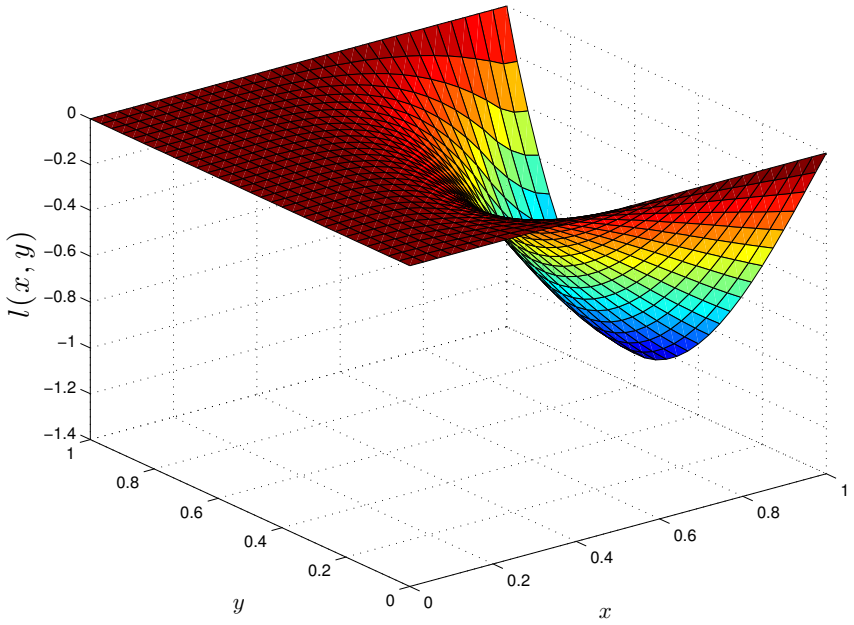

Figure 3.3: The gain kernel $l(x,y)$, with ffect of triangular forcing function $f(x,y)$ observed.

exponentially at best.

The construction of the simulation is also non-trivial. The study of methods to numerically solve coupled hyperbolic-parabolic mixed class systems is still a somewhat active field, due to the different behaviors explored necessitating different requirements in discretization. For this problem, however, the finite-element methods suffice, albeit with some condition.

3.6 Conclusion

A control algorithm for exponentionally stabilizing a unidirectionally coupled mixed-type hyperbolic-parabolic PDE system in the $L^2 \times H^1$ sense is presented. The gain kernel PDE, also consisting of a hyperbolic-parabolic coupled system, is required to be solved, which raises the question of existence of solutions. The existence of solutions is shown, and the gain kernel PDE numerically solved. The overall system is simulated with the control law to illustrate the effectiveness of the control algorithm.

The results in this chapter raise an interesting question for backstepping as a tool in PDE

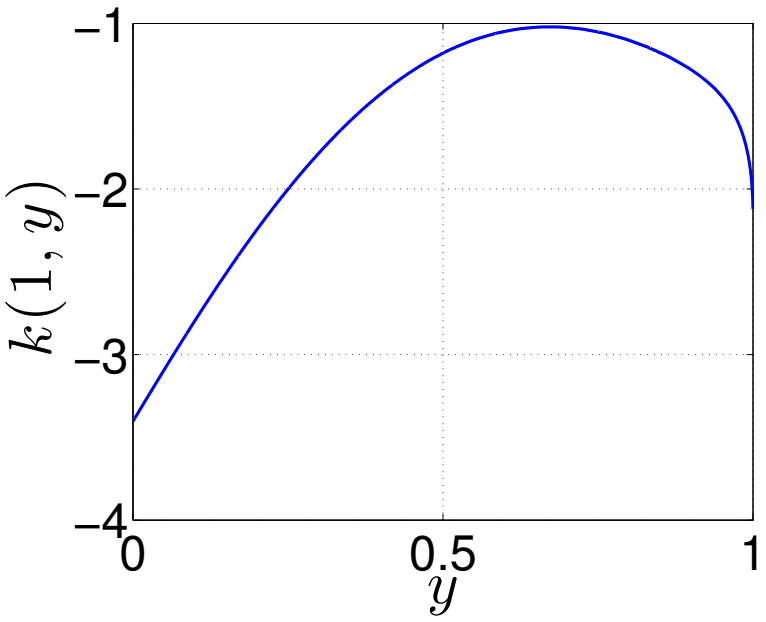

Figure 3.4: $k(1,y)$ gain kernel

control. It is widely known that many tools in PDEs are constrained to within a certain class (examples include method of characteristics for hyperbolic PDEs, and maximum principles for parabolic PDEs). However, backstepping has been successfully applied across various different classes of systems, albeit with minor modifications. This result, in particular, brings an interesting new perspective. Prior to this, few results existed for mixed-type coupled PDEs — largely in [28], which inspected a cascade structure. Now, interior coupling is beginning to be explored for various types of coupling structures. Future work will explore to what extent backstepping can be applied across mixed-type coupled PDE systems.

The coupling structure of the system explored in this paper is more restrictive than what the authors would prefer. However, depending on how the control signal enters the system and how the system is coupled in the interior, the problem ranges from tractable (this paper) to potentially impossible. Current ongoing work is exploring the extent of which coupling topologies in hyperbolic-parabolic mixed class PDEs can be stabilized using backstepping.

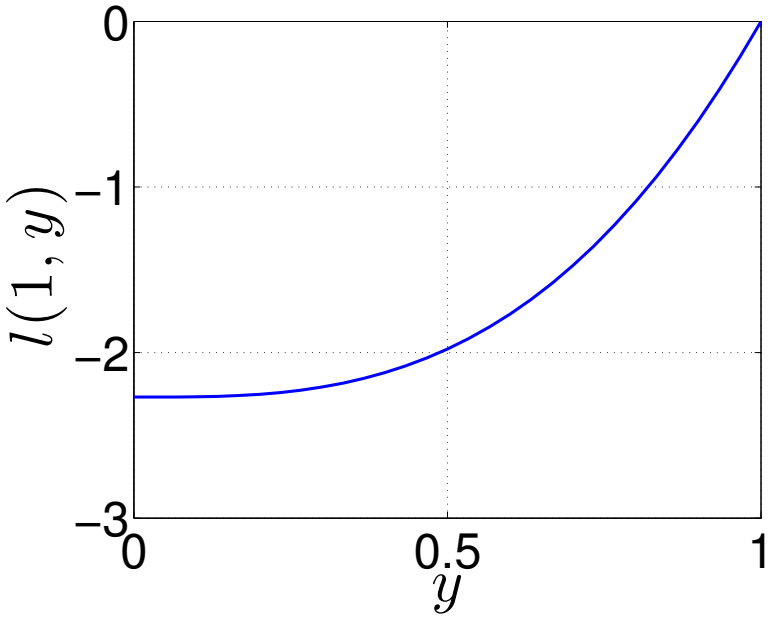

Figure 3.5: $l(1,y)$ gain kernel

3.7 Acknowledgements

Chapter 3, in part, is a reprint of the material as it appears in: S.Chen, R. Vazquez, M. Krstic. Backstepping Control Design for a Coupled Hyperbolic-Parabolic Mixed Class PDE System. Conference on Decision and Control, 2017. The dissertation author was the primary investigator and co-author of this paper.

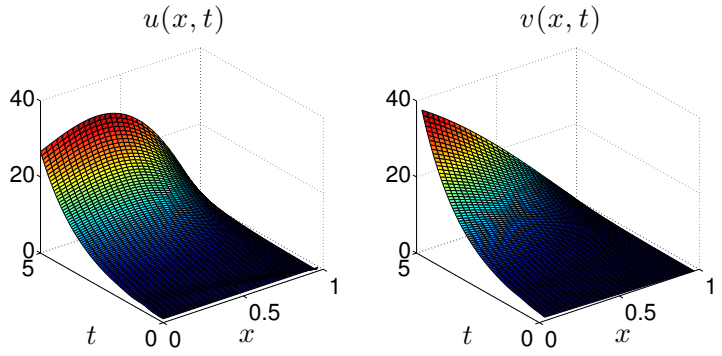

Figure 3.6: The unstable system in open-loop configuration. **Left.** $u(x,t)$. **Right.** $v(x,t)$.

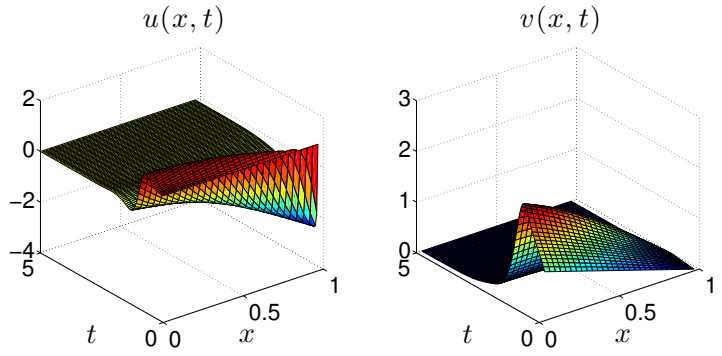

Figure 3.7: Stable closed-loop configuration. System exhibits exponential stability. **Left.** $u(x,t)$. **Right.** $v(x,t)$.

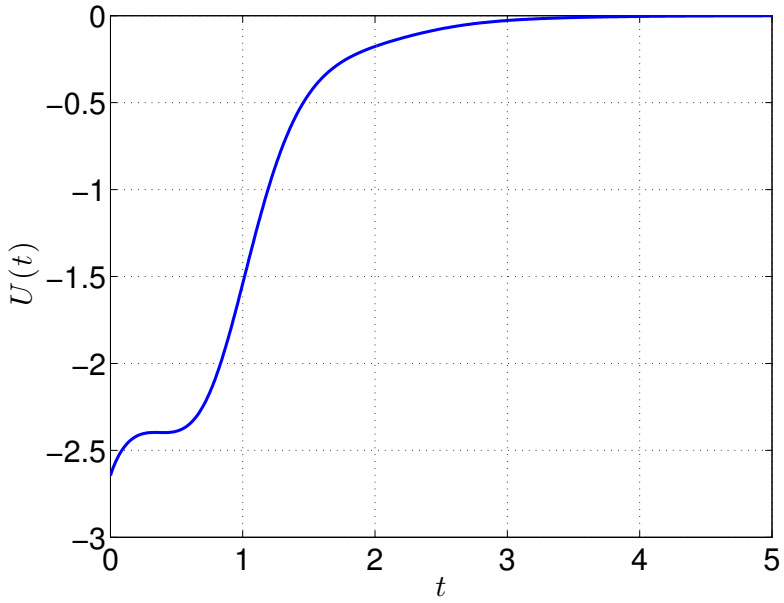

Figure 3.8: The control $U(t)$ applied to the system.

Chapter 4

Delay-compensated control for coupled parabolic systems with distinct input delays

4.1 Introduction

Control of input delay systems has been a primary focus of much work in backstepping-based boundary control of infinite-dimensional systems. Very often, the input delay is converted to a first-order hyperbolic equation [29]. Recognizing this equivalence relation between first-order hyperbolic PDEs and delays, many tools in boundary control of PDEs can be then be utilized [35],[30].

Intimately related to controlling PDEs with input delay is the control of coupled PDE systems. In the recent years, there has been a wide swath of literature with this theme, and hyperbolic PDE in particular. One of the most central (and major) results in controlling $n+1$ first-order hyperbolic equations with a single controller is found in [32]. This result was later extended in [25], which generalized the problem to $n+m$ (with $m \leq n$) first-order hyperbolic

equations with m controllers. Other results in the control of hyperbolic systems include [13], which considers the case of $1+2$ first-order hyperbolic systems with a single controller (an underactuated case), and minimum-time control of $n+m$ systems [3].

Results for parabolic PDE have also been generated in parallel. In particular, Vazquez in [45] recognized the similarity between gain kernel PDEs in both parabolic and hyperbolic backstepping control designs to great effectiveness. A more general result was generated via a different solution methodology in [18], expanding to a wider class of boundary conditions as well as including non-local interior coupling. In another direction, [33] considered output feedback control, but with constant coefficients.

The control of mixed-type (consisting of combinations of hyperbolic and parabolic) PDE is significantly more complicated than homogenous systems of PDE, but recently has been studied. A first result cast as the control of a parabolic (scalar) PDE with input delay was generated in [29], in which the system was transformed into the cascade of a first-order hyperbolic PDE (modeling the delay) with an unstable diffusion-reaction system (parabolic). An extension to this problem was considered in [12], which introduced additional in-domain coupling of strict-feedback type between the two PDE classes.

This paper acts as a matrix extension to [29], or alternatively interpreted, an extension to [45] with input delay characterstics.

4.2 Model

We will utilize the $L^2([0,1])$ and $H^1([0,1])$ function spaces over x, and the $L^2([0,\infty],\cdot)$ over t (respective to a function space in x). $L^2([0,1])$ represents the space of square-integrable functions and is written L^2 shorthand. L^2 has the norm

$$||f||_{L^2} := \sqrt{\int_0^1 |f(x)|^2 dx}.$$

Similarly, the $H^1([0,1])$ is written to be H^1 in short and has the norm:

$$||f||_{H^1} := ||f||_{L^2} + ||\partial_x f||_{L^2}\,.$$

We consider a 2×2 parabolic system

$$\partial_t U(x,t) = \Gamma\partial_x^2 U(x,t) + \Lambda(x)U(x,t) \tag{4.1}$$

$$U(0,t) = 0 \tag{4.2}$$

$$U(1,t) = \mathcal{D}_{D_1,D_2}\,\mathcal{U}(t) \tag{4.3}$$

with $U \in (L^2([0,\infty),H^1(0,1)))^2$, consisting of two scalar elements $u_i(x,t), i \in \{1,2\}$. $\Gamma = \text{diag}(\varepsilon_1,\varepsilon_2), \varepsilon_i > 0$ is taken to be a constant diagonal matrix. $\Lambda(x)$ is a matrix of functions $\lambda_{ij}(x)$. In general, $\Lambda \succ 0$ causes instability in the system. The input $\mathcal{U} = \begin{pmatrix} \mathcal{U}_1 & \mathcal{U}_2 \end{pmatrix}^T$ is operated on by the componentwise delay operator $\mathcal{D}$, which is defined as

$$\mathcal{D}_{D_1,D_2}\,\mathcal{U}(t) = \begin{pmatrix} \mathcal{U}_1(t-D_1) \\ \mathcal{U}_2(t-D_2) \end{pmatrix} \tag{4.4}$$

It is well known that delays can be represented with first-order hyperbolic PDEs. We rewrite the delays found in (4.3) with a first-order hyperbolic matrix PDE:

$$\partial_t U(x,t) = \Gamma\partial_x^2 U(x,t) + \Lambda(x)U(x,t) \tag{4.5}$$

$$\partial_t V(x,t) = \Sigma\partial_x V(x,t) \tag{4.6}$$

$$U(0,t) = 0 \tag{4.7}$$

$$U(1,t) = V(1,t) \tag{4.8}$$

$$V(2,t) = \mathcal{U}(t) \tag{4.9}$$

where $V \in (L^2([0,\infty),H^1(1,2)))^2$ consisting of two scalar elements $v_i(x,t), i \in \{1,2\}$. The component delay lengths $D_1, D_2 > 0$ are encoded in the diagonal matrix $\Sigma = \text{diag}(\sigma_1, \sigma_2)$, with the definition $\sigma_i := D_i^{-1} > 0$.

We make several assumptions on the parameter ordering:

Assumption. *Assume* $\varepsilon_1 > \varepsilon_2$ *and* $\sigma_1 > \sigma_2$.

Remark. *The assumption on the ordering of* σ_i *be relaxed by the following method. If* $\sigma_2 > \sigma_1$*, we define*

$$P = \begin{pmatrix} 0 & 1 \\ 1 & 0 \end{pmatrix}$$

and let $\bar{V} = PV$*. This permutation matrix will order the* σ_i *according to our assumption. This will change* (4.8) *into*

$$U(1,t) = P\bar{V}(1,t)$$

and the corresponding boundary condition in the target system (4.15)*. This change in boundary condition has no bearing on the stability.*

4.3 Backstepping control design

We use two backstepping transformations. The first shifts the instability of $U(x,t)$ to the $x = 1$ boundary. The second will shift the instabilitly from the $x = 1$ to the $x = 2$ boundary, where it can be neutralized by the controller $\mathcal{U}$.

The first transformation is

$$W(x,t) = U(x,t) - \int_0^x K(x,y)U(y,t)dy \tag{4.10}$$

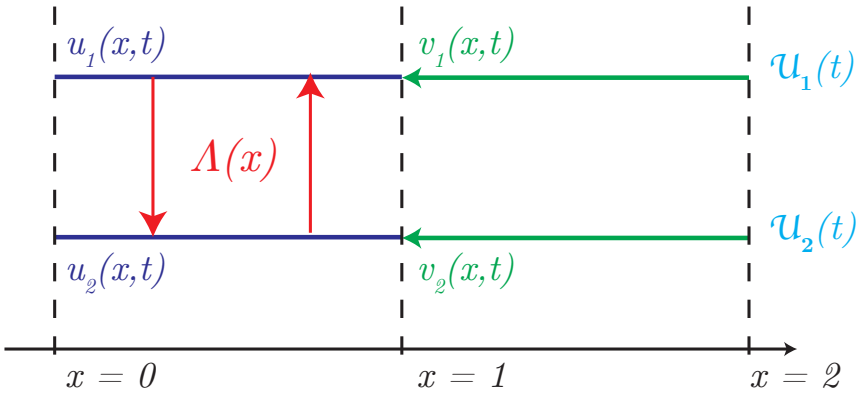

Figure 4.1: A schematic view of the plant.

where $K(x,y) : \mathcal{T}_K \to \mathbb{R}^{2\times 2}$ consists of the continuous gain kernels of the transformation. The domain of K, $\mathcal{T}_K := \{(x,y) \in \mathbb{R}^2 | 0 \leq y \leq x \leq 1\}$, is a triangular domain. This transformation for coupled parabolic systems is relatively well studied, with results found in [45],[18],[33], amongst others. In this paper, we will not concentrate our efforts on the kernel K, and instead refer the reader to the aforementioned papers. The well-posedness of K is henceforth assumed.

The second transformation is

$$\begin{aligned} Z(x,t) = V(x,t) &- \int_1^x L(x,y)V(y,t)dy \\ &- \int_0^1 M(x,y)U(y,t)dy \end{aligned} \tag{4.11}$$

where $L(x,y) : \mathcal{T}_L \to \mathbb{R}^{2\times 2}$ and $M(x,y)L(x,y) : \mathcal{T}_M \to \mathbb{R}^{2\times 2}$, where the domains are respectively defined $\mathcal{T}_L := \{(x,y) \in \mathbb{R}^2 | 1 \leq y \leq x \leq 2\}$ and $\mathcal{T}_M := \{(x,y) \in \mathbb{R}^2 | 1 \leq x \leq 2, 0 \leq y \leq 1\}$ Note that $\mathcal{T}_L$ is a triangular domain, much like $\mathcal{T}_K$; however, $\mathcal{T}_M$ is on a *square* domain. We must study the existence of these gain kernels, which is a novel contribution.

These transformations will admit the following target system:

$$\begin{aligned} \partial_t W(x,t) = \Gamma \partial_x^2 W(x,t) &- CW(x,t) \\ &- G_1(x)\partial_x W(0,t) \end{aligned} \tag{4.12}$$

$$\partial_t Z(x,t) = \Sigma \partial_x Z(x,t) + G_2(x) Z(x,t) \tag{4.13}$$

$$W(0,t) = 0 \tag{4.14}$$

$$W(1,t) = Z(1,t) \tag{4.15}$$

$$Z(2,t) = 0 \tag{4.16}$$

where $C = \text{diag}(c_1, c_2)$ is a design parameter affecting the convergence rate of the state W. The c_i must be chosen such that $\min\{c_i\} \geq \max\{1, \varepsilon_2/2\} + \delta$, with an arbitrary $\delta > 0$. This is a condition arising in [45] as well, which in a sense represents the necessity of selecting a C to dominate the effect of the trace term G_1. The matrices $G_i(x)$ have specific structures

$$G_i = \begin{pmatrix} 0 & 0 \\ g_i(x) & 0 \end{pmatrix} \tag{4.17}$$

where g_i are predetermined, and not designed. They are in fact related to the gain kernels, and will be studied later. The structure of G_1 and the regularity of the nonzero element g_1 will guarantee the exponential stability of the system. G_1 in particular arises from the kernel K. In [45], the nonzero element is explicitly defined $g_1 := -\varepsilon_1 k_{21}(x,0)$.

Theorem 9. *Consider the system given by* (4.5)-(4.9). *With the application of the feedback controller*

$$\mathcal{U}(t) = \int_0^1 M(2,y) U(y,t) dy + \int_1^2 L(2,y) V(y,t) dy \tag{4.18}$$

where M satisfies the parabolic system of PDEs given by

$$\begin{aligned} \Sigma \partial_x M(x,y) - \partial_y^2 M(x,y) \Gamma = M(x,y) \Lambda(y) \\ + G_2(x) M(x,y) \end{aligned} \tag{4.19}$$

$$M(x,1) = 0 \tag{4.20}$$

$$M(x,0) = 0 \tag{4.21}$$

$$M(1,y) = K(1,y) \tag{4.22}$$

and L satisfies the hyperbolic system of PDEs given by

$$\Sigma\partial_x L(x,y) + \partial_y L(x,y)\Sigma = G_2(x)L(x,y) \tag{4.23}$$

$$L(x,1)\Sigma = \partial_y M(x,1)\Gamma \tag{4.24}$$

where G_2 is defined by

$$G_2(x) = L(x,x)\Sigma - \Sigma L(x,x) \tag{4.25}$$

and where K arises from the gain kernel equations found in [45], the trivial solution $(U,V) = 0$ to system (4.5)-(4.9) *will be exponentially stabilized in the $H^1 \times H^1$ sense, i.e. there exist $\Xi, \Omega > 0$ such that*

$$||(U,V)||_{H^1\times H^1}(t) \leq \Xi e^{-\Omega t} ||(U,V)||_{H^1\times H^1}(0) \tag{4.26}$$

4.3.1 Lyapunov stability

To study the stability of the target system (4.12)-(4.16), we first employ a transformation in the state to make analysis simpler. First, we define the following affine transformation from W to Θ:

$$\Theta(x,t) = W(x,t) - xZ(1,t) \tag{4.27}$$

It is quite obvious that (4.27) is trivially invertible. The invertibility is a necessary condition for establishing an equivalence relation between the transformed target system and the original plant (with feedback control applied). (4.27) will admit the following coupled system:

$$\begin{aligned}\partial_t\Theta(x,t) &= \Gamma\partial_x^2\Theta(x,t) - C\Theta(x,t) \\ &\quad - G_1(x)\partial_x\Theta(0,t)) - x\Sigma\partial_x Z(1,t) \\ &\quad - (xC + G_1(x) + xG_2(1))Z(1,t) \qquad (4.28)\end{aligned}$$

$$\partial_t Z(x,t) = \Sigma\partial_x Z(x,t) + G_2(x)Z(x,t) \qquad (4.29)$$

$$\Theta(0,t) = 0 \qquad (4.30)$$

$$\Theta(1,t) = 0 \qquad (4.31)$$

$$Z(2,t) = 0 \qquad (4.32)$$

Exponential stability of $(\Theta, Z) = 0$ can be concluded using the following Lyapunov function:

$$\mathcal{V}(t) = \mathcal{V}_\Theta(t) + b\mathcal{V}_Z(t) \qquad (4.33)$$

$\mathcal{V}_\Theta$ is defined as

$$\mathcal{V}_\Theta = \int_0^1 \Theta^T Q\Theta + (\partial_x\Theta)^T Q(\partial_x\Theta)dx \qquad (4.34)$$

where the matrix $Q = \text{diag}(q_1, q_2)$ contains design parameters $q_1, q_2 > 0$. $\mathcal{V}_Z(t)$ is defined

$$\begin{aligned}\mathcal{V}_Z(t) &= \int_1^2 \exp(\kappa_1(x-1))Z^T Z \\ &\quad + \exp(\kappa_2(x-1))(\partial_x Z)^T(\partial_x Z)dx \qquad (4.35)\end{aligned}$$

where the design parameters κ_1, κ_2 must be chosen according to the following constraints:

$$\kappa_1 > \frac{2}{\sigma_2} ||g_2||_{L_\infty} \tag{4.36}$$

$$\kappa_2 > \frac{4||g_2'(x)||_{L_\infty}}{\sigma_2} + \frac{2}{\sigma_2} ||g_2||_{L_\infty} \tag{4.37}$$

Finally, the coefficient b must be chosen according to the following rule:

$$\begin{aligned} b > \frac{4}{\sigma_2 \delta} \max \{ & 2(\sigma_1 \max\{q_i\})^2, \\ & \max\{q_i\}^2 \left((\max\{c_i\} + ||g_1||_{L_\infty} + ||g_2||_{L\infty})^2 \right. \\ & \left. + (\max\{c_i\} + \left|\left|g_1'\right|\right|_{L_\infty} + ||g_2||_{L\infty})^2 \right) \Big\} \end{aligned} \tag{4.38}$$

This will allow us to find the following bound on the $H^1 \times H^1$ norm of (Θ, Z):

$$||(\Theta, Z)||_{H^1 \times H^1}(t) \leq \bar{\Xi} \exp(-\Omega t) ||(\Theta, Z)||_{H^1 \times H^1}(0) \tag{4.39}$$

where

$$\bar{\Xi} = \sqrt{\frac{\max\{b\exp(\kappa_1), b\exp(\kappa_2), q_1, q_2\}}{\min\{1, q_1, q_2\}}} \tag{4.40}$$

$$\begin{aligned} \Omega = \min \Big\{ & \delta, \frac{b}{2}\sigma_2\kappa_1 - \exp(\kappa_1) ||g_2||, \\ & \frac{b}{2}\sigma_2\kappa_2 - 2\exp(\kappa_2) \left|\left|g_2'\right|\right| - ||g_2|| \Big\} \end{aligned} \tag{4.41}$$

We will omit the derivation of the bound for the sake of space. An interesting observation one may make from (4.41) is that the analysis parameter b can be made sufficiently high, to which the rate of convergence of the target system is purely defiend by δ, the design parameter associated with choosing C.

The stability bound on (Θ, Z) can be transformed into a stability bound for (W, Z) using the invertible transformation (4.27). Then, the stability of (W, Z) can generate a stability bound for the original system (U, V) through the use of (4.10),(4.11), and their inverses (which are guaranteed to exist as long as the kernels K, L, M exist and are bounded).

4.3.2 Kernel derivations

Differentiating (4.11) once in time and twice in space, then imposing (4.5)-(4.9) and (4.12)-(4.16), the set of PDEs (4.19)-(4.24) that comprise the gain kernel equations can be recovered.

The condition (4.22) is derived from (4.10),(4.11), and (4.15). The matrix condition (4.25) actually consists of three boundary conditions and the definition for $g_2(x)$, which arises due to the assumption $\sigma_1 > \sigma_2$. Noting (4.17) and (4.25), we can find the definition for the nonzero element of $G_2(x)$ to be

$$g_2(x) := (\sigma_1 - \sigma_2) l_{21}(x, x) \tag{4.42}$$

In the following section, we will drop the (x, y) arguments on k_{ij}, l_{ij} unless otherwise specified for compact notation (i.e., if the arguments are not included, then they are assumed to be (x, y)). If one writes out the component equations for L, one finds

$$\sigma_1 \partial_x l_{11} + \sigma_1 \partial_y l_{11} = 0 \tag{4.43}$$

$$\sigma_1 \partial_x l_{12} + \sigma_2 \partial_y l_{12} = 0 \tag{4.44}$$

$$\sigma_2 \partial_x l_{21} + \sigma_1 \partial_y l_{21} = g_2(x) l_{11} \tag{4.45}$$

$$\sigma_2 \partial_x l_{22} + \sigma_2 \partial_y l_{22} = g_2(x) l_{12} \tag{4.46}$$

If one writes out the component equations for M, one finds

$$\partial_x m_{11} = \frac{\varepsilon_1}{\sigma_1}\partial_y^2 m_{11} + \frac{\lambda_{11}(y)}{\sigma_1} m_{11} + \frac{\lambda_{21}(y)}{\sigma_1} m_{12} \tag{4.47}$$

$$\partial_x m_{12} = \frac{\varepsilon_2}{\sigma_1}\partial_y^2 m_{12} + \frac{\lambda_{12}(y)}{\sigma_1} m_{11} + \frac{\lambda_{22}(y)}{\sigma_1} m_{12} \tag{4.48}$$

$$\partial_x m_{21} = \frac{\varepsilon_1}{\sigma_2}\partial_y^2 m_{21} + \frac{\lambda_{11}(y)}{\sigma_2} m_{21} + \frac{\lambda_{21}(y)}{\sigma_2} m_{22} + \frac{g_2(x)}{\sigma_2} m_{11} \tag{4.49}$$

$$\partial_x m_{22} = \frac{\varepsilon_2}{\sigma_2}\partial_y^2 m_{22} + \frac{\lambda_{12}(y)}{\sigma_2} m_{21} + \frac{\lambda_{22}(y)}{\sigma_2} m_{22} + \frac{g_2(x)}{\sigma_2} m_{12} \tag{4.50}$$

Immediately apparent in (4.43)-(4.46) is a cascading problem arising from the structure of G_2. (4.43),(4.44) are readily solvable, which then proceed to act as source functions in (4.45),(4.46).

Likewise, (4.47)-(4.50) exhibits the same cascading nature. One must first solve (4.47), (4.48) simultaneously (a vector diffusion-reaction equation). Then, the solutions m_{11}, m_{12} are then utilized to solve (4.49),(4.50).

One additional difficulty that the reader may have noticed is the presence of $g_2(x)$ in (4.45). g_2 is an evaluation of l_{21} at $y = x$, as according to (4.42). This term affects the evolution of l_{21}. Thus, we must take care in solving (4.45). However, with this solution in hand, (4.46) becomes very straightforward. (4.49)-(4.50) also depend on g_2, which will further complexify the solution, as the initial data of (4.45) depends boundary data of m_{21}. This cascading of problem data is depicted in the block diagram Figure 4.2, with each subsystem arranged by color. The following procedure is followed to fully solve the gain kernel equations:

1. Solve (4.47),(4.48),(4.43),(4.44).

2. Solve (4.45), expressing the solution as an operator of (m_{21}, m_{22}).

3. Solve (4.49),(4.50) with the operator expression for l_{21}.

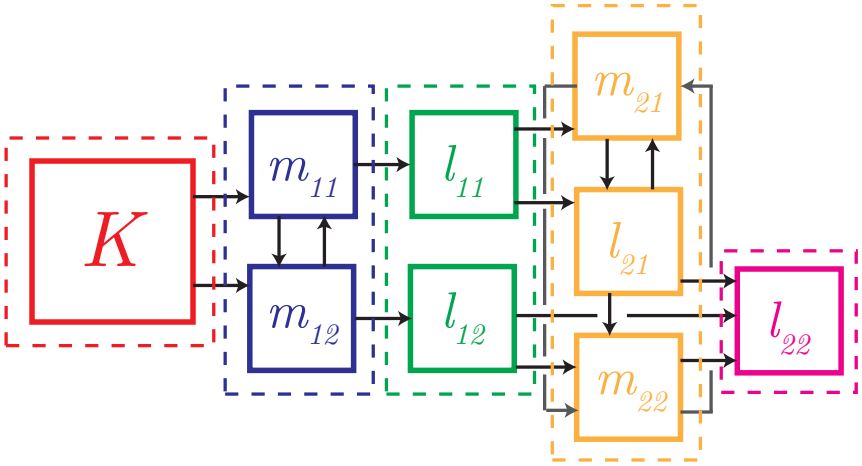

Figure 4.2: The gain kernels propagate data via in-domain and boundary coupling. There is some cascading structure (marked with color) that makes solving the system more tractable.

4. Solve (4.46).

To show existence of (weak) solutions to this system of coupled gain kernel PDEs, we reduce the work to finding existence of solutions to the subsystem (l_{21}, m_{21}, m_{22}), while the rest follow from classical results and application of method of characteristics.

$$\sigma_2 \partial_x l_{21} = -\sigma_1 \partial_y l_{21} + (\sigma_1 - \sigma_2) l_{21}(x,x) l_{11} \tag{4.51}$$

$$\begin{aligned} \partial_x m_{21} = \frac{\varepsilon_1}{\sigma_2} \partial_y^2 m_{21} + \frac{\lambda_{11}(y)}{\sigma_2} m_{21} + \frac{\lambda_{21}(y)}{\sigma_2} m_{22} \\ + \frac{(\sigma_1 - \sigma_2)}{\sigma_2} l_{21}(x,x) m_{11} \end{aligned} \tag{4.52}$$

$$\begin{aligned} \partial_x m_{22} = \frac{\varepsilon_2}{\sigma_2} \partial_y^2 m_{22} + \frac{\lambda_{12}(y)}{\sigma_2} m_{21} + \frac{\lambda_{22}(y)}{\sigma_2} m_{22} \\ + \frac{(\sigma_1 - \sigma_2)}{\sigma_2} l_{21}(x,x) m_{12} \end{aligned} \tag{4.53}$$

with the boundary conditions

$$l_{21}(x,1) = \frac{\varepsilon_1}{\sigma_1} \partial_y m_{21}(x,1) \tag{4.54}$$

$$m_{21}(x,0) = m_{21}(x,1) = 0 \tag{4.55}$$

$$m_{22}(x,0) = m_{22}(x,1) = 0 \tag{4.56}$$

$$m_{21}(1,y) = k_{21}(1,y) \tag{4.57}$$

$$m_{22}(1,y) = k_{22}(1,y) \tag{4.58}$$

4.4 Well-posedness of gain kernel equations for l_{21}, m_{21}, m_{22}

We will first begin with (4.51), and attempt to express the value of the solution at $y = x$ as an integral equation.

A direct application of method of characteristics to the expression (4.51) can be integrated to find a representation for $l_{21}(x,y)$, which is then evaluated at $y = x$. A change of integration variables leads to:

$$\begin{aligned} l_{21}(x,x) = &\frac{\varepsilon_1}{\sigma_1}\partial_y m_{21}\left(a(x),1\right) \\ &- \int_{a(x)}^{x} \frac{\sigma_1 - \sigma_2}{\sigma_2} l_{21}\left(\zeta,\zeta\right) \\ &\quad \times l_{11}\left(\zeta, a(x) + \frac{\sigma_1^2 - \sigma_2^2}{\sigma_1\sigma_2}\zeta\right) d\zeta \end{aligned} \tag{4.59}$$

where for ease of reading we have defined

$$a(x) := \left(1 - \frac{\sigma_2}{\sigma_1}\right) x + \frac{\sigma_2}{\sigma_1}. \tag{4.60}$$

We now define the following iteration for l_{21} in the spirit of successive approximations:

$$\begin{aligned} \hat{l}_{n+1}(x) = &\frac{\varepsilon_1}{\sigma_1}\partial_y m_{21}\left(a(x),1\right) \\ &- \int_{a(x)}^{x} \frac{\sigma_1 - \sigma_2}{\sigma_2} \\ &\quad \times l_{11}\left(\zeta, a(x) + \frac{\sigma_1^2 - \sigma_2^2}{\sigma_1\sigma_2}\zeta\right) \hat{l}_n\left(\zeta\right) d\zeta \end{aligned} \tag{4.61}$$

where if the above integral equation is a contraction, the limit of the iterations will approach the solution, i.e.

$$\lim_{n\to\infty} \hat{l}_n(x) = l_{21}(x,x) \tag{4.62}$$

By defining $\Delta\hat{l}_n := \hat{l}_{n+1} - \hat{l}_n$, we find the following relation:

$$\begin{aligned}\Delta\hat{l}_{n+1}(x) = \int_{a(x)}^{x} & \frac{\sigma_1-\sigma_2}{\sigma_2} \\ & \times l_{11}\left(\zeta, a(x) + \frac{\sigma_1^2-\sigma_2^2}{\sigma_1\sigma_2}\zeta\right)\Delta\hat{l}_n(\zeta)\,d\zeta\end{aligned} \tag{4.63}$$

Where now (4.62) can be rewritten as an infinite sum:

$$l_{21}(x,x) = \hat{l}_0(x) + \sum_{n=0}^{\infty}\Delta\hat{l}_n(x) \tag{4.64}$$

Choosing $\hat{l}_0(x) = 0$, one can find a representation of the solution $l_{21}(x,x)$ to be

$$\begin{aligned}l_{21}(x,x) = & \frac{\varepsilon_1}{\sigma_1}\partial_y m_{21}(a(x),1) \\ & + \sum_{n=1}^{\infty}\int_{a(x)}^{x}\int_{a(\zeta_{n-1})}^{\zeta_{n-1}}\cdots\int_{a(\zeta_2)}^{\zeta_2} \\ & \left(\frac{\sigma_1-\sigma_2}{\sigma_2}\right)^n P_n(x,\zeta_1,\zeta_2,\ldots,\zeta_n) \\ & \times \frac{\varepsilon_1}{\sigma_1}\partial_y m_{21}(a(\zeta_1),1)\,d\zeta_1\ldots d\zeta_n\end{aligned} \tag{4.65}$$

where we have defined $P_n(x,\zeta_1,\zeta_2,\ldots,\zeta_n)$ as

$$\begin{aligned}P_n = & l_{11}\left(\zeta_n, a(x) + \frac{\sigma_1^2-\sigma_2^2}{\sigma_1\sigma_2}\zeta_n\right) \\ & \times \prod_{m=1}^{n-1} l_{11}\left(\zeta_m, a(\zeta_{m+1}) + \frac{\sigma_1^2-\sigma_2^2}{\sigma_1\sigma_2}\zeta_m\right)\end{aligned} \tag{4.66}$$

Let $l_{21}(x,x) := \Psi m_{21}$, where Ψ is an operator (for notational simplicity). We seek a bound on Ψm_{21} from above, which will guarantee the existence of the solution.

$$|\Psi m_{21}| \leq \left|\frac{\varepsilon_1}{\sigma_1}\partial_y m_{21}\left(a(x),1\right)\right|$$

$$+\sum_{n=1}^{\infty}\int_{a(x)}^{x}\int_{a(\zeta_{n-1})}^{\zeta_{n-1}}\cdots\int_{a(\zeta_2)}^{\zeta_2} \left|\frac{\varepsilon_1}{\sigma_1}\right|\left|\frac{\sigma_1-\sigma_2}{\sigma_2}\right|^n |P_n| \times \left|\partial_y m_{21}\left(a(\zeta_1),1\right)\right| d\zeta_1\ldots d\zeta_n \tag{4.67}$$

Note that since $a(x) \leq x, \forall x$

$$\left|\partial_y m_{21}\left(a(\zeta_1),1\right)\right| \leq \sup_{1\leq z\leq x} C\,||m_{21}(z,\cdot)||_{H^2} \tag{4.68}$$

where C is a scaling constant as a result of H^1 being continuously embedded in L_∞ [19]. Next, we can majorize $l_{11}(x,y)$ by its pointwise sup-norm:

$$l_{11}(x,y) \leq \sup_{(x,y)}|l_{11}(x,y)| =: ||l_{11}||_{L_\infty} \tag{4.69}$$

which will allow us to bound P_n in the following way:

$$|P_n(x,\zeta_1,\ldots,\zeta_n)| \leq ||l_{11}||_{L_\infty}^n \tag{4.70}$$

This will ultimately allow us to establish the bound (7.117) as

$$|\Psi m_{21}| \leq \left|\frac{\varepsilon_1}{\sigma_1}\right| \exp\left(\left(\frac{\sigma_1-\sigma_2}{\sigma_2}||l_{11}||_{L_\infty}\right)(x-1)\right)$$

$$\times \sup_{1\leq z\leq x} C\,||m_{21}(z)||_{H^2} \tag{4.71}$$

Thus, if we find existence of H^2 solutions for m_{21}, then l_{21} exists. Nevertheless, we have an expression for l_{21} as an operator of m_{21}. This allows us to express g_2 as an operator on m_{21}, and finally, study the existence of solutions for m_{21} and m_{22}.

We let $m_1 = \begin{pmatrix} m_{11} & m_{12} \end{pmatrix}^T$ and $m_2 = \begin{pmatrix} m_{21} & m_{22} \end{pmatrix}^T$ for compact notation, and define parameter matrices accordingly.

$$\begin{aligned} \partial_x m_2(x,y) &= \Gamma_m \partial_y^2 m_2(x,y) + \Lambda_m(y) m_2(x,y) \\ &\quad + G_m[m_2](x) m_1(x,y) \end{aligned} \tag{4.72}$$

$$m_2(x,0) = m_2(x,1) = 0 \tag{4.73}$$

$$m_2(1,y) = \begin{pmatrix} k_{21}(1,y) & k_{22}(1,y) \end{pmatrix}^T \tag{4.74}$$

where m_1 is known from the bounded solution of (4.47),(4.48). The entries in $\Gamma_m, \Lambda_m, G_m[m_2]$ naturally follow from (4.49)-(4.50). (7.112) is a vector *parabolic* PDE, where x acts as a "time" like variable on the finite domain $[1,2]$. A very similar parabolic PDE consisting of diffusion and reaction terms with one additional boundary term entering the evolution was studied in [12],

Lemma 10 (A priori H^2 energy estimates for m_2)**.** *We can find the following energy estimate bound on m_2:*

$$||m_2(x)||_{H^2} \leq e^{\alpha(x)}\,||m_2(1)||_{H^2} \tag{4.75}$$

The proof nicely follows due to linearity allowing us to employ coercivity estimates for the "nice" diffusion and reaction terms, and the only challenge thus comes from the $G_m[m_2](x)m_1(x,y)$ trace term in (7.112). We will merely sketch the novel part of the proof, and refer the reader to [19] for much of the details.

Proof. Taking the inner product of m_2 with (7.112),

$$\int_0^1 m_2(x,y)^T \partial_x m_2(x,y) dy = \int_0^1 m_2(x,y)^T \left[\Gamma_m \partial_y^2 m_2(x,y) + \Lambda_m(y) m_2(x,y) + G_m[m_2](x) m_1(x,y) \right] dy \tag{4.76}$$

$$\Rightarrow \frac{1}{2}\frac{d}{dx}||m_2(x)||_{L_2}^2 \leq ||\Lambda_2||_{L_\infty} ||m_2(x)||_{L_2}^2 + |(\sigma_1 - \sigma_2)| |\Psi m_{21}| \times \int_0^1 |m_1(x)||m_2(x)| dy \tag{4.77}$$

By using the bound on Ψm_{21},

$$\begin{aligned} &\frac{1}{2}\frac{d}{dx}||m_2(x)||_{L_2}^2 \\ &\quad \leq ||\Lambda_m||_{L_\infty} ||m_2(x)||_{L^2}^2 + |(\sigma_1 - \sigma_2)| \left| \frac{\varepsilon_1}{\sigma_1} \right| \\ &\qquad \times \exp\left(\left(\frac{\sigma_1 - \sigma_2}{\sigma_2} ||l_{11}||_{L_\infty} \right) (x-1) \right) \\ &\qquad \times \sup_{1 \leq z \leq x} C ||m_2(z)||_{H^2} \\ &\qquad \times \int_0^1 |m_1(x)||m_2(x)| dy \end{aligned} \tag{4.78}$$

where we have additionally employed the fact that $||m_{21}(x)||_{H^2} \leq ||m_2(x)||_{H^2}, \forall x$. Next, we do the same process, but differentiate (7.112) once in y, and take the inner product of $\partial_y m_2$. Much of the work is similar, but most importantly, note that $G_m[m_2](x)$ is purely a function of x, and therefore is unaffected by differentiation in y. That is, we will utilize the bound on Ψm_{21} (as opposed to $\Psi \partial_y m_{21}$), which will give H^2 estimates. We will again do this once more for $\partial_y^2 m_2$, and similar results hold. Then the sum of the three bounds, $||m_2||_{L_2}, ||\partial_y m_2||_{L_2}, ||\partial_y^2 m_2||_{L_2}$ will

allow us to find a differential inequality on $||m_2||_{H^2}$.

$$\begin{aligned}
&\frac{1}{2}\frac{d}{dx}||m_2(x)||^2_{H^2} \\
&\quad\leq \left(||\Lambda_m||_{L_\infty} + 2\left|\left|\Lambda_m'\right|\right|_{L_\infty} + \left|\left|\Lambda_m''\right|\right|_{L_\infty}\right)||m_2(x)||^2_{H^2} \\
&\qquad + |(\sigma_1-\sigma_2)|\left|\frac{\varepsilon_1}{\sigma_1}\right| \sup_{1\leq z\leq x} C\,||m_2(z)||_{H^2} \\
&\qquad \times \exp\left(\left(\frac{\sigma_1-\sigma_2}{\sigma_2}||l_{11}||_{L_\infty}\right)^n (x-1)\right) \\
&\qquad \times ||m_1(x)||_{H^2}\,||m_2(x)||_{H^2}
\end{aligned} \tag{4.79}$$

where we have applied Young's inequality to the integral terms to arrive at a product of H^2 norms.

Now let $M(x) := ||m_2(x)||^2_{H^2}$ and note that $\forall x, M(x) \geq 0$. Associate the following differential equation in $\bar{M}(x)$ to the differential inequality (7.132):

$$\begin{aligned}
\frac{1}{2}\frac{d}{dx}\bar{M}(x) &= A\bar{M}(x) \\
&\quad + B(x)\left(\sup_{1\leq z\leq x}\sqrt{\bar{M}(z)}\right)\sqrt{\bar{M}(x)}
\end{aligned} \tag{4.80}$$

where the parameters $A, B(x)$ are defined by

$$A = ||\Lambda_m||_{L_\infty} + 2\left|\left|\Lambda_m'\right|\right|_{L_\infty} + \left|\left|\Lambda_m''\right|\right|_{L_\infty} \tag{4.81}$$

$$\begin{aligned}
B(x) &= |(\sigma_1-\sigma_2)|\left|\frac{\varepsilon_1}{\sigma_1}\right| ||m_1(x)||_{H^2} \\
&\quad \times \exp\left(\left(\frac{\sigma_1-\sigma_2}{\sigma_2}||l_{11}||_{L_\infty}\right)^n (x-1)\right)
\end{aligned} \tag{4.82}$$

where the initial condition is taken to be $\bar{M}(1) = M(1) = ||m_2(1,\cdot)||^2_{H^1}$. Noting that the right hand side of (7.135) is nonnegative, the supremum of $\bar{M}(z)$ in the interval $[1,x]$ is clearly at $z = x$.

Thus, the differential equation (7.135) becomes

$$\frac{1}{2}\frac{d}{dx}\bar{M}(x) = (A + B(x))\bar{M}(x) \tag{4.83}$$

and one can easily see via the integrating factor method

$$\bar{M}(x) = \exp\left(\int_1^x 2(A + B(z))dz\right)\bar{M}(1) \tag{4.84}$$

Thus, by the comparison principle,

$$||m_2(x)||_{H^2} \leq \exp\left(\int_1^x (A + B(z))dz\right)||m_2(1)||_{H^2} \tag{4.85}$$

Letting $\alpha(x) = \int_1^x A + B(z)dz$, we arrive at our resullt. □

Theorem 11 (Existence of weak solutions m_2)**.** *A weak solution in* $L_2([1,2], H^2((0,1))$ *to* (7.112) *exists.*

We will omit the proof and refer the reader to [19]. To give a sketch this approach, first, Galerkin approximations are used to project m_2 into a finite subspace spanned by a truncated set of orthonormal basis functions ϕ_k for H^2, i.e.

$$m_{2,k}(x) = \sum_{j=1}^{k} \langle m_2(x), \phi_k \rangle \tag{4.86}$$

Then the projection of (7.112) into this finite subspace spanned by ϕ_k will admit a system of k *ordinary* differential equations, and therefore, existence and uniqueness come as a result of classical theory. Noting that $\left|\left|m_{2,k}(x)\right|\right| \leq ||m_2(x)||$ for all k, one can then use energy estimates uniform in k to guarantee weak convergence of $m_{2,k} \to m_2$.

4.5 Conclusion

We have presented results in the control of coupled parabolic PDEs with distinct input delays. The assumption on the ordering of the delays in the system was mostly used for simplicity, and with the choice of a non-identity permuation matrix P, one can prove the same results. This result sits naturally as a matrix extension to [29], as well as the input delay extension to [43].

The work in this paper extends the work in mixed-type coupled PDEs further, in which coupled systems of more than 1 type per PDE are considered. The work also naturally leads to more interesting problems, such as the generalization to n-th order coupled systems of mixed type, which possibly could be interpreted as an analagous result to [25]. However, the primary difficulty with mixed-type PDE, as usual, is two-fold – the choice of a stable target system is not always very obvious, as well as the gain kernel PDEs often being difficult to show well-posedness. Unlike systems of coupled PDE of the same class, which always give *hyperbolic* gain kernels, mixed-type PDE will give *mixed-type* gain kernels, which must be solved using different methods.

The problem solved also leads naturally to future work in $n \times n$ systems, as well as an interesting and newly considered problem of "folded" PDE. In particular, bilateral control (in 1-D) has recently been considered in parabolic and hyperbolic contexts [43]. Such systems can be "folded," and expressed as a system of coupled PDE along the "folding" points. This has huge ramifications in the design of bilateral controllers, as it will put the system in the context of a coupled PDE system, albeit with an exotic boundary condition that must be considered.

4.6 Acknowledgements

Chapter 4, in part, is a reprint of the material as it appears in: S.Chen, R. Vazquez, M. Krstic. Backstepping Boundary Control of a 1-D 2×2 Unstable Diffusion-Reaction PDE System with Distinct Input Delays. American Control Conference, 2019. The dissertation author was the primary investigator and co-author of this paper.

Chapter 5

Bilateral Backstepping Boundary Control for an Unstable Parabolic PDE with Distinct Input Delays via Artifical Delay

5.1 Introduction

Bilateral backstepping control of a one dimensional parabolic partial differential equation is a natural extension to the standard, unilateral backstepping control design. It may be more natural to consider having control actuation on both boundaries in many applications.

In extreme ultraviolet light generation (EUV), liquid tin droplets are expelled by a droplet generator, which then travel in a stream. They are then energized into tin plasma by a CO2 drive laser, which generates a photon of the correct wavelength. However, this energized tin plasma acts as a disturbance to the droplet stream, which may have plasma collision like effects. These effects can be modeled by a parabolic partial differential equation. Thus, one can formulate the control objective to stabilize this plasma effect through the two actuators available – the droplet generator and the energizing CO2 laser.

Bilateral backstepping control is a relatively new concept, but one that is naturally interpreted and has much relevance. Bilateral control for partial differential equations can open the door to fault-tolerant designs (in the case one actuator fails). An additional benefit is that the presence of a second actuator can lead to less control effort per actuator, and thus extending the operating life cycle of the system significantly. Lastly, as one can intuit, the single acutator case falls under the bilateral control case, and thus, one can see that bilateral control is the natural extension to pre-existing backstepping boundary control. Previously, bilateral backstepping control has been initially developed by [43] for both parabolic and second-order hyperbolic equation cases. This work is extremely relevant, as this paper builds upon this result. Other results in bilateral control have been explored in first-order hyperbolic system contexts ([5],[4]), and most recently, in a parabolic context of trajectory tracking for a viscous Hamilton-Jacobi equation [8].

Input delay is a more commonly studied field, as it has direct relevance to many control problems (existing as actuator, communication, computational delays). There exists a wide swath of literature exploring many different variations of delay problems casted as partial differential equations, but few in input delay for parabolic equations. A large part of this is due to the mixed-class nature of these problems, as they entail a coupled system of a delay (hyperbolic) with the physical plant (parabolic). Interestingly, the gain PDE to be solved that arises from these types of problems maintain the mixed-class character of the plant (as opposed to homogeneous class systems, which always have a hyperbolic gain PDE). The most basic case of this mixed-class system has been explored in [28], where an unstable diffusion-reaction equation is considered with an arbitrariliy long input delay. This work was further extended in [12], where unidirectional in-domain coupling was next considered for systems of mixed-class type.

In this paper, we solve the problem of having distinct input delays to the bilateral control problem for an unstable parabolic equation. To approach this, we first state the main result in Section 5.2. We first establish the result for the identical delay case in Section 5.3, and use this

result in showing our approach for the distinct delay case in Section 5.4. Finally, we conclude our paper in Section 8.5.

5.2 Model and main result

We study a reaction-diffusion partial differential equation in one dimension with two Neumann boundary inputs, with delay.

$$\partial_t u(x,t) = \partial_x^2 u(x,t) + \lambda u(x,t) \tag{5.1}$$

$$\partial_x u(-L,t) = U_1(t-(D+\gamma)) \tag{5.2}$$

$$\partial_x u(L,t) = U_2(t-D) \tag{5.3}$$

where $u \in H^1([-L,L]) \times C^1([0,\infty))$. Without loss of generality, we let $\gamma \geq 0$ ($\gamma = 0$ being the case of the identical delay). Thus, the parameter $D \geq 0$ represents smaller of the two delays, and the parameter γ signifies the difference of the two input delays.

We can alternatively interpret this system as a coupled mixed-class (of parabolic and hyperbolic type) partial differential equation system as follows:

$$\partial_t u(x,t) = \partial_x^2 u(x,t) + \lambda u(x,t) \tag{5.4}$$

$$\partial_t v(x,t) = -\partial_x v(x,t) \tag{5.5}$$

$$\partial_t w(x,t) = \partial_x w(x,t) \tag{5.6}$$

$$\partial_x u(-L,t) = v(-L,t) \tag{5.7}$$

$$\partial_x u(L,t) = w(L,t) \tag{5.8}$$

$$v(-L-(D+\gamma),t) = U_1(t) \tag{5.9}$$

$$w(L+D,t) = U_2(t) \tag{5.10}$$

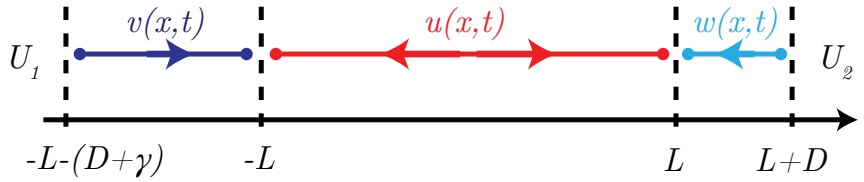

Figure 5.1: Schematic of system: the source of instability is purely in $u(x,t)$. To stabilize the system we actuate U_1, U_2 through delays.

with $u \in H^1([-L,L]) \times L_2([0,\infty))$, $v \in L_2([-L-(D+\gamma),-L]) \times L_2([0,\infty))$, $v \in L_2([L,L+D]) \times L_2([0,\infty))$. The problem is thusly transformed into a bilateral control problem of a mixed-class system, and pre-existing results in bilateral control (CITATION) and mixed-class systems (CITATIONS) can be extended to this case.

Theorem 12. *With the plant model given by* (5.4)-(5.10)*, and with the control laws*

$$\begin{aligned} U_1(t) &= \int_{-L-(D+\gamma)}^{-L} k(-L-(D+\gamma),y)v(y,t)dy \\ &+ \int_{-L}^{L} l(-L-(D+\gamma),y)u(y,t)dy \\ &+ \int_{L}^{L+D} m(-L-(D+\gamma),y)w(y,t)dy \\ &+ \int_{0}^{\gamma} m(-L-(D+\gamma),L+D+y)U_2^*(t+y-\gamma)dy \qquad (5.11) \\ U_2(t) &= \int_{L}^{L+D} p(L+D+\gamma,y)w(y,t-\gamma)dy \\ &+ \int_{-L}^{L} q(L+D+\gamma,y)u(y,t-\gamma)dy \\ &+ \int_{-L}^{-L-(D+\gamma)} r(L+D+\gamma,y)v(y,t-\gamma)dy \\ &+ \int_{0}^{\gamma} p(L+D+\gamma,L+D+y)U_2(t+y`-\gamma)dy \qquad (5.12) \end{aligned}$$

where the prediction of U_2 is denoted U_2^* and is computed using the following relation:

$$U_2^*(t) = \int_{L}^{L+D} p(L+D+\gamma,y)w(y,t)dy$$

$$+\int_{-L}^{L} q(L+D+\gamma,y)u(y,t)dy$$
$$+\int_{-L}^{-L-(D+\gamma)} r(L+D+\gamma,y)v(y,t)dy$$
$$+\int_{0}^{\gamma} p(L+D+\gamma,L+D+y)U_2^*(t+y-\gamma)dy \tag{5.13}$$

The equilibrium solution $(u,v,w)=0$ *is exponentially stabilized in the* $L_2\times H^1\times H^1$ *sense.*

5.3 Identical delay ($\gamma=0$)

5.3.1 Backstepping transformation

We use a series of two Volterra transformations to establish equivalency to a desireable target system. The first transformation directly comes from [43], and is as follows:

$$\eta(x,t)=u(x,t)-\int_{-x}^{x}\beta(x,y)u(y,t)dy \tag{5.14}$$

This will admit a gain kernel PDE on a sideways "hourglass" domain shape.

$$\partial_x^2\beta(x,y)-\partial_y^2\beta(x,y)=(\lambda+c)\beta(x,y) \tag{5.15}$$
$$\beta(x,x)=-\frac{(\lambda+c)}{2}x \tag{5.16}$$
$$\beta(x,-x)=0 \tag{5.17}$$

where $\beta\in H^1([-L,L])\times H^1([-L,L])$.

The second transformation is

$$\xi(x,t)=v(x,t)-\int_{x}^{-L}k(x,y)v(y,t)dy$$
$$-\int_{-L}^{L}l(x,y)u(y,t)dy$$

$$- \int_L^{-x} m(x,y)w(y,t)dy \tag{5.18}$$

$$\begin{aligned}\omega(x,t) = w(x,t) &- \int_L^{x} p(x,y)w(y,t)dy \\ &- \int_{-L}^{L} q(x,y)u(y,t)dy \\ &- \int_{-L}^{-x} r(x,y)v(y,t)dy \end{aligned} \tag{5.19}$$

$$\tag{5.20}$$

Differentiating (5.18) once in time and applying integration by parts admits

$$\begin{aligned}\partial_t \xi(x,t) = &-\partial_x v(x,t) + (k(x,-L) + l(x,-L))v(-L,t) \\ &+ (m(x,L) - l(x,L))w(L,t) - k(x,x)v(x,t) \\ &- m(x,-x)w(-x,t) \\ &+ \partial_y l(x,L)u(L,t) - \partial_y l(x,-L)u(-L,t) \\ &- \int_x^{-L} \partial_y k(x,y)v(y,t)dy \\ &+ \int_L^{-x} \partial_y m(x,y)w(y,t)dy \\ &- \int_{-L}^{L} (\partial_y^2 l(x,y) + \lambda)u(y,t)dy \end{aligned} \tag{5.21}$$

Differentiating (5.18) once in space:

$$\begin{aligned}\xi_x(x,t) = v_x(x,t) &+ k(x,x)v(x,t) + m(x,-x)w(-x,t) \\ &- \int_x^{-L} k_x(x,y)v(y,t)dy \\ &- \int_{-L}^{L} l_x(x,y)u(y,t)dy \\ &- \int_L^{-x} m_x(x,y)w(y,t)dy \end{aligned} \tag{5.22}$$

Differentiating (5.19) once in time and applying integration by parts admits

$$\begin{aligned}\partial_t \omega(x,t) = {} & \partial_x w(x,t) + (-p(x,L)+q(x,L))w(L,t) \\ & - (r(x,-L)-q(x,-L))v(-L,t) + p(x,x)w(x,t) \\ & + r(x,-x)v(-x,t) \\ & + \partial_y q(x,L)u(L,t) - \partial_y q(x,-L)u(-L,t) \\ & + \int_L^x \partial_y p(x,y)w(y,t)dy \\ & + \int_{-L}^{-x} \partial_y r(x,y)v(y,t)dy \\ & - \int_{-L}^{L} (\partial_y^2 l(x,y) + \lambda)u(y,t)dy \end{aligned} \tag{5.23}$$

Differentiating (5.19) once in space:

$$\begin{aligned}\partial_x \omega(x,t) = {} & \partial_x w(x,t) - p(x,x)w(x,t) + r(x,-x)v(-x,t) \\ & - \int_L^x \partial_x p(x,y)v(y,t)dy \\ & - \int_{-L}^{L} \partial_x l(x,y)u(y,t)dy \\ & - \int_{-L}^{-x} \partial_x r(x,y)v(y,t)dy \end{aligned} \tag{5.24}$$

These partial derivatives ω_t and ω_x leads to gain kernel PDEs for k,l,m,p,q,r:

$$\partial_x k(x,y) + \partial_y k(x,y) = 0 \tag{5.25}$$

$$k(x,-L) = -l(x,-L) \tag{5.26}$$

$$\partial_x m(x,y) - \partial_y m(x,y) = 0 \tag{5.27}$$

$$m(x,L) = l(x,L) \tag{5.28}$$

$$\partial_x l(x,y) = -\partial_y^2 l(x,y) - \lambda l(x,y) \tag{5.29}$$

$$\partial_y l(x,-L) = 0 \tag{5.30}$$

$$\partial_y l(x,L) = 0 \tag{5.31}$$

$$l(-L,y) = \beta(-L,y) \tag{5.32}$$

where now $k \in L^2([-L-D,-L]) \times L^2([-L-D,-L])$, $m \in L^2([-L-D,-L]) \times L^2([L,L+D])$ and $l \in L^2([-L-D,-L]) \times H^1([-L,L])$. Similarly,

$$\partial_x p(x,y) + \partial_y p(x,y) = 0 \tag{5.33}$$

$$p(x,L) = q(x,L) \tag{5.34}$$

$$\partial_x r(x,y) - \partial_y r(x,y) = 0 \tag{5.35}$$

$$r(x,-L) = -q(x,-L) \tag{5.36}$$

$$\partial_x q(x,y) = \partial_y^2 q(x,y) + \lambda q(x,y) \qquad y \in (-L,L) \tag{5.37}$$

$$\partial_y q(x,-L) = 0 \tag{5.38}$$

$$\partial_y q(x,L) = 0 \tag{5.39}$$

$$q(L,y) = \beta(L,y) \tag{5.40}$$

where now $p \in L^2([L,L+D]) \times L^2([L,L+D])$, $r \in L^2([L,L+D]) \times L^2([-L-D,-L))$ and $q \in L^2([L,L+D]) \times H^1([-L,L])$.

As one can note in Figure 5.2, we have essentially constructed a larger sideways hourglass domain. One may naturally be inclined to ask why the gain kernels cannot be solved all at once in this larger domain. The subtlety is in the mixed-class character of the gain kernels (which arise from the mixed-class nature of the model). The l,q kernels cannot be solved via method of characteristics like the k,m,p,r,β kernels can, as l,q are parabolic PDEs. Thus, one must initially solve the hyperbolic gain kernel PDE β (which has an terminal and initial condition emanating from $x = y = 0$ due to the Goursat nature of the PDE). β will then provide the sufficient terminal

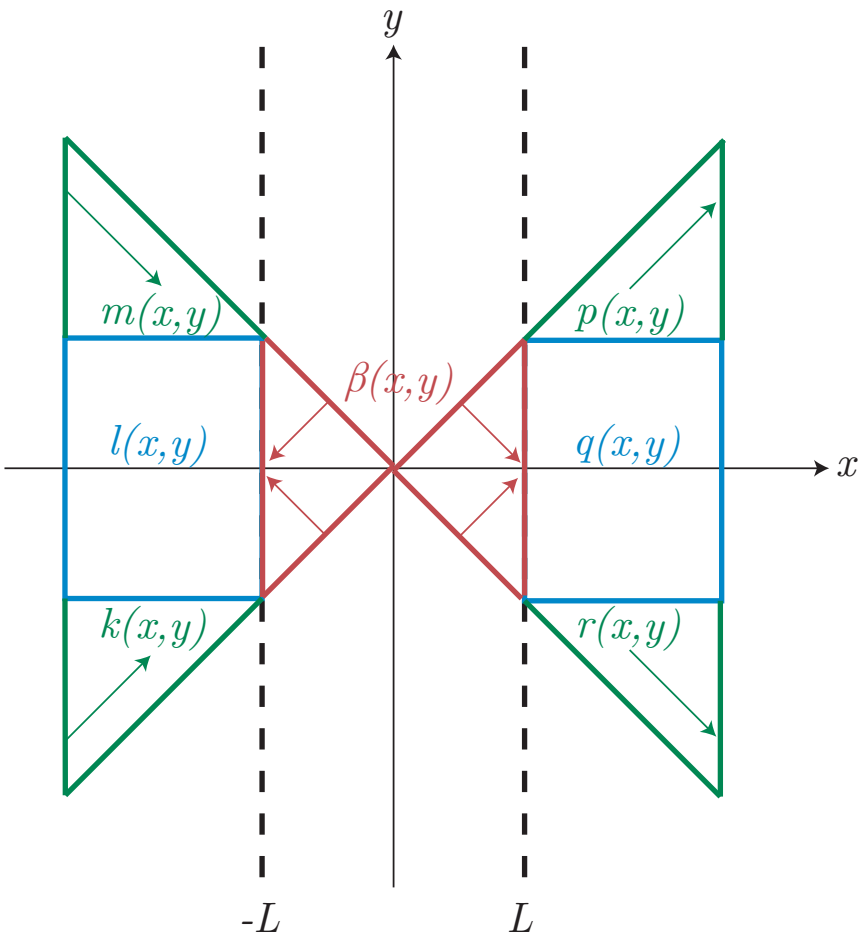

Figure 5.2: Domains of the gain kernels and how their boundary conditions interact

and initial conditions for l and q, respectively.

One may now question the viability of solving l; specifically l has a negative diffusion coefficient. This may initially appear to be suspicious, as backwards heat equations are ill-posed. However, we provide the *terminal* condition $l(-L,y)$, which leads us to, in fact, a well-posed problem for l. Therefore, there is no worry of ill-posedness in any of the equations.

After solving the parabolic gain kernels l,q, we are provided with the initial and terminal conditions to k,m,p,r, which can be trivially solved via method of characteristics.

These gain kernels will admit the following target system:

$$\partial_t \beta(x,t) = \partial_x^2 \beta(x,t) - c\beta(x,t) \tag{5.41}$$

$$\partial_t \xi(x,t) = -\partial_x \xi(x,t) \tag{5.42}$$

$$\partial_t \omega(x,t) = \partial_x \omega(x,t) \tag{5.43}$$

$$\partial_x \beta(-L,t) = \xi(-L,t) \tag{5.44}$$

$$\partial_x \beta(L,t) = \omega(L,t) \tag{5.45}$$

$$\xi(-L-D,t) = 0 \tag{5.46}$$

$$\omega(L+D,t) = 0 \tag{5.47}$$

5.3.2 Stability of target system

The target system given by (5.41)-(5.47) must be shown to be exponentially stable. We propose the following transformation to make this proof more tractable:

$$\begin{aligned} \phi(x,t) = \beta(x,t) - f(x)\xi(-L,t) \\ - g(x)\omega(L,t) \end{aligned} \tag{5.48}$$

where f, g are defined by

$$f(x) = \left(-\frac{1}{L}x^2 + \frac{1}{2}x\right) \tag{5.49}$$

$$g(x) = \left(\frac{1}{L}x^2 + \frac{1}{2}x\right) \tag{5.50}$$

This transformation allows us to find the following system:

$$\partial_t \phi(x,t) = \partial_x^2 \phi(x,t) - c\phi(x,t)$$

$$+a(x)\xi(-L,t)+b(x)\omega(L,t)$$
$$-f(x)\partial_x\xi(-L,t)-g(x)\partial_x\omega(L,t) \tag{5.51}$$
$$\partial_t\xi(x,t)=-\partial_x\xi(x,t) \tag{5.52}$$
$$\partial_t\omega(x,t)=\partial_x\omega(x,t) \tag{5.53}$$
$$\partial_x\phi(-L,t)=0 \tag{5.54}$$
$$\partial_x\phi(L,t)=0 \tag{5.55}$$
$$\xi(-L-D,t)=0 \tag{5.56}$$
$$\omega(L+D,t)=0 \tag{5.57}$$

where a,b are defined as

$$a(x)=cf(x)-\frac{1}{2L} \tag{5.58}$$
$$b(x)=cg(x)+\frac{1}{2L} \tag{5.59}$$

We let $\bar{a},\bar{b},\bar{f},\bar{g}$ be the sup norm for their respective functions.

Lemma 13. *The system given by* (5.51)-(5.57) *is exponentially stable in the* $L^2\times H^1\times H^1$ *sense.*

Proof. Consider the Lyapunov function

$$\begin{aligned}V(t)=&\int_{-L}^{L}\frac{1}{2}\phi(x,t)^2dx\\&+\int_{-L-D}^{-L}\frac{d_1}{2}e^{-\delta_1 x}\xi(x,t)^2dx\\&+\int_{-L-D}^{-L}\frac{h_1}{2}e^{-\eta_1 x}\partial_x\xi(x,t)^2dx\\&+\int_{L}^{L+D}\frac{d_2}{2}e^{\delta_2 x}\omega(x,t)^2dx\\&+\int_{L}^{L+D}\frac{h_2}{2}e^{\eta_2 x}\partial_x\omega(x,t)^2dx\end{aligned} \tag{5.60}$$

The Lie derivative of this Lyapunov function gives

$$\begin{aligned}
\dot{V} = &\int_{-L}^{L} \phi(x,t)\partial_x^2\phi(x,t)dx \\
&- \int_{-L}^{L} c\phi(x,t)^2 dx \\
&+ \int_{-L}^{L} a(x)\phi(x,t)\xi(-L,t)dx \\
&+ \int_{-L}^{L} b(x)\phi(x,t)\omega(L,t)dx \\
&- \int_{-L}^{L} f(x)\phi(x,t)\partial_x\xi(-L,t)dx \\
&- \int_{-L}^{L} g(x)\phi(x,t)\partial_x\omega(L,t)dx \\
&- \int_{-L-D}^{-L} \frac{d_1}{2} e^{\delta_1 x}\xi(x,t)\partial_x\xi(x,t)dx \\
&- \int_{-L-D}^{-L} \frac{h_1}{2} e^{\eta_1 x}\partial_x\xi(x,t)\partial_x^2\xi(x,t)dx \\
&+ \int_{L}^{L+D} \frac{d_2}{2} e^{\delta_2 x}\omega(x,t)\partial_x\omega(x,t)dx \\
&+ \int_{L}^{L+D} \frac{h_2}{2} e^{\eta_2 x}\partial_x\omega(x,t)\partial_x^2\omega(x,t)dx
\end{aligned} \tag{5.61}$$

Then, integrating by parts, and applying Young's and Poincare's inequalities appropriately admits

$$\begin{aligned}
\dot{V} \leq &- \int_{-L}^{L} \left(c + \frac{1}{2}\right)\phi(x,t)^2 dx \\
&+ \int_{-L}^{L} \left(\frac{\bar{a}}{2\varepsilon_1} + \frac{\bar{b}}{2\varepsilon_2} + \frac{\bar{f}}{2\varepsilon_3} + \frac{\bar{g}}{2\varepsilon_4}\right)\phi(x,t)^2 dx \\
&- \int_{-L-D}^{-L} \frac{d_1\delta_1}{2} e^{-\delta_1 x}\xi(x,t)^2 dx \\
&- \int_{-L-D}^{-L} \frac{h_1\eta_1}{2} e^{-\eta_1 x}\partial_x\xi(x,t)^2 dx \\
&- \left(\frac{d_1}{2}e^{-\delta_1 L} - \varepsilon_1\bar{a}L\right)\xi(-L,t)^2 \\
&- \left(\frac{h_1}{2}e^{-\eta_1 L} - \varepsilon_3\bar{f}L\right)\partial_x\xi(-L,t)^2
\end{aligned}$$

$$
\begin{aligned}
&- \int_L^{L+D} \frac{d_2\delta_2}{2} e^{\delta_2 x}\omega(x,t)^2 dx \\
&- \int_L^{L+D} \frac{h_2\eta_2}{2} e^{\eta_2 x}\partial_x\omega(x,t)^2 dx \\
&- \left(\frac{d_2}{2}e^{\delta_2 L} - \varepsilon_2\bar{b}L\right)\omega(L,t)^2 \\
&- \left(\frac{h_2}{2}e^{\eta_2 L} - \varepsilon_4\bar{g}L\right)\partial_x\omega(L,t)^2
\end{aligned}
\tag{5.62}
$$

Where $\varepsilon_i > 0$ for $i = 1,2,3,4$ are to be chosen. These parameters arise from the application of Young's inequality. It is then clear that one can choose these ε_i sufficiently large so that $c + \frac{1}{2} > \frac{\bar{a}}{2\varepsilon_1} + \frac{\bar{b}}{2\varepsilon_2} + \frac{\bar{f}}{2\varepsilon_3} + \frac{\bar{g}}{2\varepsilon_4}$. Following this, one can select the pairs d_i, δ_i and h_i, η_i for $i = 1,2$ such that the conditions $\frac{d_1}{2}e^{-\delta_1 L} > \varepsilon_1\bar{a}L, \frac{h_1}{2}e^{-\eta_1 L} - \varepsilon_3\bar{f}L$, $\frac{d_2}{2}e^{\delta_2 L} > \varepsilon_2\bar{b}L$ and $\frac{h_2}{2}e^{\eta_2 L} > \varepsilon_4\bar{g}L$ are fulfilled. By enforcing these conditions with our choices of $\varepsilon_i, d_j, \delta_j, h_j, \eta_j$, we can collapse the inequality into a relatively simple form:

$$
\dot{V}(t) \leq -CV(t) \tag{5.63}
$$

where now C is now defined by

$$
\begin{aligned}
C = \min\Bigg\{ & c + \frac{1}{2} - \left(\frac{\bar{a}}{2\varepsilon_1} + \frac{\bar{b}}{2\varepsilon_2} + \frac{\bar{f}}{2\varepsilon_3} + \frac{\bar{g}}{2\varepsilon_4}\right), \\
& \frac{\delta_1}{2}, \frac{\delta_2}{2}, \frac{\eta_1}{2}, \frac{\eta_2}{2} \Bigg\}
\end{aligned}
\tag{5.64}
$$

Applying the comparison principle to (5.63), one can find

$$
V(t) \leq e^{-Ct}V(0) \tag{5.65}
$$

It follows that there exists some constant M where now

$$||(\phi,\xi,\omega)|| \leq Me^{-\frac{C}{2}t}||\phi(0),\xi(0),\omega(0)|| \tag{5.66}$$

where this norm is defined as $||(\phi,\xi,\omega)|| = ||\phi||_{L_2} + ||\xi||_{H^1} + ||\omega||_{H^1}$. This concludes the proof. □

Due to the invertibility of the transformations (5.14),(5.18),(5.19),(5.48), we can establish an equivalent stability condition on the original system with the designed feedback control applied.

5.3.3 Feedback control laws

The feedback control laws are found from evaluating (5.18) and (5.19) at their respective control boundaries $x = -L-D$ and $x = L+D$, and are found to be

$$\begin{aligned} U_1(t) &= \int_{-L-D}^{-L} k(-L-D,y)v(y,t)dy \\ &\quad + \int_{-L}^{L} l(-L-D,y)u(y,t)dy \\ &\quad + \int_{L}^{L+D} m(-L-D,y)w(y,t)dy \end{aligned} \tag{5.67}$$

$$\begin{aligned} U_2(t) &= \int_{L}^{L+D} p(L+D,y)w(y,t)dy \\ &\quad + \int_{-L}^{L} q(L+D,y)u(y,t)dy \\ &\quad + \int_{-L}^{-L-D} r(L+D,y)v(y,t)dy \end{aligned} \tag{5.68}$$

5.4 Distinct delay

In the distinct delay case, one controller (with the longer input delay) will no longer be feasible, as this controller must begin to anticipate future values of the opposing controller,

leading to a noncausal formulation.

The proposed workaround to accommodate the distinct delay case involves *domain extension*. We begin by defining a new auxiliary control $U^*(t)$, and the augmented system

$$\partial_t \bar{w}(x,t) = \partial_x \bar{w}(x,t) \tag{5.69}$$

$$\bar{w}(L+(D+\delta),t) = U_2^*(t) \tag{5.70}$$

The augmented system (5.69),(5.70) serve to extend the system (5.6),(5.10). By choosing our controller U_2 as

$$U_2(t) = U_2^*(t-\delta) \tag{5.71}$$

one can note that the solution of $\bar{w}$ can be expressed in the following piecewise form:

$$\bar{w}(x,t) = \begin{cases} w(x,t) & x \in (L, L+D) \\ U_2^*(t+(x-(L+D))) & \text{otherwise} \end{cases} \tag{5.72}$$

The main takeaway from this is that by applying our control via the relation (5.71), a relation is established between the extended system $\bar{w}$ and the original system w.

This allows us to design a controller in the identical input delay case for $D+\gamma$, and select the controller U_2 from the designed control U_2^*.

From the previous section (but with the domain as $D+\gamma$), we have the following controllers for the augmented system $(u, v, \bar{w})$:

$$\begin{aligned} U_1(t) = &\int_{-L-(D+\gamma)}^{-L} k(-L-(D+\gamma),y)v(y,t)dy \\ &+ \int_{-L}^{L} l(-L-(D+\gamma),y)u(y,t)dy \\ &+ \int_{L}^{L+D} m(-L-(D+\gamma),y)\bar{w}(y,t)dy \end{aligned} \tag{5.73}$$

$$U_2^*(t) = \int_L^{L+D} p(L+D+\gamma,y)\bar{w}(y,t)dy + \int_{-L}^{L} q(L+D+\gamma,y)u(y,t)dy + \int_{-L}^{-L-(D+\gamma)} r(L+D+\gamma,y)v(y,t)dy \tag{5.74}$$

$$\tag{5.75}$$

Using the representation (5.72) in conjunction with the relationship between the predicted controller U_2^* and U_2 (5.71), one can derive the feedback controllers (5.11),(5.12), and (5.13).

5.5 Conclusion

A method for designing bilateral backstepping feedback controllers for a parabolic equation with input delays is presented. The unstable parabolic equation with input delays is transformed into a mixed-class system of three partial differential equations. Due to the mixed-class nature of this system, the gain PDEs that are solved are also of a mixed-class type. Since there exists favorable structure in the system, a solution can be determined through cascading the solutions of the gain kernel PDEs.

The problem is initially solved for the case of identical delays, which is then extended to the distinct delay case. The method of how the distinct delays is solved is somewhat lackluster, in the sense that the controller essentially adds "artificial" delay to build a prediction of the future states. For simpler systems (and perhaps even more complex ones), if one can find a prediction method that does not rely on adding delay, the stabilization of systems such as these would be faster, as well as being more of an elegant solution.

The results in this paper, however, do raise several new questions in bilateral backstepping control – dealing primarily with the domain of the control kernel, and its impact in the type of systems we can stabilize using the basic Volterra transformation. In this paper, the sideways

hourglass domain was augmented by additional square and triangular domains to construct a "larger" hourglass domain. One may ask the questions "Must this domain be an hourglass? How might one incorporate different domains, and how would this affect the control design process?" These questions are subject to future work, and may provide insight into developing a more general, nonlinear backstepping transformation for PDEs.

5.6 Acknowledgements

Chapter 5 is unpublished research co-authored between S.Chen, R. Vazquez, M. Krstic. The dissertation author was the primary investigator and co-author of this work.

Chapter 6

Folding Bilateral Backstepping Output-Feedback Control Design For an Unstable Parabolic PDE

6.1 Introduction

Parabolic partial differential equations (PDEs) describe numerous physical processes, which include but are not limited to heat transfer, chemical reaction-diffusion processes, tumor angiogenesis [11], predator-prey Lotka-Volterra population models [23], opinion dynamics (of the Fischer-Kolmogorov-Petrovsky-Piskunov type equation [2]), free-electron plasma diffusion, and flows through porous media [42].

Previous results in boundary control for 1-D PDEs has been largely focused on unilateral boundary controllers, i.e. controllers acting on a single boundary. Results have been generated for a wide variety of parabolic PDE systems and objectives, beginning with the classical scalar 1-D PDE with homogeneous media results [30]. Other extensions to the parabolic PDE boundary control case introduce nonhomgeneous media (such as [37]), parallel interconnected parabolic

PDE systems [45], series interconnected parabolic PDE systems [41], and output feedback extensions for coupled parabolic PDE [33]. Some work that is tangentially related is that of [50],[51], which investigates a problem of using an in-domain actuation to control a parabolic PDE.

The notion of bilateral boundary control is partially motivated by boundary control of balls in $\mathbb{R}^n$ [44], in which the controls actuate on the surface of the n-dimensional ball. The analogous case (in 1-D) is a controller actuating on the boundary of the 1-dimensional ball, i.e., the endpoints of an interval. Bilateral control has been studied in some contexts for both hyperbolic and parabolic PDE systems. [5] studies bilateral controllers achieving minimum-time convergence in coupled first-order hyperbolic systems via a Fredholm transformation technique, while [43] additionally studies bilateral control for diffusion-reaction equations, albeit with the limitatin of a symmetric Volterra transformation. [8] studies a nonlinear viscous Hamilton-Jacobi PDE, which likewise uses the symmetric Volterra transformation from [43].

Boundary observer design is of equal (and perhaps arguably more) importance when compared with the boundary controller design. Many results have been generated as a dual problem to the boundary controller case. In [36], a boundary observer design for parabolic PDEs is formulated, with measurements taken at a boundary (in both collocated and anticollocated cases). [6] studies a coupled parabolic PDE system with identical diffusion coefficients. [10] recovers a result for coupled parabolic PDEs with varying diffusion coefficients.

The main contribution of the paper are results for bilateral control of diffusion-reaction equations with spatially-varying reaction via the method of "folding," i.e. using an arbitrarily defined domain separation and transformation to design the boundary controllers. The idea of folding has been touched upon in the hyperbolic context [17], where the authors have explored a linearized Rijke tube model. The folding technique admits a design parameter (called the folding point) whose choice influences the control effort exerted by the boundary controllers. Additionally, a state-estimator is designed to complement the state-feedback controller. The

state-estimator is an interesting new development in which collocated measurements are taken from any arbitrary point in the interior of the PDE, and the folding approach applied. Finally, the output feedback is formulated by combining both the state-feedback and state-estimation.

The state observer design is an interesting development, as it generates a result where measurements are taken at a single measure zero point in the interior. It is of physical importance, as measurements at the boundary are not necessarily guaranteed for a given realization. [40] has also investigated observer designs where measurements are not given at a boundary, rather, as a weighted average (the state appearing underneath a bounded integral operator). A related result is [20], in which the authors consider the combination of boundary measurements with a single interior measurement to achieve estimation convergence for semilinear parabolic problems.

The primary technical difficulty in the paper is compensating the folding-type boundary conditions, which arises due to the regularity property of the solutions. In hyperbolic PDE, this constitutes an imposition of continuity – a first-order compatibility condition. However, in parabolic PDE, one must treat second-order compatibility conditions existing at the same point, which will require additional correctional designs to compensate.

The paper is organized as follows: the notations and model are introduced in Section 8.1. The output feedback controller consisting of the state-feedback and state-estimator designs is developed in Section 6.3. The gain kernel well posedness is studied in Section 8.4. Some simulations for various folding scenarios are given and analyzed in Section 6.5. Finally, the paper is concluded in Section 6.6.

6.2 Preliminaries

6.2.1 Notation

The partial operator is notated using the del-notation, i.e.

$$\partial_x f := \frac{\partial f}{\partial x}$$

$L^2(I_o)$ is defined as the the L^2 space on the interval I_o, equipped with the norm

$$||f||_{L^2(I_o)} = \left(\int_{I_o} f^2 \, d\mu \right)^{\frac{1}{2}}$$

We also consider the standard inner product (that induces the standard norm) for L^2:

$$\langle f, g \rangle_{L^2(I_o)} = \int_{I_o} f \cdot g \, d\mu$$

For compact notation, we will let $L^2(I_o)$ be represented merely as L^2, where the interval is implied by the function. The norm notation ($||\cdot||$) is used to notate the function norm over the vector 2-norm (notated with $|\cdot|_2$). If the norm is taken over a matrix function, then the induced 2-norm is implied, i.e. for vector-valued function f and matrix-valued function F:

$$||f||_{L^2} := \left(\int_{I_o} ||f||_2^2 \, d\mu \right)^{\frac{1}{2}} \quad ||F||_{L^2} := \left(\int_{I_o} ||F||_{2,i}^2 \, d\mu \right)^{\frac{1}{2}}$$

Furthermore, if f is a function of the space-time tuple (x,t), the norm is assumed to be the norm in space (x) unless otherwise stated. The written x-dependence is dropped, i.e.

$$||f(x,t)||_{L^2} = ||f(t)||_{L^2} := \left(\int_{I_o} |f(t)|_2^2 \, d\mu \right)^{\frac{1}{2}}$$

We will introduce the notion of stability in the sense of a norm. Rigorously, this refers to the norm in which stability is derived. Per example, stability in the sense of L^2 refers to a stability estimate using L^2 norms:

$$||f(t)||_{L^2} \leq M\,||f(t_0)||_{L^2}$$

Elements of a matrix A are denoted with lowercase a_{ij}, with the subscripts defining the i-th row and j-th column.

6.2.2 Model and problem formulation

We consider the following reaction-diffusion PDE for u on the domain $[0,\infty)\times(-1,1)$:

$$\partial_t \bar{u}(y,t) = \varepsilon\partial_y^2\bar{u}(y,t) + \nu(y)\partial_y\bar{u}(y,t) + \bar{\lambda}(y)\bar{u}(y,t) \tag{6.1}$$

$$\bar{u}(-1,t) = \bar{\mathcal{U}}_1(t) \tag{6.2}$$

$$\bar{u}(1,t) = \bar{\mathcal{U}}_2(t) \tag{6.3}$$

It is assumed that $\varepsilon > 0$ for well-posedness, and $\nu,\bar{\lambda} \in C^1((-1,1))$. The controllers operate at $x = 1$ and $x = -1$, and are denoted $\bar{\mathcal{U}}_1(t), \bar{\mathcal{U}}_2(t)$, respectively. We define the following transformation:

$$u(y,t) = \exp\left(\int_{-1}^{y} \frac{\nu(z)}{2\varepsilon}dz\right)\bar{u}(y,t) \tag{6.4}$$

and with the appropriate parameter definitions, we find the equivalent system

$$\partial_t u(y,t) = \varepsilon\partial_y^2 u(y,t) + \lambda(y)u(y,t) \tag{6.5}$$

$$u(-1,t) = \bar{\mathcal{U}}_1(t) =: \mathcal{U}_1(t) \tag{6.6}$$

$$u(1,t) = \exp\left(\int_{-1}^{1} \frac{\nu(z)}{2\varepsilon} dz\right) \bar{\mathcal{U}}_2(t) =: \mathcal{U}_2(t) \tag{6.7}$$

The transformation (6.4) removes the advection/convection term in (6.1). The attenuation and/or amplification of control effort in the controllers matches intuition – the controller upstream of the "average" convection requires less control effort, while the controller downstream requires more control effort (average, as the sign of ν can vary across the domain). In this paper, we will assume that $\nu = 0$, but in general, the methodology can compensate convection phenomena.

6.3 Output-feedback control design

The output feedback is designed via solving two subproblems: the state-feedback design, and state-estimator design. The output-feedback result is then recovered by replacing the state-feedback control law with the state-estimate, and the resulting stability of the interconnected systems is proven.

6.3.1 Model transformation for control via folding

The folding approach entails selecting a point $y_0 \in (-1,1)$ in which the scalar parabolic PDE system u is "folded" into a 2×2 coupled parabolic system. A special case $y_0 = 0$ (dividing into a symmetric problem) recovers the result of [43]. We define the the folding spatial transformations as

$$x = (y_0 - y)/(1 + y_0) \qquad y \in (-1, y_0) \tag{6.8}$$

$$x = (y - y_0)/(1 - y_0) \qquad y \in (y_0, 1) \tag{6.9}$$

admits the following states:

$$U(x,t) := \begin{pmatrix} u_1(x,t) \\ u_2(x,t) \end{pmatrix} = \begin{pmatrix} u(y_0 - (1+y_0)x, t) \\ u(y_0 + (1-y_0)x, t) \end{pmatrix} \tag{6.10}$$

whose dynamics are governed by the following system:

$$\partial_t U(x,t) = E\partial_x^2 U(x,t) + \Lambda(x)U(x,t) \tag{6.11}$$

$$\alpha U_x(0,t) = -\beta U(0,t) \tag{6.12}$$

$$U(1,t) = \mathcal{U}(t) \tag{6.13}$$

with the parameters given by :

$$\begin{aligned} E &:= \operatorname{diag}(\varepsilon_1, \varepsilon_2) \\ &:= \operatorname{diag}\left(\frac{\varepsilon}{(1+y_0)^2}, \frac{\varepsilon}{(1-y_0)^2} \right) \end{aligned} \tag{6.14}$$

$$\begin{aligned} \Lambda(x) &:= \operatorname{diag}(\lambda_1(x), \lambda_2(x)) \\ &:= \operatorname{diag}(\lambda(y_0 - (1+y_0)x), \lambda(y_0 + (1-y_0)x)) \end{aligned} \tag{6.15}$$

$$\alpha := \begin{pmatrix} 1 & a \\ 0 & 0 \end{pmatrix} \tag{6.16}$$

$$\beta := \begin{pmatrix} 0 & 0 \\ 1 & -1 \end{pmatrix} \tag{6.17}$$

$$a := (1+y_0)/(1-y_0) \tag{6.18}$$

The boundary conditions at $x = 0$ are curious. While they may initially appear to be encapsulated as Robin boundary conditions in (8.9), they are actually compatibility conditions that arise from imposing continuity in the solution at the folding point. Analogous conditions have been

considered in some previous parabolic backstepping work in [41], albeit in a differing context.

Assumption. *The folding point y_0 is constricted to the half domain $(-1,0]$ without loss of generality. The case $y_0 \in [0,1)$ can be recovered by using a change in spatial variables $\hat{y} = -y$ and performing the same folding technique. By choosing y_0 in this manner, we impose an ordering $\varepsilon_1 > \varepsilon_2$.*

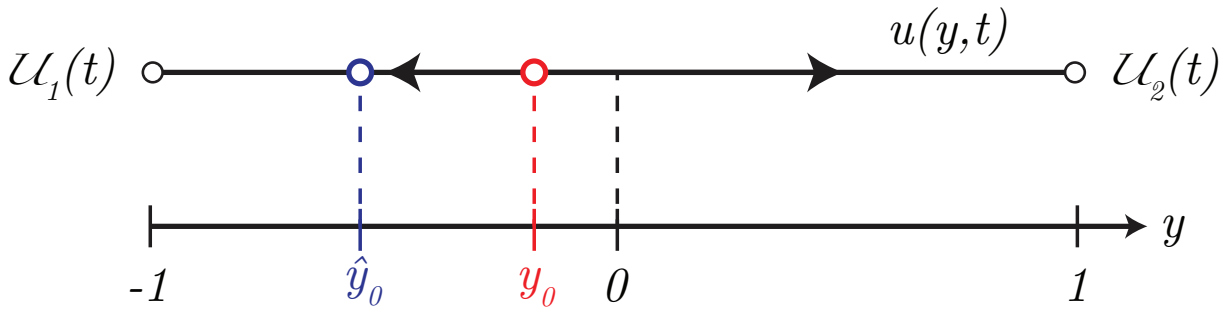

Figure 6.1: System schematic of diffusion-reaction equation with two boundary inputs. The control folding point y_0 and the measurement location $\hat{y}_0$ can be arbitrarily chosen on the interior, independent of one another.

6.3.2 State-feedback design

The backstepping state-feedback control design is accomplished with two consecutive backstepping transformations. The first transformation is a 2×2 Volterra integral transformation of the second kind:

$$W(x,t) = U(x,t) - \int_0^x K(x,y)U(y,t)dy \tag{6.19}$$

where $K(x,y) \in C^2(\mathcal{T})$ is a 2×2 matrix of kernel elements (k_{ij}), with $\mathcal{T} := \{(x,y) \in \mathbb{R}^2 | 0 \leq y \leq x \leq 1\}$, and $W(x,t) := \begin{pmatrix} w_1(x,t) & w_2(x,t) \end{pmatrix}^T$. The inverse transformation is analogous:

$$U(x,t) = W(x,t) - \int_0^x \bar{K}(x,y)W(y,t)dy \tag{6.20}$$

The corresponding target system for (6.19) is chosen to be

$$\partial_t W(x,t) = E\partial_x^2 W(x,t) - CW(x,t) + G[K](x)W(x,t) \tag{6.21}$$

$$\alpha\partial_x W(0,t) = -\beta W(0,t) \tag{6.22}$$

$$W(1,t) = \mathcal{V}(t) \tag{6.23}$$

where $\mathcal{V}(t) = \begin{pmatrix} 0 & \nu_2(t) \end{pmatrix}^T$ is an auxiliary control which is designed later in the paper. The controller $\mathcal{U}(t)$ can be expressed as an operator of $\mathcal{V}(t)$ by evaluating (6.19) for $x = 1$:

$$\mathcal{U}(t) := \mathcal{V}(t) + \int_0^1 K(1,y)U(y,t)dy \tag{6.24}$$

The matrix C can be arbitrarily chosen such that $C \succ 0$, but for simplicity of analysis, we select a diagonal matrix $C = \text{diag}(c_1, c_2)$ with $c_1, c_2 > 0$. The matrix-valued operator $G[\cdot](x)$ acting on K is given by

$$G[K](x) = \begin{pmatrix} 0 & 0 \\ (\varepsilon_2 - \varepsilon_1)\partial_y k_{21}(x,x) & 0 \end{pmatrix} =: \begin{pmatrix} 0 & 0 \\ g[k_{21}](x) & 0 \end{pmatrix} \tag{6.25}$$

Imposing the conditions (8.8), (8.9), (6.19), (8.20)-(8.22) admits the following companion gain kernel PDE system for $K(x,y)$:

$$\begin{aligned} E\partial_x^2 K(x,y) - \partial_y^2 K(x,y)E &= K(x,y)\Lambda(y) + CK(x,y) \\ &\quad - G[K](x)K(x,y) \end{aligned} \tag{6.26}$$

$$\begin{aligned} \partial_y K(x,x)E + E\partial_x K(x,x) &= -E\frac{d}{dx}K(x,x) - \Lambda(x) \\ &\quad - C + G[K](x) \end{aligned} \tag{6.27}$$

$$EK(x,x) - K(x,x)E = 0 \tag{6.28}$$

$$K(x,0)E\partial_x U(0) = \partial_y K(x,0)EU(0) \tag{6.29}$$

It is clear to see that by imposing (6.28), the definition for $G[K](x)$ can be recovered from (6.27) Upon first inspection, the resulting kernel PDE is very similar to those found in [45],[18]. However, one may see that (6.29) is different, and in fact quite new in backstepping designs. (6.29) arises due to the folding boundary condition (8.9). Surprisingly enough, if one analyzes (6.29) componentwise and employs (8.9), "anti-folding" conditions on K can be recovered, which preserve continuity in the spatial derivative of the state (as opposed to folding conditions preserving continuity in the state). The folding conditions that arise from (6.29) are:

$$\varepsilon_1 k_{11}(x,0) - a\varepsilon_2 k_{12}(x,0) = 0 \tag{6.30}$$

$$\varepsilon_1 \partial_y k_{11}(x,0) + \varepsilon_2 \partial_y k_{12}(x,0) = 0 \tag{6.31}$$

$$\varepsilon_1 k_{21}(x,0) - a\varepsilon_2 k_{22}(x,0) = 0 \tag{6.32}$$

$$\varepsilon_1 \partial_y k_{21}(x,0) + \varepsilon_2 \partial_y k_{22}(x,0) = 0 \tag{6.33}$$

or, more compactly written,

$$\tilde{\alpha} K(x,0) = \tilde{\beta} \partial_y K(x,0) \tag{6.34}$$

where

$$\tilde{\alpha} := \begin{pmatrix} 1 & -a \\ 0 & 0 \end{pmatrix}, \quad \tilde{\beta} := \begin{pmatrix} 0 & 0 \\ 1 & 1 \end{pmatrix} \tag{6.35}$$

The kernel equations for the inverse kernels $\bar{K}$ are similar to those of K, and are derived in an analogous manner:

$$\begin{aligned} E\partial_x^2\bar{K}(x,y) - \partial_y^2\bar{K}(x,y)E &= -\bar{K}(x,y)(C - G[\bar{K}](y)) \\ &\quad - \Lambda(x)\bar{K}(x,y) \end{aligned} \tag{6.36}$$

$$\begin{aligned} \partial_y\bar{K}(x,x)E + E\partial_x\bar{K}(x,x) &= -E\frac{d}{dx}\bar{K}(x,x) + \Lambda(x) \\ &\quad + C - G[\bar{K}](x) \end{aligned} \tag{6.37}$$

$$E\bar{K}(x,x) - \bar{K}(x,x)E = 0 \tag{6.38}$$

$$\bar{K}(x,0)E\partial_x W(0) = \partial_y\bar{K}(x,0)EW(0) \tag{6.39}$$

The second transformation is designed to admit an expression for the auxiliary controller $\mathcal{V}(t) = \begin{pmatrix} 0 & \nu_2(t) \end{pmatrix}^T$. The goal of $\nu_2(t)$ is to remove the potentially destabilizing effect of the coupling term $G[K](x)$. The second set of transformations is:

$$\omega_1(x,t) = w_1(x,t) \tag{6.40}$$

$$\begin{aligned} \omega_2(x,t) = w_2(x,t) &- \int_0^x \begin{pmatrix} q(x,y) & p(x-y) \end{pmatrix} W(y,t)dy \\ &- \int_x^1 \begin{pmatrix} r(x,y) & 0 \end{pmatrix} W(y,t)dy \end{aligned} \tag{6.41}$$

Let $\Omega(x,t) := \begin{pmatrix} \omega_1(x,t) & \omega_2(x,t) \end{pmatrix}^T$. The inverse transformations are given by

$$w_1(x,t) = \omega_1(x,t) \tag{6.42}$$

$$\begin{aligned} w_2(x,t) = \omega_2(x,t) &- \int_0^x \begin{pmatrix} \bar{q}(x,y) & \bar{p}(x-y) \end{pmatrix} \Omega(y,t)dy \\ &- \int_x^1 \begin{pmatrix} \bar{r}(x,y) & 0 \end{pmatrix} \Omega(y,t)dy \end{aligned} \tag{6.43}$$

We impose the following target system dynamics:

$$\partial_t \Omega(x,t) = E\partial_x^2 \Omega(x,t) - C\Omega(x,t) \tag{6.44}$$

$$\alpha\partial_x \Omega(0,t) = -\beta\Omega(0,t) \tag{6.45}$$

$$\Omega(1,t) = 0 \tag{6.46}$$

Noting that $G[K](x)$ is parametrized by the difference in diffusion coefficients $\varepsilon_1 - \varepsilon_2$, one can interpret (6.41) to be the *correction* factor to the first transformation in presence of selecting a non-trivial folding point. Indeed, when the folding point is chosen to be the midpoint, $G[K](x) \equiv 0$ (and therefore (6.41) becomes an identity transformation). This necessity for correction factors is to compensate for the behavior unique to bilateral control design in parabolic PDE, and is not observed in the results featuring bilateral control design of hyperbolic PDE systems [5].

The transformation (6.41) features two major components – a Volterra integral operator in w_2 characterized by kernel p, a Volterra integral operator in w_1 characterized by kernel q, and an *forwarding* type of transformation in w_1 characterized by kernel r. The kernels p,q are defined on the domain $\mathcal{T}$, while r is defined on the domain $\mathcal{T}_{\mathrm{u}} := \{(x,y) \in \mathbb{R}^2 | 0 \leq x \leq y \leq 1\}$.

The transformation (6.41) with the conditions (8.20)-(8.22),(6.44)-(6.46) imposed will admit the following definition for p and kernel PDE for q:

$$p(x) = a^{-1} q(x,0) \tag{6.47}$$

$$\begin{aligned} \varepsilon_2 \partial_x^2 q(x,y) - \varepsilon_1 \partial_y^2 q(x,y) &= (c_2 - c_1) q(x,y) \\ &\quad + g[k_{21}](y) p(x-y) \end{aligned} \tag{6.48}$$

$$\varepsilon_2 \partial_x^2 r(x,y) - \varepsilon_1 \partial_y^2 r(x,y) = (c_2 - c_1) r(x,y) \tag{6.49}$$

subject to the following boundary conditions:

$$\partial_y q(x,x) = \partial_y r(x,x) + \frac{g[k_{21}](x)}{\varepsilon_2 - \varepsilon_1} \tag{6.50}$$

$$r(x,x) = q(x,x) \tag{6.51}$$

$$\partial_y q(x,0) = a^2 p'(x) = a\partial_x q(x,0) \tag{6.52}$$

$$r(x,1) = 0 \tag{6.53}$$

In addition, two initial conditions on r can be found from enforcing (8.21) on (6.41):

$$r(0,y) = 0 \tag{6.54}$$

$$\partial_x r(0,y) = \mathbf{1}_{\{y=0\}}(y)\frac{g[k_{21}](0)}{\varepsilon_2 - \varepsilon_1} \tag{6.55}$$

where $\mathbf{1}_{\{y=0\}}(y)$ is the indicator function equal to 1 on the set $\{y=0\}$ and 0 otherwise. This is quite unusual when compared to standard backstepping techniques, but is necessary to resolve the condition (6.50),(6.51) at $x = y = 0$. Despite having this unusual initial condition, the target system and gain kernels are unaffected as $\partial_x r(0,y)$ only appears underneath an integration operation. The kernel equations for the inverse kernels $\bar{p}, \bar{q}, \bar{r}$ are similar to those of p, q respectively:

$$\bar{p}(x) = a^{-1}\bar{q}(x,0) \tag{6.56}$$

$$\begin{aligned}\varepsilon_2\partial_x^2\bar{q}(x,y) - \varepsilon_1\partial_y^2\bar{q}(x,y) &= (c_1 - c_2)\bar{q}(x,y) \\ &\quad - g[k_{21}](x)\bar{p}(x-y)\end{aligned} \tag{6.57}$$

$$\varepsilon_2\partial_x^2\bar{r}(x,y) - \varepsilon_1\partial_y^2\bar{r}(x,y) = (c_2 - c_1)\bar{r}(x,y) \tag{6.58}$$

with boundary conditions

$$\partial_y \bar{q}(x,x) = \partial_y \bar{r}(x,x) + \frac{g[k_{21}](x)}{\varepsilon_1 - \varepsilon_2} \tag{6.59}$$

$$\bar{r}(x,x) = \bar{q}(x,x) \tag{6.60}$$

$$\partial_y \bar{q}(x,0) = -a^2 \bar{p}'(x) = -a\partial_x \bar{q}(x,0) \tag{6.61}$$

As in the forward transformation, initial conditions on $\bar{r}$ can be found:

$$r(0,y) = 0 \tag{6.62}$$

$$\partial_x r(0,y) = \mathbf{1}_{\{y=0\}}(y) \frac{g[k_{21}](0)}{\varepsilon_1 - \varepsilon_2} \tag{6.63}$$

An interpretation of the (p,q,r) coupled kernel is that of a hyperbolic PDE (q,r) defined on the square $\mathcal{T} \cup \mathcal{T}_{\mathrm{u}}$, subject to non-local coupling and memory phenomena via p. Transmission conditions between q,r exist at the interface $y = x$, where operator $g[k_{21}](x)$ acts as a point forcing through the interface. This interpretation will motivate the well-posedness study of (p,q,r). A point of interest to be raised is on the postulated continuity of the solutions. From (6.51), continuity is imposed between q,r, however, due to (6.50), the partial derivatives will not exhibit the same property. One may expect piecewise differentiability, in which the derivative loses continuity at the interface $y = x$.

Lemma 14. *The trivial solution* $\Omega \equiv 0$ *of the target system* (6.44)-(6.46) *is exponentially stable in the sense of the* L^2 *norm. That is,*

$$||\Omega(\cdot,t)||_{L^2} \leq \Pi \exp\left(-\gamma(t-t_0)\right) ||\Omega(\cdot,t_0)||_{L^2} \tag{6.64}$$

where the constants Π, γ *are given by*

$$\Pi = a^{-\frac{3}{2}} \tag{6.65}$$

$$\gamma = \min\{a^3 c_1, c_2\} + \frac{\varepsilon_2}{4} \tag{6.66}$$

Proof. We define a Lyapunov functional V_1 as follows:

$$V(t) := \int_0^1 \Omega(x,t)^T A \Omega(x,t) dx \tag{6.67}$$

where $A = \text{diag}(a^3, 1)$. $V(t)$ is equivalent to the squared norm in L^2:

$$V(t) \geq a^3 \left|\left|\Omega(\cdot,t)\right|\right|_{L^2}^2 \tag{6.68}$$

$$V(t) \leq \left|\left|\Omega(\cdot,t)\right|\right|_{L^2}^2 \tag{6.69}$$

Barring the details of the derivation, one can find the following bound on $\dot{V}$ through integration by parts:

$$\begin{aligned} \dot{V}(t) \leq & -2\Omega(0,t)^T AE \partial_x \Omega(0,t) - 2\pi_1 \left|\left|\partial_x \Omega(\cdot,t)\right|\right|_{L^2}^2 \\ & - 2\pi_2 \left|\left|\Omega(\cdot,t)\right|\right|_{L^2}^2 \end{aligned} \tag{6.70}$$

where the constants $\pi_i, i \in \{1,2\}$ are given by

$$\pi_1 = \varepsilon_2 \tag{6.71}$$

$$\pi_2 = \min\{a^3 c_1, c_2\} \tag{6.72}$$

Noting A, the term $-2\Omega(0,t)^T AE \partial_x \Omega(0,t) = 0$. From one application of the Poincare inequality, (6.70) results in the following inequality for $\dot{V}_1(t)$:

$$\dot{V}(t) \leq -2\left(\pi_2 + \frac{\pi_1}{4}\right) \left|\left|\Theta(\cdot,t)\right|\right|_{L^2}^2 \leq -2\gamma V(t) \tag{6.73}$$

Applying the comparison principle to above, the differential inequality in V can be converted to a

bound on $V(t)$.

$$V(t) \leq \exp\left(-2\gamma(t-t_0)\right) V(t_0) \tag{6.74}$$

By using (6.68),(6.69), one can arrive at the inequality in the theorem:

$$||\Omega(\cdot,t)||_{L^2} \leq \Pi \exp(-\gamma(t-t_0)) \, ||\Omega(\cdot,t_0)||_{L^2} \tag{6.75}$$

□

With Lemma 23, we are equipped to establish state feedback result.

Theorem 15. *The trivial solution of the system* (6.1)-(6.3) *is exponentially stable in the sense of the L^2 norm under the pair of state feedback control laws $\bar{\mathcal{U}}_1, \bar{\mathcal{U}}_2$:*

$$\begin{pmatrix} \bar{\mathcal{U}}_1(t) \\ \bar{\mathcal{U}}_2(t) \end{pmatrix} = \int_{-1}^{1} \begin{pmatrix} F_1(y) \\ F_2(y) \end{pmatrix} \bar{u}(y,t) dy \tag{6.76}$$

with feedback gains F_1, F_2 defined as

$$F_1(y) = \begin{cases} (1+y_0)^{-1} k_{11}\left(1, \frac{y_0-y}{1+y_0}\right) & y \leq y_0 \\ (1-y_0)^{-1} k_{12}\left(1, \frac{y-y_0}{1-y_0}\right) & y > y_0 \end{cases} \tag{6.77}$$

$$F_2(y) = \begin{cases} (1+y_0)^{-1} h_1\left(\frac{y_0-y}{1+y_0}\right) & y \leq y_0 \\ (1-y_0)^{-1} h_2\left(\frac{y-y_0}{1-y_0}\right) & y > y_0 \end{cases} \tag{6.78}$$

$$\begin{aligned} h_1(y) &= k_{21}(1,y) + q(1,y) - \int_y^1 \big[p(1-z)k_{21}(z,y) \\ &\qquad + q(1,z)k_{11}(z,y)\big] dz \\ h_2(y) &= k_{22}(1,y) + p(1-y) - \int_y^1 \big[p(1-z)k_{22}(z,y) \end{aligned} \tag{6.79}$$

$$+q(1,z)k_{12}(z,y)\big]dz \tag{6.80}$$

where k_{ij}, p, q *are* $C^2(\mathcal{T})$ *solutions to the kernel equations* (6.26),(8.47),(8.48) *respectively (with associated boundary conditions). That is, under the controllers* $\bar{\mathcal{U}}_1(t), \bar{\mathcal{U}}_2(t)$*, there exists a constant* $\bar{\Pi}$ *such that*

$$||\bar{u}(\cdot,t)||_{L^2} \leq \bar{\Pi}\exp\left(-\gamma(t-t_0)\right)||\bar{u}(\cdot,t_0)||_{L^2} \tag{6.81}$$

Proof. The feedback controllers (8.74) are derived via evaluating transforms (6.19),(6.41) at the boundary $x = 1$. From (6.41):

$$\begin{aligned} W(1,t) = \mathcal{V}(t) &= \begin{pmatrix} 0 \\ \nu_2(t) \end{pmatrix} \\ &= \begin{pmatrix} 0 \\ \int_0^1 \begin{pmatrix} q(1,y) & p(1-y) \end{pmatrix} W(y,t)dy \end{pmatrix} \end{aligned} \tag{6.82}$$

From (6.19),(8.24):

$$\mathcal{U}(t) = \int_0^1 K(1,y)U(y,t)dy + \mathcal{V}(t) \tag{6.83}$$

Or componentwise,

$$\begin{aligned} \mathcal{U}_1(t) &= \int_0^1 \begin{pmatrix} k_{11}(1,y) & k_{12}(1,y) \end{pmatrix} U(y,t)dy \\ \mathcal{U}_2(t) &= \int_0^1 \begin{pmatrix} k_{21}(1,y) & k_{22}(1,y) \end{pmatrix} U(y,t)dy \\ &\quad + \int_0^1 \begin{pmatrix} q(1,y) & p(1-y) \end{pmatrix} U(y,t)dy \end{aligned} \tag{6.84}$$

$$-\int_0^1 \int_0^y K(y,z)U(z,t)dzdy \tag{6.85}$$

By exchanging the order of integrals in the nested integrals, and applying the inverse folding transformations (8.7), the controllers (8.74) can be recovered.

The proof of the bound (8.80) relies on the well-posedness of the kernel PDEs, studied in Section 8.4. Specifically, Lemmas 25,26,22 state that continuous solutions exist and are unique. By Morrey's inequality (5.6.2 Theorem 4 in [19]), the continuous embedding $C^1(\mathcal{T}) \subseteq L^2(\mathcal{T})$ holds, and therefore $C^1(\mathcal{T})$ functions possess a bounded $L^2(\mathcal{T})$ norm. The boundedness (in $L^2(\mathcal{T})$) of the kernels K, p, q, r (and their inverses $\bar{K}, \bar{p}, \bar{q}, \bar{r}$, via the bounded inverse theorem) are required, but can be shown from their continuity properties on the compact sets $\mathcal{T}, \mathcal{T}_{\text{u}}$.

From (6.41), (6.43), one can derive the following equivalence:

$$M_1^{-1} ||W(\cdot,t)||_{L^2}^2 \leq ||\Omega(\cdot,t)||_{L^2}^2 \leq \bar{M}_1 ||W(\cdot,t)||_{L^2}^2 \tag{6.86}$$

where the coefficient M_1 depends on kernels p, q, r, and is given by

$$M_1 = (1 - ||q||_{L^2} - ||p||_{L^2} - ||r||_{L^2})^2 \tag{6.87}$$

and $\bar{M}_1$ is analogous with inverse kernels $\bar{p}, \bar{q}, \bar{r}$. Similarly, from (6.19),(8.19), the following equivalence can be derived:

$$\bar{M}_2^{-1} ||U(\cdot,t)||_{L^2}^2 \leq ||W(\cdot,t)||_{L^2}^2 \leq M_2 ||U(\cdot,t)||_{L^2}^2 \tag{6.88}$$

with

$$M_2 = (1 - ||K||_{L^2})^2 \tag{6.89}$$

and $\bar{M}_2$ analogous with inverse kernel $\bar{K}$. Then, applying (6.86),(6.88) to the bound (8.58) in Lemma 23, one can arrive at (8.80), with

$$\bar{\Pi} = \left(\sqrt{M_1\bar{M}_1M_2\bar{M}_2}\right)\Pi \tag{6.90}$$

□

6.3.3 Model transformation for estimation via folding

In the state-estimation problem, we tackle the related problem to the state-feedback problem. Rather than the controllers existing at either opposing boundary, we establish a problem which has two collocated measurements (of state and flux) in the interior of the PDE at some point $\hat{y}_0$. We also note that the sensor location $\hat{y}_0$ need not to be chosen equal to the control folding point y_0. The output, denoted $\mathcal{Y}$, is formulated as

$$\mathcal{Y}(t) = \begin{pmatrix} u(\hat{y}_0,t) \\ \partial_y u(\hat{y}_0,t) \end{pmatrix} \tag{6.91}$$

Much like the control case, applying a folding transformation about $\hat{y}_0$ will recover a coupled parabolic system. The transformation

$$\hat{x} = (\hat{y}_0 - y)/(1+\hat{y}_0) \qquad y \in (-1,\hat{y}_0) \tag{6.92}$$

$$\hat{x} = (y - \hat{y}_0)/(1-\hat{y}_0) \qquad y \in (\hat{y}_0,1) \tag{6.93}$$

will admit the following folded states:

$$\breve{U}(\hat{x},t) := \begin{pmatrix} \breve{u}_1(\hat{x},t) \\ \breve{u}_2(\hat{x},t) \end{pmatrix} = \begin{pmatrix} u(\hat{y}_0 - (1+\hat{y}_0)\hat{x},t) \\ u(\hat{y}_0 + (1-\hat{y}_0)\hat{x},t) \end{pmatrix} \tag{6.94}$$

The evolution of $\check{U}(x,t)$ governed by the following dynamics:

$$\partial_t \check{U}(x,t) = \check{E}\partial_x^2 \check{U}(x,t) + \check{\Lambda}(x)\check{U}(x,t) \tag{6.95}$$

$$\check{\alpha}\partial_x \check{U}(0,t) = -\beta \check{U}(0,t) \tag{6.96}$$

$$\check{U}(1,t) = \mathcal{U}(t) \tag{6.97}$$

The hat notation on $\hat{x}$ has been dropped for simplicity and the spatial domains are defined within the context of the equation in which it arises. The parameter matrices are then as follows:

$$\begin{aligned} \check{E} &:= \operatorname{diag}(\check{\varepsilon}_1, \check{\varepsilon}_2) \\ &:= \operatorname{diag}\left(\frac{\varepsilon}{(1+\hat{y}_0)^2}, \frac{\varepsilon}{(1-\hat{y}_0)^2}\right) \end{aligned} \tag{6.98}$$

$$\begin{aligned} \check{\Lambda}(x) &:= \operatorname{diag}(\check{\lambda}_1(x), \check{\lambda}_2(x)) \\ &:= \operatorname{diag}(\lambda(\hat{y}_0 - (1+\hat{y}_0)x), \lambda(\hat{y}_0 + (1-\hat{y}_0)x)) \end{aligned} \tag{6.99}$$

$$\check{\alpha} := \begin{pmatrix} 1 & \check{a} \\ 0 & 0 \end{pmatrix} \tag{6.100}$$

$$\check{a} := (1+\hat{y}_0)/(1-\hat{y}_0) \tag{6.101}$$

Certainly, if $\hat{y}_0 = y_0$, then the observation and control folded models are identical.

6.3.4 Backstepping state estimator design

Note that the sensor values in the folded coordinates can be expressed in the following manner:

$$\begin{pmatrix} u(\hat{y}_0,t) \\ \partial_y u(\hat{y}_0,t) \end{pmatrix} = \begin{pmatrix} u_1(0,t) \\ -(1+y_0)^{-1}\partial_x u_1(0,t) \end{pmatrix} \tag{6.102}$$

$$= \begin{pmatrix} u_2(0,t) \\ (1-y_0)^{-1}\partial_x u_2(0,t) \end{pmatrix} \tag{6.103}$$

With the two sensor values collocated at a single point, the design of the state estimator can be uncoupled into two near-identical subproblems. Specifically, we choose the following the estimator structure (indexed by $i \in \{1,2\}$):

$$\begin{aligned} \partial_t \hat{u}_i = {} & \check{\varepsilon}_i \partial_x^2 \hat{u}_i(x,t) + \check{\lambda}_i(x)\hat{u}_i(x,t) \\ & + \phi_i(x)\left(\partial_x u_i(0,t) - \partial_x \hat{u}_i(0,t)\right) \end{aligned} \tag{6.104}$$

$$\hat{u}_i(0,t) = u(0,t) \tag{6.105}$$

$$\hat{u}_i(1,t) = \mathcal{U}_i(t) \tag{6.106}$$

We define the error systems of the estimators as $\tilde{u}_i(x,t) := u_i(x,t) - \hat{u}_i(x,t)$. They are governed by

$$\begin{aligned} \partial_t \tilde{u}_i = {} & \check{\varepsilon}_i \partial_x^2 \tilde{u}_i(x,t) + \check{\lambda}_i(x)\tilde{u}_i(x,t) \\ & - \phi_i(x)\partial_x \tilde{u}_i(0,t) \end{aligned} \tag{6.107}$$

$$\tilde{u}_i(0,t) = 0 \tag{6.108}$$

$$\tilde{u}_i(1,t) = 0 \tag{6.109}$$

We can then design the $\phi_i(x)$ independently to stabilize trivial solutions $\tilde{u}_i(x,t) \equiv 0$ of the error systems $\tilde{u}_i$. We employ the following pair of backstepping transformations

$$\tilde{w}_i(x,t) = \tilde{u}_i(x,t) - \int_0^x \Phi_i(x,y)\tilde{u}_i(y,t)dy \tag{6.110}$$

with the following target systems:

$$\partial_t \tilde{w}_i(x,t) = \check{\varepsilon}_i \partial_x^2 \tilde{w}_i(x,t) - \check{c}_i \tilde{w}_i(x,t) \tag{6.111}$$

$$\tilde{w}_i(0,t) = 0 \tag{6.112}$$

$$\tilde{w}_i(1,t) = 0 \tag{6.113}$$

The inverse transformations are postulated to be

$$\tilde{u}_i(x,t) = \tilde{w}_i(x,t) - \int_0^x \bar{\Phi}_i(x,y)\tilde{w}_i(y,t)dy \tag{6.114}$$

where $\bar{\Phi}_i(x,y)$ will satisfy similar kernel equations to Φ.

Lemma 16. *For the choice of coefficients $\check{c}_i > 0, i \in \{1,2\}$, the trivial solutions $(\tilde{w}_i, \tilde{v}_i) \equiv 0$ of the observer error target systems* (6.111)-(6.113) *are exponentially stable in the $L^2 \times H^1$ sense, that is, there exist coefficients $\check{\Pi}_i, \check{\gamma}_i > 0$ such that for $i \in \{1,2\}$,*

$$||\tilde{w}_i(\cdot,t)||_{L^2} \leq \check{\Pi}_i \exp\left(-\check{\gamma}_i(t-t_0)\right) ||\tilde{w}_i(\cdot,t_0)||_{L^2} \tag{6.115}$$

The proof of Lemma 16 can be found in [36].

The companion gain kernel PDEs for ϕ_i can be found from imposing conditions arising from (6.95)-(6.97), (6.111)-(6.113), and the transformation (6.110).

$$\partial_x^2 \Phi_i(x,y) - \partial_y^2 \Phi_i(x,y) = -\frac{\lambda_i(x) + c_i}{\varepsilon_i} \Phi_i(x,y) \tag{6.116}$$

$$\Phi_i(1,y) = 0 \tag{6.117}$$

$$\Phi_i(x,x) = \int_x^1 \frac{\lambda_i(y) + c_i}{2\varepsilon_i} dy \tag{6.118}$$

In addition, one additional condition is imposed, which defines the observation gain $\phi_i(x)$ in terms of the transformation kernel $\Phi_i(x,y)$.

$$\phi_i(x) = -\varepsilon_i \Phi_i(x,0) \tag{6.119}$$

Lemma 17. *The Klein-Gordon PDEs defined by* (6.116)-(6.118) *admit unique $C^2(\mathcal{T})$ solutions. As a direct result, the gain kernels ϕ_i are bounded in the domain $\mathcal{T}$, that is,*

$$||\Phi_i||_{L^\infty} := \max_{(x,y)\in\mathcal{T}} |\Phi_i(x,y)| \leq \bar{\Phi}_i < \infty \tag{6.120}$$

The proof of Lemma (17) is given in [37].

Remark. *For the special case $\lambda_i(x) = \lambda_i$ is a constant, an explicit solution to* (6.116)-(6.118) *can be found:*

$$\Phi_i(x,y) = -\frac{\lambda_i + c_i}{\varepsilon_i}(1-x)\frac{I_1(z)}{z} \tag{6.121}$$

$$z = \sqrt{\frac{\lambda_i + c_i}{\varepsilon_i}(2-x-y)} \tag{6.122}$$

where $I_1(z)$ is the modified Bessel function of the first kind.

Theorem 18. *Consider the original system* (8.1)-(8.3) *and the auxiliary observer system defined in* (6.104)-(6.106) *with measurements $u(0,t), \partial_y u(0,t)$. Define the state estimate*

$$\hat{u}(y,t) := \begin{cases} \hat{u}_1\left(\frac{\hat{y}_0 - y}{1+\hat{y}_0}\right) & y \leq \hat{y}_0 \\ \hat{u}_2\left(\frac{y-\hat{y}_0}{1-\hat{y}_0}\right) & y > \hat{y}_0 \end{cases} \tag{6.123}$$

and

$$\hat{\bar{u}}(y,t) := \exp\left(-\int_{-1}^{y} \frac{\nu(z)}{2\varepsilon} dz\right) \hat{u}(y,t) \tag{6.124}$$

Then $\hat{\bar{u}}(y,t) \to \bar{u}(y,t)$ *exponentially fast in the sense of the* L^2 *norm, i.e. there exist coefficients* $\breve{\Pi}, \breve{\gamma}_{min} > 0$ *such that*

$$\begin{aligned} &\left|\left|\bar{u}(\cdot,t) - \hat{\bar{u}}(\cdot,t)\right|\right|_{L^2} \\ &\quad \leq \breve{\Pi} \exp\left(-\breve{\gamma}_{min}(t-t_0)\right) \left|\left|\bar{u}(\cdot,t_0) - \hat{\bar{u}}(\cdot,t_0)\right|\right|_{L^2} \end{aligned} \tag{6.125}$$

Proof. The proof follows from Lemmas 16, 17. The boundedness of the kernel Φ_i implies the existence of invertible transformations (6.114). Then one can directly apply the transformation (6.110) to (6.115) to recover the following bound:

$$\begin{aligned} &||u(\cdot,t) - \hat{u}(\cdot,t)||_{L^2} \\ &\quad \leq \breve{\Pi}_{\max} \exp\left(-\breve{\gamma}_{\min}(t-t_0)\right) ||u(\cdot,t_0) - \hat{u}(\cdot,t_0)||_{L^2} \end{aligned} \tag{6.126}$$

where the coefficients $\breve{\Pi}_{\max}, \breve{\gamma}_{\min}$ are defined:

$$\breve{\Pi}_{\max} = \max\{\breve{\Pi}_1, \breve{\Pi}_2\} \tag{6.127}$$

$$\breve{\gamma}_{\min} = \min\{\breve{\gamma}_1, \breve{\gamma}_2\} \tag{6.128}$$

and $\breve{\Pi}_i, i \in \{1,2\}$ are

$$\breve{\Pi}_i = (1 + ||\Phi_i||_{L^2})^2 (1 + \left|\left|\bar{\Phi}_i\right|\right|_{L^2})^2 \breve{\Pi}_i \tag{6.129}$$

Finally, by applying the transformation (6.4), one can recover (6.125) with the coefficient $\breve{\breve{\Pi}}$ defined as follows:

$$\breve{\breve{\Pi}} = \exp\left(\max_{y\in[-1,1]}\int_{-1}^{y}\frac{\nu(z)}{2\varepsilon}dz + \min_{y\in[-1,1]}\int_{-1}^{y}\frac{\nu(z)}{2\varepsilon}dz\right)\breve{\breve{\Pi}}_{\max} \tag{6.130}$$

□

6.3.5 Output-feedback controller

The output feedback controller proposed is the composition of the state observer with the state feedback. We state the main result below:

Theorem 19 (Separation principle)**.** *Consider the original system* (8.1)-(8.3) *and the auxiliary observer system defined in* (6.104)-(6.106) *with measurements* $u(0,t), \partial_y u(0,t)$*. With the state estimate* (6.123)*, the feedback controller pair* $\bar{\mathcal{U}}_1(t), \bar{\mathcal{U}}_2(t)$*:*

$$\begin{pmatrix}\bar{\mathcal{U}}_1(t)\\ \bar{\mathcal{U}}_2(t)\end{pmatrix} = \int_{-1}^{1}\begin{pmatrix}F_1(y)\\ F_2(y)\end{pmatrix}\hat{\bar{u}}(y,t)dy \tag{6.131}$$

with the gains F_1, F_2 *defined in* (8.75),(8.76) *will stabilize* $(\bar{u},\hat{\bar{u}}) \equiv 0$ *exponentially in the* L^2 *sense – that is, there exist constants* $\bar{\bar{\Pi}}, \bar{\bar{\gamma}} > 0$ *such that*

$$\left|\left|(\bar{u},\hat{\bar{u}})(\cdot,t)\right|\right|_{L^2} \leq \bar{\bar{\Pi}}\exp(\bar{\bar{\gamma}}(t-t_0))\left|\left|(\bar{u},\hat{\bar{u}})(\cdot,t_0)\right|\right|_{L^2} \tag{6.132}$$

Proof. The output feedback control law (6.131) is rewritten in the $(\bar{u},\tilde{\bar{u}})$ coordinates (recalling

that $\tilde{\bar{u}} := \bar{u} - \hat{\bar{u}}$):

$$\begin{pmatrix} \bar{\mathcal{U}}_1(t) \\ \bar{\mathcal{U}}_2(t) \end{pmatrix} = \int_{-1}^{1} \begin{pmatrix} F_1(y) \\ F_2(y) \end{pmatrix} \bar{u}(y,t)dy + \int_{-1}^{1} \begin{pmatrix} F_1(y) \\ F_2(y) \end{pmatrix} \tilde{\bar{u}}(y,t)dy \tag{6.133}$$

Applying the transformations (6.19),(6.41) will yield the same target system (6.44),(6.45), with the modified boundary condition

$$\Omega(1,t) = \int_{-1}^{1} \begin{pmatrix} F_1(y) \\ F_2(y) \end{pmatrix} \tilde{\bar{u}}(y,t)dy \tag{6.134}$$

Applying the Cauchy-Schwarz inequality and the bound from Theorem 18, we can bound this boundary condition in the following manner:

$$\begin{aligned} ||\Omega(1,t)||_2 \leq \check{\bar{\Pi}} \left|\left| \begin{pmatrix} F_1(y) \\ F_2(y) \end{pmatrix} \right|\right|_{L^2} & ||\tilde{\bar{u}}(\cdot,t_0)||_{L^2} \\ & \times \exp\left(-\check{\gamma}_{\min}(t-t_0)\right) \end{aligned} \tag{6.135}$$

Following the proof of Lemma 23 and Theorem 24, one can arrive at the following inequality on the L^2 norm of the system state:

$$\begin{aligned} ||\bar{u}(\cdot,t)||_{L^2} \leq \bar{\Pi} \exp\left(-\bar{\gamma}(t-t_0)\right) & ||\bar{u}(\cdot,t_0)||_{L^2} \\ + \hat{\bar{\Pi}} \exp\left(-\min\{\bar{\gamma},\check{\gamma}\}(t-t_0)\right) & ||\tilde{\bar{u}}(\cdot,t_0)||_{L^2} \end{aligned} \tag{6.136}$$

where

$$\hat{\bar{\Pi}} = (1 + ||p||_{L^2} + ||q||_{L^2})(1 + ||K||_{L^2})$$

$$\times \left|\left| \begin{pmatrix} F_1 \\ F_2 \end{pmatrix} \right|\right|_{L^2} \frac{\check{\bar{\Pi}}}{\sqrt{2|\bar{\gamma}-\check{\gamma}_{\max}|}} \tag{6.137}$$

Taking the root sum square of (6.125) and (6.136), one can arrive at an exponential stability result for $(\bar{u},\tilde{\bar{u}})$:

$$||(\bar{u},\tilde{\bar{u}})(\cdot,t)||_{L^2} \leq \tilde{\bar{\Pi}} \exp\left(-\bar{\bar{\gamma}}(t-t_0)\right) ||(\bar{u},\tilde{\bar{u}})(\cdot,t_0)||_{L^2} \tag{6.138}$$

where

$$\tilde{\bar{\Pi}} = \max\{\bar{\Pi}, \hat{\bar{\Pi}} + \check{\bar{\Pi}}\} \tag{6.139}$$

$$\bar{\bar{\gamma}} = \min\{\bar{\gamma}, \check{\gamma}\} \tag{6.140}$$

Finally, transforming back into the $(\bar{u},\hat{\bar{u}})$ coordinates, (6.132) can be recovered, with $\bar{\bar{\Pi}} = 4\tilde{\bar{\Pi}}$. □

6.4 Gain kernel well-posedness studies

A necessary and sufficient condition for the invertibility of (6.19), (6.41) (and their respective inverse transforms) is the existence of bounded kernels K, p, q on their respective domains. It is not trivially obvious that the kernel PDEs (6.26)-(6.29), (8.47),(8.48) are well-posed. The goal of this section is to establish and characterize the existence and uniqueness (and regularity) properties of these kernel PDEs.

6.4.1 Well-posedness of K

For K, we note that the kernel PDE is very similar to that of [45], and thus apply an adjusted approach to (6.26)-(6.28), (6.34). We use the following definition:

$$\check{K}(x,y) = \sqrt{E}\partial_x K(x,y) + \partial_y K(x,y)\sqrt{E} \tag{6.141}$$

which allows us to transform the 2×2 system of 2nd-order hyperbolic PDE K into the following $2\times 2\times 2$ 1st-order hyperbolic PDE system $(K,\check{K})$. Due to G possessing triangular structure (8.25) (a result of Assumption 8.2), we can separate the kernel PDEs into cascading sets of PDE systems.

Well-posedness of first row $K,\check{K}$: $(k_{1i},\check{k}_{1i})$

The first set of kernel PDEs we study is $(k_{11},k_{12},\check{k}_{11},\check{k}_{12})$. These kernels comprise an autonomous system of first-order hyperbolic PDEs on a bounded triangular domain, and are *linear and x-invariant* PDEs. Thus, our expectation is that the energy of a (potentially weak) solution can only grow (in x) at an exponential rate at best.

The component-wise kernels are

$$\sqrt{\varepsilon_1}\partial_x k_{11}(x,y) + \sqrt{\varepsilon_1}\partial_y k_{11}(x,y) = \check{k}_{11}(x,y) \tag{6.142}$$

$$\sqrt{\varepsilon_1}\partial_x k_{12}(x,y) + \sqrt{\varepsilon_2}\partial_y k_{12}(x,y) = \check{k}_{12}(x,y) \tag{6.143}$$

$$\sqrt{\varepsilon_1}\partial_x \check{k}_{11}(x,y) - \sqrt{\varepsilon_1}\partial_y \check{k}_{11}(x,y) = (\lambda_1(y)+c_1)k_{11}(x,y) \tag{6.144}$$

$$\sqrt{\varepsilon_1}\partial_x \check{k}_{12}(x,y) - \sqrt{\varepsilon_2}\partial_y \check{k}_{12}(x,y) = (\lambda_2(y)+c_1)k_{12}(x,y) \tag{6.145}$$

with boundary conditions

$$k_{11}(x,0) = \frac{a\varepsilon_2}{\varepsilon_1(a\varepsilon_2+\sqrt{\varepsilon_1\varepsilon_2})}$$

$$\times \int_0^x \sqrt{\varepsilon_1}\check{k}_{11}(y,0)+\sqrt{\varepsilon_2}\check{k}_{12}(y,0)dy \tag{6.146}$$

$$k_{12}(x,0)=\frac{1}{a\varepsilon_2+\sqrt{\varepsilon_1\varepsilon_2}} \times \int_0^x \sqrt{\varepsilon_1}\check{k}_{11}(y,0)+\sqrt{\varepsilon_2}\check{k}_{12}(y,0)dy \tag{6.147}$$

$$k_{12}(x,x)=0 \tag{6.148}$$

$$\check{k}_{11}(x,x)=-\frac{\lambda_1(x)+c_1}{2\sqrt{\varepsilon_1}} \tag{6.149}$$

$$\check{k}_{12}(x,x)=0 \tag{6.150}$$

The system of kernel equations $(k_{1i},\check{k}_{1i})$ is self contained. Due to Assumption 8.2, the characteristics of the kernel equations $k_{12},\check{k}_{12}$ will have sub-unity slope, in turn neccessitating two boundary condtions on k_{12} at the $y=0$ and $y=x$ boundaries.

Lemma 20. *The system of first-order hyperbolic PDEs* (8.94)-(8.97) *and associated boundary conditions admit a unique set of* $k_{11},k_{12}\in C^2(\mathcal{T})$, $\check{k}_{11},\check{k}_{12}\in C^1(\mathcal{T})$ *solutions.*

Proof. With a direct application of the method of characteristcs to (8.94)-(8.97), Volterra-type integral equations can be recovered:

$$k_{11}(x,y)=c_1a^3\int_0^{x-y}\sqrt{\varepsilon_1}\check{k}_{11}(z,0)+\sqrt{\varepsilon_2}\check{k}_{12}(z,0)dz + \int_0^{\sqrt{\varepsilon_1^{-1}}y}\check{k}_{11}(\sqrt{\varepsilon_1}z+x-y,\sqrt{\varepsilon_1}z)dz \tag{6.151}$$

$$k_{12}(x,y)=\begin{cases} k_{12,l} & \sqrt{\varepsilon_1}y\le\sqrt{\varepsilon_2}x \\ k_{12,u} & \sqrt{\varepsilon_1}y\ge\sqrt{\varepsilon_2}x \end{cases} \tag{6.152}$$

$$\check{k}_{11}(x,y)=-\frac{\lambda_1\left(\frac{x+y}{2}\right)+c_1}{2\sqrt{\varepsilon_1}} + \int_0^{\frac{x-y}{2\sqrt{\varepsilon_1}}}\left(\lambda_1\left(-\sqrt{\varepsilon_1}z+\frac{x+y}{2}\right)+c_1\right) \times k_{11}\left(\sqrt{\varepsilon_1}z+\frac{x+y}{2},-\sqrt{\varepsilon_1}z+\frac{x+y}{2}\right)dz \tag{6.153}$$

$$\check{k}_{12}(x,y) = \int_0^{\frac{x-y}{\sqrt{\varepsilon_1}+\sqrt{\varepsilon_2}}} \lambda_2(-\sqrt{\varepsilon_2}z+\sigma_3(x,y)+c_1) \times k_{12}(\sqrt{\varepsilon_1}z+\sigma_3(x,y),-\sqrt{\varepsilon_2}z+\sigma_3(x,y))dz \tag{6.154}$$

where $k_{12,u}, k_{12,l}$ is defined by

$$k_{12,l}(x,y) = \int_0^{\sigma_1(x,y)} \sqrt{\varepsilon_1}\check{k}_{11}(z,0)+\sqrt{\varepsilon_2}\check{k}_{12}(z,0)dz + \int_0^{\sqrt{\varepsilon_2^{-1}}y} \check{k}_{12}(\sqrt{\varepsilon_1}z+\sigma_1(x,y),\sqrt{\varepsilon_2}z)dz \tag{6.155}$$

$$k_{12,u}(x,y) = \int_0^{\frac{x-y}{\sqrt{\varepsilon_1}-\sqrt{\varepsilon_2}}} \check{k}_{12}(\sqrt{\varepsilon_1}z+\sigma_2(x,y), \sqrt{\varepsilon_2}z+\sigma_2(x,y))dz \tag{6.156}$$

and the functions σ_i given by

$$\sigma_1(x,y) = \sqrt{\varepsilon_2^{-1}}(\sqrt{\varepsilon_2}x-\sqrt{\varepsilon_1}y) \tag{6.157}$$

$$\sigma_2(x,y) = (\sqrt{\varepsilon_1}-\sqrt{\varepsilon_2})^{-1}(\sqrt{\varepsilon_1}y-\sqrt{\varepsilon_2}x) \tag{6.158}$$

$$\sigma_3(x,y) = (\sqrt{\varepsilon_1}+\sqrt{\varepsilon_2})^{-1}(\sqrt{\varepsilon_2}x+\sqrt{\varepsilon_1}y) \tag{6.159}$$

From substituting (6.154) into (6.152) on the domain $\mathcal{T}_u := \{(x,y) \in \mathbb{R}^2 | 0 \le \sqrt{\varepsilon_2/\varepsilon_1}x \le y \le x \le 1\}$, one can immediately notice $k_{12,u}(x,y) = \check{k}_{12}(x,y) \equiv 0, (x,y) \in \mathcal{T}_u$.

Using (6.151)-(6.154), the following integral equation relations can be established:

$$\begin{pmatrix} k_{11} \\ k_{12} \end{pmatrix} = \Gamma_1 \left[\begin{pmatrix} \check{k}_{11} \\ \check{k}_{12} \end{pmatrix} \right] := I_1 \left[\begin{pmatrix} \check{k}_{11} \\ \check{k}_{12} \end{pmatrix} \right] (x,y) + \Psi_1(x,y) \tag{6.160}$$

$$\begin{pmatrix} \check{k}_{11} \\ \check{k}_{12} \end{pmatrix} = \Gamma_2 \left[\begin{pmatrix} k_{11} \\ k_{12} \end{pmatrix} \right] := I_2 \left[\begin{pmatrix} k_{11} \\ k_{12} \end{pmatrix} \right] (x,y) + \Psi_2(x,y) \tag{6.161}$$

where the operators Γ_1, Γ_2 over $(x,y) \in \mathcal{T}$) encapsulate the affine integral equations (6.151)-(6.154), and I_1, I_2 represent the linear part in $k, \check{k}$, while Ψ_1, Ψ_2 represent the constant part. We establish the following iteration via the method of successive approximations to recover a solution:

$$\begin{pmatrix} k_{11,n+1} \\ k_{12,n+1} \end{pmatrix} = (\Gamma_1 \circ \Gamma_2) \left[\begin{pmatrix} k_{11,n} \\ k_{12,n} \end{pmatrix} \right] \tag{6.162}$$

The existence of a solution (k_{11}, k_{12}) through the iteration (6.162) will imply the existence of a solution $(\check{k}_{11}, \check{k}_{12})$ via (6.161). To show that this iteration converges, we first define

$$\Delta k_{1,n} := \begin{pmatrix} \Delta k_{11,n} \\ \Delta k_{12,n} \end{pmatrix} := \begin{pmatrix} k_{11,n+1} - k_{11,n} \\ k_{12,n+1} - k_{12,n} \end{pmatrix} \tag{6.163}$$

Applying (6.163) to (6.162) and utilizing the properties of affine operators, one can recover the following iteration for $\Delta k_{1,n}$:

$$\Delta k_{1,n+1} = (I_1 \circ I_2)[\Delta k_{1,n}](x,y) \tag{6.164}$$

As $\Gamma_1 \circ \Gamma_2$ is a continuous mapping over the complete convex space of bounded continuous functions, then the following statement holds via the Schauder fixed point theorem.

$$\lim_{n \to \infty} \begin{pmatrix} k_{11,n} \\ k_{12,n} \end{pmatrix} = \begin{pmatrix} k_{11,0} \\ k_{12,0} \end{pmatrix} + \sum_{n=0}^{\infty} \Delta k_{1,n} = \begin{pmatrix} k_{11} \\ k_{12} \end{pmatrix} \tag{6.165}$$

Choosing $k_{11,0} = k_{12,0} = 0$, one can compute the following bound on $\Delta k_{1,0}$ directly:

$$||\Delta k_{1,0}||_1 \leq (\bar{\lambda} + c_1) \left(c_1 a^3 + \varepsilon_1^{-1} + 1 \right) x \tag{6.166}$$

where we have taken the liberty of defining

$$\bar{\lambda} := \max\{||\lambda_1||_{L^\infty}, ||\lambda_2||_{L^\infty}\} = ||\lambda||_{L^\infty} \tag{6.167}$$

It is important to note that the norm $||\Delta k_{1,0}||_1$ is the *vector* 1-norm and not the L^1 function norm. That is,

$$||\Delta k_{1,n}||_1 := |\Delta k_{11,n}(x,y)| + |\Delta k_{12,n}(x,y)| \tag{6.168}$$

By using (6.166) in (6.164), one can find the following bound on $||\Delta k_{1,n}||_1$ indexed by iteration n:

$$||\Delta k_{1,n}||_1 \leq \frac{2^n((\bar{\lambda}+c_1)(c_1a^3+\varepsilon_1^{-1}+1))^{n+1}}{(2n+1)!}x^{2n+1} \tag{6.169}$$

Due to the bounded domain $\mathcal{T}$, one can find *uniform* convergence properties (where the uniform bound is simply evaluated for $x^{2n+1} \leq 1, \forall x \in [0,1]$). From (6.165),

$$\left|\left|\begin{pmatrix} k_{11} \\ k_{12} \end{pmatrix}\right|\right|_1 \leq \sum_{n=0}^{\infty} \frac{2^n((\bar{\lambda}+c_1)(c_1a^3+\varepsilon_1^{-1}+1))^{n+1}}{(2n+1)!}x^{2n+1} \tag{6.170}$$

To recover the $C^2(\mathcal{T})$ regularity, one can directly reference (6.165). Noting that the set $C^n(\mathcal{T})$ is closed under addition for $n \in \mathbb{N}$ along with the *integral* iteration (6.164), it is easy to see that $\lambda_1, \lambda_2 \in C^1([0,1])$ generates the regularity $k_{11}, k_{12} \in C^2(\mathcal{T})$. □

Well-posedness of second row $K, \check{K}$: ($k_{2i}, \check{k}_{2i}$)

The second set of kernels is $(k_{21}, k_{22}, \check{k}_{21}, \check{k}_{22})$. These feature the kernels k_{11}, k_{12} acting as source terms, however, by employing estimates of k_{11}, k_{12} from Lemma 25, we can simplify the system significantly. However, the structure of the problem is different, most notably in how the characteristics evolve.

To account for the different nature of these characteristics, we perform one more transformation on the kernels for k_{2i}:

$$\hat{k}_{2i}(x,y) = \sqrt{\varepsilon_2}\partial_x k_{2i}(x,y) - \sqrt{\varepsilon_i}\partial_y k_{2i}(x,y) \tag{6.171}$$

where $i \in \{1,2\}$. We then turn our attention to the gain kernel system $(\hat{k}_{21}, \check{k}_{21}, \hat{k}_{22}, \check{k}_{22})$.

The component system of kernel PDEs for $(\hat{k}_{21}, \check{k}_{21}, \hat{k}_{22}, \check{k}_{22})$ is

$$\begin{aligned}
\sqrt{\varepsilon_2}\partial_x \hat{k}_{21}(x,y) + \sqrt{\varepsilon_1}\partial_y \hat{k}_{21}(x,y) &= (\lambda_1(y) + c_2)k_{21}(x,y) \\
&\quad - g[k_{21}](x)k_{11}(x,y) && (6.172)\\
\sqrt{\varepsilon_2}\partial_x \hat{k}_{22}(x,y) + \sqrt{\varepsilon_2}\partial_y \hat{k}_{22}(x,y) &= (\lambda_2(y) + c_2)k_{22}(x,y) \\
&\quad - g[k_{21}](x)k_{12}(x,y) && (6.173)\\
\sqrt{\varepsilon_2}\partial_x \check{k}_{21}(x,y) - \sqrt{\varepsilon_1}\partial_y \check{k}_{21}(x,y) &= (\lambda_1(y) + c_2)k_{21}(x,y) \\
&\quad - g[k_{21}](x)k_{11}(x,y) && (6.174)\\
\sqrt{\varepsilon_2}\partial_x \check{k}_{22}(x,y) - \sqrt{\varepsilon_2}\partial_y \check{k}_{22}(x,y) &= (\lambda_2(y) + c_2)k_{22}(x,y) \\
&\quad - g[k_{21}](x)k_{12}(x,y) && (6.175)
\end{aligned}$$

subject to the following boundary conditions:

$$\hat{k}_{21}(x,0) = -\frac{1-a^2}{1+a^2}\check{k}_{21}(x,0) + \frac{2a^3}{1+a^2}\check{k}_{22}(x,0) \tag{6.176}$$

$$\hat{k}_{22}(x,0) = \frac{2}{a(1+a^2)}\check{k}_{21}(x,0) + \frac{1-a^2}{1+a^2}\check{k}_{22}(x,0) \tag{6.177}$$

$$\check{k}_{21}(x,x) = -\frac{\sqrt{\varepsilon_1} - \sqrt{\varepsilon_2}}{\sqrt{\varepsilon_1} + \sqrt{\varepsilon_2}}\hat{k}_{21}(x,x) \tag{6.178}$$

$$\check{k}_{22}(x,x) = -\frac{\lambda_2(x) + c_2}{2\sqrt{\varepsilon_2}} \tag{6.179}$$

where the inverse transformations are given to be

$$k_{21}(x,y) = \frac{1}{2\sqrt{\varepsilon_2}} \int_y^x \check{k}_{21}(z,y) + \hat{k}_{21}(z,y) dz \tag{6.180}$$

$$\begin{aligned} k_{22}(x,y) = &- \int_0^y \frac{\lambda_2(z) + c_2}{2\sqrt{\varepsilon_2}} dz \\ &+ \frac{1}{2\sqrt{\varepsilon_2}} \int_y^x \check{k}_{22}(z,y) + \hat{k}_{22}(z,y) dz \end{aligned} \tag{6.181}$$

and the function $g[k_{21}](x)$ can be expressed in terms of $\hat{k}_{21}, \check{k}_{21}$:

$$g[k_{21}](x) = \frac{(\varepsilon_2 - \varepsilon_1)}{2\sqrt{\varepsilon_1}} (\check{k}_{21}(x,x) - \hat{k}_{21}(x,x)) \tag{6.182}$$

Without the estimates given by Lemma 25, the system of gain kernels would in fact be *nonlinear*, a significantly harder problem.

Lemma 21. *The system of first-order hyperbolic PDE* (8.107)-(8.110) *and associated boundary conditions admit a unique set of* $\hat{k}_{21}, \check{k}_{21}, \hat{k}_{22}, \check{k}_{22} \in C^1(\mathcal{T})$ *solutions.*

Proof. The primary technical difficulty of this proof is incorporating the boundary conditions (8.111),(8.113). While in standard integral equation solutions one can apply successive approximations to recover a convergent sum of monomial terms (in increasing powers), the trace term $g[k_{21}](x)$ presents issues with this approach. Thus, we utilize an approach inspired from [5],[10] involving a recursion relating to the finite volume of integration (of the domain $\mathcal{T}$).

We apply the method of characteristics to (8.107)-(8.110) to recover the following system of coupled integro-algebraic equations:

$$\begin{aligned} \hat{k}_{21}(x,y) &= \hat{k}_{21}(\sigma_4(x,y), 0) + \hat{I}_{21}[\hat{k}_{21}, \check{k}_{21}](x,y) \\ \hat{k}_{22}(x,y) &= \hat{k}_{22}(x-y, 0) + \hat{I}_{22}[\hat{k}_{22}, \check{k}_{22}, \hat{k}_{21}](x,y) \end{aligned} \tag{6.183}$$

$$- \int_0^{\frac{y}{\sqrt{\varepsilon_2}}} \left[\frac{\lambda_2(\sqrt{\varepsilon_2}z) + c_2}{2\sqrt{\varepsilon_2}} \times \int_0^{\sqrt{\varepsilon_2}z} (\lambda_2(\xi) + c_2) d\xi \right] dz \tag{6.184}$$

$$\check{k}_{21}(x,y) = \check{k}_{21}\left(\sigma_5(x,y), \sigma_5(x,y)\right) + \check{I}_{21}[\hat{k}_{21}, \check{k}_{21}](x,y) \tag{6.185}$$

$$\begin{aligned} \check{k}_{22}(x,y) = {} & \check{k}_{22}\left(\frac{x+y}{2}, \frac{x+y}{2}\right) + \check{I}_{22}[\hat{k}_{22}, \check{k}_{22}, \hat{k}_{21}](x,y) \\ & - \int_0^{\frac{x-y}{2\sqrt{\varepsilon_2}}} \left[\frac{\lambda_2\left(-\sqrt{\varepsilon_2}z + \frac{x+y}{2}\right) + c_2}{2\sqrt{\varepsilon_2}} \times \int_0^{-\sqrt{\varepsilon_2}z + \frac{x+y}{2}} (\lambda_2(\xi) + c_2) d\xi \right] dz \end{aligned} \tag{6.186}$$

where

$$\sigma_4(x,y) := x - \frac{\sqrt{\varepsilon_2}}{\sqrt{\varepsilon_1}} y \tag{6.187}$$

$$\sigma_5(x,y) := \frac{\sqrt{\varepsilon_1}x + \sqrt{\varepsilon_2}y}{\sqrt{\varepsilon_1} + \sqrt{\varepsilon_2}} \tag{6.188}$$

and the integral operators $\hat{I}_{21}, \hat{I}_{22}, \check{I}_{21}, \check{I}_{22}$ are defined

$$\begin{aligned} & \hat{I}_{21}[\hat{k}_{21}, \check{k}_{21}](x,y) \\ & := \int_0^{\frac{y}{\sqrt{\varepsilon_1}}} \left[- \frac{\varepsilon_2 - \varepsilon_1}{\sqrt{\varepsilon_1} + \sqrt{\varepsilon_2}} k_{11}(\sqrt{\varepsilon_2}z + \sigma_4(x,y), \sqrt{\varepsilon_1}z) \right. \\ & \qquad \times \hat{k}_{21}(\sqrt{\varepsilon_2}z + \sigma_4(x,y), \sqrt{\varepsilon_2} + \sigma_4(x,y)) \\ & \quad + \frac{\lambda_1(\sqrt{\varepsilon_1}z) + c_2}{2\sqrt{\varepsilon_2}} \int_{\sqrt{\varepsilon_1}z}^{\sqrt{\varepsilon_2}z + \sigma_4(x,y)} \left(\check{k}_{21}(\xi, \sqrt{\varepsilon_1}z) \right. \\ & \qquad \left. \left. + \hat{k}_{21}(\xi, \sqrt{\varepsilon_1}z) \right) d\xi \right] dz \end{aligned} \tag{6.189}$$

$$\begin{aligned} & \hat{I}_{22}[\hat{k}_{22}, \check{k}_{22}, \hat{k}_{21}](x,y) \\ & := \int_0^{\frac{y}{\sqrt{\varepsilon_2}}} \left[- \frac{\varepsilon_2 - \varepsilon_1}{\sqrt{\varepsilon_1} + \sqrt{\varepsilon_2}} k_{12}(\sqrt{\varepsilon_2}z + x - y, \sqrt{\varepsilon_2}z) \right. \\ & \qquad \left. \times \hat{k}_{21}(\sqrt{\varepsilon_2}z + x - y, \sqrt{\varepsilon_2} + x - y) \right. \end{aligned}$$

$$+\frac{\lambda_2(\sqrt{\varepsilon_2}z)+c_2}{2\sqrt{\varepsilon_2}}\Bigg(\int_{\sqrt{\varepsilon_2}z}^{\sqrt{\varepsilon_2}z+x-y}\Bigg(\check{k}_{22}(\xi,\sqrt{\varepsilon_2}z)+\hat{k}_{22}(\xi,\sqrt{\varepsilon_2}z)\Bigg)d\xi\Bigg)\Bigg]dz \tag{6.190}$$

$$\begin{aligned}
&\check{I}_{21}[\hat{k}_{21},\check{k}_{21}](x,y)\\
&:=\int_0^{\frac{x-y}{\sqrt{\varepsilon_1}+\sqrt{\varepsilon_2}}}\Bigg[-\frac{\varepsilon_2-\varepsilon_1}{\sqrt{\varepsilon_1}+\sqrt{\varepsilon_2}}k_{11}(\sqrt{\varepsilon_2}z+\sigma_5(x,y)\\
&\qquad,-\sqrt{\varepsilon_1}z+\sigma_5(x,y))\\
&\qquad\times\hat{k}_{21}(\sqrt{\varepsilon_2}z+\sigma_5(x,y),\sqrt{\varepsilon_2}+\sigma_5(x,y))\\
&\quad+\frac{\lambda_1(-\sqrt{\varepsilon_1}z+\sigma_5(x,y))+c_2}{2\sqrt{\varepsilon_2}}\\
&\times\int_{-\sqrt{\varepsilon_1}z+\sigma_5(x,y)}^{\sqrt{\varepsilon_2}z+\sigma_5(x,y)}\Bigg(\check{k}_{21}(\xi,-\sqrt{\varepsilon_1}z+\sigma_5(x,y))\\
&\qquad+\hat{k}_{21}(\xi,-\sqrt{\varepsilon_1}z+\sigma_5(x,y))\Bigg)d\xi\Bigg]dz
\end{aligned} \tag{6.191}$$

$$\begin{aligned}
&\check{I}_{22}[\hat{k}_{22},\check{k}_{22},\hat{k}_{21}](x,y)\\
&:=\int_0^{\frac{x-y}{2\sqrt{\varepsilon_2}}}\Bigg[-\frac{\varepsilon_2-\varepsilon_1}{\sqrt{\varepsilon_1}+\sqrt{\varepsilon_2}}\\
&\qquad\times k_{12}\left(\sqrt{\varepsilon_2}z+\frac{x+y}{2},-\sqrt{\varepsilon_2}z+\frac{x+y}{2}\right)\\
&\qquad\times\hat{k}_{21}\left(\sqrt{\varepsilon_2}z+\frac{x+y}{2},\sqrt{\varepsilon_2}+\frac{x+y}{2}\right)\\
&\quad+\frac{\lambda_2\left(-\sqrt{\varepsilon_2}z+\frac{x+y}{2}\right)+c_2}{2\sqrt{\varepsilon_2}}\\
&\qquad\times\Bigg(\int_{-\sqrt{\varepsilon_2}z+\frac{x+y}{2}}^{\sqrt{\varepsilon_2}z+\frac{x+y}{2}}\Bigg(\check{k}_{22}\left(\xi,-\sqrt{\varepsilon_2}z+\frac{x+y}{2}\right)\\
&\qquad+\hat{k}_{21}\left(\xi,-\sqrt{\varepsilon_2}z+\frac{x+y}{2}\right)\Bigg)d\xi\Bigg)\Bigg]dz
\end{aligned} \tag{6.192}$$

From enforcing (8.111)-(8.114) on (8.118)-(8.121) recursively, one can eventually arrive at an integral equation system representation for $(\hat{k}_{21},\hat{k}_{22},\check{k}_{21},\check{k}_{22})$ involving infinite sums of integral operators. The infinite sums appear due to the reflection boundary conditions

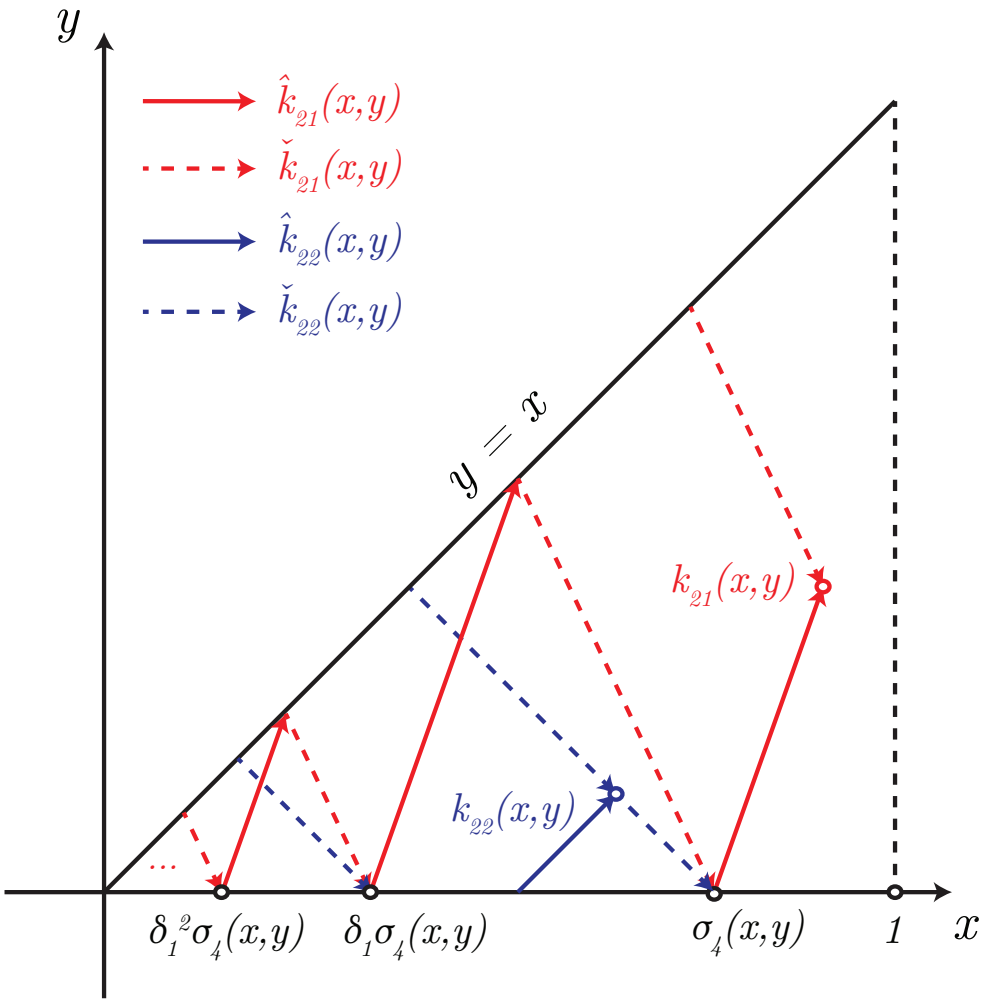

Figure 6.2: Characteristics of $\hat{k}_{21}, \hat{k}_{22}, \check{k}_{21}, \check{k}_{22}$ featuring an infinite number of reflection boundary conditions.

(8.111),(8.113) observed in the system.

$$\begin{aligned}
&\hat{k}_{21}(x,y) = \\
&\quad \lim_{n\to\infty}\Big[-\delta_1^n\delta_2^{n+1}\check{k}_{21}\left(\delta_1^n\sigma_4(x,y),0\right) \\
&\qquad\qquad +\delta_1^n\delta_2^n\frac{2a^3}{1+a^2}\check{k}_{22}(\delta_1^n\sigma_4(x,y),0)\Big] \\
&\quad -\sum_{n=0}^{\infty}\Big[\delta_1^n\delta_2^n\frac{2a^3}{1+a^2}\Big(\frac{\lambda_2(\delta_1^n\sigma_4(x,y))+c_2}{2\sqrt{\varepsilon_2}}
\end{aligned}$$

$$
\begin{aligned}
&+\int_0^{\frac{1}{2\sqrt{\varepsilon_2}}\delta_1^n\sigma_4(x,y)}\Bigg(\frac{\lambda_2(-\sqrt{\varepsilon_1}z+\frac{1}{2}\delta_1^n\sigma_4(x,y))+c_2}{2\sqrt{\varepsilon_2}}\\
&\qquad\times\int_0^{-\sqrt{\varepsilon_2}z+\frac{1}{2}\delta_1^n\sigma_4(x,y)}(\lambda_2(\xi)+c_2)d\xi\Bigg)dz\Bigg]\\
&+\sum_{n=0}^{\infty}\Bigg[\delta_1^n\delta_2^n\hat{I}_{21}[\hat{k}_{21},\check{k}_{21}](\delta_3^n\sigma_4(x,y),\delta_3^n\sigma_4(x,y))\\
&\quad-\delta_1^n\delta_2^{n+1}\check{I}_{21}[\hat{k}_{21},\check{k}_{21}](\delta_1^n\sigma_4(x,y),0)\\
&\quad+\delta_1^n\delta_2^n\frac{2a^3}{1+a^2}\check{I}_{22}[\hat{k}_{22},\check{k}_{22},\hat{k}_{21}](\delta_1^n\sigma_4(x,y),0)\Bigg]\\
&+\hat{I}_{21}[\hat{k}_{21},\check{k}_{21}](x,y)
\end{aligned}
\tag{6.193}
$$

$$
\begin{aligned}
&\hat{k}_{22}(x,y)=\\
&\frac{2}{a(1+a^2)}\lim_{n\to\infty}\Bigg[\delta_1^n\delta_2^n\check{k}_{21}(\delta_1^n(x-y),0)\Bigg]\\
&-\delta_2\left(\frac{\lambda_2\left(\frac{x-y}{2}\right)+c_2}{2\sqrt{\varepsilon_2}}\right)\\
&+\frac{4a^2}{(1+a^2)^2}\sum_{n=1}^{\infty}\Bigg[(-1)^n\delta_1^n\delta_2^n\Bigg(\frac{\lambda_2(\delta_1^n(x-y))+c_2}{2\sqrt{\varepsilon_2}}\\
&\quad-\int_0^{\delta_3^n\frac{x-y}{2\sqrt{\varepsilon_2}}}\Bigg[\frac{\lambda_2\left(-\sqrt{\varepsilon_2}z+\delta_3^n\frac{x-y}{2}\right)+c_2}{2\sqrt{\varepsilon_2}}\\
&\qquad\qquad\times\int_0^{-\sqrt{\varepsilon_2}z+\delta_3^n\frac{x-y}{2}}(\lambda_2(\xi)+c_2)d\xi\Bigg]dz\Bigg)\Bigg]\\
&+\frac{2}{a(1+a^2)}\sum_{n=1}^{\infty}\Bigg[(-1)^n\delta_1^n\delta_2^{n-1}\\
&\qquad\qquad\times\hat{I}_{21}[\hat{k}_{21},\check{k}_{21}](\delta_3^n(x-y),\delta_3^n(x-y))\\
&\quad+\delta_1^{n-1}\delta_2^{n-1}\check{I}_{21}[\hat{k}_{21},\check{k}_{21}](\delta_1^n(x-y),0)\\
&\quad+(-1)^n\delta_1^n\delta_2^{n-1}\frac{2a}{1+a^3}\check{I}_{22}[\hat{k}_{22},\check{k}_{22},\hat{k}_{21}](\delta_3^n(x-y),0)\Bigg]\\
&+\delta_2\check{I}_{22}[\hat{k}_{22},\check{k}_{22},\hat{k}_{21}](x-y,0)+\hat{I}_{22}[\hat{k}_{22},\check{k}_{22},\hat{k}_{21}](x,y)\\
&-\int_0^{\frac{y}{\sqrt{\varepsilon_2}}}\Bigg[\frac{\lambda_2(\sqrt{\varepsilon_2}z)+c_2}{2\sqrt{\varepsilon_2}}\int_0^{\sqrt{\varepsilon_2}z}(\lambda_2(\xi)+c_2)d\xi\Bigg]dz\\
&-\int_0^{\frac{x-y}{2\sqrt{\varepsilon_2}}}\delta_2\Bigg[\frac{\lambda_2\left(-\sqrt{\varepsilon_2}z+\frac{x-y}{2}\right)+c_2}{2\sqrt{\varepsilon_2}}
\end{aligned}
$$

$$\times \int_0^{-\sqrt{\varepsilon_2}z+\frac{x-y}{2}} (\lambda_2(\xi)+c_2)d\xi\Bigg]dz \tag{6.194}$$

$$\begin{aligned}
&\check{k}_{21}(x,y) = \\
&\quad \lim_{n\to\infty}\left[\delta_1^n\delta_2^n\check{k}_{21}(\delta_1^n\sigma_5(x,y),\delta_1^n\sigma_5(x,y))\right] \\
&\quad + \sum_{n=0}^{\infty}\Bigg[\delta_1^{n+1}\delta_2^n\Bigg(\frac{\lambda_2\left(\frac{1}{2}\frac{\delta_1}{\delta_3}\delta_1^n\sigma_5(x,y)\right)+c_2}{2\sqrt{\varepsilon_2}} \\
&\quad - \int_0^{\frac{\delta_1}{\delta_3}\delta_1^n\frac{\sigma_5(x,y)}{2\sqrt{\varepsilon_2}}}\Bigg[\frac{\lambda_2\left(-\sqrt{\varepsilon_2}z+\frac{\delta_1}{\delta_3}\delta_1^n\frac{\sigma_5(x,y)}{2}\right)+c_2}{2\sqrt{\varepsilon_2}} \\
&\qquad\qquad \times \int_0^{-\sqrt{\varepsilon_2}z+\frac{\delta_1}{\delta_3}\delta_1^n\frac{\sigma_5(x,y)}{2}} (\lambda_2(\xi)+c_2)d\xi\Bigg]dz\Bigg)\Bigg] \\
&\quad + \sum_{n=0}^{\infty}\Bigg[-\delta_1^{n+1}\delta_2^n\hat{I}_{21}[\hat{k}_{21},\check{k}_{21}](\delta_1^n\sigma_5(x,y),\delta_1^n\sigma_5(x,y)) \\
&\qquad - \frac{2a^3}{1+a^2}\delta_1^{n+1}\delta_2^n\check{I}_{22}[\hat{k}_{22},\check{k}_{22},\hat{k}_{21}]\left(\frac{\delta_1}{\delta_3}\delta_1^n\sigma_5(x,y),0\right) \\
&\qquad + \delta_1^{n+1}\delta_2^{n+1}\check{I}_{21}[\check{k}_{21},\hat{k}_{21}]\left(\frac{\delta_1}{\delta_3}\delta_1^n\sigma_5(x,y),0\right)\Bigg] \\
&\quad + \check{I}_{21}[\hat{k}_{21},\check{k}_{21}](x,y)
\end{aligned} \tag{6.195}$$

$$\begin{aligned}
&\check{k}_{22}(x,y) = \\
&\quad - \frac{\lambda_2(\frac{x+y}{2})+c_2}{2\sqrt{\varepsilon_2}} + \check{I}_{22}[\hat{k}_{22},\check{k}_{22},\hat{k}_{21}](x,y) \\
&\quad - \int_0^{\frac{x-y}{2\sqrt{\varepsilon_2}}}\Bigg[\frac{\lambda_2\left(-\sqrt{\varepsilon_2}z+\frac{x+y}{2}\right)+c_2}{2\sqrt{\varepsilon_2}} \\
&\qquad\qquad \times \int_0^{-\sqrt{\varepsilon_2}z+\frac{x+y}{2}} (\lambda_2(\xi)+c_2)d\xi\Bigg]dz
\end{aligned} \tag{6.196}$$

where δ_1, δ_2 are defined

$$\delta_1 = \frac{\sqrt{\varepsilon_1}-\sqrt{\varepsilon_2}}{\sqrt{\varepsilon_1}+\sqrt{\varepsilon_2}} \tag{6.197}$$

$$\delta_2 = \frac{1-a^2}{1+a^2} \tag{6.198}$$

$$\delta_3 = \frac{\sqrt{\varepsilon_1}}{\sqrt{\varepsilon_1} + \sqrt{\varepsilon_2}} \tag{6.199}$$

Since $a < 1, \varepsilon_1 > \varepsilon_2$ as per Assumption 8.2, the coefficients $\delta_{1,2,3} \in (0,1)$. It is unclear initially whether the limit and infinite sum terms are convergent, however, as one may notice from Figure 6.2, the contracting volume of integration and the reflection coefficients (appearing in the δ_i coefficients) will guarantee convergence.

Like in the proof of Lemma 25, we will define the integral equations (8.128)-(8.131) in terms of operators for notational compactness. Let $k_2 := \left(\hat{k}_{21}, \hat{k}_{22}, \check{k}_{21}, \check{k}_{22}\right)$, and

$$k_2 = I_3[k_2](x,y) + \Theta[k_2](x,y) + \Psi_3(x,y) \tag{6.200}$$

where I_3 is the operator involving the integral operators $\hat{I}_{2i}, \check{I}_{2i}$, Θ is the operator involving limits, and Ψ_3 collects the terms independent of $\hat{k}_{2i}, \check{k}_{2i}$. We establish an iteration $k_{2,n}$ as

$$k_{2,n+1} = I_3[k_{2,n}](x,y) + \Theta[k_{2,n}](x,y) + \Psi_3(x,y) \tag{6.201}$$

with the iteration residual $\Delta k_{2,n} := k_{2,n+1} - k_{2,n}$ defining the iteration

$$\Delta k_{2,n+1} = I_3[\Delta k_{2,n}](x,y) + \Theta[\Delta k_{2,n}](x,y) \tag{6.202}$$

We note that (6.200) is a continuous mapping over the complete (convex) metric space of bounded continuous functions (via the Schauder fixed point theorem), and make the following statement:

$$\lim_{n\to\infty} k_{2,n} = k_{2,0} + \sum_{n=0}^{\infty} \Delta k_{2,n} = k_2 \tag{6.203}$$

Supposing that $k_{2,0} = 0$,

$$\begin{aligned} ||\Delta k_{2,0}||_1 = ||\Psi_3||_1 &\leq \left(\frac{\bar{\lambda} + c_2}{2\sqrt{\varepsilon_2}} + \frac{1}{2}\left(\frac{\bar{\lambda} + c_2}{2\sqrt{\varepsilon_2}} \right)^2 \right) \\ &\quad \times \left(1 + \frac{1}{1 - \delta_1\delta_2} + \frac{2a^3}{1+a^2}\frac{1}{1-\delta_1\delta_2} \right. \\ &\quad \left. + \frac{4a^2}{(1+a^2)^2}\frac{1}{1-\delta_1\delta_2} \right) \\ &\leq \bar{\Psi}_{3,0} \end{aligned} \tag{6.204}$$

From iterating $||\Delta k_{2,0}||_1$ through (6.202), one can achieve successive bounds on $\Delta k_{2,n}$:

$$\begin{aligned} ||\Delta k_{2,n}||_1 \leq \frac{1}{n!} \Bigg[3 \Bigg(\left(1 + \frac{2}{1 - \delta_1\delta_2} \right) + \frac{2}{a(1+a^2)} \frac{1}{1-\delta_1\delta_2} \Bigg) \\ \times \left(a^{-1} \left|\left| \begin{pmatrix} k_{11} \\ k_{12} \end{pmatrix} \right|\right|_{1,L^\infty} + \frac{\bar{\lambda} + c_2}{\varepsilon_2} \right) \Bigg]^n \bar{\Psi}_{3,0} x^n \end{aligned} \tag{6.205}$$

We remark that it is easy to see for any polynomial bound $||\Delta k_{2,n}||_1$, $||\Theta[\Delta k_{2,n}](x,y)||_1 \leq 0$ due to continuity (and boundedness). Then, via (6.203) and noting $x \in [0,1]$, we can arrive at the following bound on k_2:

$$||k_2||_1 \leq \sum_{n=0}^{\infty} ||\Delta k_{2,n}||_1 \tag{6.206}$$

which is the power series representation of an exponential bound. The regularity of the solution k_2 is also derived from (6.203), where noting that the initial choice of $k_{2,0} = 0$ admits $\Delta k_{2,0} = \Psi_3$, which is $C^1(\mathcal{T})$ as it involves sums of $\lambda_2 \in C^1([0,1])$. Then from (8.115),(8.116), a single integration yields $k_{21}, k_{22} \in C^2(\mathcal{T})$.

□

6.4.2 Well-posedness of p,q,r

As aformentioned, the (p,q,r)-system of kernel PDEs comprise a fairly interesting structure, the heart of which is a wave equation with an interface, whereby forcing is introduced via the differential transmission condition (6.50) at the interface. It is quite trivial to see that if one can show a solution exists for q, then necessarily, a solution p must exist as well.

To faciliate the study of the kernels, we will apply the Riemann invariant transformation as before found in the K kernel. As q,r share congruent characteristics, the solution method is much more straightforward and involves tracing characteristics through the square $\mathcal{T}\cup\mathcal{T}_{\mathrm{u}}$.

In this section, we have used the relation (8.47) to reduce the (p,q,r) system to (q,r), albeit at the cost of introducing trace terms into the q-PDE.

We begin by apply the following definition to derive the Rienmann invariants:

$$\hat{q}(x,y)=\sqrt{\varepsilon_2}\partial_x q(x,y)-\sqrt{\varepsilon_1}\partial_y q(x,y) \tag{6.207}$$

$$\check{q}(x,y)=\sqrt{\varepsilon_2}\partial_x q(x,y)+\sqrt{\varepsilon_1}\partial_y q(x,y) \tag{6.208}$$

which admit the following coupled PDEs for $(\hat{q},\check{q})$ defined on $\mathcal{T}$:

$$\sqrt{\varepsilon_2}\partial_x\hat{q}(x,y)+\sqrt{\varepsilon_1}\partial_y\hat{q}(x,y)=I_q[\hat{q},\check{q}](x,y) \tag{6.209}$$

$$\sqrt{\varepsilon_2}\partial_x\check{q}(x,y)-\sqrt{\varepsilon_1}\partial_y\check{q}(x,y)=I_q[\hat{q},\check{q}](x,y) \tag{6.210}$$

where the operator $I_q[\hat{q},\check{q}]$ is a linear integral operator defined as

$$\begin{aligned} I_q[\hat{q},\check{q}](x,y)=&\frac{c_2-c_1}{2\sqrt{\varepsilon_2}}\int_0^x\check{q}(z,0)dz\\ &+\frac{c_2-c_1}{2\sqrt{\varepsilon_1}}\int_0^y(\check{q}(x,z)-\hat{q}(x,z))dz\\ &+\frac{a^{-1}g[k_{21}](y)}{2\sqrt{\varepsilon_2}}\int_0^{x-y}\check{q}(z,0)dz \end{aligned} \tag{6.211}$$

In a similar manner, we define the Riemann invariants for r on $\mathcal{T}_{\mathrm{u}}$:

$$\hat{r}(x,y) = \sqrt{\varepsilon_2}\partial_x r(x,y) - \sqrt{\varepsilon_1}\partial_y r(x,y) \tag{6.212}$$

$$\check{r}(x,y) = \sqrt{\varepsilon_2}\partial_x r(x,y) + \sqrt{\varepsilon_1}\partial_y r(x,y) \tag{6.213}$$

which admits the coupled PDE:

$$\sqrt{\varepsilon_2}\partial_x \hat{r}(x,y) + \sqrt{\varepsilon_1}\partial_y \hat{r}(x,y) = I_r[\hat{r},\check{r}](x,y) \tag{6.214}$$

$$\sqrt{\varepsilon_2}\partial_x \check{r}(x,y) - \sqrt{\varepsilon_1}\partial_y \check{r}(x,y) = I_r[\hat{r},\check{r}](x,y) \tag{6.215}$$

where $I_r[\hat{r},\check{r}]$ is a linear integral operator defined as

$$I_r[\hat{r},\check{r}](x,y) = \frac{c_2 - c_1}{2\sqrt{\varepsilon_2}} \int_0^x (\hat{r}(z,y) + \check{r}(z,y))dz \tag{6.216}$$

The PDEs given by (6.209),(6.210),(6.214),(6.215) are subject to the following boundary conditions, which consist of transmission and reflection boundary conditions:

$$\hat{q}(x,0) = 0 \tag{6.217}$$

$$\check{q}(x,x) = \check{r}(x,x) - (\sqrt{\varepsilon_1} + \sqrt{\varepsilon_2})^{-1} g[k_{21}](x) \tag{6.218}$$

$$\hat{r}(0,y) = \check{r}(0,y) = 0 \tag{6.219}$$

$$\hat{r}(x,x) = \hat{q}(x,x) - (\sqrt{\varepsilon_1} - \sqrt{\varepsilon_2})^{-1} g[k_{21}](x) \tag{6.220}$$

$$\check{r}(x,1) = -\hat{r}(x,1) \tag{6.221}$$

An additional condition employed implicity in the derivation of $(\hat{q},\check{q},\hat{r},\check{r})$ is the following point condition:

$$q(0,0) = r(0,0) = 0 \tag{6.222}$$

Lemma 22. *The system of first-order hyperbolic PDE* (6.209),(6.210),(6.214),(6.215) *with associated boundary conditions admit a unique set of solutions* $(\hat{q},\check{q}) \in C^1(\mathcal{T})$ *and* $(\hat{r},\check{r}) \in C^1(\mathcal{T}_u)$.

Proof. We can directly apply the method of characteristics to (6.209),(6.210),(6.214),(6.215) to recover the following linear integral equations:

$$\hat{q}(x,y) = \int_0^{\frac{y}{\sqrt{\varepsilon_1}}} I_q[\hat{q},\check{q}](\sigma_6(x,y)+\sqrt{\varepsilon_2}z, \sqrt{\varepsilon_1}z)dz \tag{6.223}$$

$$\begin{aligned}\check{q}(x,y) = {} & \check{r}(\sigma_7(x,y),\sigma_7(x,y)) \\ & - (\sqrt{\varepsilon_1}+\sqrt{\varepsilon_2})^{-1} g[k_{21}](\sigma_7(x,y)) \\ & + \int_0^{\frac{x-y}{\sqrt{\varepsilon_1}+\sqrt{\varepsilon_2}}} I_q[\hat{q},\check{q}](\sqrt{\varepsilon_2}z+\sigma_7(x,y), \\ & \qquad -\sqrt{\varepsilon_1}z+\sigma_7(x,y))dz\end{aligned} \tag{6.224}$$

where $\sigma_6, \sigma_7, \sigma_8$ are defined as

$$\sigma_6(x,y) = x - \sqrt{\frac{\varepsilon_2}{\varepsilon_1}}y \tag{6.225}$$

$$\sigma_7(x,y) = \frac{\sqrt{\varepsilon_1}x+\sqrt{\varepsilon_2}y}{\sqrt{\varepsilon_1}+\sqrt{\varepsilon_2}} \tag{6.226}$$

while for $\hat{r},\check{r}$, we recover piecewise defined linear integral equations which arises due to the mixing of initial and boundary conditions.

$$\hat{r}(x,y) = \begin{cases} \hat{r}_l(x,y) & x \le \sqrt{\varepsilon_2/\varepsilon_1}y \\ 0 & x > \sqrt{\varepsilon_2/\varepsilon_1}y \end{cases} \tag{6.227}$$

$$\check{r}(x,y) = \begin{cases} \check{r}_u(x,y) & x \le \sqrt{\varepsilon_2/\varepsilon_1} \\ \check{r}_l(x,y) & \sqrt{\varepsilon_2/\varepsilon_1} < x \le \sqrt{\varepsilon_2/\varepsilon_1} \\ 0 & x < \sqrt{\varepsilon_2/\varepsilon_1}y \end{cases} \tag{6.228}$$

where

$$\begin{aligned}\hat{r}_l(x,y) &= \hat{q}(\sigma_8(x,y),\sigma_8(x,y)) \\ &\quad -(\sqrt{\varepsilon_1}-\sqrt{\varepsilon_2})^{-1} g[k_{21}](\sigma_8(x,y)) \\ &\quad + \int_0^{\frac{y-x}{\sqrt{\varepsilon_1}-\sqrt{\varepsilon_2}}} I_r[\hat{r},\check{r}](\sqrt{\varepsilon_2}z+\sigma_8(x,y), \\ &\qquad\qquad \sqrt{\varepsilon_1}z+\sigma_8(x,y))dz \end{aligned} \tag{6.229}$$

$$\begin{aligned}\check{r}_u(x,y) &= -\hat{r}(\sigma_9(x,y),1) \\ &\quad + \int_0^{\frac{1-y}{\sqrt{\varepsilon_1}}} I_r[\hat{r},\check{r}](\sqrt{\varepsilon_2}z+\sigma_9(x,y), \\ &\qquad\qquad -\sqrt{\varepsilon_1}z+1)dz \end{aligned} \tag{6.230}$$

$$\begin{aligned}\check{r}_l(x,y) &= \int_0^{\frac{\sqrt{\varepsilon_1}-\sqrt{\varepsilon_2}}{2\sqrt{\varepsilon_1}}} I_r[\hat{r},\check{r}](\sqrt{\varepsilon_2}z+\sigma_{10}(x,y), \\ &\qquad\qquad -\sqrt{\varepsilon_1}z+\sigma_{10}(x,y))dz \end{aligned} \tag{6.231}$$

with $\sigma_8, \sigma_9, \sigma_{10}$ defned as

$$\sigma_8(x,y) = \frac{\sqrt{\varepsilon_1}x-\sqrt{\varepsilon_2}y}{\sqrt{\varepsilon_1}-\sqrt{\varepsilon_2}} \tag{6.232}$$

$$\sigma_9(x,y) = x+\sqrt{\frac{\varepsilon_2}{\varepsilon_1}}(y-1) \tag{6.233}$$

$$\sigma_{10}(x,y) = x+\sqrt{\frac{\varepsilon_2}{\varepsilon_1}}y \tag{6.234}$$

To study the well-posedness $\hat{q},\check{q},\hat{r},\check{r}$ system, it is helpful to study the characteristics geometrically, which are depicted in Figure 6.3.

Much like the analysis of the K kernel, we establish the following operator representation for the affine integral equations that govern $\rho := (\hat{q},\check{q},\hat{r},\check{r})$:

$$\rho = \Gamma_3[\rho](x,y) := I_4[\rho](x,y)+\Psi_4(x,y) \tag{6.235}$$

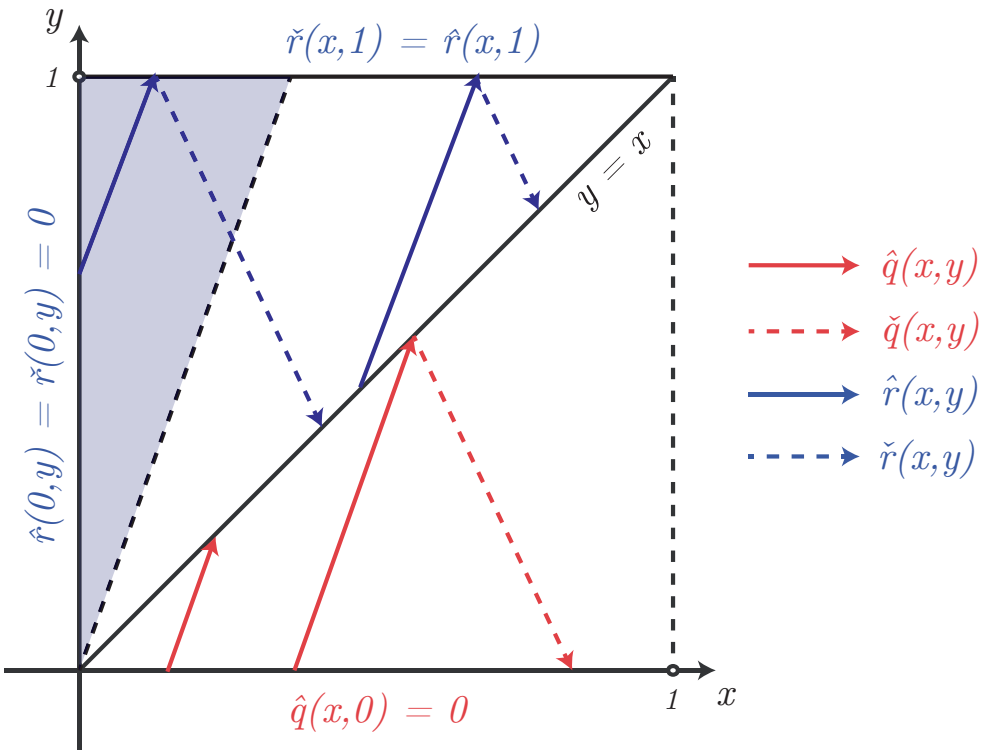

Figure 6.3: Solution characteristics of $\hat{q},\check{q},\hat{r},\check{r}$. An interface between the solutions exists at $y = x$ defining a jump discontinuity. Because of the initial conditons imposed, $\hat{r} = \check{r} = 0$ in the shaded triangle.

where analogous to before, Γ_3 encapsulates the affine integral equations given by (6.223),(6.224), (6.227),(6.228). We separate the operator into the linear operator I_4 and the constant Ψ_4. Ψ_4 is evaluated to be

$$\Psi_4(x,y) := \begin{pmatrix} 0 & \Psi_{4,1}(x,y) & \Psi_{4,2}(x,y) & \Psi_{4,3}(x,y) \end{pmatrix}^T \tag{6.236}$$

$$\begin{aligned}
\Psi_{4,1}(x,y) &= (\sqrt{\varepsilon_1} - \sqrt{\varepsilon_2})^{-1} \\
&\quad \times g[k_{21}](\sigma_8(\sigma_9(\sigma_7(x,y),\sigma_7(x,y)),1)) \\
&\quad - (\sqrt{\varepsilon_1} + \sqrt{\varepsilon_2})^{-1} g[k_{21}](\sigma_7(x,y)) \\
\Psi_{4,2}(x,y) &= -(\sqrt{\varepsilon_1} - \sqrt{\varepsilon_2})^{-1} g[k_{21}](\sigma_8(x,y)) \\
\Psi_{4,3}(x,y) &= (\sqrt{\varepsilon_1} - \sqrt{\varepsilon_2})^{-1} g[k_{21}](\sigma_8(\sigma_9(x,y),1))
\end{aligned}$$

Intuitively, one can understand Ψ_4 to represent the nonzero data of the problem. If, perchance the folding point is chosen $y_0 = 0$, then $g[k_{21}] \equiv 0 \Leftrightarrow \Psi_4 \equiv 0$. It is precisely the unmatched artifact from the first transformation, $g[k_{21}]$, that acts as the sole forcing to the (q,r) PDE, as expected.

We carry out the same methodology as for K, and establish an iteration ρ_k for $n \in \mathbb{N}$:

$$\rho_{n+1} = I_4[\rho_n](x,y) + \Psi_4(x,y) \tag{6.237}$$

The residual $\Delta\rho_n := \rho_{n+1} - \rho_n$ will obey the following linear integral equation,

$$\Delta\rho_n = I_4[\Delta\rho_n](x,y) \tag{6.238}$$

which arises from abusing the linear property of I_4. We note that in the complete space of bounded continuous functions, the iteration (6.237) will converge (via the Schauder fixed point theorem) if we can show uniform Cauchy convergence. The iteration limit thus can be rewritten as an infinite summation:

$$\lim_{n\to\infty} \rho_n = \rho_0 + \sum_{n=0}^{\infty} \Delta\rho_n = \rho \tag{6.239}$$

It is quite clear from imposing (6.237),(6.238) that by choosing $\rho_0 = 0$, $\Delta\rho_0$ can be computed to be

$$\begin{aligned} \Delta\rho_0 &= \Psi_4 \\ \Rightarrow ||\Delta\rho_0||_1 = ||\Psi_4||_1 &\leq \frac{4\sqrt{\varepsilon_1} + 2\sqrt{\varepsilon_2}}{\varepsilon_1 - \varepsilon_2} \, ||g[k_{21}]||_{L^\infty} \end{aligned} \tag{6.240}$$

From using (6.240) in the iteration (6.238), one can find the successive bounds on the residuals:

$$||\Delta\rho_n||_1 \leq \frac{1}{n!} \left(\frac{2\varepsilon_2^{-1}(2|c_1 - c_2| + ||g[k_{21}]||_{L^\infty}}{2} x \right)^n ||\Psi_4||_1 \tag{6.241}$$

Noting (6.239), it is quite trivial to see that ρ is bounded (in vector 1-norm) by an exponential. This guarantees the existence of a solution ρ, and thus $(\hat{q}, \check{q}, \hat{r}, \check{r})$ admit a solution. In fact, due to the linearity of the PDEs (6.209),(6.210),(6.214),(6.215), it is not difficult to show that this solution is also unique. □

6.5 Folding point analysis and numerical study

Table 6.1: Simulation parameters

Parameter	Value
ε	1
$\lambda(x)$	$-4x^2 - 2x + 6$
y_0	$-0.05, -0.30$
$\hat{y}_0$	$0.05, -0.45$
c_1, c_2	5
$\check{c}_1, \check{c}_2$	1

The parameters chosen for simulation are given in Table 6.1. λ is specifically chosen to not be symmetric about $x = 0$, and actually attains a maximum at $x = -0.25$. This is motivated by the intuition that choosing a folding point not at the point of symmetry $x = 0$ may afford better performance according a preferred index. It is also important to note that $c_1, c_2, \check{c}_1, \check{c}_2$ all influence the system response in some manner that is not wholly independent from the choices $y_0, \hat{y}_0$.

6.5.1 Folding point selection

It is difficult to directly characterize the size of the controller gains F_1, F_2 (defined in (8.75),(8.76)), but one may glean intuition for how the controllers grow based upon what the bounds on the gain kernels suggest.

As one may note from Figure 6.4, the control gains are not necessarily continuous at the selected folding point. Surely, as $y_0 \to 0$ (the point of symmetry), one recovers the continuous case. However, as the folding point is chosen to be more and more biased (for the same set of

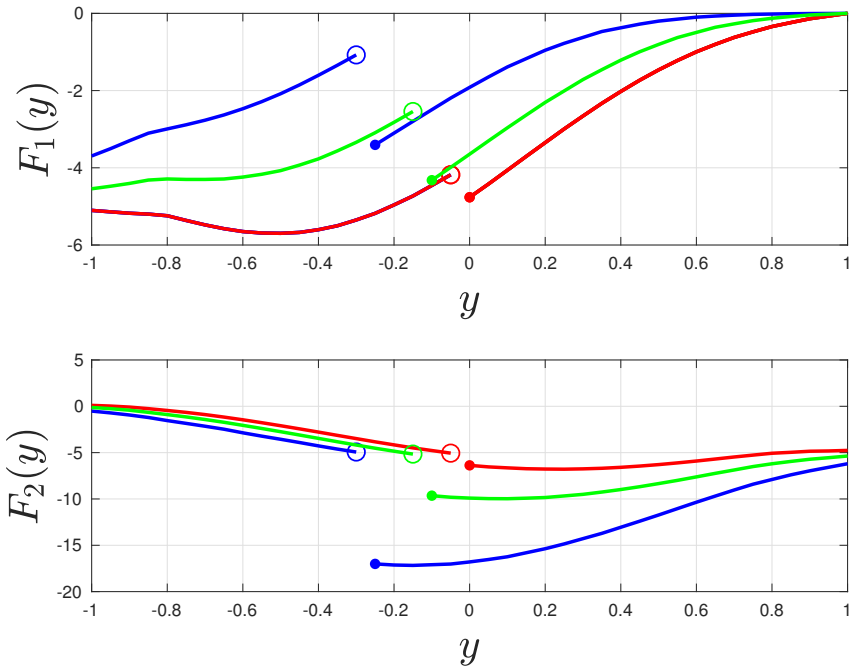

Figure 6.4: Numerically computed gains for given reaction coefficient λ for three separate folding cases: **(red)** $y_0 = -0.05$, **(green)** $y_0 = -0.15$, **(blue)** $y_0 = -0.30$

target system reaction coefficients c_i), one control gain grows smaller (less effort) while the other is magnified (more effort).

Although not provable, the bounds (6.170),(6.206),(6.241) suggest this behavior as well. In (6.170), the bound on the controller gains k_{1i} arise as an exponential in a^3. In (6.206),(6.241), the control gains k_{2i}, p, q are parametrized (exponentially as well) in a^{-1}.

6.5.2 Numerical results for output-feedback

Due to the choice of a sufficiently large positive λ, the open-loop system is unstable and therefore necessitates feedback control. Two choices of control folding points y_0 and two choices of measurement points $\hat{y}_0$ are simulated, with the control folding point y_0 marked in red and the measurement point $\hat{y}_0$ marked in blue.

Comparing Figures 6.5, 6.7 with Figurues 6.6,6.8 gives insight to how changing the

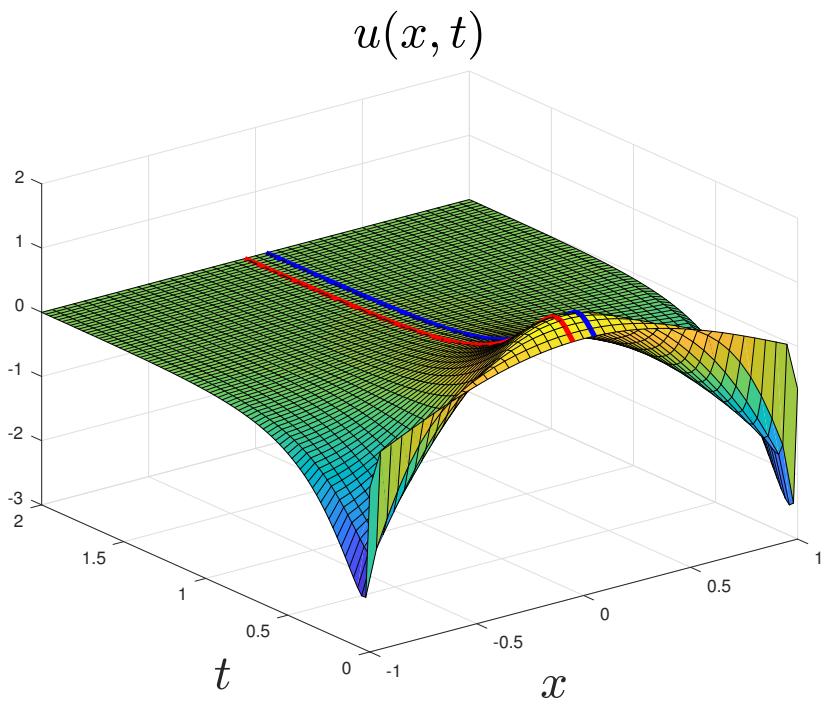

Figure 6.5: Closed-loop response $u(x,t)$ with folding points chosen to be $y_0 = -0.05, \hat{y}_0 = 0.05$.

control folding point affects the response – the controller $\mathcal{U}_1$ has a lower peak value in the biased case (Figure 6.6,6.8) than that of the close-to-symmetric case (Figure 6.5,6.7). However, it is quite clear to note that the controller $\mathcal{U}_2$ pays the cost in having a much higher peak value.

Comparing Figures 6.5,6.6 with Figures 6.7,6.8 gives insight to how changing the measurement point $\hat{y}_0$ affects the system response. One can note that the closer the measurement is to the boundary, the performance will improve (uniformly).

The controller responses are given in Figures 6.13,6.14. It can be noted that the selection of the control folding point appears to suggest an inherent waterbed effect in L^2 versus L^∞ (in time. The numerical simulations suggest that as $y_0 \to -1$ (the biased case), the controller improves in the L^2 sense at the cost of the peak value. Conversely, as $y_0 \to 0$ (the symmetric case), the controller improves in the L^∞ sense at the cost of the convergence speed (related to L^2).

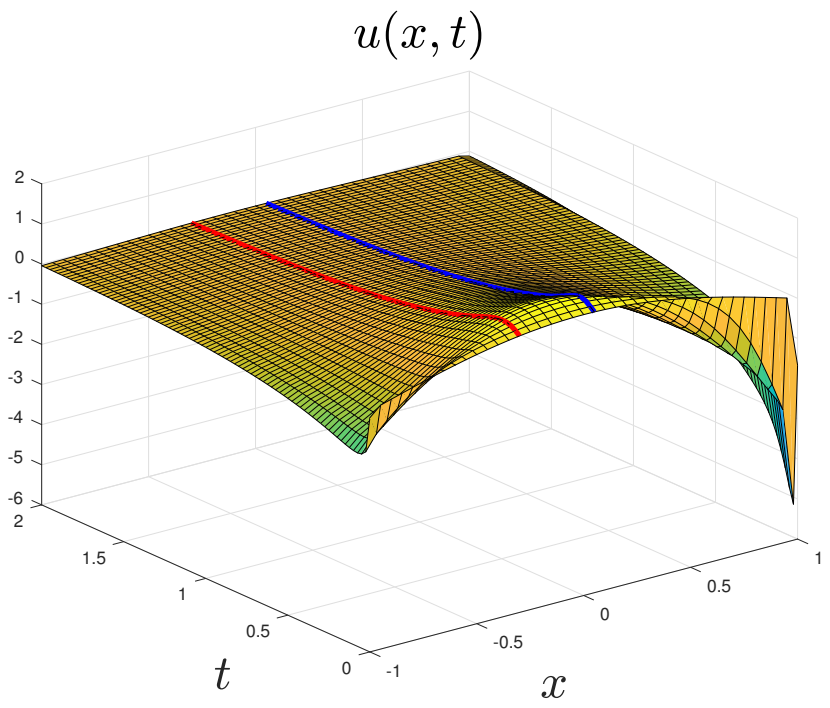

Figure 6.6: Closed-loop response $u(x,t)$ with folding points chosen to be $y_0 = -0.30, \hat{y}_0 = 0.05$.

6.6 Conclusion

A methodology for designing output feedback bilateral boundary controllers for linear parabolic class PDEs is generated as the main result of the paper. Compared with existing bilateral control designs for parabolic PDEs, the folding appraoch affords additional design degrees of freedom in not only control but also estimator design.

The primary advantage that the folding approach admits is a generalization of bilateral control design. A design for a given performance index e.g. energy (L^2) or boundedness (L^∞) can be achieved in a straightforward manner. The unilateral control design is recoverable in the limit from the folding control design; therefore, the design is far more flexible as a methodology.

Without explicit solutions to the gain kernel equations, the effect of the design parameters on system response is difficult to quantify. However, numerical analysis is given which suggests at least qualitative intuition for selecting folding points for desired behavior. A waterbed effect is

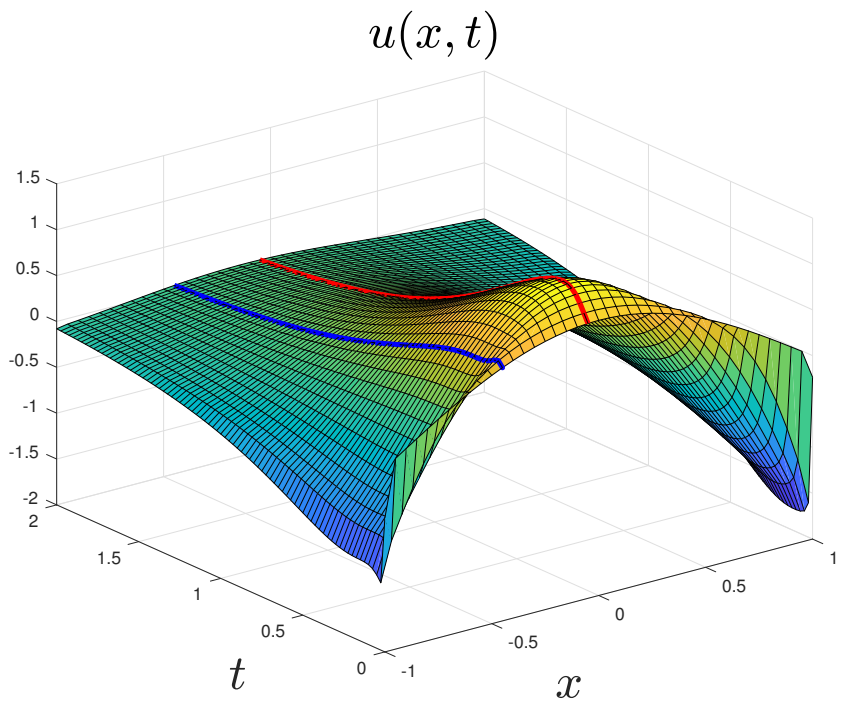

Figure 6.7: Closed-loop response $u(x,t)$ with folding points chosen to be $y_0 = -0.05, \hat{y}_0 = -0.45$.

noted, in which the controller energy (L^2) exhibits an inherent trade off with boundedness (L^∞).

The observer result as a stand alone result is particularly interesting theoretically, as it no longer technically falls within the "boundary" observer design any more. Of future interest is developing methodology for design of estimators with arbitrarily placed measure zero measurments in the interior. One may even begin to ask more fundamental questions about conditions about the number of measurements needed to make and allowable locations, because it is not immediately obvious how either affects the observability of the system.

The folding approach also opens the door to potential results involving 1-D PDEs exhibiting coupling structures at points on the interior, as opposed to spatially distributed coupling or boundary coupling. An extension to the folding framework, involving an unstable ODE coupled on an arbitrary point on the interior, is explored in [14]. Certainly, one may begin to explore additional couplings, which involve feedback coupling between the unstable ODE and

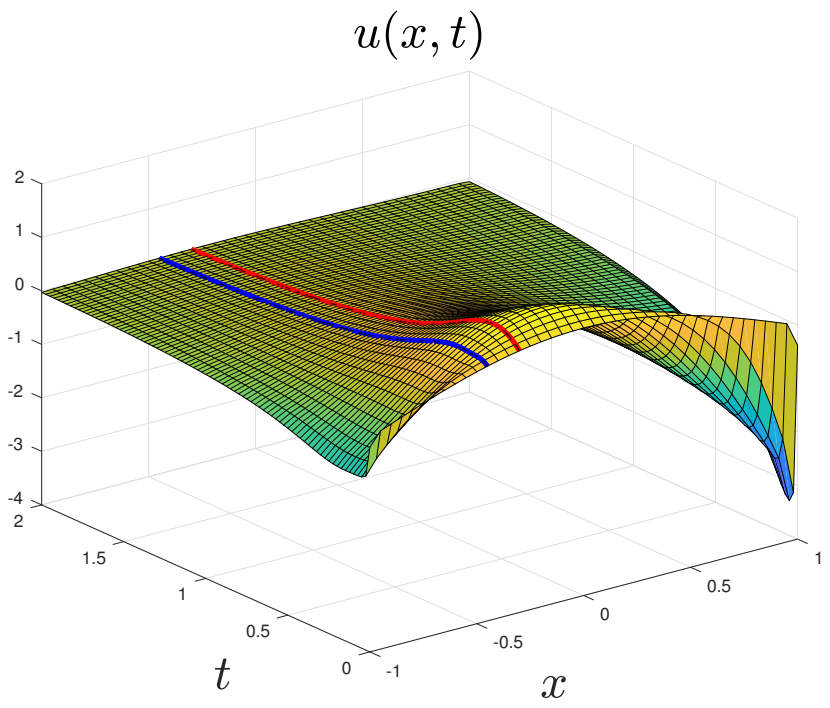

Figure 6.8: Closed-loop response $u(x,t)$ with folding points chosen to be $y_0 = -0.30, \hat{y}_0 = -0.45$.

the parabolic PDE, or even coupling other 1-D PDEs at the boundary.

6.7 Acknowledgements

Chapter 6 is, in part, a reprint of work found in "Bilateral Boundary Backstepping Control of a 1-D Unstable Parabolic PDE via a Folding Approach" presented at the 3rd IFAC Joint Workshop on PDE Control and Distributed Parameter Systems (CPDE/CDPS), 2019 co-authored with R. Vazquez and M. Krstic. The dissertation author was the primary investigator and author of this paper. Chapter 6 also contains the extension of this work to state-estimation and output-feedback, which is a reprint of the work "Folding Bilateral Backstepping Output-Feedback Control Design For an Unstable Parabolic PDE," submitted for publication to IEEE Transactions on Automatic Control, 2019 co-authored with R. Vazquez and M. Krstic. The dissertation author

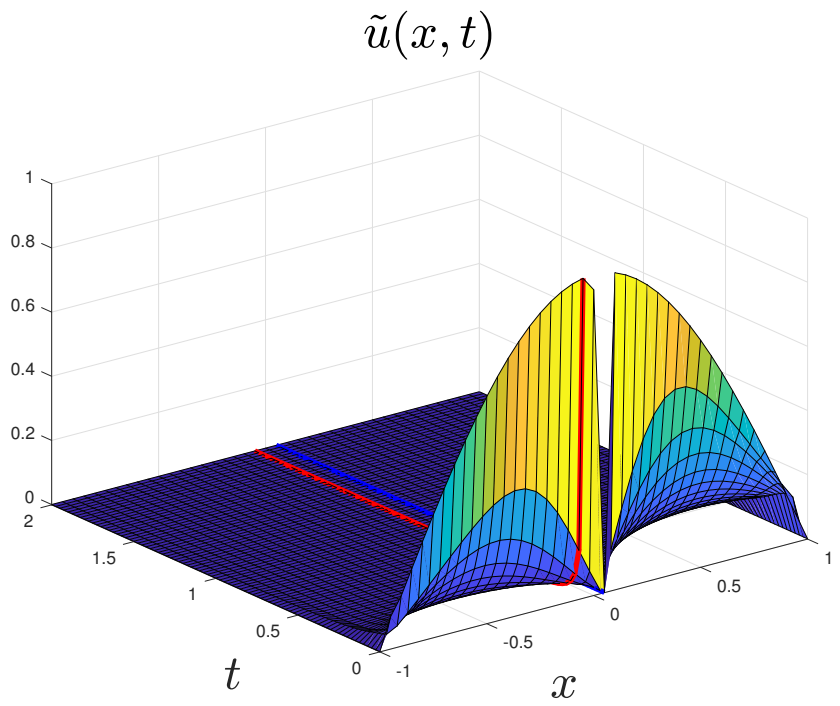

Figure 6.9: Observer error $\tilde{u}(x,t)$ with folding points chosen to be $y_0 = -0.05, \hat{y}_0 = 0.05$.

was also the primary investigator and author of this paper.

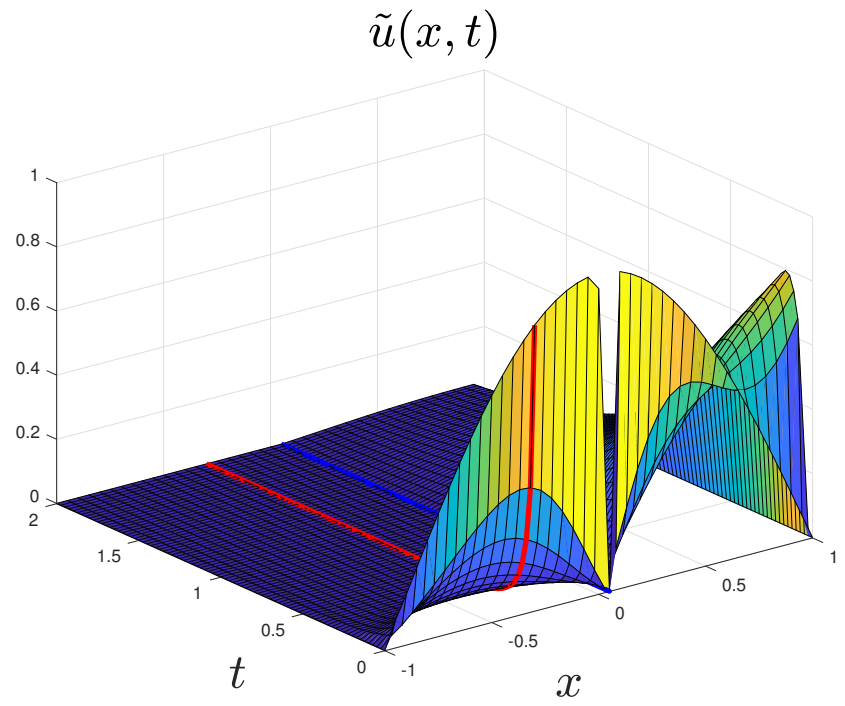

Figure 6.10: Observer error $\tilde{u}(x,t)$ with folding points chosen to be $y_0 = -0.30, \hat{y}_0 = 0.05$.

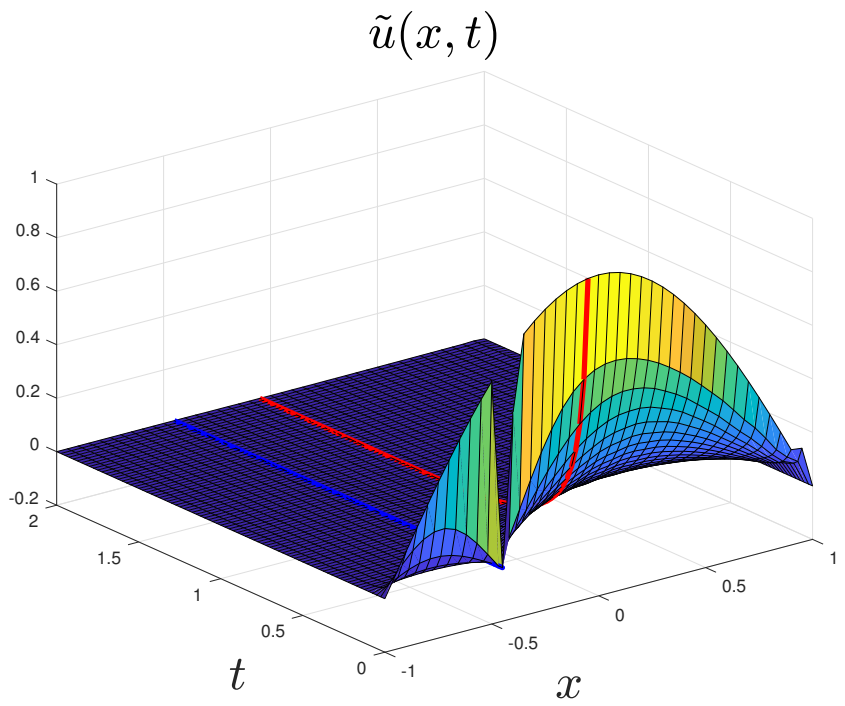

Figure 6.11: Observer error $\tilde{u}(x,t)$ with folding points chosen to be $y_0 = -0.05, \hat{y}_0 = -0.45$.

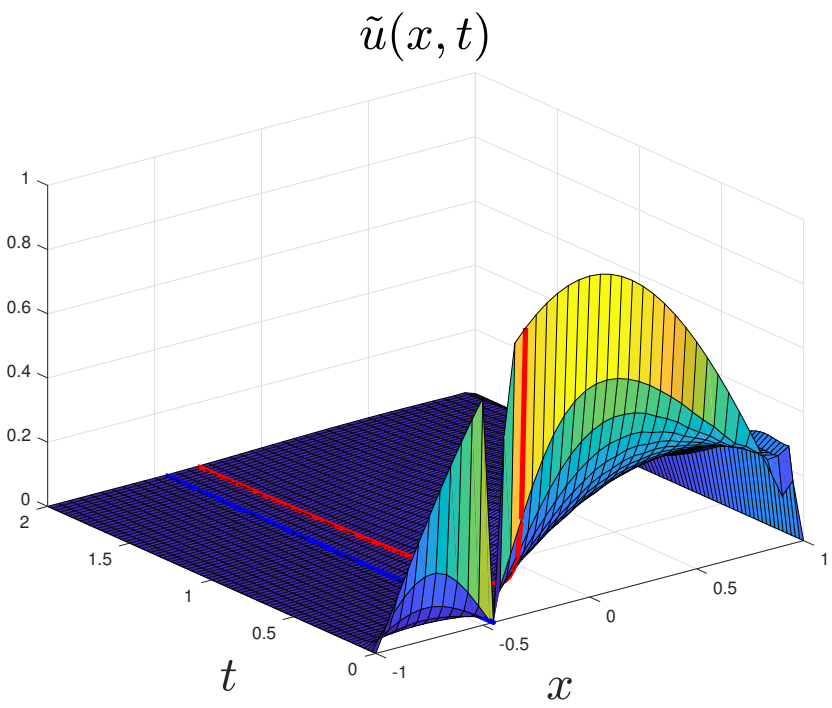

Figure 6.12: Observer error $\tilde{u}(x,t)$ with folding points chosen to be $y_0 = -0.30, \hat{y}_0 = -0.45$.

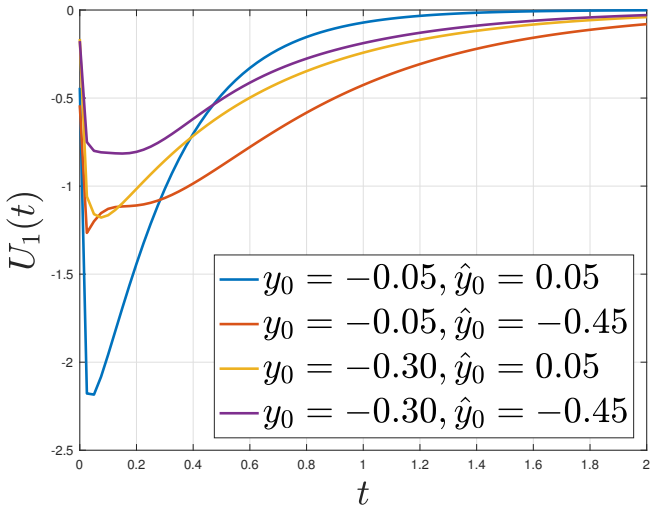

Figure 6.13: Comparison of control effort by left controller ($\mathcal{U}_1(t)$) over different folding choices

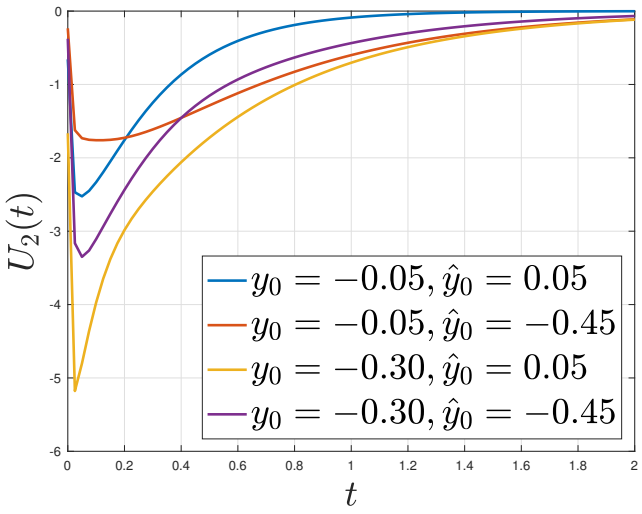

Figure 6.14: Comparison of control effort by right controller ($\mathcal{U}_2(t)$) over different folding choices

Chapter 7

A Folding Approach to Bilateral Control of a 1-D Unstable Parabolic PDE with Distinct Input Delays

7.1 Introduction

We return to the problem investigated in Chapter 5 involving bilateral control design for a 1-D parabolic PDE subject to distinct input delays. However, rather than to resort to using artifical delay (an infinite-dimensional analogue to dynamic extension), we will apply the folding approach developed in the previous chapter to admit a system representation that can account for the distinctness of the input delays without using artifical delay.

Bilateral backstepping control is a relatively new concept, but one that is naturally interpreted and has much relevance. Bilateral control for partial differential equations can open the door to fault-tolerant designs (in the case one actuator fails). An additional benefit is that the presence of a second actuator can lead to less control effort per actuator, and thus extending the operating life cycle of the system significantly. Lastly, as one can intuit, the single

acutator case falls under the bilateral control case, and thus, one can see that bilateral control is the natural extension to pre-existing backstepping boundary control. Previously, bilateral backstepping control has been initially developed by [43] for both parabolic and second-order hyperbolic equation cases, and the previous work by the author in [15]. Other results in bilateral control have been explored in first-order hyperbolic system contexts ([5],[4]), and most recently, in a parabolic context of trajectory tracking for a viscous Hamilton-Jacobi equation [8].

Input delay is a more commonly studied field, as it has direct relevance to many control problems (existing as actuator, communication, computational delays). There exists a wide swath of literature exploring many different variations of delay problems casted as partial differential equations, but relatively few in input delay for parabolic equations. A large part of this is due to the mixed-class nature of these problems, as they entail a coupled system of a delay (hyperbolic) with the physical plant (parabolic). Interestingly, the gain PDE to be solved that arises from these types of problems maintain the mixed-class character of the plant (as opposed to homogeneous class systems, which always have a hyperbolic gain PDE). The most basic case of this mixed-class system has been explored in [28], where an unstable diffusion-reaction equation is considered with an arbitrariliy long input delay. This work was further extended in [12], where unidirectional in-domain coupling was next considered for systems of mixed-class type.

In this paper, we solve the problem of having distinct input delays to the bilateral control problem for an unstable parabolic equation via the method of folding.

7.2 Model and "folding" transformation

We consider the problem of an unstable diffusion-reaction equation with distinct input delays $D_v, D_w > 0$.

$$\partial_t u(y,t) = \varepsilon \partial_{yy} u(y,t) + \lambda(y) u(y,t) \tag{7.1}$$

$$\partial_x u(-1,t) = \mathcal{U}_1(t - D_v) \tag{7.2}$$

$$\partial_x u(1,t) = \mathcal{U}_2(t - D_w) \tag{7.3}$$

with $y \in (-1,1)$. It is well known that delays can be represented with first-order hyperbolic PDEs. We rewrite the delays found in (7.2),(7.3) as first-order hyperbolic PDEs:

$$\partial_t v(x,t) = -\partial_x v(x,t) \tag{7.4}$$

$$\partial_t w(z,t) = \partial_z w(z,t) \tag{7.5}$$

$$v(-1 - D_v, t) = \mathcal{U}_1(t) \tag{7.6}$$

$$w(1 + D_w, t) = \mathcal{U}_2(t) \tag{7.7}$$

Where $x \in (-1 - D_v, -1), z \in (1, 1 + D_w)$. Thus, (7.2),(7.3) become

$$\partial_x u(-1,t) = -v(-1,t) \tag{7.8}$$

$$\partial_x u(1,t) = w(1,t) \tag{7.9}$$

We select an arbiitary point $y_0 \in (-1,1)$ to "fold" the parabolic equation (7.1) around. We first use the following piecewise definition of $u(y,t)$ as:

$$u(y,t) = \begin{cases} u_1(y,t) & y \in (-1, y_0) \\ u_2(y,t) & y \in (y_0, 1) \end{cases} \tag{7.10}$$

and define the following spatial transformations in x, y, z:

$$x_1 = (y_0 - y)/(1 + y_0) \qquad y \in (-1, y_0) \tag{7.11}$$

$$x_2 = (y - y_0)/(1 - y_0) \qquad y \in (y_0, 1) \tag{7.12}$$

$$x_3 = -\frac{1}{D_v}(x+1)+1 \tag{7.13}$$

$$x_4 = \frac{1}{D_w}(z-1)+1 \tag{7.14}$$

Note that $x_1, x_2 \in [0,1]$ and $x_3, x_4 \in [1,2]$. This set of scaling and folding transformations will allow us to map the system (7.1)-(7.8) into the following system in matrix form:

$$\partial_t U(x,t) = E\partial_{xx}U(x,t) + \Lambda(x)u(x,t) \tag{7.15}$$

$$\partial_t V(x,t) = \Sigma\partial_x v(x,t) \tag{7.16}$$

$$\alpha U_x(0,t) = -\beta U(0,t) \tag{7.17}$$

$$U_x(1,t) = V(1,t) \tag{7.18}$$

$$V(2,t) = \mathcal{U}(t) \tag{7.19}$$

We have dropped the subscript indexing on x for simplicity. The states $U : [0,1]\times[0,\infty) \to \mathbb{R}^2$ and $V : [1,2]\times[0,\infty) \to \mathbb{R}^2$ are defined as

$$U(x,t) := \begin{pmatrix} u_1(y_0 - (1+y_0)x, t) \\ u_2(y_0 + (1-y_0)x, t) \end{pmatrix} \tag{7.20}$$

$$V(x,t) := \begin{pmatrix} v(-1 - D_v(x+1), t) \\ w(x,t) \end{pmatrix} \tag{7.21}$$

while the control $\mathcal{U} : [0,\infty) \to \mathbb{R}^2$ is defined

$$\mathcal{U} := \begin{pmatrix} \mathcal{U}_1(t) \\ \mathcal{U}_2(t) \end{pmatrix} \tag{7.22}$$

and the parameter matrices are defined by

$$E := \mathrm{diag}(\varepsilon_1, \varepsilon_2) \tag{7.23}$$

$$\Lambda(x) := \mathrm{diag}(\lambda_1(x), \lambda_2(x)) \tag{7.24}$$

$$\Sigma := \mathrm{diag}(\sigma_1, \sigma_2) \tag{7.25}$$

$$\alpha := \begin{pmatrix} 1 & 1 \\ 0 & 0 \end{pmatrix} \tag{7.26}$$

$$\beta := \begin{pmatrix} 0 & 0 \\ 1 & -1 \end{pmatrix} \tag{7.27}$$

$$\varepsilon_1 = \frac{\varepsilon}{(1+y_0)^2} \tag{7.28}$$

$$\varepsilon_2 = \frac{\varepsilon}{(1-y_0)^2} \tag{7.29}$$

$$\lambda_1(x) = \lambda(y_0 - (1+y_0)x) \tag{7.30}$$

$$\lambda_2(x) = \lambda(y_0 + (1-y_0)x) \tag{7.31}$$

$$\sigma_1 = D_v^{-1} \tag{7.32}$$

$$\sigma_2 = D_w^{-1} \tag{7.33}$$

The conditions encoded in the α, β matrices arise from imposing compatibility conditions between u_1 and u_2 at $x = 0$.

7.3 Backstepping control design

We use two sets of backstepping transformations. The first shifts the instability of $U(x,t)$ to the $x = 1$ boundary. The second will shift the instabilitly from the $x = 1$ to the $x = 2$ boundary, where it can be neutralized by the controller $\mathcal{U}$.

The first transformation is

$$W(x,t) = U(x,t) - \int_0^x K(x,y)U(y,t)dy \tag{7.34}$$

where $K(x,y) : \mathbb{R} \times \mathbb{R} \to \mathbb{R}^{2\times 2}$ are the continuous gain kernels of the transformations. The existence of K is studied in [18]. For brevity, we will skip over the details in determining K in this paper.

The second transformation is

$$\begin{aligned} Z(x,t) = V(x,t) &- \int_1^x L(x,y)V(y,t)dy \\ &- \int_0^1 M(x,y)U(y,t)dy \end{aligned} \tag{7.35}$$

where, again, $L(x,y), M(x,y) : \mathbb{R} \times \mathbb{R} \to \mathbb{R}^{2\times 2}$. We must study the existence of these gain kernels, which is a novel contribution.

These transformations will admit the following target system (depending on parameters):

$$\begin{aligned} \partial_t W(x,t) &= E\partial_{xx} W(x,t) - \mu W(x,t) \\ &\quad - C_1(x)(F_1 F_1^T W(0,t) + F_2 F_2^T \partial_x W(0,t)) \end{aligned} \tag{7.36}$$

$$\partial_t Z(x,t) = \Sigma \partial_x Z(x,t) + C_2(x)Z(x,t) \tag{7.37}$$

$$\alpha \partial_x W(0,t) = -\beta W(0,t) \tag{7.38}$$

$$\partial_x W(1,t) = Z(1,t) \tag{7.39}$$

$$Z(2,t) = 0 \tag{7.40}$$

where $\mu \in \mathbb{R}_+$ is a design parameter affecting the convergence rate of the state, and F_1,F_2 are

indicator vectors defined as

$$F_1 = \begin{pmatrix} 1 & 0 \end{pmatrix}^T \qquad F_2 = \begin{pmatrix} 0 & 1 \end{pmatrix}^T \tag{7.41}$$

The structure of $C_1(x)$ will change according to the parameters $\varepsilon_1, \varepsilon_2$:

$$C_1(x) = \begin{cases} \begin{pmatrix} 0 & 0 \\ c_1(x) & 0 \end{pmatrix} & \varepsilon_1 > \varepsilon_2 \\ \begin{pmatrix} 0 & c_1(x) \\ 0 & 0 \end{pmatrix} & \varepsilon_1 < \varepsilon_2 \\ 0 & \varepsilon_1 = \varepsilon_2 \end{cases} \tag{7.42}$$

The structure of the matrix-valued functions $C_2(x)$ is analagous to $C_1(x)$ in structure, but instead according to the parameters σ_1, σ_2, i.e.

$$C_2(x) = \begin{cases} \begin{pmatrix} 0 & 0 \\ c_2(x) & 0 \end{pmatrix} & \sigma_1 > \sigma_2 \\ \begin{pmatrix} 0 & c_2(x) \\ 0 & 0 \end{pmatrix} & \sigma_1 < \sigma_2 \\ 0 & \sigma_1 = \sigma_2 \end{cases} \tag{7.43}$$

The system will be exponentially stable due to the structure of these matrix valued functions. The $c_i(x)$ are predefined (in fact related to the gain kernel functions, which will be defined in a later section).

For the sake of brevity in this paper, we will make the following assumption:

Assumption. *Assume the case* $\varepsilon_1 > \varepsilon_2$ *and* $\sigma_1 > \sigma_2$. *By a simple permutation of states, this is*

equivalent to the case $\varepsilon_2 > \varepsilon_1$ *and* $\sigma_2 > \sigma_1$.

Remark. *Based upon this assumption, also note that the product* $C_2F_2F_2^T = 0$.

Remark. *The unconsidered cases of* $(\varepsilon_1 < \varepsilon_2, \sigma_1 > \sigma_2)$ *and* $(\varepsilon_2 < \varepsilon_1, \sigma_2 > \sigma_1)$ *are equivalent via a permutation of states. For this case,* $C_1F_1F_1^T = 0$. *Therefore, the stability analysis for this case is mildly different, owing to a slightly different target system, but nevertheless naturally extends from the stability analysis in this paper.*

These remarks follow directly from a special 2×2 case found in [18].

7.3.1 Kernel derivations for L, M

Differentiating (7.35) once in time admits

$$\begin{aligned}\partial_t Z(x,t) &= \partial_t V(x,t) - \int_1^x L(x,y)\partial_t V(y,t)dy \\ &\quad - \int_0^1 M(x,y)\partial_t U(y,t)dy \qquad (7.44)\\ &= \Sigma\partial_x V(x,t) - \int_1^x L(x,y)\Sigma\partial_y V(y,t)dy \\ &\quad - \int_0^1 M(x,y)\left[E\partial_{yy}U(y,t) + \Lambda(y)U(y,t)\right]dy \qquad (7.45)\end{aligned}$$

Integrating by parts,

$$\begin{aligned}&= \Sigma\partial_x V(x,t) - L(x,x)\Sigma V(x,t) + L(x,1)\Sigma V(1,t) \\ &\quad + \int_1^x \partial_y L(x,y)\Sigma V(y,t)dy \\ &\quad - M(x,1)E\partial_x U(1,t) + M(x,0)E\partial_x U(0,t) \\ &\quad + \partial_y M(x,1)EU(1,t) - \partial_y M(x,0)EU(0,t) \\ &- \int_0^1 \left[\partial_{yy}M(x,y)E + M(x,y)\Lambda(y)\right]U(y,t)dy \qquad (7.46)\end{aligned}$$

While differentiating (7.35) once in space admits

$$\begin{aligned}\partial_x Z(x,t) = \partial_x V(x,t) - L(x,x)V(x,t) \\ - \int_1^x \partial_x L(x,y)V(y,t)dy \\ - \int_0^1 \partial_x M(x,y)U(y,t)dy \end{aligned} \tag{7.47}$$

By imposing (7.1)-(7.7) and (7.36)-(7.40), we can recover the following set of conditions on L, M that comprise a coupled mixed-type PDE:

$$\Sigma\partial_x L(x,y) + \partial_y L(x,y)\Sigma = C_2(x)L(x,y) \tag{7.48}$$

$$\Sigma L(x,x) - L(x,x)\Sigma = -C_2(x) \tag{7.49}$$

$$L(x,1)\Sigma = M(x,1)E \tag{7.50}$$

$$\begin{aligned}\Sigma\partial_x M(x,y) - \partial_{yy} M(x,y)E = M(x,y)\Lambda(y) \\ + C_2(x)M(x,y)\end{aligned} \tag{7.51}$$

$$\partial_y M(x,1)E = 0 \tag{7.52}$$

$$\partial_y M(x,0)EU(0,t) = M(x,0)E\partial_x U(0,t) \tag{7.53}$$

The matrix condition (7.49) actually consists of three boundary conditions and one *definition*, which arises due to the assumption $\sigma_1 \geq \sigma_2$. Noting (7.43), we can find the definition for the nonzero element of $C_2(x)$ to be

$$c_2(x) = (\sigma_1 - \sigma_2)l_{21}(x,x) \tag{7.54}$$

Additionally, the gain kernel has a dependence on $U, \partial_x U$. However, the structure of the plant allows for some very interesting reductions. Due to the singularity of the matrices α, β found in (7.17), we will have to analyze this boundary condition componentwise. The α matrix

encodes the continuity of the spatial derivative of the state, $\partial_x u_1(0,t) = -\partial_x u_2(0,t)$ (analgous condition regarding the state and β). Using this knowledge, we can rewrite (7.53) as

$$M(x,0)E\begin{pmatrix}1\\-1\end{pmatrix}\partial_x u_1(0,t) - M_y(x,0)E\begin{pmatrix}1\\1\end{pmatrix}u_1(0,t) = 0 \tag{7.55}$$

From this, we can derive two sufficient conditions:

$$M(x,0)E\begin{pmatrix}1\\-1\end{pmatrix} = 0 \tag{7.56}$$

$$\partial_y M(x,0)E\begin{pmatrix}1\\1\end{pmatrix} = 0 \tag{7.57}$$

In its current form, the M gain kernel appears to be overdefined. However, one can notice that writing out these two conditions componentwise, they actually encode sets of *folding* boundary conditions on M! This is an interesting symmetry between the plant and the gain kernel, in the sense that we have folded the parabolic equation in the plant, and proceed to unfold the parabolic equation in the kernel. The equations written out are:

$$m_{11}(x,0)\varepsilon_1 - m_{12}(x,0)\varepsilon_2 = 0 \tag{7.58}$$

$$m_{21}(x,0)\varepsilon_1 - m_{22}(x,0)\varepsilon_2 = 0 \tag{7.59}$$

$$\partial_y m_{11}(x,)\varepsilon_1 + \partial_y m_{12}(x,0)\varepsilon_2 = 0 \tag{7.60}$$

$$\partial_y m_{21}(x,0)\varepsilon_1 + \partial_y m_{22}(x,0)\varepsilon_2 = 0 \tag{7.61}$$

Thus, one can rewrite the m_{11}, m_{12} component gain kernel PDEs into a single PDE, and

the same for m_{21}, m_{22}. By defining m_1, m_2 as the following:

$$m_1(x,y) := \begin{cases} \frac{\varepsilon_1}{\varepsilon_2} m_{11}(x,-y) & y \in (-1,0) \\ m_{12}(x,y) & y \in (0,1) \end{cases} \tag{7.62}$$

$$m_2(x,y) := \begin{cases} \frac{\varepsilon_1}{\varepsilon_2} m_{21}(x,-y) & y \in (-1,0) \\ m_{22}(x,y) & y \in (0,1) \end{cases} \tag{7.63}$$

we can consolidate the four (m_{ij}) component parabolic gain kernel PDEs into two reaction-diffusion equations with identically zero Neumann boundary conditions:

$$\partial_x m_1(x,y) = D_1(y)\partial_{yy} m_1(x,y) + \Lambda_1(y) m_1(x,y) \tag{7.64}$$

$$\partial_y m_1(x,-1) = 0 \tag{7.65}$$

$$\partial_y m_1(x,1) = 0 \tag{7.66}$$

$$m_1(1,y) = \begin{cases} \frac{\varepsilon_1}{\varepsilon_2} \partial_x k_{11}(1,-y) & y \in (-1,0) \\ \partial_x k_{12}(1,y) & y \in (0,1) \end{cases} \tag{7.67}$$

$$\begin{aligned} \partial_x m_2(x,y) = {} & D_2(y)\partial_{yy} m_2(x,y) + \Lambda_2(y) m_2(x,y) \\ & + \Phi(x,y) \end{aligned} \tag{7.68}$$

$$\partial_y m_2(x,-1) = 0 \tag{7.69}$$

$$\partial_y m_2(x,1) = 0 \tag{7.70}$$

$$m_2(1,y) = \begin{cases} \frac{\varepsilon_1}{\varepsilon_2} \partial_x k_{21}(1,-y) & y \in (-1,0) \\ \partial_x k_{22}(1,y) & y \in (0,1) \end{cases} \tag{7.71}$$

where the parameters are now defined spatially as

$$D_1(y) := \begin{cases} \varepsilon_1/\sigma_1 & y \in (-1,0) \\ \varepsilon_2/\sigma_1 & y \in (0,1) \end{cases} \tag{7.72}$$

$$\Lambda_1(y) := \begin{cases} \varepsilon_2\lambda_1(y)/\varepsilon_1\sigma_1 & y \in (-1,0) \\ \lambda_2(y)/\sigma_1 & y \in (0,1) \end{cases} \tag{7.73}$$

$$D_2(y) := \begin{cases} \varepsilon_1/\sigma_2 & y \in (-1,0) \\ \varepsilon_2/\sigma_2 & y \in (0,1) \end{cases} \tag{7.74}$$

$$\Lambda_2(y) := \begin{cases} \varepsilon_2\lambda_1(y)/\varepsilon_1\sigma_2 & y \in (-1,0) \\ \lambda_2(y)/\sigma_2 & y \in (0,1) \end{cases} \tag{7.75}$$

and Φ is a function defined as

$$\Phi(x,y) := \begin{cases} \frac{\varepsilon_2}{\varepsilon_1} c_2(x) m_1(x,y) & y \in (-1,0) \\ 0 & y \in (0,1) \end{cases} \tag{7.76}$$

where we have used the lower triangular structure of the matrix valued function $C_2(x)$ alongside the condition (7.49) to define $\Phi(x,y)$ appropriately.

Curiously, this brings up an interesting structure in the gain kernels. One must actually solve the m_1 equation prior to attempting to solve the m_2 equation, due to the cascading found in $F(x,y)$. Fortunately, the solution m_1 only requires information of the gain kernel $K(x,y)$, which is readily available.

As for the gain kernel PDEs in L, there exists some difficulty. Due to the structure of the coefficient γ (which in itself is a necessity for well-posedness), one must approach these gain kernels in a componentwise fashion.

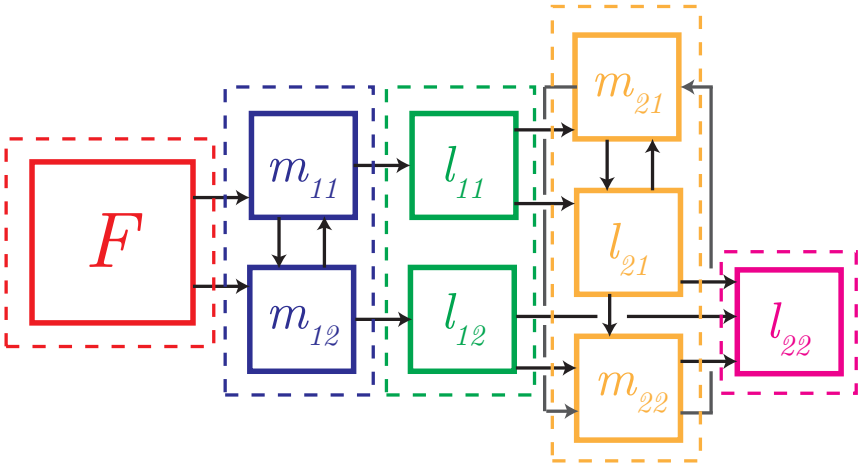

Figure 7.1: The gain kernels express a cascaded nature which can be exploited to recover linear PDE problems solved in succession.

The first set of gain kernels, m_1, one can directly observe that they in fact are merely reaction-diffusion equations with spatially varying reaction. In fact, one can solve these directly using the method of separation of variables.

The next set of gain kernel PDEs are simple to solve. For l_{11}, l_{12}, we can express them as simply:

$$\partial_x l_{11}(x,y) + \partial_y l_{11}(x,y) = 0 \tag{7.77}$$

$$l_{11}(x,1) = \frac{\varepsilon_2}{\sigma_1} m_1(x,-1) \tag{7.78}$$

$$\sigma_1 \partial_x l_{12}(x,y) + \sigma_2 \partial_y l_{12}(x,y) = 0 \tag{7.79}$$

$$l_{12}(x,1) = \frac{\varepsilon_2}{\sigma_2} m_1(x,1) \tag{7.80}$$

$$l_{12}(x,x) = 0 \tag{7.81}$$

l_{12} requires two boundary conditions for $y = 1$ and $y = x$, as per the assumption $\sigma_1 \geq \sigma_2$.

The second set of gain kernel PDEs are a little more involved, due to $C_2(x)$ introducing

additonal coupling structures. They are expressed in the following manner:

$$\sigma_2 \partial_x l_{21}(x,y) + \sigma_1 \partial_y l_{21}(x,y) = c_2(x) l_{11}(x,y) \tag{7.82}$$

$$l_{21}(x,1) = \frac{\varepsilon_2^2}{\varepsilon_1 \sigma_1} m_2(x,-1) \tag{7.83}$$

$$\partial_x l_{22}(x,y) + \partial_y l_{22}(x,y) = c_2(x) l_{11}(x,y) \tag{7.84}$$

$$l_{22}(x,1) = \frac{\varepsilon_2}{\sigma_2} m_2(x,1) \tag{7.85}$$

Herein lies the difficulty of showing existence or otherwise solving the gain kernel PDEs. In the second set of gain kernel PDEs consisting of l_{21}, l_{22}, one notes that l_{11} enters the equation. This is not a problem, as we can merely solve via cascading the solution of l_{11} into these equations. However, the more difficult part is noticing that l_{21} is introudced into the equations as well (through the coupling term $c_2(x)$) and the equations become far more difficult to solve as it contains a nonlocal term, $l_{21}(x,x)$. Moreover, the boundary condition given for this equation depends on m_2, which (if the reader may recall in (7.68),(7.76)) depends on l_{21}.

Thus, one must attempt to solve l_{21} and m_2 simultaneously before being able to solve l_{22}. The gain kernel equations (and definitions) relevant and reiterated are then:

$$\begin{aligned} \partial_x \sigma_2 l_{21}(x,y) = &-\partial_y \sigma_1 l_{21}(x,y) \\ &+ (\sigma_1 - \sigma_2) l_{21}(x,x) l_{11}(x,y) \end{aligned} \tag{7.86}$$

$$l_{21}(x,1) = \frac{\varepsilon_2^2}{\varepsilon_1 \sigma_1} m_2(x,-1) \tag{7.87}$$

$$\begin{aligned} \partial_x m_2(x,y) = &D_2(y) m_{yy}^2(x,y) + \Lambda_2(y) m_2(x,y) \\ &+ \Phi(x,y) \end{aligned} \tag{7.88}$$

$$\partial_y m_2(x,-1) = 0 \tag{7.89}$$

$$\partial_y m_2(x,1) = 0 \tag{7.90}$$

$$m_2(1,y) = \begin{cases} \frac{\varepsilon_1}{\varepsilon_2}\partial_x k_{21}(1,-y) & y \in (-1,0) \\ \partial_x k_{22}(1,y) & y \in (0,1) \end{cases} \tag{7.91}$$

$$\Phi(x,y) := \begin{cases} \frac{\varepsilon_2}{\varepsilon_1}(\sigma_1 - \sigma_2) & \\ \quad \times l_{21}(x,x)m_1(x,y) & y \in (-1,0) \\ 0 & y \in (0,1) \end{cases} \tag{7.92}$$

where one can assume that $l_{11}, m_1, k_x^{21}, k_x^{22}$ exist and have sufficient regularity.

7.3.2 Well-posedness of gain kernel equations for $l_{21}(x,y), m_2(x,y)$

We will first begin with the l_{21} equation, and attempt to express the solution at the boundary $y = x$,$l_{21}(x,x)$, as an integral equation.

By method of characteristics, we find

$$\frac{dx}{ds} = \sigma_2 \tag{7.93}$$

$$\frac{dy}{ds} = \sigma_1 \tag{7.94}$$

$$\frac{dl_{21}}{ds} = (\sigma_1 - \sigma_2) l_{11}(x(s), y(s)) l_{21}(x(s), x(s)) \tag{7.95}$$

The evolution of x, y along the characteristics is simple to find:

$$x(s) = x_0 + \sigma_2 s \tag{7.96}$$

$$y(s) = 1 + \sigma_1 s \tag{7.97}$$

One can also show that given a pair (x,y), s, x_0 can be found accordingly:

$$s = \frac{1}{\sigma_1}(y-1) \tag{7.98}$$

$$x_0 = x - \frac{\sigma_2}{\sigma_1}(y-1) \tag{7.99}$$

Then, the expression (7.95) can be integrated to find

$$\begin{aligned} l_{21}(x,y) = {} & l_{21}\left(x - \frac{\sigma_2}{\sigma_1}(y-1), 1\right) \\ & - \int_0^{\frac{1}{\sigma_1}(y-1)} l_{11}\left(x - \frac{\sigma_2}{\sigma_1}(y-1) + \sigma_2 z, 1 + \sigma_1 z\right) \\ & \times l_{21}\left(x - \frac{\sigma_2}{\sigma_1}(y-1) + \sigma_2 z, x - \frac{\sigma_2}{\sigma_1}(y-1) + \sigma_2 z\right) \\ & \times (\sigma_1 - \sigma_2) dz \end{aligned} \tag{7.100}$$

Evaluating this expression at $y = x$,

$$\begin{aligned} l_{21}(x,x) = {} & l_{21}\left(\left(1 - \frac{\sigma_2}{\sigma_1}\right)x + \frac{\sigma_2}{\sigma_1}, 1\right) \\ & - \int_0^{\frac{1}{\sigma_1}(x-1)} l_{11}\left(\left(1 - \frac{\sigma_2}{\sigma_1}\right)x + \frac{\sigma_2}{\sigma_1} + \sigma_2 z, 1 + \sigma_1 z\right) \\ & \times l_{21}\left(\left(1 - \frac{\sigma_2}{\sigma_1}\right)x + \frac{\sigma_2}{\sigma_1} + \sigma_2 z, \right. \\ & \left. \left(1 - \frac{\sigma_2}{\sigma_1}\right)x + \frac{\sigma_2}{\sigma_1} + \sigma_2 z\right)(\sigma_1 - \sigma_2) dz \end{aligned} \tag{7.101}$$

Making the following substitution for the variable of integration

$$\zeta = a(x) + \sigma_2 z \tag{7.102}$$

$$a(x) := \left(1 - \frac{\sigma_2}{\sigma_1}\right)x + \frac{\sigma_2}{\sigma_1} \tag{7.103}$$

The integral equation for $l_{21}(x,x)$ becomes

$$l_{21}(x,x) = l_{21}\left(a(x), 1\right)$$

$$-\int_{a(x)}^{x}\frac{\sigma_1-\sigma_2}{\sigma_2}l_{11}\left(\zeta,\left(1-\frac{\sigma_1}{\sigma_2}\right)x+\frac{\sigma_1}{\sigma_2}\zeta\right)l_{21}(\zeta,\zeta)\,d\zeta \tag{7.104}$$

$$=\frac{\varepsilon_2^2}{\varepsilon_1\sigma_1}m_2(a(x),-1)$$

$$-\int_{a(x)}^{x}\frac{\sigma_1-\sigma_2}{\sigma_2}$$

$$\times l_{11}\left(\zeta,\left(1-\frac{\sigma_1}{\sigma_2}\right)x+\frac{\sigma_1}{\sigma_2}\zeta\right)l_{21}(\zeta,\zeta)\,d\zeta \tag{7.105}$$

We can now define the following iteration for l_{21} in the spirit of successive approximations:

$$\hat{l}_{n+1}(x)=\frac{\varepsilon_2^2}{\varepsilon_1\sigma_1}m_2(a(x),-1)$$
$$-\int_{a(x)}^{x}\frac{\sigma_1-\sigma_2}{\sigma_2}$$
$$\times l_{11}\left(\zeta,\left(1-\frac{\sigma_1}{\sigma_2}\right)x+\frac{\sigma_1}{\sigma_2}\zeta\right)\hat{l}_n(\zeta)\,d\zeta \tag{7.106}$$

where if the above integral equation is a contraction, the limit of the iterations will approach the solution, i.e.

$$\lim_{n\to\infty}\hat{l}_n(x)=l_{21}(x,x) \tag{7.107}$$

By defining $\Delta\hat{l}_n:=\hat{l}_{n+1}-\hat{l}_n$, we find the following relation:

$$\Delta\hat{l}_{n+1}(x)=\int_{\left(1-\frac{\sigma_2}{\sigma_1}\right)x+\frac{\sigma_2}{\sigma_1}}^{x}\frac{\sigma_1-\sigma_2}{\sigma_2}$$
$$\times l_{11}\left(\zeta,\left(1-\frac{\sigma_1}{\sigma_2}\right)x+\frac{\sigma_1}{\sigma_2}\zeta\right)\Delta\hat{l}_n(\zeta)\,d\zeta \tag{7.108}$$

Where now (7.107) can be rewritten as an infinite sum:

$$l_{21}(x,x)=\hat{l}_0(x)+\sum_{n=0}^{\infty}\Delta\hat{l}_n(x) \tag{7.109}$$

Choosing $\hat{l}_0(x) = 0$, one can find the solution $l_{21}(x,x)$ to be

$$\begin{aligned} l_{21}(x,x) &= \frac{\varepsilon_2^2}{\varepsilon_1\sigma_1} m_2\left(a(x),-1\right) \\ &\quad + \sum_{n=1}^{\infty} \int_{a(x)}^{x} \int_{a(\zeta_{n-1})}^{\zeta_{n-1}} \cdots \int_{a(\zeta_2)}^{\zeta_2} \\ &\quad \left(\frac{\sigma_1-\sigma_2}{\sigma_2}\right)^n P_n(x,\zeta_1,\zeta_2,\ldots,\zeta_n) \\ &\quad \times \frac{\varepsilon_2^2}{\varepsilon_1\sigma_1} m_2\left(a(\zeta_1),-1\right) d\zeta_1 \ldots d\zeta_n \end{aligned} \tag{7.110}$$

$$\begin{aligned} P_n(x,\zeta_1,\ldots,\zeta_n) &= l_{11}\left(\zeta_n, \left(1-\frac{\sigma_1}{\sigma_2}\right)x + \frac{\sigma_1}{\sigma_2}\zeta_n\right) \\ &\quad \times \prod_{m=1}^{n-1} l_{11}\left(\zeta_m, \left(1-\frac{\sigma_1}{\sigma_2}\right)\zeta_{m+1} + \frac{\sigma_1}{\sigma_2}\zeta_m\right) \end{aligned} \tag{7.111}$$

One can now proceed to study the existence of solutions to m_2. The existence of l_{21} is contigent on the existence of m_2. Letting $l_{21}(x,x) := \Psi[m_2](x)$ as defined above,

$$\begin{aligned} \partial_x m_2(x,y) &= D_2(y)\partial_{yy} m_2(x,y) + \Lambda_2(y) m_2(x,y) \\ &\quad + \Phi(x,y) \end{aligned} \tag{7.112}$$

$$\partial_y m_2(x,-1) = 0 \tag{7.113}$$

$$\partial_y m_2(x,1) = 0 \tag{7.114}$$

$$m_2(1,y) = \begin{cases} \frac{\varepsilon_1}{\varepsilon_2}\partial_x k_{21}(1,-y) & y \in (-1,0) \\ \partial_x k_{22}(1,y) & y \in (0,1) \end{cases} \tag{7.115}$$

$$\Phi(x,y) := \begin{cases} \frac{\varepsilon_2}{\varepsilon_1}(\sigma_1-\sigma_2) & \\ \qquad \times m_1(x,y)\Psi[m_2](x) & y \in (-1,0) \\ 0 & y \in (0,1) \end{cases} \tag{7.116}$$

We will attempt to establish energy estimates on m_2. First we will bound the term $\Psi[m_2](x)$

as defined above.

$$
\begin{aligned}
|\Psi[m_2](x)| \leq & \left| \frac{\varepsilon_2^2}{\varepsilon_1 \sigma_1} m_2 \left(\left(1 - \frac{\sigma_2}{\sigma_1} \right) x + \frac{\sigma_2}{\sigma_1}, -1 \right) \right| \\
& + \sum_{n=1}^{\infty} \int_{a(x)}^{x} \int_{a(\zeta_{n-1})}^{\zeta_{n-1}} \cdots \int_{a(\zeta_2)}^{\zeta_2} \\
& \left| \frac{\varepsilon_2^2}{\varepsilon_1 \sigma_1} \right| \left| \frac{\sigma_1 - \sigma_2}{\sigma_2} \right|^n |P_n(x, \zeta_1, \zeta_2, \ldots, \zeta_n)| \\
& \times \left| m_2 \left(\left(1 - \frac{\sigma_2}{\sigma_1} \right) \zeta_1 + \frac{\sigma_2}{\sigma_1}, -1 \right) \right| d\zeta_1 \ldots d\zeta_n
\end{aligned} \tag{7.117}
$$

Note that since $a(x) \leq x, \forall x$

$$
\begin{aligned}
|m_2(a(x), -1)| &\leq \sup_{y \in [-1,1]} |m_2(a(x), y)| && (7.118) \\
&\leq ||m_2(a(x), \cdot)||_{L_\infty} && (7.119) \\
&\leq \sup_{1 \leq z \leq x} ||m_2(z, \cdot)||_{L_\infty} && (7.120) \\
&\leq C ||m_2(z, \cdot)||_{H^1} && (7.121)
\end{aligned}
$$

where C is a scaling constant as a result of H^1 being continuously embedded in L_∞. Likewise, we can majorize $l_{11}(x,y)$ by its pointwise sup-norm:

$$
l_{11}(x,y) \leq \sup_{(x,y)} |l_{11}(x,y)| =: ||l_{11}||_{L_\infty} \tag{7.122}
$$

which will allow us to bound P_n in the following way:

$$
|P_n(x, \zeta_1, \ldots, \zeta_n)| \leq ||l_{11}||_{L_\infty}^n \tag{7.123}
$$

We can then redefine (7.117) as

$$
\begin{aligned}
|\Psi[m_2](x)| \leq & \left|\frac{\varepsilon_2^2}{\varepsilon_1\sigma_1}\right| \left| \sup_{1\leq z\leq x} C||m_2(z,\cdot)||_{H^1} \right| \\
& + \sum_{n=1}^{\infty} \int_1^x \int_1^{\zeta_{n-1}} \cdots \int_1^{\zeta_2} \left|\frac{\sigma_1-\sigma_2}{\sigma_2}\right|^n \\
& \quad \times ||l_{11}||_{L_\infty}^n \left|\frac{\varepsilon_2^2}{\varepsilon_1\sigma_1}\right| \\
& \quad \times \sup_{1\leq z\leq x} C||m_2(z,\cdot)||_{H^1} d\zeta_1 \ldots d\zeta_n \qquad (7.124) \\
& \leq \frac{\varepsilon_2^2}{\varepsilon_1\sigma_1} \\
& \times \left(1 + \sum_{n=1}^{\infty} \int_1^x \int_1^{\zeta_{n-1}} \cdots \int_1^{\zeta_2} \right. \\
& \quad \left. \left|\frac{\sigma_1-\sigma_2}{\sigma_2}\right|^n ||l_{11}||_{L_\infty}^n d\zeta_1 \ldots d\zeta_n \right) \\
& \times \sup_{1\leq z\leq x} C||m_2(z,\cdot)||_{H^1} \qquad (7.125) \\
& \leq \frac{\varepsilon_2^2}{\varepsilon_1\sigma_1} \exp\left(\left(\frac{\sigma_1-\sigma_2}{\sigma_2} ||l_{11}||_{L_\infty} \right) (x-1) \right) \\
& \times \sup_{1\leq z\leq x} C||m_2(z,\cdot)||_{H^1} \qquad (7.126)
\end{aligned}
$$

Taking the inner product of m_2 with (7.112),

$$
\begin{aligned}
\int_{-1}^{1} \partial_x m_2(x,y) m_2(x,y) dy = & \\
& \int_{-1}^{1} D_2(y) \partial_{yy} m(x,y) m(x,y) dy \\
& \quad + \int_{-1}^{1} \Lambda_2(y) m(x,y)^2 dy \\
& \qquad + \int_{-1}^{1} \Phi(x,y) m_2(x,y) dy \qquad (7.127)
\end{aligned}
$$

$$\Rightarrow \frac{1}{2}\frac{d}{dx}||m_2(x,\cdot)||_{L_2}^2 \leq ||\Lambda_2||_{L_\infty}||m_2(x,\cdot)||_{L_2}^2 + \int_{-1}^{1}\Phi(x,y)m_2(x,y)dy \tag{7.128}$$

$$\leq ||\Lambda_2||_{L_\infty}||m_2(x,\cdot)||_{L_2}^2 + \left|\frac{\varepsilon_2}{\varepsilon_1}(\sigma_1-\sigma_2)\right||\Psi[m_2](x)| \times \int_{-1}^{0}|m_1(x,y)||m_2(x,y)|dy \tag{7.129}$$

By using the bound on Ψ,

$$\frac{1}{2}\frac{d}{dx}||m_2(x,\cdot)||_{L_2}^2 \leq ||\Lambda_2||_{L_\infty}||m_2(x,\cdot)||_{H^1}^2 + \left|\frac{\varepsilon_2}{\varepsilon_1}(\sigma_1-\sigma_2)\right|\frac{\varepsilon_2^2}{\varepsilon_1\sigma_1} \times \exp\left(\left(\frac{\sigma_1-\sigma_2}{\sigma_2}||l_{11}||_{L_\infty}\right)^n(x-1)\right) \times \sup_{1\leq z\leq x} C||m_2(z,\cdot)||_{H^1} \times \int_{-1}^{0}|m_1(x,y)||m_2(x,y)|dy \tag{7.130}$$

Also by differentiating (7.112) once in y, and taking the inner product with $\partial_y m_2$,

$$\frac{1}{2}\frac{d}{dx}||\partial_y m_2(x,\cdot)||_{L_2}^2 \leq \left(||\Lambda_2||_{L_\infty}+||\Lambda_2'||_{L_\infty}\right)||m_2(x,\cdot)||_{H^1}^2 + \left|\frac{\varepsilon_2}{\varepsilon_1}(\sigma_1-\sigma_2)\right|\frac{\varepsilon_2^2}{\varepsilon_1\sigma_1} \times \exp\left(\left(\frac{\sigma_1-\sigma_2}{\sigma_2}||l_{11}||_{L_\infty}\right)^n(x-1)\right) \times \sup_{1\leq z\leq x} C||m_2(z,\cdot)||_{H^1} \times \int_{-1}^{0}|\partial_y m_1(x,y)||\partial_y m_2(x,y)|dy \tag{7.131}$$

Then one can see simply that from the sum of the two bounds,

$$\begin{aligned}\frac{1}{2}\frac{d}{dx}||m_2(x,\cdot)||_{H^1}^2 \leq & \left(||\Lambda_2||_{L_\infty}+\left|\left|\Lambda_2'\right|\right|_{L_\infty}\right)||m_2(x,\cdot)||_{H^1}^2 \\ & +2\left|\frac{\varepsilon_2}{\varepsilon_1}(\sigma_1-\sigma_2)\right|\frac{\varepsilon_2^2}{\varepsilon_1\sigma_1} \\ & \times\exp\left(\left(\frac{\sigma_1-\sigma_2}{\sigma_2}||l_{11}||_{L_\infty}\right)^n(x-1)\right) \\ & \times\sup_{1\leq z\leq x} C||m_2(z,\cdot)||_{H^1} \\ & \times||m_1(x,\cdot)||_{H^1}||m_2(x,\cdot)||_{H^1} \end{aligned} \tag{7.132}$$

Now let $M(x) := ||m_2(x,\cdot)||_{H^1}^2$ and note that $\forall x, M(x) \geq 0$. Associate the following differential equation in $\bar{M}(x)$ to the differential inequality (7.132):

$$\frac{1}{2}\frac{d}{dx}\bar{M}(x) = a\bar{M}(x)+b(x)\left(\sup_{1\leq z\leq x}\sqrt{\bar{M}(z)}\right)\sqrt{\bar{M}(x)} \tag{7.133}$$

$$a = ||\Lambda_2||_{L_\infty}+\left|\left|\Lambda_2'\right|\right|_{L_\infty} \tag{7.134}$$

$$\begin{aligned} b(x) = & 2C\left|\frac{\varepsilon_2}{\varepsilon_1}(\sigma_1-\sigma_2)\right|\frac{\varepsilon_2^2}{\varepsilon_1\sigma_1} \\ & \times\exp\left(\left(\frac{\sigma_1-\sigma_2}{\sigma_2}||l_{11}||_{L_\infty}\right)^n(x-1)\right) \\ & \times||m_1(x,\cdot)||_{H^1} \end{aligned} \tag{7.135}$$

where the initial condition is taken to be $\bar{M}(1) = M(1) = ||m_2(1,\cdot)||_{H^1}^2$. Noting that the right hand side of (7.135) is nonnegative, the supremum of $\bar{M}(z)$ in the interval $[1,x]$ is clearly at $z = x$. Thus, the differential equation (7.135) becomes

$$\frac{1}{2}\frac{d}{dx}\bar{M}(x) = (a+b(x))\bar{M}(x) \tag{7.136}$$

and one can easily see via the integrating factor method

$$\bar{M}(x) = \exp\left(\int_1^x 2(a+b(z))dz\right)\bar{M}(1) \tag{7.137}$$

Thus, by the comparison principle,

$$M(x) \leq \exp\left(\int_1^x 2(a+b(z))dz\right)M(1) \tag{7.138}$$

$$||m_2(x,\cdot)||_{H^1} \leq \exp\left(\int_1^x (a+b(z))dz\right)||m_2(1,\cdot)||_{H^1} \tag{7.139}$$

The implicatiton here is that the energy quantity $||m_2(x,\cdot)||_{H^1}$ is bounded only by its initial condition $m_2(1,\cdot)$ on the finite interval $[1, 1+D]$ (and by the nature of using the H^1 norm, $m_2(x,\cdot)$ can be noted to be bounded pointwise as well), and therefore a weak solution will exist. One merely needs to additionally construct Galerkin approximations to m_2, and take the limit. The energy estimate (which is uniform with respect to the sequence of Galerkin approximations) will guarantee the weak convergence of the sequence to a weak solution.

7.4 Conclusions

A delay compensation design augmenting the technique the folding technique for designing bilateral controllers with distinct input delays is presented in this paper. The delay compensation for parabolic PDEs can be cast as a mixed-type (hyperbolic-parabolic) PDE system, which motivates the use of new and different techniques. Namely, the gain kernel that arises from applying backstepping to mixed-type PDEs is of differing type than homogeneous-type PDE systems. As a result, parabolic PDEs are found in the resulting gain kernel PDE system, which necessitates the well-posedness analysis not by method of characteristcs (as of typical fashion in classical backstepping with purely hyperbolic kernel PDE), rather, applying a Galerkin-type argument to show existence and uniqueness properties. Conditions on the parameters of the

system can be imposed to demand a certain regularity of the kernel solutions if necessary, but in general, a weak solution with discontinuities over measure zero sets is sufficient, as the kernel appears strictly under an integration.

The development of these results motivate further study into mixed-type PDEs, in particular, ones with "harder" coupling between the hyperbolic and parabolic equations. Some coupling in-domain had previously been considered, but in the sense that the strict feedback structure (spatial causality) from the control boundary is preserved. However, it does not seem wholly unreasonable that even more intricate coupling can be considered.

7.5 Acknowledgements

Chapter 7, in part, is a reprint of the material as it appears in: S.Chen, R. Vazquez, M. Krstic. Bilateral Boundary Control Design for Unstable Parabolic PDE Subject to Distinct Input Delays. Submitted to Systems and Control Letters, 2019. The dissertation author was the primary investigator and co-author of this paper.

Chapter 8

Bilateral boundary control design for a cascaded diffusion-ODE system coupled at an arbitrary interior point

8.1 Preliminaries

8.1.1 Introduction

Systems modeled by parabolic partial differential equations are relevant in many engineering and social systems, with applications found in field as varied as heat transfer, chemical reaction-diffusion processes, tumor angiogenesis [11], predator-prey Lotka-Volterra population models [23], opinion dynamics (of the Fischer-Kolmogorov-Petrovsky-Piskunov type equation [2]), free-electron plasma diffusion, and flows through porous media [42]. Often times, there is some control objective associated with these systems, especially that of stabilization.

Also of interest are systems that involve various couplings of infinite-dimensional and finite-dimensional systems. This subject, in the context of control design, has been explored significantly, of various coupling structures of equations of varying class. In particular, cascading

structures with parabolic and hyperbolic actuation paths entering linear and nonlinear ODEs – in the parabolic case, one can think of a "smearing" phenomena affecting the control input. The stabilization problem of parabolic PDEs coupled with ODEs via backstepping boundary control has been studied by [27]. This initial result has been extended to consider various different coupling topologies, including different boundary conditions ([38]), bidirectional coupling ([39]), and sliding mode control designs ([49]).

A majority of boundary backstepping designs (in 1-D) are *unilateral*, meaning a single scalar controller actuates at precisely one boundary. A wide variety of results have been developed for a broad class of systems under this paradigm. However, in higher dimensions, the analogous control design would be to only actuate at some subset of the boundary (rather than on the entire boundary surface). The fully actuated high dimensional boundary control case (studied on n-D ball geometry by [44]) motivates the study of *bilateral* control design in 1-D, which, as the name suggests, involves two scalar controls two boundary points (the boundary surface of a 1-D ball). The two controllers are coupled implicitly through the equation. Intuitively, the addition of one more controller augments the controllability of the system – a analogy to having two hands versus one when performing tasks. Some bilateral boundary control design techniques for 1-D PDEs has been studied prior in other specific contexts: for parabolic PDEs in [43] and [15], for heterodirectional hyperbolic PDE systems ([5]), and nonlinear viscous Hamilton-Jacobi PDE ([8]), amongst others.

The system in question in this paper involves an unstable linear ODE coupled not at a boundary, rather, at an interior point. Previous work by [53] has studied this problem in the context of unilateral control design, employing a nontraditional Fredholm transformation technique with separable kernels. This is in contrast to the work proposed in this paper, which utilizes a methodology of bilateral control design called *folding*. The folding approach (detailed in [15]) involves using a transformation to "fold" the system around an interior point into a coupled parabolic PDE with a degree of freedom in choosing the folding point. In this particular case, we

select the coupling point to fold about to recover a type of cascaded coupled PDE-ODE system.

The ODE coupling appearing in the interior of the PDE falls in a special class of so-called "sandwich" systems–systems that have a tri-layer (possibly more) of systems coupled together. Certain results exist for these systems in the unilateral sense – for example, for ODEs "sandwiched" between first-order hyperbolic PDEs as in [52]. This idea exists for ODEs sandwiched by parabolic equations in the work by Zhou [53]. An addition to parabolic-ODE sandwich systems is related work by Koga involving the two-phase Stefan problem, a special case of an ODE sandwiched by parabolic equations whose domains evolve as a function of the ODE (a nonlinear bidirectional coupling) [26]. Finally, results also exist for ODEs sandwiched by second-order hyperbolic PDEs in the context of the Rijke tube, a phenomena found in thermoacoustics [17]. The problem considered in this paper of the heat equation with an ODE coupled at the interior point is an example of such a sandwiched system.

The paper is structured as follows: in Section 8.2, the model is introduced and the folding transformation is applied to recover the equivalent coupled PDE-ODE system. In Section 8.3, the controller is designed via applying a two-tiered backstepping approach to recover a target system with a trivial solution possessing desirable stability properties. The stability is shown via the method of Lyapunov, and the feedback controllers (in the original coordinates) are derived. In Section 8.4, the well-posedness of the transformations from Section 8.3 is investigated. The existence of the transformations are shown, verifying the equivalence relation between the original plant under feedback with the chosen target system. Finally, the paper is concluded in Section 8.5.

8.1.2 Notation

The partial operator is notated using the del-notation, i.e.

$$\partial_x f := \frac{\partial f}{\partial x}$$

We will consider several different spaces and their Cartensian products. $\mathbb{R}^n$ is the standard real n-dimensional space. An element $v \in \mathbb{R}^n$ has elements notated $v_i, i \in \{1,...,n\}$. The p-norm denoted

$$|v|_p := \left(\sum_{k=1}^{n} |v_k|^p \right)^{\frac{1}{p}}$$

We also consider the space of square-integrable functions $L^2(I)$ over two different closed intervals I. For notational compactness, we label the spaces $L^2(I)$ as merely L^2, where the domain is implicit in the function considered. The L^2 space is endowed with the norm

$$||f||_{L^2} := \left(\int_I |f|_2^2 \, d\mu \right)^{\frac{1}{2}}$$

The Cartesian product space $L^2 \times \mathbb{R}^n$ induces a norm $||\cdot||$

$$||(f,v)|| := \sqrt{||f||_{L^2}^2 + |v|_2^2}$$

Elements of a matrix A are denoted by a_{ij}, in reference to the i-th row and j-th column.

8.2 Model and problem formulation

We consider the following coupled PDE-ODE system consisting of a diffusion PDE with an unstable ODE:

$$\partial_t u(y,t) = \varepsilon \partial_y^2 u(y,t) \tag{8.1}$$

$$Z'(t) = AZ(t) + Bu(y_0,t) \tag{8.2}$$

$$u(-1,t) = \mathcal{U}_1(t) \tag{8.3}$$

$$u(1,t) = \mathcal{U}_2(t) \tag{8.4}$$

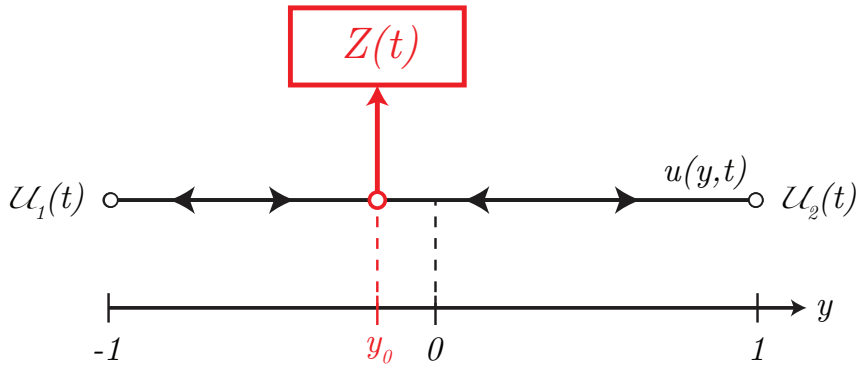

Figure 8.1: System schematic of heat equation coupled with interior ODE with two boundary inputs. The ODE system $Z(t)$ is located at some arbitrary interior point y_0.

with solutions $u : [-1,1] \times [0,\infty) \to \mathbb{R}, Z : [0,\infty) \to \mathbb{R}^n$. It is assumed that $\varepsilon > 0$ for well-posedness. The controllers operate at $x = 1$ and $x = -1$, and are denoted $\bar{\mathcal{U}}_1(t), \bar{\mathcal{U}}_2(t)$, respectively. The ODE (8.2) is forced by the state of the heat equation at an interior point $y_0 \in (-1,1)$, which is assumed to be known *a priori*. The pair (A,B) is assumed to be stabilizable.

Remark. *In general, a general class of reaction-advection-diffusion equations with spatially varying advection and reaction can be chosen rather than the pure heat equation, i.e. equations of the form*

$$\partial_t u(y,t) = \varepsilon \partial_y^2 u(y,t) + b(y)\partial_y u(y,t) + \lambda(y)u(y,t)$$

For clarity in the paper, we merely use the pure heat equation, but the analysis is analogous to the work in [15].

We perform a folding transformation about y_0, in which the scalar parabolic PDE system u is "folded" into a 2×2 coupled parabolic system. We define the the folding spatial transformations as

$$x = (y_0 - y)/(1 + y_0) \qquad y \in (-1, y_0) \tag{8.5}$$

$$x = (y - y_0)/(1 - y_0) \qquad y \in (y_0, 1) \tag{8.6}$$

admitting the following states:

$$U(x,t) := \begin{pmatrix} u_1(x,t) \\ u_2(x,t) \end{pmatrix} = \begin{pmatrix} u(y_0 - (1+y_0)x, t) \\ u(y_0 + (1-y_0)x, t) \end{pmatrix} \tag{8.7}$$

whose dynamics are governed by the following system:

$$\partial_t U(x,t) = E\partial_x^2 U(x,t) \tag{8.8}$$

$$Z'(t) = AZ(t) + B\Theta U(0,t) \tag{8.9}$$

$$\alpha U_x(0,t) = -\beta U(0,t) \tag{8.10}$$

$$U(1,t) = \mathcal{U}(t) \tag{8.11}$$

with the parameters given by :

$$\begin{aligned} E &:= \operatorname{diag}(\varepsilon_1, \varepsilon_2) \\ &:= \operatorname{diag}\left(\frac{\varepsilon}{(1+y_0)^2}, \frac{\varepsilon}{(1-y_0)^2} \right) \end{aligned} \tag{8.12}$$

$$\alpha := \begin{pmatrix} 1 & a \\ 0 & 0 \end{pmatrix} \tag{8.13}$$

$$\beta := \begin{pmatrix} 0 & 0 \\ 1 & -1 \end{pmatrix} \tag{8.14}$$

$$a := (1+y_0)/(1-y_0) \tag{8.15}$$

$$\Theta = \begin{pmatrix} \theta & 1-\theta \end{pmatrix}, \theta \in [0,1] \tag{8.16}$$

In particular, the boundary conditions (8.10) are curious. While they may initially appear to be Robin boundary conditions, they actually encapsulate compatibility conditions arising from imposing continuity in the solution at the folding point. Some related conditions have been

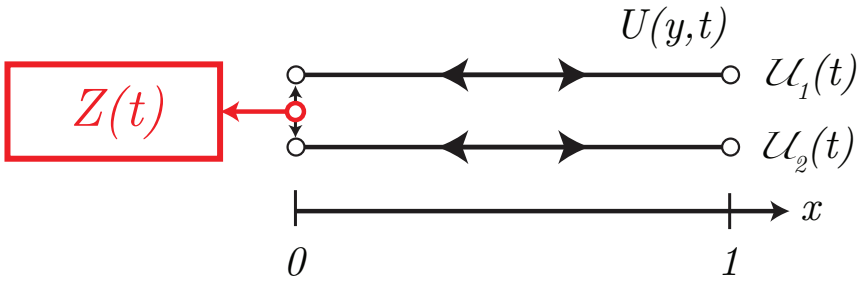

Figure 8.2: System schematic of folded system. The system becomes equivalent to a coupled parabolic PDE system with folding conditions imposed at the distal boundary. The folding conditions also enter the ODE as an input.

considered in some previous parabolic backstepping work in [41], albeit with differing context. This is contrasted with more typical boundary conditions which impose a single condition at a single boundary.

From Figure 8.2, it is quite clear to see the control problem after folding becomes equivalent to stabilizing an ODE system through a coupled parabolic PDE actuation path, however, one which has the distal end "pinned" together. The control designs for $\mathcal{U}_{1,2}$ will be coupled.

Assumption. *The ODE location y_0 is constricted to the half domain $(-1,0]$ without loss of generality. The case $y_0 \in [0,1)$ can be recovered by using a change in spatial variables $\hat{y} = -y$ and performing the same folding technique. By choosing y_0 in this manner, we impose an ordering* $\varepsilon_1 > \varepsilon_2$.

8.3 State-feedback design

The backstepping state-feedback control design is accomplished with two PDE backstepping steps. First, we will assume the existence of a stabilizing nominal control.

Assumption. *There exists $\Gamma_0 \in \mathbb{R}^{1\times n}$ such that the matrix $A + B\Gamma_0$ is Hurwitz.*

Assumption 8.3 is a direct consequence of the stabilizability of the pair (A,B).

8.3.1 First transformation K

The first PDE backstepping transformation is a 2×2 Volterra integral transformation of the second kind:

$$W(x,t) = U(x,t) - \int_0^x K(x,y)U(y,t)dy - \Gamma(x)Z(t) \tag{8.17}$$

where $K \in C(\mathcal{T})$, with $\mathcal{T} := \{(x,y) \in \mathbb{R}^2 | 0 \leq y \leq x \leq 1\}$ and $\Gamma : [0,1] \to \mathbb{R}^{2\times n}$. We suppose the row elements of Γ are denoted with the index $i = 1,2$, i.e.

$$\Gamma(x) := \begin{pmatrix} \Gamma_1(x) \\ \Gamma_2(x) \end{pmatrix} \tag{8.18}$$

where $\Gamma_1(x), \Gamma_2(x) \in \mathbb{R}^{1\times n}$. The associated inverse transformation is given by

$$U(x,t) = W(x,t) - \int_0^x \bar{K}(x,y)W(y,t)dy - \bar{\Gamma}(x)Z(t) \tag{8.19}$$

with $\bar{K} \in C(\mathcal{T})$ and $\bar{\Gamma} : [0,1] \to \mathbb{R}^{2\times n}$. The corresponding target system for (8.17) is chosen to be

$$\partial_t W(x,t) = E\partial_x^2 W(x,t) + G[K](x)W(x,t) \tag{8.20}$$

$$Z'(t) = (A + B\Gamma_0)Z(t) + B\Theta W(0,t) \tag{8.21}$$

$$\alpha\partial_x W(0,t) = -\beta W(0,t) \tag{8.22}$$

$$W(1,t) = \mathcal{V}(t) \tag{8.23}$$

where $\mathcal{V}(t) = \begin{pmatrix} 0 & \nu_2(t) \end{pmatrix}^T$ is an auxiliary control which is designed later in the paper. The controller $\mathcal{U}(t)$ can be expressed as an operator of $\mathcal{V}(t)$ by evaluating (8.17) for $x = 1$:

$$\mathcal{U}(t) := \mathcal{V}(t) + \int_0^1 K(1,y)U(y,t)dy \tag{8.24}$$

The matrix-valued operator $G[\cdot](x)$ acting on K is given by

$$G[K](x) = \begin{pmatrix} 0 & 0 \\ (\varepsilon_2 - \varepsilon_1)\partial_y k_{21}(x,x) & 0 \end{pmatrix} =: \begin{pmatrix} 0 & 0 \\ g[k_{21}](x) & 0 \end{pmatrix} \tag{8.25}$$

From enforcing conditions (8.8)-(8.11), (8.20)-(8.23), the following cascaded ODE-PDE kernel can be recovered from (8.17):

$$E\partial_x^2 K(x,y) - \partial_y^2 K(x,y)E = G[K](x)K(x,y) \tag{8.26}$$

$$E\Gamma''(x) - \Gamma(x)A + G[K](x)\Gamma(x) = 0 \tag{8.27}$$

subject to boundary conditions

$$EK(x,x) - K(x,x)E = 0 \tag{8.28}$$

$$E\partial_x K(x,x) + \partial_y K(x,x)E + E\frac{d}{dx}K(x,x) = G[K](x) \tag{8.29}$$

$$K(x,0)E\partial_x U(0) = 0 \tag{8.30}$$

$$(\Gamma(x)B\Theta - \partial_y K(x,0)E)U(0) = 0 \tag{8.31}$$

$$\Gamma(0) = \begin{pmatrix} \Gamma_0 \\ \Gamma_0 \end{pmatrix} \tag{8.32}$$

$$\Gamma'(0) = \begin{pmatrix} 0 \\ 0 \end{pmatrix} \tag{8.33}$$

The intial condition (8.32) arises from two conditions on $W(0)$: (8.21), (8.22). Evaluating (8.17) at $x = 0$ admits

$$W(0,t) = U(0,t) - \Gamma(0)Z(t) \tag{8.34}$$

From (8.9) and (8.21), we recover a condition on $\Gamma(0)$:

$$\Theta\Gamma(0) = \Gamma_0 \tag{8.35}$$

Additionally, from (8.22),(8.34), we can note

$$\Gamma_1(0) = \Gamma_2(0) \tag{8.36}$$

(8.35),(8.36) uniquely determine (8.32). The conditions (8.33) are derived in an analogous manner.

A symmetry with the plant is observed with (8.30),(8.31) encapsulating folding conditions on K. By imposing (8.10) onto (8.30),(8.31), one can recover the scalar conditions

$$\varepsilon_1 k_{11}(x,0) - a\varepsilon_2 k_{12}(x,0) = 0 \tag{8.37}$$

$$\varepsilon_1 k_{21}(x,0) - a\varepsilon_2 k_{22}(x,0) = 0 \tag{8.38}$$

$$\varepsilon_1 \partial_y k_{11}(x,0) + \varepsilon_2 \partial_y k_{12}(x,0) = \Gamma_1(x)B \tag{8.39}$$

$$\varepsilon_1 \partial_y k_{21}(x,0) + \varepsilon_2 \partial_y k_{22}(x,0) = \Gamma_2(x)B \tag{8.40}$$

8.3.2 Second transformation (p,q)

A second transformation is designed to compensate for the term $G[K](x)$ in (8.20). One can see this as the correction factor needed to compensate the interaction between the two controllers. Indeed, if one inspects the structure of the operator G, one may note two things. Firstly, the coupling is from the faster equation (associated with ε_1) to the slower equation (associaterd with ε_2). That is, the slower equation will have additional dynamics. Secondly, the nonzero element g depends on the *difference* of the diffusion coefficients. For the symmetric folding (ODE located at $x = 0$) case, the coupling does not appear.

The following transformation for designing the compensation controller $\mathcal{V}(t)$ is considered:

$$\Omega(x,t) = W(x,t) - \int_0^x \begin{pmatrix} 0 & 0 \\ q(x,y) & p(x-y) \end{pmatrix} W(y,t)dy \tag{8.41}$$

The corresponding inverse is given by

$$W(x,t) = \Omega(x,t) - \int_0^x \begin{pmatrix} 0 & 0 \\ \bar{q}(x,y) & \bar{p}(x-y) \end{pmatrix} \Omega(y,t)dy \tag{8.42}$$

We define our target system (Ω, Z) as

$$\partial_t \Omega(x,t) = E\partial_x^2 \Omega(x,t) \tag{8.43}$$

$$Z'(t) = (A + B\Gamma_0)Z(t) + B\Theta\Omega(0,t) \tag{8.44}$$

$$\alpha\partial_x \Omega(0,t) = -\beta\Omega(0,t) \tag{8.45}$$

$$\Omega(1,t) = 0 \tag{8.46}$$

The transformation (8.41), original system model (8.8)-(8.11), and target system (8.43)-(8.46) will impose a set of conditions on p, q that comprise a scalar nonlocal Goursat problem:

$$p(x) = a^{-1}q(x,0) \tag{8.47}$$

$$\begin{aligned} \varepsilon_2\partial_x^2 q(x,y) - \varepsilon_1\partial_y^2 q(x,y) &= (c_2 - c_1)q(x,y) \\ &\quad + g[k_{21}](y)p(x-y) \end{aligned} \tag{8.48}$$

subject to the following boundary conditions:

$$\partial_y q(x,x) = \frac{g[k_{21}](x)}{\varepsilon_2 - \varepsilon_1} \tag{8.49}$$

$$q(x,x) = 0 \tag{8.50}$$

$$\partial_y q(x,0) = a^2 p'(x) = a\partial_x q(x,0) \tag{8.51}$$

The kernel equations for the inverse kernels $\bar{p}, \bar{q}$ are similar to those of p, q respectively:

$$\bar{p}(x) = a^{-1}\bar{q}(x,0) \tag{8.52}$$

$$\begin{aligned}\varepsilon_2\partial_x^2\bar{q}(x,y) - \varepsilon_1\partial_y^2\bar{q}(x,y) &= (c_1 - c_2)\bar{q}(x,y) \\ &\quad - g[k_{21}](x)\bar{p}(x-y)\end{aligned} \tag{8.53}$$

with boundary conditions

$$\partial_y \bar{q}(x,x) = \frac{g[k_{21}](x)}{\varepsilon_1 - \varepsilon_2} \tag{8.54}$$

$$\bar{q}(x,x) = 0 \tag{8.55}$$

$$\partial_y \bar{q}(x,0) = -a^2 \bar{p}'(x) = -a\partial_x \bar{q}(x,0) \tag{8.56}$$

The PDE (8.47),(8.48) and associated boundary conditions (8.50),(8.51) are studied in previous work on folding bilateral control. The controller $\mathcal{V}(t)$ can be computed by evaluating (8.41) at $x = 1$ and using the appropriate boundary conditions:

$$\mathcal{V}(t) = \begin{pmatrix} 0 \\ \nu_2(t) \end{pmatrix} = \int_0^1 \begin{pmatrix} 0 & 0 \\ q(1,y) & p(1-y) \end{pmatrix} W(y,t)dy \tag{8.57}$$

8.3.3 Stability of target system (Ω, Z)

Lemma 23. *The trivial solution* $(\Omega, Z) \equiv 0$ *of the target system* (8.43)-(8.46) *is exponentially stable in the sense of the* $L^2 \times \mathbb{R}^n$ *norm. That is, there exist constants* $\Pi, \mu > 0$ *such that*

$$||(\Omega(\cdot,t), Z(t))|| \leq \Pi \exp\left(-\mu(t-t_0)\right) ||(\Omega(\cdot,t_0), Z(t_0))|| \tag{8.58}$$

Proof. The proof of Lemma 23 is relatively straightforward. First consider the a Lyapunov function of the form

$$V(\Omega(\cdot,t), Z) = Z(t)^T P Z(t) + \int_0^1 \left[\Omega(x,t)^T M \Omega(x,t)\right] dx \tag{8.59}$$

where $M = \text{diag}(a^3 m, m), m > 0$ is an analysis parameter to be chosen later, and $P \succ 0$ is the (symmetric) solution to the Lyapunov equation

$$P(A + B\Gamma_0) + (A + B\Gamma_0)^T P = -Q \tag{8.60}$$

for a chosen $Q \succ 0$. The symmetric solution $P \succ 0$ is guaranteed to exist since $A + B\Gamma_0$ is designed to be Hurwitz. We note that $V(t)$ is equivalent to the $L^2 \times \mathbb{R}^n$ norm:

$$\Pi_1 ||(\Omega(\cdot,t), Z(t))||^2 \leq V(t) \leq \Pi_2 ||(\Omega(\cdot,t), Z(t))||^2 \tag{8.61}$$

where the coefficients Π_i are:

$$\Pi_1 = \min\{\lambda_{\min}(P), a^3 m\} \tag{8.62}$$

$$\Pi_2 = \max\{\lambda_{\max}(P), m\} \tag{8.63}$$

Differentiating (8.59) in time, one finds

$$\begin{aligned}\dot{V}(t) \leq (\Omega(0,t)^T \Theta^T B^T + Z(t)^T (A+B\Gamma_0)^T))PZ(t) \\ + Z(t)^T P((A+B\Gamma_0)Z(t) + B\Theta\Omega(0,t)) \\ + \int_0^1 \left[\partial_x^2 \Omega(x,t)^T EM\Omega(x,t)\right. \\ \left. + \Omega(x,t)^T ME\partial_x^2 \Omega(x,t)\right] dx \end{aligned} \tag{8.64}$$

Using integration by parts and (8.60) will admit

$$\begin{aligned}\dot{V}(t) &\leq -Z(t)^T QZ(t) + 2Z(t)^T PB\Theta\Omega(0,t) \\ &\quad - \int_0^1 \left[2\partial_x \Omega(x,t)^T EM\partial_x \Omega(x,t)\right] dx \\ &\leq -\lambda_{\min}(Q)|Z(t)|_2^2 + 2Z(t)^T PB\Theta\Omega(0,t) \\ &\quad - 2a^3 m\varepsilon_2 \,||\partial_x \Omega(\cdot,t)||_{L^2}^2 \end{aligned} \tag{8.65}$$

Applying Young's inequality,

$$\dot{V}(t) \leq -\mu_1 |Z(t)|_2^2 - 4\mu_2 \,||\partial_x \Omega(\cdot,t)||_{L^2}^2 \tag{8.66}$$

where

$$\mu_1 = \lambda_{\min}(Q) - \delta |P|_{2,i} |B|_{2,i} \tag{8.67}$$

$$\mu_2 = \frac{1}{4}\left(2a^3 \varepsilon_2 m - \frac{1}{\delta}|P|_{2,i}|B|_{2,i}\right) \tag{8.68}$$

The analysis parameters δ, m_1, m_2 must be chosen such that $\mu_{1,2} > 0$. This is easily achievable by

choosing

$$\delta < \frac{\lambda_{\min}(Q)}{\lambda_{\max}(P)|B|_{2,i}} \tag{8.69}$$

$$m > \frac{\lambda_{\max}(P)|B|_{2,i}}{2\delta a^3 \varepsilon_2} \tag{8.70}$$

Applying Young's inequality and (8.61) to (8.66), one finds

$$\dot{V}(t) \leq -\frac{\min\{\mu_1, \mu_2\}}{\Pi_1} V(t) \tag{8.71}$$

which via the comparison principle admits the bound

$$V(t) \leq \exp(-2\mu(t - t_0))V(t_0) \tag{8.72}$$

where

$$\mu := \frac{\min\{\mu_1, \mu_2\}}{2\Pi_1} \tag{8.73}$$

Applying the equivalence (8.61) once more recovers the bound (8.58) with $\Pi = \sqrt{\Pi_2/\Pi_1}$. This completes the proof. □

8.3.4 Main result: closed-loop stability

Theorem 24. *The trivial solution of the system* (8.1)-(8.4) *is exponentially stable in the sense of the* $L^2 \times \mathbb{R}^n$ *norm under the pair of state feedback control laws* $\mathcal{U}_1, \mathcal{U}_2$*:*

$$\begin{pmatrix} \mathcal{U}_1(t) \\ \mathcal{U}_2(t) \end{pmatrix} = \int_{-1}^{1} \begin{pmatrix} F_1(y) \\ F_2(y) \end{pmatrix} u(y,t)dy + F_3 Z(t) \tag{8.74}$$

with feedback gains F_1, F_2 defined as

$$F_1(y) = \begin{cases} (1+y_0)^{-1} k_{11}\left(1, \frac{y_0 - y}{1+y_0}\right) & y \le y_0 \\ (1-y_0)^{-1} k_{12}\left(1, \frac{y - y_0}{1-y_0}\right) & y > y_0 \end{cases} \tag{8.75}$$

$$F_2(y) = \begin{cases} (1+y_0)^{-1} h_1\left(\frac{y_0 - y}{1+y_0}\right) & y \le y_0 \\ (1-y_0)^{-1} h_2\left(\frac{y - y_0}{1-y_0}\right) & y > y_0 \end{cases} \tag{8.76}$$

$$\begin{aligned} h_1(y) = k_{21}(1,y) + q(1,y) - \int_y^1 \big[& p(1-z) k_{21}(z,y) \\ & + q(1,z) k_{11}(z,y) \big] dz \end{aligned} \tag{8.77}$$

$$\begin{aligned} h_2(y) = k_{22}(1,y) + p(1-y) - \int_y^1 \big[& p(1-z) k_{22}(z,y) \\ & + q(1,z) k_{12}(z,y) \big] dz \end{aligned} \tag{8.78}$$

$$F_3 = \begin{pmatrix} \Gamma_1(1) \\ \Gamma_2(1) - \int_0^1 [q(1,y)\Gamma_1(y) + p(1-y)\Gamma_2(y)] dy \end{pmatrix} \tag{8.79}$$

where $k_{ij}, p, q \in C(\mathcal{T})$ are solutions to the kernel PDE equations (8.26),(8.47),(8.48) *respectively (with associated boundary conditions), and $\Gamma_{1,2} \in C([0,1])$ are solutions to the kernel ODE equations*(8.27)*. That is, under the feedback controllers* (8.74)*, there exists a constant $\bar{\Pi}$ such that*

$$||(u(\cdot,t), Z(t))|| \le \bar{\Pi} \exp\left(-\mu(t - t_0)\right) ||(u(\cdot,t_0), Z(t_0))|| \tag{8.80}$$

The proof of Theorem 24 is not given but is analogous to the proofs found in [15]. The proof involves utilizing the invertability of the transformations (8.7),(8.17),(8.41) that arise either trivially (folding), or from the boundedness of the kernels (studied in Section 8.4). The forward and inverse transform give estimates on the equivalence relation between the target system

(8.43)-(8.46) and the original system (8.1)-(8.4), which are applied to (8.80).

8.4 Well-posedness of K, Γ kernel system

The PDE gain kernel K and ODE kernel Γ must be shown to be well-posed. The following lemmas establish these results.

8.4.1 Γ kernel

The ODE system (8.27) is written into into two separate n-th order ODEs:

$$\Gamma_1''(x) = \varepsilon_1^{-1}\Gamma_1(x)A \tag{8.81}$$

$$\Gamma_2''(x) = \varepsilon_2^{-1}\Gamma_2(x)A + \varepsilon_2^{-1}g[k_{21}](x)\Gamma_1(x) \tag{8.82}$$

where the initial conditions can be found from (8.32),(8.33) to be

$$\Gamma_1(0) = \Gamma_0 \tag{8.83}$$

$$\Gamma_1'(0) = 0 \tag{8.84}$$

$$\Gamma_2(0) = \Gamma_0 \tag{8.85}$$

$$\Gamma_2'(0) = 0 \tag{8.86}$$

From the variation of constants formula, it is easy to see that the solutions for Γ_1 can be expressed via

$$\Gamma_1(x) = \begin{pmatrix} \Gamma_0 & 0 \end{pmatrix} \exp\left(\begin{pmatrix} 0 & I \\ \varepsilon_1^{-1}A & 0 \end{pmatrix} x \right) \begin{pmatrix} I \\ 0 \end{pmatrix} \tag{8.87}$$

while Γ_2 is

$$\Gamma_2(x) = \Bigg[\begin{pmatrix} \Gamma_0 & 0 \end{pmatrix} \exp\left(\begin{pmatrix} 0 & I \\ \varepsilon_2^{-1} A & 0 \end{pmatrix} x \right) + \int_0^x \begin{pmatrix} 0 & \varepsilon_2^{-1} g[k_{21}](\xi)\Gamma_1(\xi) \end{pmatrix} \times \exp\left(\begin{pmatrix} 0 & I \\ \varepsilon_2^{-1} A & 0 \end{pmatrix} (x-\xi) \right) d\xi \Bigg] \begin{pmatrix} I \\ 0 \end{pmatrix} \tag{8.88}$$

Noting that $\Gamma_2(x)$ depends on $g[k_{21}](x)$, an element of K, we define the operator formulation $(\check{\Gamma}_2 \circ g)[k_{21}] := \Gamma_2$. We will additionally define the operator $\Phi : C(\mathcal{T};\mathbb{R}) \to C([0,1];\mathbb{R}^{2\times n})$ as

$$\Phi[f](x) := \begin{pmatrix} \Gamma_1(x) \\ (\check{\Gamma}_2 \circ g)[f](x) \end{pmatrix} \tag{8.89}$$

where $\Phi[f]$ maps from the scalar $C(\mathcal{T};\mathbb{R})$ to the multidimensional $C([0,1];\mathbb{R}^{2\times n})$ function space. From this definition, it naturally follows that $\Phi[k_{21}] = \Gamma$. This operator representation will be used in the well-posedness analysis for the PDE kernel K.

Of interest are bounds on $\Gamma_1(x), \Gamma_2(x)$. The following bound on $\Gamma_1(x)$ is trivial to find:

$$|\Gamma_1(x)| \leq |\Gamma_0|_2 S(x) \tag{8.90}$$

where

$$S(x) = \sigma_{\max}\left(\exp\left(\begin{pmatrix} 0 & I \\ \varepsilon_2^{-1} A & 0 \end{pmatrix} x \right) \right) \tag{8.91}$$

and $\sigma_{\max}(X)$ denotes the largest singular value of the matrix X (the induced 2-norm). It is important to note that the largest singular value of the matrix exponential is bounded on the

compact set $[0,1]$, i.e. $|S(x)| < \infty, \forall x \in [0,1]$. With a bound on Γ_1, the following bound on $(\check{\Gamma}_2 \circ g)[k_{21}](x)$ can be found, which will be used in the proof of well-posedness for K.

$$\begin{aligned}|(\check{\Gamma}_2 \circ g)[k_{21}](x)| \leq |\Gamma_0|_2 S(x) \\ + \int_0^x \frac{\varepsilon_1 - \varepsilon_2}{\varepsilon_2} ||\Gamma_1||_{L^\infty} S(x-\xi) \\ \times |\partial_y k_{21}(\xi,\xi)| d\xi \end{aligned} \tag{8.92}$$

8.4.2 K kernel

The K-kernel must be approached in two sets of equations: (k_{11}, k_{12}) and (k_{21}, k_{22}). The reason for this is that the operator $G[K]$ introduces coupling between the two sets of kernels. We first apply a transformation to gain kernel (8.26)

$$\check{K}(x,y) = \sqrt{E}\partial_x K(x,y) + \partial_y K(x,y)\sqrt{E} \tag{8.93}$$

which transforms the kernel PDE into a 2×2 system of coupled first-order hyperbolic PDEs.

(k_{11}, k_{12})-system

The transform (8.93) will admit the following coupled 2×2 system

$$\sqrt{\varepsilon_1}\partial_x k_{11}(x,y) + \sqrt{\varepsilon_1}\partial_y k_{11}(x,y) = \check{k}_{11}(x,y) \tag{8.94}$$

$$\sqrt{\varepsilon_1}\partial_x k_{12}(x,y) + \sqrt{\varepsilon_2}\partial_y k_{12}(x,y) = \check{k}_{12}(x,y) \tag{8.95}$$

$$\sqrt{\varepsilon_1}\partial_x \check{k}_{11}(x,y) - \sqrt{\varepsilon_1}\partial_y \check{k}_{11}(x,y) = 0 \tag{8.96}$$

$$\sqrt{\varepsilon_1}\partial_x \check{k}_{12}(x,y) - \sqrt{\varepsilon_2}\partial_y \check{k}_{12}(x,y) = 0 \tag{8.97}$$

with boundary conditions

$$k_{11}(x,0) = \frac{a\varepsilon_2}{\varepsilon_1(a\varepsilon_2+\sqrt{\varepsilon_1\varepsilon_2})} \times \int_0^x [\sqrt{\varepsilon_1}\check{k}_{11}(y,0)+\sqrt{\varepsilon_2}\check{k}_{12}(y,0) - \Gamma_1(y)B]dy \tag{8.98}$$

$$k_{12}(x,0) = \frac{1}{a\varepsilon_2+\sqrt{\varepsilon_1\varepsilon_2}} \times \int_0^x [\sqrt{\varepsilon_1}\check{k}_{11}(y,0)+\sqrt{\varepsilon_2}\check{k}_{12}(y,0) - \Gamma_1(y)B]dy \tag{8.99}$$

$$k_{12}(x,x) = 0 \tag{8.100}$$

$$\check{k}_{11}(x,x) = 0 \tag{8.101}$$

$$\check{k}_{12}(x,x) = 0 \tag{8.102}$$

Lemma 25. *The system of first-order hyperbolic PDEs* (8.94)-(8.97) *and associated boundary conditions admit a unique set of* $k_{11}, k_{12} \in C(\mathcal{T})$ *solutions.*

Proof. (k_{11}, k_{12}) can actually be solved explicitly via the method of characteristics. First, note that (8.96),(8.97),(8.101),(8.102) imply that $(\check{k}_{11}, \check{k}_{12}) = 0$, the solution can be simplified significantly:

$$k_{11}(x,y) = \frac{a\varepsilon_2}{\varepsilon_1(a\varepsilon_2+\sqrt{\varepsilon_1\varepsilon_2})}\int_0^{x-y}\Gamma_1(z)Bdz \tag{8.103}$$

$$k_{12}(x,y) = \begin{cases} k_{12,l}(x,y) & \sqrt{\varepsilon_2}x \geq \sqrt{\varepsilon_1}y \\ 0 & \text{otherwise} \end{cases} \tag{8.104}$$

$$k_{12,l}(x,y) = \frac{1}{a\varepsilon_2+\sqrt{\varepsilon_1\varepsilon_2}}\int_0^{x-\sqrt{\frac{\varepsilon_1}{\varepsilon_2}}y}\Gamma_1(z)Bdz \tag{8.105}$$

□

It is not difficult to see that $k_{11} \in C^\infty(\mathcal{T}) \subset C(\mathcal{T})$ from the matrix exponential properties, while $k_{12} \in C(\mathcal{T})$.

(k_{21}, k_{22})-system

The (k_{21}, k_{22}) system must be treated in a differing manner than the (k_{11}, k_{12}) system, due to the existence of a nonlocal trace term To account for the different nature of these characteristics, we perform one more transformation on the kernels for k_{2i}:

$$\hat{k}_{2i}(x,y) = \sqrt{\varepsilon_2}\partial_x k_{2i}(x,y) - \sqrt{\varepsilon_i}\partial_y k_{2i}(x,y) \tag{8.106}$$

where $i \in \{1,2\}$. We then turn our attention to the gain kernel system $(\hat{k}_{21}, \check{k}_{21}, \hat{k}_{22}, \check{k}_{22})$.

The component system of kernel PDEs for $(\hat{k}_{21}, \check{k}_{21}, \hat{k}_{22}, \check{k}_{22})$ is

$$\sqrt{\varepsilon_2}\partial_x \hat{k}_{21}(x,y) + \sqrt{\varepsilon_1}\partial_y \hat{k}_{21}(x,y) = -g[k_{21}](x)k_{11}(x,y) \tag{8.107}$$

$$\sqrt{\varepsilon_2}\partial_x \hat{k}_{22}(x,y) + \sqrt{\varepsilon_2}\partial_y \hat{k}_{22}(x,y) = -g[k_{21}](x)k_{12}(x,y) \tag{8.108}$$

$$\sqrt{\varepsilon_2}\partial_x \check{k}_{21}(x,y) - \sqrt{\varepsilon_1}\partial_y \check{k}_{21}(x,y) = -g[k_{21}](x)k_{11}(x,y) \tag{8.109}$$

$$\sqrt{\varepsilon_2}\partial_x \check{k}_{22}(x,y) - \sqrt{\varepsilon_2}\partial_y \check{k}_{22}(x,y) = -g[k_{21}](x)k_{12}(x,y) \tag{8.110}$$

subject to the following boundary conditions:

$$\begin{aligned}\hat{k}_{21}(x,0) = &-\frac{1-a^2}{1+a^2}\check{k}_{21}(x,0) + \frac{2a^3}{1+a^2}\check{k}_{22}(x,0) \\ &- \frac{2a^2}{\sqrt{\varepsilon_1}(1+a^2)}(\check{\Gamma}_2 \circ g)[k_{21}](x)B\end{aligned} \tag{8.111}$$

$$\begin{aligned}\hat{k}_{22}(x,0) = &\frac{2}{a(1+a^2)}\check{k}_{21}(x,0) + \frac{1-a^2}{1+a^2}\check{k}_{22}(x,0) \\ &- \frac{2}{\sqrt{\varepsilon_2}(1+a^2)}(\check{\Gamma}_2 \circ g)[k_{21}](x)B\end{aligned} \tag{8.112}$$

$$\check{k}_{21}(x,x) = -\frac{\sqrt{\varepsilon_1}-\sqrt{\varepsilon_2}}{\sqrt{\varepsilon_1}+\sqrt{\varepsilon_2}}\hat{k}_{21}(x,x) \tag{8.113}$$

$$\check{k}_{22}(x,x) = 0 \tag{8.114}$$

where the inverse transformations are given to be

$$k_{21}(x,y) = \frac{1}{2\sqrt{\varepsilon_2}} \int_y^x \check{k}_{21}(z,y) + \hat{k}_{21}(z,y) dz \tag{8.115}$$

$$k_{22}(x,y) = \frac{1}{2\sqrt{\varepsilon_2}} \int_y^x \check{k}_{22}(z,y) + \hat{k}_{22}(z,y) dz \tag{8.116}$$

and the function $g[k_{21}](x)$ can be expressed in terms of $\hat{k}_{21}, \check{k}_{21}$:

$$\begin{aligned} g[k_{21}](x) &= \frac{(\varepsilon_2 - \varepsilon_1)}{2\sqrt{\varepsilon_1}} (\check{k}_{21}(x,x) - \hat{k}_{21}(x,x)) \\ &= (\sqrt{\varepsilon_1} - \sqrt{\varepsilon_2}) \hat{k}_{21}(x,x) \end{aligned} \tag{8.117}$$

Lemma 26. *The system of first-order hyperbolic PDE* (8.107)-(8.110) *and associated boundary conditions admit a unique set of* $\hat{k}_{21}, \check{k}_{21}, \hat{k}_{22}, \check{k}_{22} \in C(\mathcal{T})$ *solutions.*

Proof. We recognize that $(\hat{k}_{21}, \check{k}_{21}, \hat{k}_{22}, \check{k}_{22})$ are similar in structure to the (previous result), albeit with an additional non-local recirculation term appearing in the boundaries (8.111),(8.112). The non-local term in the boundary does not change the method of the proof by too much, however, additional care must be given to incorporate the behavior.

The solutions for the $\hat{k}_{21}$ can be recovered via a direct application of the method of characteristics:

$$\hat{k}_{21}(x,y) = \hat{k}_{21}(\sigma_4(x,y), 0) + \hat{I}_{21}[\hat{k}_{21}](x,y) \tag{8.118}$$

$$\hat{k}_{22}(x,y) = \hat{k}_{22}(x-y, 0) + \hat{I}_{22}[\hat{k}_{21}](x,y) \tag{8.119}$$

$$\check{k}_{21}(x,y) = \check{k}_{21}(\sigma_5(x,y), \sigma_5(x,y)) + \check{I}_{21}[\hat{k}_{21}](x,y) \tag{8.120}$$

$$\check{k}_{22}(x,y) = \check{k}_{22}\left(\frac{x+y}{2}, \frac{x+y}{2}\right) + \check{I}_{22}[\hat{k}_{21}](x,y) \tag{8.121}$$

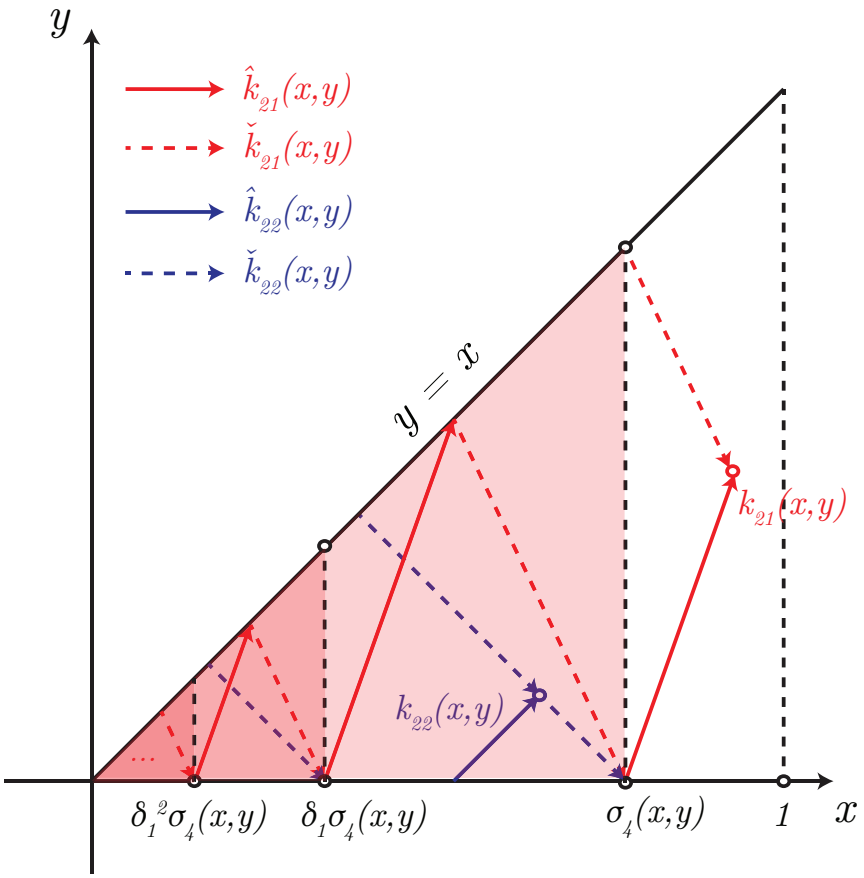

Figure 8.3: Characteristics of $\hat{k}_{21}, \hat{k}_{22}, \check{k}_{21}, \check{k}_{22}$. To solve for a given point, the solution must be known on a triangle of smaller volume.

$$\sigma_4(x,y) := x - \frac{\sqrt{\varepsilon_2}}{\sqrt{\varepsilon_1}} y \tag{8.122}$$

$$\sigma_5(x,y) := \frac{\sqrt{\varepsilon_1}x + \sqrt{\varepsilon_2}y}{\sqrt{\varepsilon_1} + \sqrt{\varepsilon_2}} \tag{8.123}$$

and the integral operators $\hat{I}_{21}, \hat{I}_{22}, \check{I}_{21}, \check{I}_{22}$ are defined

$$\begin{aligned} &\hat{I}_{21}[\hat{k}_{21}](x,y) \\ &:= \int_0^{\frac{y}{\sqrt{\varepsilon_1}}} \Bigg[-\frac{\varepsilon_2 - \varepsilon_1}{\sqrt{\varepsilon_1} + \sqrt{\varepsilon_2}} k_{11}(\sqrt{\varepsilon_2}z + \sigma_4(x,y), \sqrt{\varepsilon_1}z) \\ &\qquad \times \hat{k}_{21}(\sqrt{\varepsilon_2}z + \sigma_4(x,y), \sqrt{\varepsilon_2} + \sigma_4(x,y)) \Bigg] dz \end{aligned} \tag{8.124}$$

$$\hat{I}_{22}[\hat{k}_{21}](x,y)$$
$$:= \int_0^{\frac{y}{\sqrt{\varepsilon_2}}} \Bigg[-\frac{\varepsilon_2-\varepsilon_1}{\sqrt{\varepsilon_1}+\sqrt{\varepsilon_2}} k_{12}(\sqrt{\varepsilon_2}z+x-y, \sqrt{\varepsilon_2}z) \times \hat{k}_{21}(\sqrt{\varepsilon_2}z+x-y, \sqrt{\varepsilon_2}+x-y) \Bigg] dz \tag{8.125}$$

$$\check{I}_{21}[\hat{k}_{21}](x,y)$$
$$:= \int_0^{\frac{x-y}{\sqrt{\varepsilon_1}+\sqrt{\varepsilon_2}}} \Bigg[-\frac{\varepsilon_2-\varepsilon_1}{\sqrt{\varepsilon_1}+\sqrt{\varepsilon_2}} k_{11}(\sqrt{\varepsilon_2}z+\sigma_5(x,y), -\sqrt{\varepsilon_1}z+\sigma_5(x,y)) \times \hat{k}_{21}(\sqrt{\varepsilon_2}z+\sigma_5(x,y), \sqrt{\varepsilon_2}+\sigma_5(x,y)) \Bigg] dz \tag{8.126}$$

$$\check{I}_{22}[\hat{k}_{21}](x,y)$$
$$:= \int_0^{\frac{x-y}{2\sqrt{\varepsilon_2}}} \Bigg[-\frac{\varepsilon_2-\varepsilon_1}{\sqrt{\varepsilon_1}+\sqrt{\varepsilon_2}} \times k_{12}\left(\sqrt{\varepsilon_2}z+\frac{x+y}{2}, -\sqrt{\varepsilon_2}z+\frac{x+y}{2}\right) \times \hat{k}_{21}\left(\sqrt{\varepsilon_2}z+\frac{x+y}{2}, \sqrt{\varepsilon_2}+\frac{x+y}{2}\right) \Bigg] dz \tag{8.127}$$

From enforcing (8.111)-(8.114) on (8.118)-(8.121) recursively, one can eventually arrive at an integral equation system representation for $(\hat{k}_{21}, \hat{k}_{22}, \check{k}_{21}, \check{k}_{22})$ involving infinite sums of Volterra-type integral operators. The infinite sums appear due to the reflection boundary conditions (8.111),(8.113) observed in the system.

$$\hat{k}_{21}(x,y) = \lim_{n\to\infty} \Bigg[-\delta_1^n \delta_2^{n+1} \check{k}_{21}(\delta_1^n \sigma_4(x,y), 0) + \delta_1^n \delta_2^n \frac{2a^3}{1+a^2} \check{k}_{22}(\delta_1^n \sigma_4(x,y), 0) \Bigg]$$

$$
\begin{aligned}
&+\sum_{n=0}^{\infty}\Big[\delta_1^n\delta_2^n\hat{I}_{21}[\hat{k}_{21}](\delta_3^n\sigma_4(x,y),\delta_3^n\sigma_4(x,y))\\
&\quad-\delta_1^n\delta_2^{n+1}\check{I}_{21}[\hat{k}_{21}](\delta_1^n\sigma_4(x,y),0)\\
&\quad+\delta_1^n\delta_2^n\frac{2a^3}{1+a^2}\check{I}_{22}[\hat{k}_{21}](\delta_1^n\sigma_4(x,y),0)\\
&\quad-\delta_1^n\delta_2^n\frac{2a^2}{\sqrt{\varepsilon_1}(1+a^2)}(\check{\Gamma}_2\circ g)[k_{21}](\delta_1^n\sigma_4(x,y))\Big]\\
&+\hat{I}_{21}[\hat{k}_{21}](x,y)
\end{aligned}
\tag{8.128}
$$

$$
\begin{aligned}
&\hat{k}_{22}(x,y)=\\
&\quad\frac{2}{a(1+a^2)}\lim_{n\to\infty}\Big[\delta_1^n\delta_2^n\check{k}_{21}(\delta_1^n(x-y),0)\Big]\\
&\quad+\frac{2}{a(1+a^2)}\sum_{n=1}^{\infty}\Big[(-1)^n\delta_1^n\delta_2^{n-1}\\
&\qquad\qquad\times\hat{I}_{21}[\hat{k}_{21}](\delta_3^n(x-y),\delta_3^n(x-y))\\
&\quad+\delta_1^{n-1}\delta_2^{n-1}\check{I}_{21}[\hat{k}_{21}](\delta_1^n(x-y),0)\\
&\quad+(-1)^n\delta_1^n\delta_2^{n-1}\frac{2a}{1+a^3}\check{I}_{22}[\hat{k}_{21}](\delta_3^n(x-y),0)\\
&\quad+\delta_1^n\delta_2^{n-1}\frac{2a^2}{\sqrt{\varepsilon_1}(1+a^2)}(\check{\Gamma}_2\circ g)[k_{21}](\delta_1^n(x-y))\Big]\\
&\quad+\delta_2\check{I}_{22}[\hat{k}_{21}](x-y,0)+\hat{I}_{22}[\hat{k}_{21}](x,y)\\
&\quad-\frac{2}{\sqrt{\varepsilon_2}(1+a^2)}(\check{\Gamma}_2\circ g)[k_{21}](x-y)B
\end{aligned}
\tag{8.129}
$$

$$
\begin{aligned}
&\check{k}_{21}(x,y)=\\
&\quad\lim_{n\to\infty}\Big[\delta_1^n\delta_2^n\check{k}_{21}(\delta_1^n\sigma_5(x,y),\delta_1^n\sigma_5(x,y))\Big]\\
&\quad+\sum_{n=0}^{\infty}\Big[-\delta_1^{n+1}\delta_2^n\hat{I}_{21}[\hat{k}_{21}](\delta_1^n\sigma_5(x,y),\delta_1^n\sigma_5(x,y))\\
&\quad-\frac{2a^3}{1+a^2}\delta_1^{n+1}\delta_2^n\check{I}_{22}[\hat{k}_{21}]\left(\frac{\delta_1}{\delta_3}\delta_1^n\sigma_5(x,y),0\right)\\
&\quad-\delta_1^{n+1}\delta_2^n\frac{2a^2}{\sqrt{\varepsilon_1}(1+a^2)}(\check{\Gamma}_2\circ g)[k_{21}]\left(\frac{\delta_1}{\delta_3}\delta_1^n\sigma_5(x,y)\right)\\
&\quad+\delta_1^{n+1}\delta_2^{n+1}\check{I}_{21}[\hat{k}_{21}]\left(\frac{\delta_1}{\delta_3}\delta_1^n\sigma_5(x,y),0\right)\Big]
\end{aligned}
$$

$$+\check{I}_{21}[\hat{k}_{21}](x,y) \tag{8.130}$$

$$\check{k}_{22}(x,y) = \check{I}_{22}[\hat{k}_{21}](x,y) \tag{8.131}$$

with

$$\delta_1 = \frac{\sqrt{\varepsilon_1} - \sqrt{\varepsilon_2}}{\sqrt{\varepsilon_1} + \sqrt{\varepsilon_2}} \tag{8.132}$$

$$\delta_2 = \frac{1-a^2}{1+a^2} \tag{8.133}$$

$$\delta_3 = \frac{\sqrt{\varepsilon_1}}{\sqrt{\varepsilon_1} + \sqrt{\varepsilon_2}} \tag{8.134}$$

Since $a < 1, \varepsilon_1 > \varepsilon_2$ as per Assumption 8.2, the coefficients $\delta_{1,2,3} \in (0,1)$. It is unclear initially whether the limit and infinite sum terms even converge, however, as one may notice in Figure 8.3, the contracting volume of integration and the reflection coefficients (appearing implicitly in the δ_i coefficients) will guarantee the convergence.

The argument is similar to that of [15], but the additional non-local term $(\check{\Gamma}_2 \circ g)[k_{21}]$ must be accounted for. As we have shown in (8.92), the operator $\check{\Gamma}_2 \circ g)$ is a bounded Volterra operator on the transformed variable $\hat{k}_{21}$. It is easy to see that if a solution $\hat{k}_{21}$ exists, then the solutions $\check{k}_{21}, \hat{k}_{22}, \check{k}_{22}$ follow from direct evaluation. Thus, in this proof, we will merely show that $\hat{k}_{21}$ exists.

We establish an iteration $\hat{k}_{21,i}$ as

$$\begin{aligned}
&\hat{k}_{21,i}(x,y) = \\
&\quad \sum_{n=0}^{\infty} \Big[\delta_1^n \delta_2^n \hat{I}_{21}[\hat{k}_{21,i}](\delta_3^n \sigma_4(x,y), \delta_3^n \sigma_4(x,y)) \\
&\qquad - \delta_1^n \delta_2^{n+1} \check{I}_{21}[\hat{k}_{21,i}](\delta_1^n \sigma_4(x,y), 0) \\
&\qquad + \delta_1^n \delta_2^n \frac{2a^3}{1+a^2} \check{I}_{22}[\hat{k}_{21,i}](\delta_1^n \sigma_4(x,y), 0)
\end{aligned}$$

$$
\begin{aligned}
&\quad - \delta_1^n \delta_2^n \frac{2a^2}{\sqrt{\varepsilon_1}(1+a^2)} (\check{\Gamma}_2 \circ g)[k_{21,i}](\delta_1^n \sigma_4(x,y)) \Big] \\
&+ \hat{I}_{21}[\hat{k}_{21,i}](x,y)
\end{aligned} \tag{8.135}
$$

We seek the existence fixed point of the iteration (in the complete space $C(\mathcal{T})$), that is, $\lim_{i\to\infty} \hat{k}_{21,i} = \hat{k}_{21}$. For the limit to converge, we can seek for *uniform* bounds over $\mathcal{T}$, which will imply uniform convergence. For simplicity of analysis, we study the residuals of the iteration, $\Delta\hat{k}_{21,i} := \hat{k}_{21,i+1} - \hat{k}_{21,i}$. Noting the linearitiy of the integral operators, and evaluating the infinite geometric sum, one can eventually find the following iterative bound:

$$
\begin{aligned}
&|\Delta\hat{k}_{21,i+1}(x,y)| \leq \\
&\quad \frac{1}{1-\delta_1\delta_2} \Bigg[|\hat{I}_{21}[|\Delta\hat{k}_{21,i}|](\delta_3^n\sigma_4(x,y), \delta_3^n\sigma_4(x,y))| \\
&\qquad\qquad + \delta_2 |\check{I}_{21}[|\Delta\hat{k}_{21,i}|](\delta_1^n\sigma_4(x,y), 0)| \\
&\qquad\qquad + \frac{2a^3}{1+a^2} |\check{I}_{22}[|\Delta\hat{k}_{21,i}|](\delta_1^n\sigma_4(x,y), 0)| \\
&\qquad\qquad + \frac{2a^2}{\sqrt{\varepsilon_1}(1+a^2)} \int_0^{\delta_1^n\sigma_4(x,y)} \frac{\sqrt{\varepsilon_1} - \sqrt{\varepsilon_2}}{\varepsilon_2} \\
&\qquad\qquad\qquad \times ||\Gamma_1||_{L^\infty} ||S||_{L^\infty} |\Delta\hat{k}_{21,i}(\xi,\xi)| d\xi \Bigg] \\
&\quad + |\hat{I}_{21}[|\Delta\hat{k}_{21,i}|](x,y)|
\end{aligned} \tag{8.136}
$$

where now we can establish the postulated fixed point as

$$
\hat{k}_{21} = \lim_{i\to\infty} \hat{k}_{21,i} = \hat{k}_{21,0} + \sum_{i=0}^{\infty} \Delta\hat{k}_{21,i} \tag{8.137}
$$

The equivalent condition for convergence of the residuals is showing that the sum in (8.137) converges uniformly, which we will show via the Weierstrass M-test. We select $\hat{k}_{21,0} = 0$, and

from (8.135), we can find

$$\Delta\hat{k}_{21,0} \leq \frac{1}{1-\delta_1\delta_2}\frac{2a^2}{\sqrt{\varepsilon_1}(1+a^2)}|\Gamma_0|_2\,||S||_{L^\infty} =: \Psi_0 \tag{8.138}$$

Noting this, one may substitute Ψ_0 into (8.136) to compute successive bounds on $\Delta\hat{k}_{21,i}$, which can be encapsulated into the following bound:

$$|\Delta k_{21,i}(x,y)| \leq 3\Psi_0\frac{1}{n!}\Psi^n x^n \tag{8.139}$$

where

$$\begin{aligned}\Psi = \max\Bigg\{ &\left(\frac{1}{1-\delta_1\delta_2}\right)\left(1+\delta_2+\frac{2a^3}{1+a^2}\right)\\ &\times\left(\frac{\sqrt{\varepsilon_1}-\sqrt{\varepsilon_2}}{\sqrt{\varepsilon_2}}\,||k_{11}||_{L^\infty}\right),\\ &\left(\frac{1}{1-\delta_1\delta_2}\right)\left(\frac{2}{\varepsilon_2}\,||\Gamma_1||_{L^\infty}||S||_{L^\infty}\right),\\ &\frac{\sqrt{\varepsilon_1}-\sqrt{\varepsilon_2}}{\sqrt{\varepsilon_2}}\,||k_{11}||_{L^\infty}\Bigg\}\end{aligned} \tag{8.140}$$

Then it is quite clear that

$$\sum_{i=0}^{\infty}|\Delta k_{21,i}(x,y)| \leq 3\Psi_0\exp(\Psi x) < \infty \tag{8.141}$$

since $x \in [0,1]$. By the Weierstrass M-test we can conclude the uniform (and absolute) convergence of (8.137) in $C(\mathcal{T})$. This proves the existence of $\hat{k}_{21} \in C(\mathcal{T})$ via the Schauder fixed point theorem.

As mentioned previously, the existence of $\hat{k}_{21} \in C(\mathcal{T})$ will imply the existence of $\hat{k}_{22}, \check{k}_{21}, \check{k}_{22} \in C(\mathcal{T})$ by a mere straightforward evaluation of (8.129),(8.130),(8.131).

□

Lemma 27. *The ODE* (8.27) *and associated initial conditions admit a unique* $C([0,1])$ *solution.*

Proof. The proof directly follows from (8.87),(8.88) and Lemmas 25,26. It is trivial to see that $\Gamma_1 \in C^\infty([0,1])$ by virtue of the matrix exponential.

The regularity of Γ_2 can be recovered noting that Γ_2 involves a convolution of the operator $g[k_{21}](x)$ with a matrix exponential (seen in (8.88)). As the exponential is $C^\infty([0,1])$, it is quite clear that it acts as a mollifier to recover a $C^\infty([0,1])$ solution for Γ_2. □

8.5 Conclusion

A control design methodology via folding and infinte-dimensional backstepping is detailed in the paper. The result comes as a natural extension to the folding framework to designing bilateral controllers.

Of great interest is an alternative interpretation of the folded system with an ODE. The control of an ODE through two distinct controllers can be seen to play a cooperative "game", whose objective is to stabilize the ODE through the coupled actuation path. This interpretation naturally raises the question of casting a noncooperative game, where perhaps the two controllers are designed independently of one another. Such a formulation may lead to more robust bilateral implementations, where the failure of one controller does not compromise the stability of the system.

A nautral extension to consider is state estimation. Some work by Camacho-Solario has explored a similar problem, albeit for a single parabolic equation (as opposed to two distinct parabolic input paths) [9]. The state estimation analogue to the problem has been considered without the ODE in (...), where two collocated measurements of state and flux are taken at an arbitrary interior point (independent of the ODE coupling/folding point). When only the ODE is measured, however, the designer can really only generate an estimate of the state at the point of coupling, and not necessarily of the flux – an undersensed system. This problem is of great engineering interest, and is under investigation.

8.6 Acknowledgements

Chapter 8, in part, is a reprint of the material as it appears in: S.Chen, R. Vazquez, M. Krstic. Bilateral Boundary Control Design for a Cascaded Diffusion-ODE System Coupled at an Arbitrary Interior Point. Submitted to Automatica, 2019. The dissertation author was the primary investigator and co-author of this paper.

Bibliography

[1] "Boundary control of coupled reaction-advection-diffusion equations having the same diffusivity parameter**the research leading to these results has received funding from the research project."

[2] Y. Achdou, J. B. Francisco, J. Lasry, P. Lions, and B. Moll, "Partial differential equation models in macroeconomics," *Philosophical Transactions of the Royal Society A: Mathematical, Physical and Engineering Sciences*, vol. 372, no. 2028, Nov 2014.

[3] J. Auriol and F. D. Meglio, "Minimum time control of heterodirectional linear coupled hyperbolic pdes," *Automatica*, vol. 71, pp. 300–307, 2016.

[4] ——, "Two sided boundary stabilization of heterodirectional linear coupled hyperbolic pdes," *IEEE Transactions on Automatic Control*, vol. PP, no. 99, pp. 1–1, 2017.

[5] ——, "Two-sided boundary stabilization of heterodirectional linear coupled hyperbolic pdes," *IEEE Transactions on Automatic Control*, vol. 63, no. 8, pp. 2421–2436, 2018.

[6] A. Baccoli and A. Pisano, "Anticollocated backstepping observer design for a class of coupled reaction-diffusion pdes," *Journal of Control Science and Engineering*, vol. 2015, p. 53, 2015.

[7] N. Bekiaris-Liberis and M. Krstic, "Compensation of wave actuator dynamics for nonlinear systems," *IEEE Transactions on Automatic Control*, vol. 59, pp. 1555–1570, 2014.

[8] N. Bekiaris-Liberis and R. Vazquez, "Nonlinear Bilateral Output-Feedback Control for a Class of Viscous Hamilton-Jacobi PDEs," *ArXiv e-prints*, Mar. 2018.

[9] L. Camacho-Solario, N. Velmurugan, F. D. Meglio, and M. Krstic, "Observer design for a coupled ode-pde system from a wellbore reservoir drilling model," in *Submitted to the 2019 IEEE 58th Conference on Decision and Control (CDC)*, Dec 2019.

[10] L. Camacho-Solorio, R. Vazquez, and M. Krstic, "Boundary observer design for coupled reaction-diffusion systems with spatially-varying reaction," in *2017 American Control Conference (ACC)*, May 2017, pp. 3159–3164.

[11] M. Chaplain, S. McDougall, and A. Anderson, "Mathematical modeling of tumor-induced angiogenesis," *Annual Review of Biomedical Engineering*, vol. 8, no. 1, pp. 233–257, 2006, pMID: 16834556. [Online]. Available: https://doi.org/10.1146/annurev.bioeng.8.061505.095807

[12] S. Chen, R. Vazquez, and M. Krstic, "Backstepping control design for a coupled hyperbolic-parabolic mixed class pde system," in *2017 IEEE 56th Annual Conference on Decision and Control (CDC)*, Dec 2017, pp. 664–669.

[13] ——, "Stabilization of an underactuated coupled transport-wave pde system," in *2017 American Control Conference (ACC)*, May 2017, pp. 2504–2509.

[14] ——, "Bilateral boundary control design for a cascaded diffusion-ode system coupled at an arbitrary interior point," *Submitted to Automatica and uploaded to arXiv preprint submit/2727152*, 2019.

[15] ——, "Folding bilateral backstepping output-feedback control design for an unstable parabolic pde," *Submitted to IEEE Transactions on Automatic Control and uploaded to arXiv preprint submit/2727120*, 2019.

[16] J. Coron, B. d'Andréa Novel, and G. Bastin, "A strict Lyapunov function for boundary control of hyperbolic systems of conservation laws," *IEEE Transactions on Automatic Control*, vol. 52, no. 1, pp. 2–11, 2007.

[17] G. A. de Andrade, R. Vazquez, and D. J. Pagano, "Backstepping stabilization of a linearized odepde rijke tube model," *Automatica*, vol. 96, pp. 98 – 109, 2018.

[18] J. Deutscher and K. Simon, "Backstepping control of coupled linear parabolic pides with spatially varying coefficients," *IEEE Transactions on Automatic Control*, vol. 63, no. 12, pp. 4218–4233, 2018.

[19] L. Evans, *Partial Differential Equations*. American Mathematical Society, 1998.

[20] G. Freudenthaler, F. Gttsch, and T. Meurer, "Backstepping-based extended luenberger observer design for a burgers-type pde for multi-agent deployment**financial support by the german research council (dfg) in the project me 3231/2-1 is gratefully acknowledged." *IFAC-PapersOnLine*, vol. 50, no. 1, pp. 6780 – 6785, 2017, 20th IFAC World Congress. [Online]. Available: http://www.sciencedirect.com/science/article/pii/S2405896317316956

[21] G. Hardy, J. Littlewood, and G. Polya, *Inequalities, 2nd ed.* Cambridge University Press, 1959.

[22] T. Hashimoto and M. Krstic, "Stabilization of reaction diffusion equations with state delay using boundary control input," *IEEE Transactions on Automatic Control*, vol. 61, no. 12, pp. 4041–4047, Dec 2016.

[23] A. Hastings, "Global stability in lotka-volterra systems with diffusion," *Journal of Mathematical Biology*, vol. 6, no. 2, pp. 163–168, Jul 1978. [Online]. Available: https://doi.org/10.1007/BF02450786

[24] L. Hu and F. D. Meglio, "Finite-time backstepping boundary stabilization of 3 3 hyperbolic systems," *European Control Conference 2015*, pp. 67–72, 2015.

[25] L. Hu, F. D. Meglio, R. Vazquez, and M. Krstic, "Control of homodirectional and general heterodirectional linear coupled hyperbolic pdes," *IEEE Transactions on Automatic Control*, vol. 61, no. 10, pp. 3301–3314, 2016.

[26] S. Koga and M. Krstic, "Single-boundary control of the two-phase stefan system," *arXiv preprint arXiv:1905.12735*, 2019.

[27] M. Krstic, "Compensating actuator and sensor dynamics governed by diffusion pdes," *Systems & Control Letters*, vol. 58, no. 5, pp. 372–377, 2009.

[28] ——, "Control of an unstable reaction-diffusion pde with long input delay," *Systems and Control Letters*, vol. 58, pp. 773–782, 2009.

[29] ——, *Delay compensation for nonlinear, adaptive, and PDE systems*. Springer, 2009.

[30] M. Krstic and A. Smyshlyaev, *Boundary Control of PDEs: A Course on Backstepping Designs*. SIAM, 2008.

[31] F. D. Meglio, R. Vazquez, and M. Krstic, "Backstepping stabilization of an underactuated 3x3 linear hyperbolic system of fluid flow equations," *American Control Conference 2012*, pp. 3365–3370, 2012.

[32] ——, "Stabilization of a system of coupled first-order hyperbolic linear pdes with a single boundary input," *IEEE Transactions on Automatic Control*, vol. 58, no. 12, pp. 3097–3111, 2013.

[33] Y. Orlov, A. Pisano, A. Pilloni, and E. Usai, "Output feedback stabilization of coupled reaction-diffusion processes with constant parameters," *SIAM Journal on Control and Optimization*, vol. 55, no. 6, pp. 4112–4155, 2017. [Online]. Available: https://doi.org/10.1137/15M1034325

[34] C. Prieur and E. Trlat, "Feedback stabilization of a 1-d linear reactiondiffusion equation with delay boundary control," *IEEE Transactions on Automatic Control*, vol. 64, no. 4, pp. 1415–1425, April 2019.

[35] A. Smyshlyaev and M. Krstic, "Explicit state and output feedback boundary controllers for partial differential equations," *Journal of Automatic Control*, vol. 13, pp. 1–9, 2003.

[36] ——, "Backstepping observers for a class of parabolic pdes," *Systems & Control Letters*, vol. 54, no. 7, pp. 613 – 625, 2005. [Online]. Available: http://www.sciencedirect.com/science/article/pii/S0167691104001963

[37] ——, "On control design for pdes with space-dependent diffusivity and time-dependent reactivity," *Automatica*, vol. 41, pp. 1601–1608, 2005.

[38] G. A. Susto and M. Krstic, "Control of pde-ode cascades with neumann interconnections," *Journal of the Franklin Institute*, vol. 347, no. 1, pp. 284 – 314, 2010, dynamics and Control. [Online]. Available: http://www.sciencedirect.com/science/article/pii/S0016003209001276

[39] S. Tang and C. Xie, "State and output feedback boundary control for a coupled pde-ode system," *Systems & Control Letters*, vol. 60, no. 8, pp. 540 – 545, 2011. [Online]. Available: http://www.sciencedirect.com/science/article/pii/S0167691111000922

[40] D. Tsubakino and S. Hara, "Backstepping observer design for parabolic pdes with measurement of weighted spatial averages," *Automatica*, vol. 53, 03 2015.

[41] D. Tsubakino, M. Krstic, and Y. Yamashita, "Boundary control of a cascade of two parabolic pdes with different diffusion coefficients," in *Decision and Control (CDC), 2013 IEEE 52nd Annual Conference on*. IEEE, 2013, pp. 3720–3725.

[42] J. Vázquez, *The porous medium equation: mathematical theory*. Oxford University Press, 2007.

[43] R. Vazquez and M. Krstic, "Bilateral boundary control of one-dimensional first- and second-order pdes using infinite-dimensional backstepping," in *2016 IEEE 55th Conference on Decision and Control (CDC)*, Dec 2016, pp. 537–542.

[44] ——, "Boundary control and estimation of reaction–diffusion equations on the sphere under revolution symmetry conditions," *International Journal of Control*, pp. 1–10, 2017.

[45] ——, "Boundary control of coupled reaction-advection-diffusion systems with spatially-varying coefficients," *IEEE Transactions on Automatic Control*, vol. 62, no. 4, pp. 2026–2033, April 2017.

[46] C. Wagner and N. Harned, "EUV lithography: Lithography gets extreme," *Nat Photon*, vol. 4, no. 1, pp. 24–26, 01 2010.

[47] J. Wang and M. Krstic, "Output-feedback boundary control of a heat pde sandwiched between two odes," *IEEE Transactions on Automatic Control*, pp. 1–1, 2019.

[48] J. Wang, B. Guo, and M. Krstic, "Wave equation stabilization by delays equal to even multiples of the wave propagation time," *Systems & Control Letters*, vol. 57, pp. 750–758, 2008.

[49] J. Wang, J. Liu, B. Ren, and J. Chen, "Sliding mode control to stabilization of cascaded heat pde-ode systems subject to boundary control matched disturbance," *Automatica*, vol. 52, pp. 23 – 34, 2015. [Online]. Available: http://www.sciencedirect.com/science/article/pii/S0005109814004981

[50] S. Wang and F. Woittennek, "Backstepping-method for parabolic systems with in-domain actuation," *IFAC Proceedings Volumes*, vol. 46, no. 26, pp. 43–48, 2013.

[51] F. Woittennek, S. Wang, and T. Knüppel, "Backstepping design for parabolic systems with in-domain actuation and robin boundary conditions," *IFAC Proceedings Volumes*, vol. 47, no. 3, pp. 5175–5180, 2014.

[52] H. Yu, M. Diagne, L. L. Zhang, and M. Krstic, "Bilateral boundary control of moving shockwave in lwr model of congested traffic," *arXiv preprint arXiv:1904.04303*, 2019.

[53] Z. Zhou, Z. Ren, and C. Xu, "Stabilization of a general linear heat-ode system coupling at an intermediate point," *International Journal of Robust and Nonlinear Control*, vol. 27, no. 17, pp. 3951–3970, 2017.